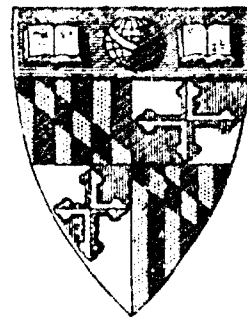
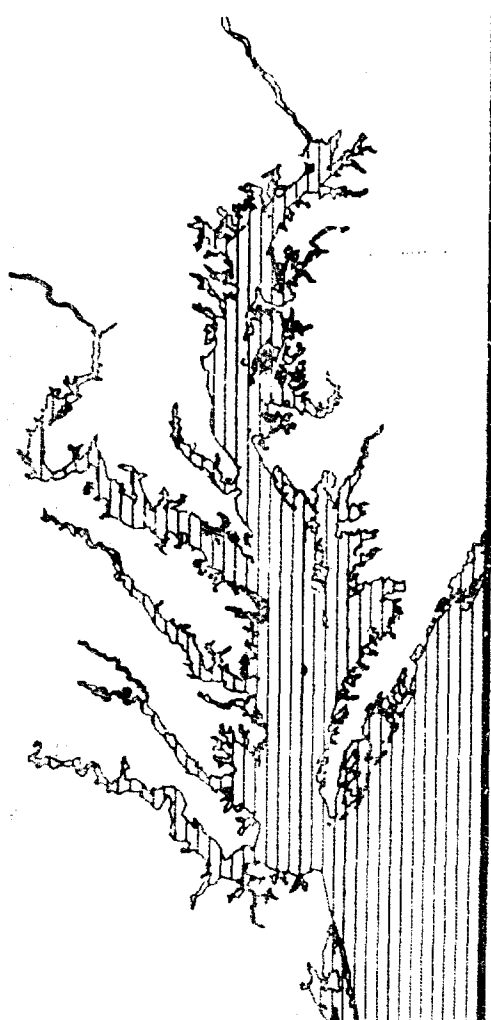


AD 671270



# CHESAPEAKE BAY INSTITUTE The Johns Hopkins University



SUSPENDED SEDIMENT OF THE  
NORTHERN CHESAPEAKE BAY

Best Available Copy

J.R. Schubel

Technical Report 35

This document has been approved  
for public release and sale; its  
distribution is unlimited.

Reference 68-2

March 1968

Published by the  
SEAFARERS HOUSE  
1000 Pennsylvania Avenue, N.W.  
Washington, D.C. 20004

27

CHESAPEAKE BAY INSTITUTE  
THE JOHNS HOPKINS UNIVERSITY

SUSPENDED SEDIMENT OF THE NORTHERN CHESAPEAKE BAY

J. R. Schubel

TECHNICAL REPORT 35

This report contains results of work carried out for the Department of Chesapeake Bay Affairs, State of Maryland, and the Bureau of Commercial Fisheries, Department of the Interior, through a jointly funded project under Public Law 88-309; for the Office of Naval Research under Project NR 083-016, Contract Nonr 4010(11); and for the Natural Resources Institute, University of Maryland.

This report does not necessarily constitute final publication of the material presented.

Reproduction in whole or in part is permitted for any purpose of the United States Government.

Reference 68-2  
March 1968

D. W. Pritchard  
Director

#### ABSTRACT

An intensive study was made of the suspended sediment of the northern Chesapeake Bay from 21 March 1966 through 31 March 1967. Samples were collected routinely at 16 stations for determinations of both the concentrations of total suspended solids and the concentrations of combustible organic matter. At selected stations samples were collected for mineral identification by X-ray diffraction and for size analysis both by a photomicrographic technique and by sedimentation.

The concentrations of suspended sediment in the Bay proper were greater than 5 mg/l throughout the year with maximum values greater than 110 mg/l occurring in March during the period of peak river flow. The concentrations of combustible organic matter were highest in the spring and summer months averaging nearly 5 mg/l and lowest during the winter months when they averaged about 3 mg/l. The concentrations of suspended sediment in the mouth of the Susquehanna River, the principal source of fluvial sediment to the study area, exceeded 140 mg/l during the period of maximum river flow. Except for the period of peak river discharge, the concentrations of suspended sediment were higher in the Bay than in the Susquehanna River.

The mean projected diameter of the suspended particles had a limited range. In nearly 80 percent of the samples analyzed it was between 1.4 and 2.0  $\mu$  and all samples were included

between 1.1 and 2.8  $\mu$ . The mean Stokes diameter ranged from 2.3 to 12.2  $\mu$ , and in nearly 70 percent of the samples it was between 3 and 6  $\mu$ . At nearly all of the stations, both the mean projected diameter and the mean Stokes diameter increased near the bottom.

The minerals of the suspended sediment consisted of the illite, chlorite, and kaolinite clay mineral "groups" and of quartz and feldspar. Illite appears to be the most abundant mineral. The seasonal and geographic variations of the relative abundances of the clay minerals were small.

During the year 1 April 1966 through 31 March 1967 the Susquehanna River discharged  $0.6 \times 10^6$  metric tons of suspended sediment into the Bay at Havre de Grace. Nearly 70 percent of the  $0.6 \times 10^6$  metric tons was discharged during peak runoff in late February and March and of this 70 percent about 80 percent was deposited within the study area. Approximately  $0.1 \times 10^6$  metric tons of silt and clay are introduced into the study area from coastal erosion.

During the period of peak runoff the upper Bay's suspended sediment population was closely linked to its major source of new sediment--the Susquehanna River. At all other times of the year however, the concentrations of suspended sediment were higher within the Bay than in the mouth of the Susquehanna River despite the dilution of the Susquehanna discharge

and the settling out which occur within the Bay. Excluding the period of maximum runoff, the concentrations of suspended sediment in the Bay were determined largely by local resuspension, and by the upstream transport of sediment in the lower layer. It is not possible to assess the relative contributions by these two mechanisms with the data we now have. It was possible however, to calculate the net flux density of sediment through the surface separating the upper and lower layers.

Although we do not have sufficient information to write a sediment budget for this segment of the Chesapeake Bay, there can be little doubt that this is an area of net deposition. The data indicate an average sedimentation rate of from 2 to 3 mm per year.

The pattern of sedimentation then, is one of fluvial domination during the period of thaw and high runoff, and cannibalism (resedimentation) during the remainder of the year.

#### ACKNOWLEDGEMENTS

This report represents a great deal of effort by a number of people. Throughout this study I have received abundant moral and material support both in the field and in the laboratory. From the first shaky cruise with apparatus held together with parachute cord to an efficient sampling procedure with apparatus held together with parachute cord, the help and advice of my friends at the Chesapeake Bay Institute Field Laboratory have been indispensable. It is impractical to mention all those who have lent a hand in the field, but I should like to thank Horace Whaley, Richard Whaley, James Booth, David Booth, Roy Kafter, and particularly William Cronin, George Anderson, and Robert Baker for all their help. In the laboratory I have been privileged to have an able and efficient technician in Mrs. Cecily Morrow.

I am grateful to Drs. Akira Okubo, Donald Pritchard, and James Carpenter for their advice for improving the manuscript, and to Harry Carter for his help on the first organizational cruises, and for his continued encouragement. I am particularly indebted to Dr. Blair Kinsman for his counsel and comfort. I wish to thank Harvey Walters for the computer programming, Richard Linfield and Mrs. Dean Loose for the illustrations, and Mrs. Kathy Shinn for typing the manuscript.

Acknowledgements continued

I would like to thank the state and federal agencies which jointly provided the funding for this program. The Department of Chesapeake Bay Affairs and the Bureau of Commercial Fisheries, Department of Interior, provided the major portion of the support through a jointly funded project under Public Law 88-309. During a portion of the study funding support was also provided from the Natural Resources Institute, University of Maryland, and from the Office of Naval Research, U.S. Navy Department.

## TABLE OF CONTENTS

	Page
Introduction	1
The Study Area	13
Hypsometry	13
Hydrographic Conditions	16
Fresh Water Inflow	16
Concentration of Suspended Solids	21
Cumbustible Organic Matter	42
Size Analysis	85
Introduction	85
Some Definitions	89
Photomicrographic Size Analysis	96
Results and Discussion	109
Size Analysis by Sedimentation using the MSA Particle Size Analyzer	129
Results and Discussion	162
Mineralogy of the Suspended Sediment	170
Sedimentation Processes	177
Suspended Sediment Discharge of the Susquehanna	179
Coastal Erosion of the Upper Bay	192
Resuspension of Bottom Sediment	198

TABLE OF CONTENTS Continued

	Page
Summary	219
Appendix A	223
Appendix B	241
Appendix C	246
Appendix D	252
Bibliography	258

## TABLES

	Page
1 Average Discharge of Rivers Flowing into the Northern Chesapeake Bay	22
2 Comparison of Large (18-50 liter) and Small (0.5-1 liter) samples	27
3 Suspended Sediment Retention Characteristics of 0.8 $\mu$ AFD Metal Membrane Filters	31
4 Inventory of Sampling Program	37
5 Statistics Based on Data Presented in Figs. 40 through 45	44
6 Ranges of Applicability of Various Microscopic Techniques	86
7 Some Definitions of Means	93
8 Statistical Properties of Particle Size Distributions Shown in Figs. 49 and 50	114
9 Stability of Photomicrographic Size Analyser	128
10 Statistical Properties of Particle Size Distributions Shown in Figs. 57 and 58	166

TABLES Continued

	Page
11 Replicate MSA Analyses of a Suspended Sediment Sample from the Upper Bay	167
12 Mineralogy Samples	171
13 Coastal Erosion Data	196
A1 Statistical Properties of Particle Size Distri- butions Shown in Figs. A-1 through A-6	230
A2 Statistical Properties of Particle Size Distri- butions Shown in Figs. 55 and 56 and in Figs. A-7 through A-12	239
D1 Statistical Properties of Particle Size Distri- butions Shown in Figs. D-1 through D-3	256

## FIGURES

	Page
1 The Chesapeake Bay Estuarine System	8
2 Map of Study Area Showing all Portions Deeper than 8 m in Black	14
3 Hypsometric Curve of the Bay from Tolchester to Turkey Pt.	15
4 Average Temperature and Salinity Along the Channel Section in the Upper Bay, Spring 1966 (15 March- 15 June)	17
5 Average Temperature and Salinity along the Channel Section in the Upper Bay, Summer 1966 (16 June- 30 September)	18
6 Average Temperature and Salinity Along the Channel Section in the Upper Bay, Autumn 1966 (1 October- 15 December)	19
7 Average Temperature and Salinity Along the Channel Section in the Upper Bay, Winter 1966-1967 (16 December- 14 March)	20
8 Station Location Map	36

FIGURES Continued

	Page
9 Distribution of Total Suspended Solids (mg/l) on 21-22 March 1966 (Cruise 1)	46
10 Distribution of Total Suspended Solids (mg/l) on 5-6 May 1966 (Cruise 2)	47
11 Distribution of Total Suspended Solids (mg/l) on 31 May-1 June 1966 (Cruise 3)	48
12 Distribution of Total Suspended Solids (mg/l) on 27-28 June 1966 (Cruise 4)	49
13 Distribution of Total Suspended Solids (mg/l) on 11-12 July 1966 (Cruise 5)	50
14 Distribution of Total Suspended Solids (mg/l) on 25-26 July 1966 (Cruise 6)	51
15 Distribution of Total Suspended Solids (mg/l) on 8-9 August 1966 (Cruise 7)	52
16 Distribution of Total Suspended Solids (mg/l) on 22-23 August 1966 (Cruise 8)	53
17 Distribution of Total Suspended Solids (mg/l) on 6-7 September 1966 (Cruise 9)	54

FIGURES Continued

	Page
18 Distribution of Total Suspended Solids (mg/l) on 19-20 September 1966 (Cruise 10)	55
19 Distribution of Total Suspended Solids (mg/l) on 3-4 October 1966 (Cruise 11)	56
20 Distribution of Total Suspended Solids (mg/l) on 17-18 October 1966 (Cruise 12)	57
21 Distribution of Total Suspended Solids (mg/l) on 1 November 1966 (Cruise 13)	58
22 Distribution of Total Suspended Solids (mg/l) on 14 November 1966 (Cruise 14)	59
23 Distribution of Total Suspended Solids (mg/l) on 30 November-1 December 1966 (Cruise 15)	60
24 Distribution of Total Suspended Solids (mg/l) on 13-14 December 1966 (Cruise 16)	61
25 Distribution of Total Suspended Solids (mg/l) on 28-29 December 1966 (Cruise 17)	62
26 Distribution of Total Suspended Solids (mg/l) on 12-13 January 1967 (Cruise 18)	63

FIGURES Continued

	Page
27 Distribution of Total Suspended Solids (mg/l) on 14-15 February 1967 (Cruise 20)	64
28 Distribution of Total Suspended Solids (mg/l) on 9-10 March 1967 (Cruise 21)	65
29 Distribution of Total Suspended Solids (mg/l) on 15 March 1967 (Cruise 22)	66
30 Distribution of Total Suspended Solids (mg/l) on 20 March 1967 (Cruise 23)	67
31 Surface and Mid-depth Concentrations of Suspended Sediment at the Susquehanna River Station and at Channel Stations Within the Bay	68
32 Surface and Mid-depth Concentrations of Suspended Sediment at the Susquehanna River Station and at Channel Stations within the Bay	69
33 Surface and Mid-depth Concentrations of Suspended Sediment at the Susquehanna River Station and at Channel Stations within the Bay	70
34 Surface and Mid-depth Concentrations of Suspended Sediment at the Susquehanna River Station and at Channel Stations within the Bay	71

FIGURES Continued

	Page
35 Surface and Mid-depth Concentrations of Suspended Sediment at the Susquehanna River Station and at Stations within the Bay	72
36 Surface and Mid-depth Concentrations of Suspended Sediment at the Susquehanna River Station and at Stations within the Bay	73
37 Surface and Mid-depth Concentrations of Suspended Sediment at the Susquehanna River Station and at Stations within the Bay	74
38 Average Distributions of Total Suspended Solids (mg/l) During Summer 1966 (16 June-30 September) and Autumn 1966 (1 October-15 December)	75
39 Average Distributions of Total Suspended Solids (mg/l) During Winter 1966-1967 (16 December-14 March) and Spring 1966 and 1967 (15 March-15 June)	76
40 Surface and Mid-depth Concentrations of Suspended Sediment at Station SUS Plotted Against the Date of Sample Collection	77

FIGURES Continued

	Page
41 Surface and Mid-depth Concentrations of Suspended Sediment at Stations IC and IE Plotted Against the Date of Sample Collection	78
42 Surface and Mid-depth Concentrations of Suspended Sediment at Stations IIB, IID, and IIE, Plotted Against the Date of Sample Collection	79
43 Surface and Mid-depth Concentrations of Suspended Sediment at Stations IIIA, IIIC, and IIIE, Plotted Against the Date of Sample Collection	80
44 Surface and Mid-depth Concentrations of Suspended Sediment at Stations IVB, IVD, and IVE, Plotted Against the Date of Sample Collection	81
45 Surface and Mid-depth Concentrations of Suspended Sediment at Stations VC, VE, and VF, Plotted Against the Date of Sample Collection	82
46 Average Distribution of the Percent of the Total Suspended Solids Accounted for by Combustible Organic Matter During Summer 1966 (16 June-30 September) and Autumn 1966 (1 October-15 December)	83

FIGURES Continued

	Page
47 Average Distributions of the Percent of the Total Suspended Solids Accounted for by Combustible Organic Matter During Winter 1966-1967 (16 December- 14 March) and Spring 1966 and 1967 (15 March-15 June)	84
48 Diagrammatic Sketch of Zeiss Particle Size Analyzer TGZ-3	105
49 Particle Size Distribution Curves of Suspended Sediment Samples from Selected Space-time Positions in the Upper Bay	110
50 Particle Size Distribution Curves of Suspended Sediment Samples from Selected Space-time Positions in the Upper Bay	111
51 Frequency Distributions of Mean Projected Suspended Sediment Particle Diameters for Three Depths	116
52 Frequency Distribution of Mean Projected Suspended Sediment Particle Diameters for all 161 Samples	117
53 Frequency Distributions of the Modal Class of Equivalent Projected Diameters ( $D_m$ ) for Samples from Various Periods of the Year	118

FIGURES Continued

	Page
54 Frequency Distributions of the Modal Class of Equivalent Projected Diameters ( $D_m$ ) for Samples from January and February 1967, and for all 161 Samples	119
55 Volume-Size Distribution Curves Obtained by Transformation of Number-size Data	122
56 Volume-Size Distribution Curves Obtained by Transformation of Number-size Data	123
57 MSA Centrifuge Determined Volume-size Distri- butions of Selected Samples of Suspended Sediment from the Upper Bay	164
58 MSA Centrifuge Determined Volume-size Distri- butions of Selected Samples of Suspended Sediment from the Upper Bay	165
59 X-ray Diffraction Patterns of the Less than 2 $\mu$ and Greater than 2 $\mu$ Fractions of the Mid-depth Mineral Assemblage at Station VF on 6 September 1966	172
60 X-ray Diffraction Patterns of the Less than 2 $\mu$ and Greater than 2 $\mu$ Fractions of the Mid-depth Mineral Assemblage at Station IVD on 20 September 1966	173

FIGURES Continued

	Page
61 Diagram of the Sources of the Suspended Sediment of the Chesapeake Bay	178
62 Discharge of the Susquehanna River at Conowingo ( $\text{cfs} \times 10^3$ ), and Mean Suspended Sediment Concentrations ( $\text{mg/l}$ ) at Havre de Grace used in Calculating the Suspended Sediment discharge of the Susquehanna	161
63 Suspended Sediment Discharge of the Susquehanna River at Havre de Grace from 1 April 1966 through 31 March 1967 Plotted as Cumulative Percent, and as the Mass of Sediment Discharged During Consecutive Periods of Varying Lengths	188
64 The Maximum Surface Concentrations of Suspended Sediment ( $C_x$ ) at each of the Channel Stations Plotted as the Percentage of the Maximum Surface Concentration of Suspended Sediment at Station SUS ( $C_{\text{SUS}}$ ). The fresh water fractions of the surface waters at the same stations are also plotted as percentages.	190
65 Map of the Upper Bay Showing Shoreline Segments used in Calculating Annual Losses due to Erosion	194

FIGURES Continued

	Page
66 Monthly Wind Rose Diagrams for the Year 1 April 1966 through 31 March 1967	199
67 Current Velocity and Suspended Sediment Concentration at the Surface and at 2 m at Station IIIC* (9.5 m) on 10-11 July 1967. Based on hourly measurements.	201
68 Current Velocity and Suspended Sediment Concentration at 4 m and at 6 m at Station IIIC* (9.5 m) on 10-11 July 1967. Based on hourly measurements.	202
69 Current Velocity and Suspended Sediment Concentration at 8 m and at 9 m at Station IIIC* on 10-11 July 1967. Based on hourly measurements.	203
70 Surface Concentrations (mg/l) of Combustible Organic Matter at Stations SUS, IIIC, and VF Plotted Against the Date of Sample Collection	206
A-1 Particle Size Distribution Curves of Suspended Sediment Samples from Selected Space-time Positions in the Upper Bay	224
A-2 Particle Size Distribution Curves of Suspended Sediment Samples from Selected Space-time Positions in the Upper Bay	225

FIGURES Continued

	Page
A-3 Particle Size Distribution Curves of Suspended Sediment Samples from Selected Space-time Positions in the Upper Bay	226
A-4 Particle Size Distribution Curves of Suspended Sediment Samples from Selected Space-time Positions in the Upper Bay	227
A-5 Particle Size Distribution Curves of Suspended Sediment Samples from Selected Space-time Positions in the Upper Bay	228
A-6 Particle Size Distribution Curves of Suspended Sediment Samples from Selected Space-time Positions in the Upper Bay	229
A-7 Volume-size Distribution Curves Obtained by Transformation of the Number-size Data	233
A-8 Volume-size Distribution Curves Obtained by Transformation of the Number-size Data	234
A-9 Volume-size Distribution Curves Obtained by Transformation of the Number-size Data	235
A-10 Volume-size Distribution Curves Obtained by Transformation of the Number-size Data	236

FIGURES Continued

	Page
A-11 Volume-size Distribution Curves Obtained by Transformation of the Number-size Data	237
A-12 Volume-size Distribution Curves Obtained by Transformation of the Number-size Data	238
B-1 Typical Acceleration Curves of MSA Centrifuge used to Determine Starting-stopping Correction Term	244
B-2 Acceleration Curves of 1200 r.p.m. MSA Centrifuge used to Determine Starting-stopping Correction Term	245
C-1 MSA Data Sheet	251
D-1 MSA Centrifuge Determined Volume-size Distributions of Selected Samples of Suspended Sediment from the Upper Bay	253
D-2 MSA Centrifuge Determined Volume-size Distributions of Selected Samples of Suspended Sediment from the Upper Bay	254
D-3 MSA Centrifuge Determined Volume-size Distributions of Selected Samples of Suspended Sediment from the Upper Bay	255

## INTRODUCTION

The study of sediments is almost as old as the science of geology itself. Sediment consists of solid material which is being transported or has been deposited at or near the Earth's surface. Transportation, although it may be no more than the detachment of particles from the parent rock, is a necessary criterion.

The kind of sediment which accumulates in an environment depends on the nature of the sources, the transport mechanisms both into and internal to the region, and the conditions prevailing within the area during and after deposition--physical, chemical, and biological. A sedimentary deposit consists of both mineral and organic matter. The mineral fraction is made up of two kinds of material, the exogenetic (clastic) and the endogenetic (precipitated) parts (Grabau, 1904). Igneous rocks are the ultimate sources of all mineral grains. The ultimate sources are, however, often remote in space and time and sediments in a region may have gone through several cycles. Since the paths connecting a sediment and its sources are often difficult and sometimes impossible to trace, a study of sediments approached through their ultimate sources is seldom instructive. It is generally more meaningful to look at the proximate sources and the transporting media of sediments.

Modern marine and estuarine sediments are best understood when source and transport are taken together instead of being considered separately. We can consider the proximate sources of an estuarine sediment to be the atmosphere, the land and its surface drainage system, the estuary, the estuarine floor, and the sea.

Students of modern sediments have concentrated their attention on deposits and sources and have almost entirely neglected the transportation of sediment into and within the deposit area. Transportation, when it is treated at all, is commonly inferred from an examination of the textures and structures of the deposits themselves; properties such as sorting and rounding on the one hand, and ripple marks and laminations on the other. There are two primary reasons for this approach. First, the techniques for measuring sediments in transport are often lacking and second, modern sediments have frequently been studied primarily for guidance in the recognition of ancient environments and the interpretation of their deposits. (See for example Shepard, 1964.) Since sedimentary textures and structures reflect average or maximum current velocities they are also useful in studies of modern sediments. Such features, however, tell us very little about the mechanics of sedimentation, about the rates involved, or about the paths of movement. Without a knowledge of these

factors our understanding of sediments must remain severely limited.

Sediments are carried in suspension and by bottom traction by the three principal agents of transportation-- air, water, and ice. Sediment forming material is also carried in solution. The mode of movement of clastic materials by water or by air depends on the Reynolds number<sup>1</sup> of the flow and on the sizes, shapes, and specific gravities of the transported particles. Coarse sediments are generally transported as bed load, and fine sediments as suspended load. Bagnold (1966) defines the suspended load as that part of total load which is supported by a fluid-transmitted stress, and the bottom load as that part which is supported wholly by a solid-transmitted stress. The saltation of particles is a transitional stage between the bottom and suspended loads.

---

<sup>1</sup> The Reynolds number,  $Ul/v$ , depends on the velocity of the flow  $U$ , on the kinematic viscosity of the fluid  $v$ , and on some characteristic dimension of the container  $l$ . Low Reynolds numbers correspond to laminar flows, high Reynolds numbers to turbulent flows. Turbulent flows are much more powerful transporting agencies than are laminar flows. Turbulent flows with very high Reynolds numbers are difficult to create in the laboratory but they are the most commonly occurring flows under natural conditions.

Suspension is the primary mode of transportation in the Chesapeake Bay. The lower reaches of the tributaries have very low gradients as a result of the drowning caused by the post glacial rise in sea level. The low gradients have decreased the competency of the rivers to the extent that very little gravel and coarse sand reach the main body of the estuary. In addition, the reservoirs of the Susquehanna have almost eliminated the introduction of any sand into the upper Chesapeake Bay.

Suspended marine and estuarine sediments have been studied by methods based on optics, on centrifuging and on filtering. The majority of these investigations have used optical methods. Measurements of optical turbidity are relatively easy to make and may be done quickly. The evaluation of the results, however, is difficult because the optical measurements vary not only with the concentration of suspended matter, but also with the size distribution, with the indices of refraction of the particles, and with other properties. Most of the centrifuge studies have been made by the Russians. The main advantage of the centrifuge technique is that large water samples can be analyzed. Lisitsin (1961) reports that water samples of 100-200 tons have been processed in their studies of oceanic suspended matter. In regions where the concentration of suspended matter is low

and where the suspended matter is inhomogeneously distributed, large samples are needed to determine average conditions. The centrifuge method has a number of disadvantages. Centrifuge analyses are time consuming and require apparatus too bulky to be easily accommodated aboard the small vessels usually available for oceanography. In addition, the method has limited success in removing particles with specific gravities close to one, and when small amounts of recovered sediment are under study losses in the transfers required by the technique can become critical.

Filtration studies require very little equipment, and analyses of water samples of two liters, or less, are relatively quick and easy to make. In well-mixed, turbid areas where the suspended solids of small volumes of water are representative of those of much larger volumes of water, filtration of a large number of small water samples provides more information than can be obtained from the few large samples which can be centrifuged in a comparable time. It was for this reason that most of the samples for this study were collected by filtration. Two kinds of filters were used, metal membrane filters and cellulose membrane filters, the first to collect material for mass determinations, and the second to collect material for microscopic examination. The metal membrane filters were chosen in preference to cellulose membrane filters for mass determinations

because they require no pretreatment, and are not hygroscopic. Samples collected in this way are not amenable to microscopic examination. Smaller auxiliary samples were collected on cellulose filters. These filters can be made transparent by the application of liquid whose index of refraction approximates that of the filter.

The upper Chesapeake Bay is a good area for an intensive study of suspended sediment. The area is small, and has only one principal fluvial source--the Susquehanna. It is a fluvio-marine region of fine-grained sedimentation in which suspension is the primary mode of transportation, and in which the concentration of suspended matter is always relatively high.

The study of the suspended sediments of natural waters is important from a number of standpoints. Suspended sediments are an important proximate source of material for bottom sediments in regions of fine-grained sedimentation, and they are a key factor in explaining the textural and mineralogical compositions of the associated bottom sediments. There is also a need for more comparisons of bottom sediments with the sediments of overlying waters in order to establish and evaluate paleogeographic and paleoceanographic indicators.

Suspended sediments are extremely important geochemically both as a reservoir, and as a site for exchange and sorption reactions.

In addition they are important biologically because organisms and their degradation products are an important constituent and because suspended matter represents an important storehouse of food for suspension feeding organisms.

The Chesapeake Bay proper and its tributaries, Fig. 1, form one of the largest estuarine systems on Earth. For convenience of discussion the term "Bay" will mean "Bay proper" unless otherwise qualified. The term estuary has been defined in various ways. Pritchard's (1952) definition is used in this paper. Pritchard defines an estuary as a semienclosed coastal body of water having free connection with the open sea and measurable dilution of sea water by land drainage. The Bay is approximately 314 km long, varies in width from 5.5 to 56 km, covers an area<sup>2</sup> of about  $6.02 \times 10^3$  km<sup>2</sup>, and has a mean low water volume of approximately  $5.07 \times 10^{10}$  m<sup>3</sup>. Its long axis runs approximately North-South, and its mouth faces East. The Bay and its tributaries<sup>3</sup> cover an area of approximately  $11.53 \times 10^3$  km<sup>2</sup> and has a mean low water volume of  $7.46 \times 10^{10}$  m<sup>3</sup>. The Chesapeake Bay system is located

---

<sup>2</sup> This and other statistics in this section have been provided by Wm. Cronin.

<sup>3</sup> The upper limits of the estuarine system are defined as the mean limits of measurable salt water intrusion.

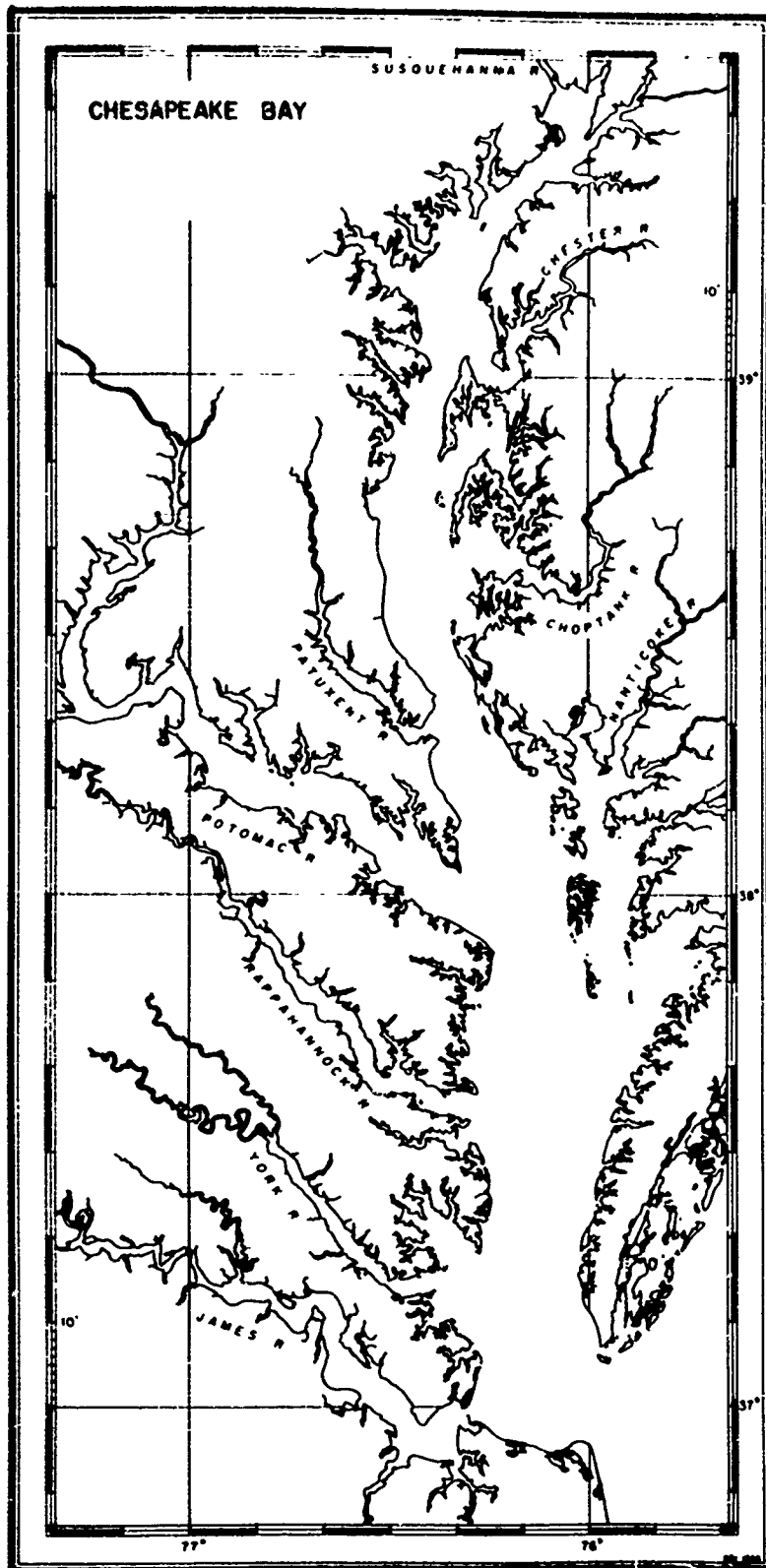


Fig. 1 The Chesapeake Bay Estuarine System

entirely within the Atlantic Coastal Plain and is surrounded by the low, rolling Maryland and Virginia countryside.

For the geologist or physical geographer, the Chesapeake Bay is a classic example of a submerged river valley, ria coast, or coastal plain estuary<sup>4</sup>. Shepard (1963) would term it a primary or youthful coast since its configuration is due largely to the sea coming to rest against a land form which has been shaped mainly by terrestrial agencies.

The Chesapeake Bay system, according to Stephenson, Cooke, and Mansfield (1933), originated during Pliocene time when the region was upwarped and the now drowned valleys of the Chesapeake Bay and its tributaries were eroded in the uplifted sediments. They believe that the Atlantic Coastal Plain was stable during the Pleistocene in the Chesapeake Bay region. The Chesapeake Bay system, however, was alternately flooded and exposed due to the large fluctuations of sea level caused by the alternate advance and retreat of the continental glaciers. At the end of the Pleistocene the region was drowned by the rise in sea level due to deglaciation. This drowning resulted in the dismemberment of the lower part of

---

<sup>4</sup> For the physical oceanographer whose interest is in the movement of the water and what drives it, it is a partially mixed or Type B estuary (Pritchard, 1955). The physical oceanographer's classification system is based upon the advection-diffusion equation for salt.

the former Susquehanna valley system. The rivers previously tributary to the Susquehanna became tributary to the broad Chesapeake Bay estuary. From an examination of Coast and Geodetic Survey charts and the available geologic data, it seems likely that the James River reached the sea separately prior to submergence, but that the York and all rivers to the North were tributaries of the Susquehanna.

The Chesapeake Bay system is shallow having a mean depth of less than 8.5 m for the Bay and less than 6.5 m for the Bay and its tributaries. The deepest portion of the Bay, with depths to nearly 50 m, occurs in a long narrow channel, Fig. 2, which according to Ryan (1953), is the part of the ancient Susquehanna River valley which has not been filled with post-Pleistocene sediments.

Local studies of Chesapeake Bay bottom sediments have been made by Young (1962), Biggs (1963), and Harrison, Lynch, and Altschaeffl (1964). The most extensive study was made by Ryan (1953) who analyzed 209 bottom samples taken from all parts of the Bay proper. A map of the bottom sediment distribution is presented in Plate 1 of his paper. Planimetry of Ryan's chart shows approximately 51 percent of the Bay floored with clayey silt, 12 percent with fine and very fine-grained sand, and approximately 37 percent with medium-grained sand. Sands occur only rarely away from near-shore areas. The region

around Tangier Sound-Smith Island is the notable exception. Near the mouth of the Bay sand is characteristic. The Bay channel, large areas west of it, and most of the tributary channels are floored with black and grey clayey silt.

For 92 mud samples Ryan found an average content of silt and clay together of 84 percent by weight. For 74 of the 92 samples he found that clay alone made up an average of 24 percent by weight. The major mineral constituent of the silt is quartz, and the major clay minerals are chlorite, illite, and kaolinite.

Our knowledge of the suspended sediments of the Chesapeake Bay is meager compared with our knowledge of the bottom sediments. Previous knowledge has been based largely on indirect measurements.

Burt (1952, 1953, 1955a,b) made over 25000 light extinction measurements with a Beckman Model DU Quartz Prism Spectrophotometer. He estimated the size distribution and the concentration of suspended matter from his measurements on the basis of the Mie Theory. He reported only eleven direct determinations of suspended load, however, and reported no direct determination of either the size distribution or the composition of the suspended matter (Burt, 1955a).

Bond and Meade (1966) analyzed eleven surface samples collected from the Chesapeake Bay during the period 6-9 June

1965. They determined the concentration of suspended matter by filtration and the percent of the total load lost by ignition. They also determined the size distribution of the recognizable mineral grains by microscopy.

In addition to the author's work, work on the suspended solids of the upper Bay by R.B. Biggs of the Chesapeake Biological Laboratory is in progress. Biggs and the author have cooperated in setting up their respective sampling programs to minimize duplication, and to improve coverage of the area both spatially and temporally.

The present study offers the first substantial information on the spatial and temporal variations in the suspended load, its sources, its size distribution, and its composition for any segment of the Chesapeake Bay.

## THE STUDY AREA

### HYPSONETRY

The region of the Bay investigated extends from Tolchester ( $39^{\circ}12'$ ) to Turkey Point ( $39^{\circ}27'$ ), Fig. 2.

The frequency distribution of the depths of this area was determined from Coast and Geodetic Survey Charts 549 and 572. The charts were contoured at 3 m intervals, and enclosed areas were determined by overlaying the charts with tracing paper, cutting out the appropriate areas and weighing. Two independent analyses were made. Taking the total area as 100 percent, the duplicate determinations of the partial areas agreed to within 0.5 percent in every case.

The largest source of uncertainty in such an analysis is in the placement of the contours. However, the density of the soundings given on the charts is high, and the contouring was carefully checked, so any changes in the frequency distribution of depth, by refinement of the contouring, would be minor.

The results are summarized in Fig. 3. The histogram and the cumulative curve show that the area is extremely shallow. More than 90 percent of the area is less than 8 m deep and the mean depth is only 4.7 m. It is also significant that nearly all areas with depths greater than 9 m are in the channel, much of which is maintained by dredging. Fig. 2 shows

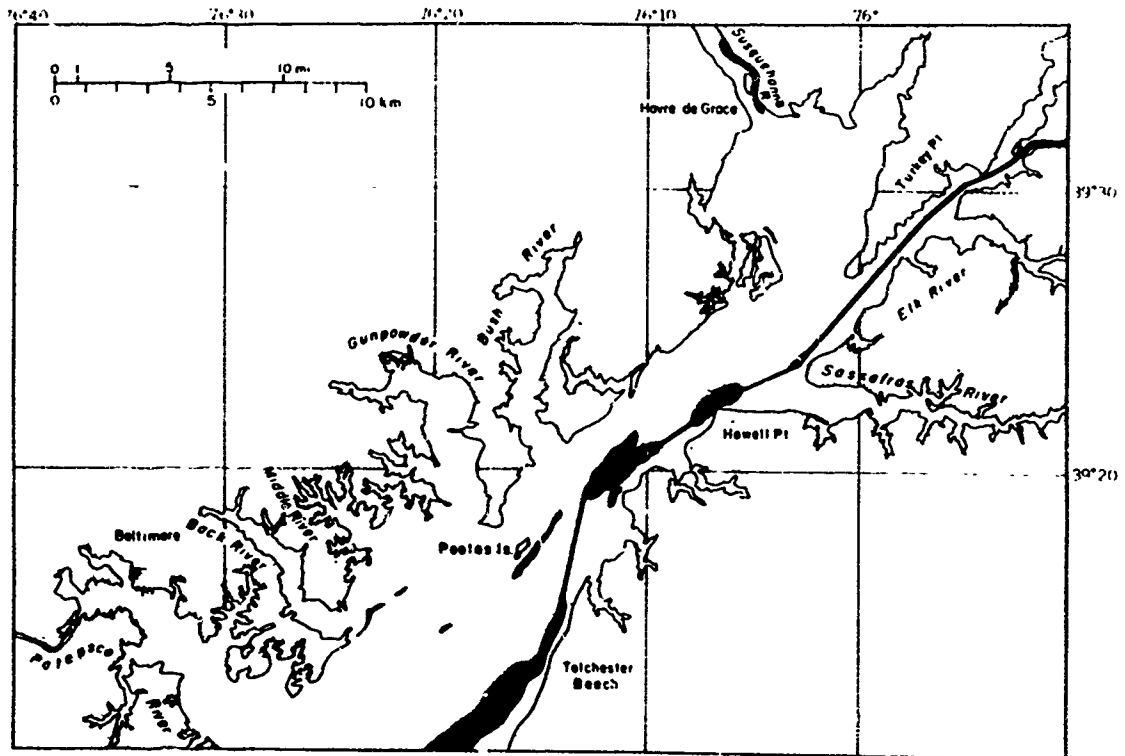


**Fig. 2** Map of Study Area Showing All Portions Deeper than 8 m in Black.

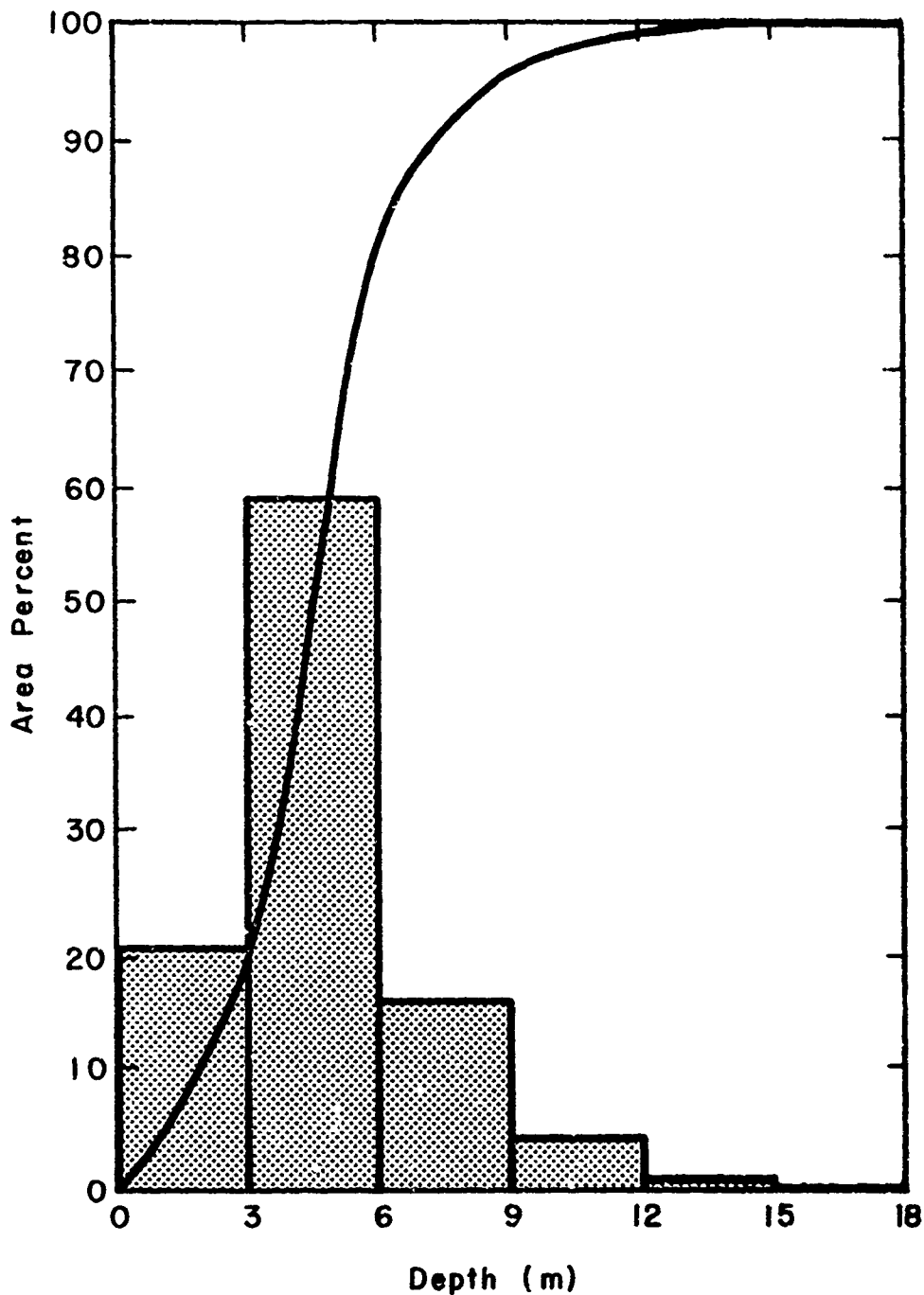


Fig. 3 Hypsometric curve of the Bay from Tolchester to Turkey Point showing the area shallower than any depth in cumulative percent. The frequency distribution of depths for 3m intervals is also shown.

all areas with depths greater than 8 m. The shallowness of the area is an important factor in the sedimentation.

#### HYDROGRAPHIC CONDITIONS

The seasonal average salinity and temperature distributions of the region are presented as vertical sections in Figs. 4 through 7. The seasons were defined as follows: spring, 15 March - 15 June; summer, 16 June - 30 September; autumn, 1 October - 15 December; winter, 16 December - 14 March. The seasonal averages were constructed by averaging the observed data over the defined seasons. Temperature and salinity observations were made weekly by the Chesapeake Bay Institute and the Chesapeake Biological Laboratory on an alternate basis during the period 15 March 1966 through 14 March 1967.

#### FRESH WATER INFLOW

The Susquehanna River provides more than 97 percent of the fresh water inflow into the Chesapeake Bay north of  $39^{\circ}12'N$ . The long term mean discharge at the Conowingo Hydroelectric Plant, which is located about nine miles above Havre de Grace, is approximately 34,800 cfs. For the period 1 April 1966 through 31 March 1967 however, the mean discharge was only 24,100 cfs. Since the fall of 1961 rainfall in the drainage

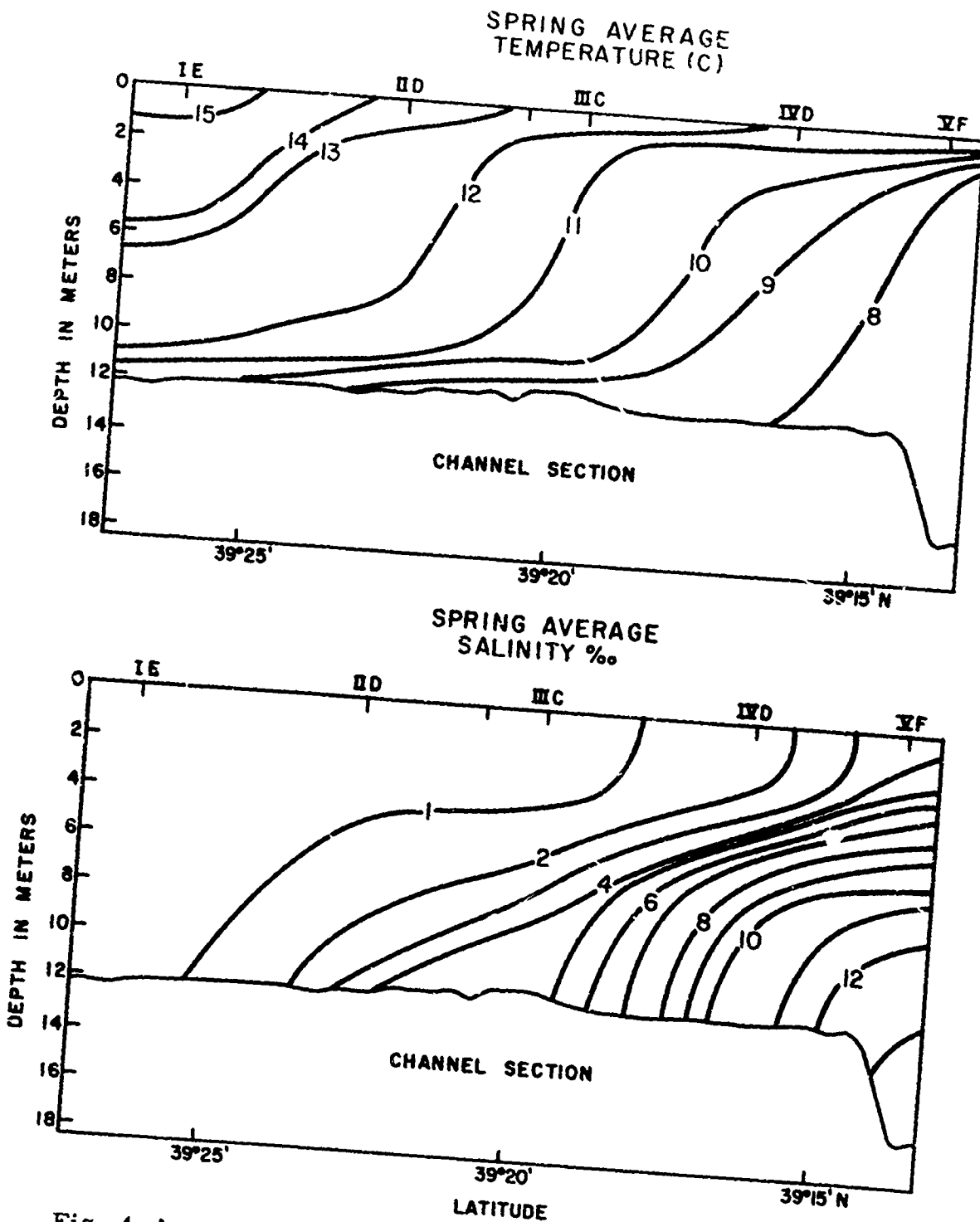


Fig. 4 Average temperature and salinity along the channel section in the upper Bay, Spring 1966 (15 March - 15 June).

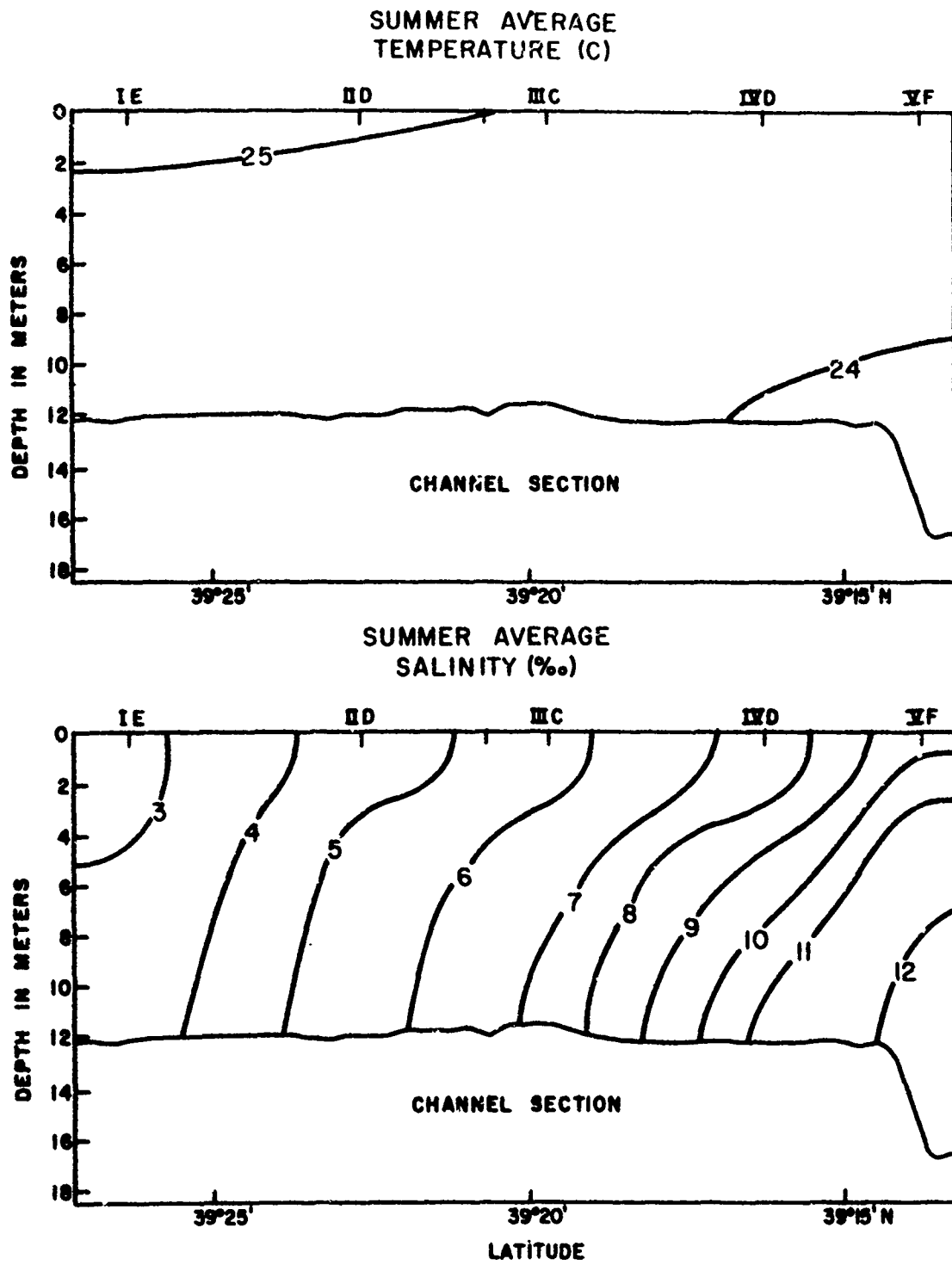
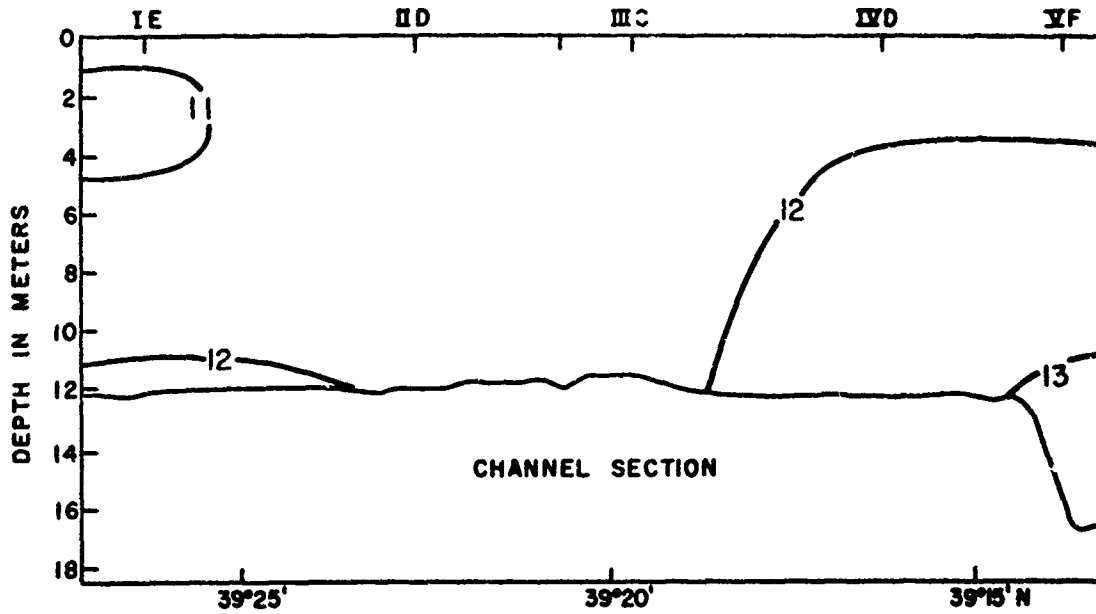


Fig. 5 Average temperature and salinity along the channel section in the upper Bay, Summer 1966 (16 June - 30 September).

AUTUMN AVERAGE  
TEMPERATURE (C)



AUTUMN AVERAGE  
SALINITY ‰

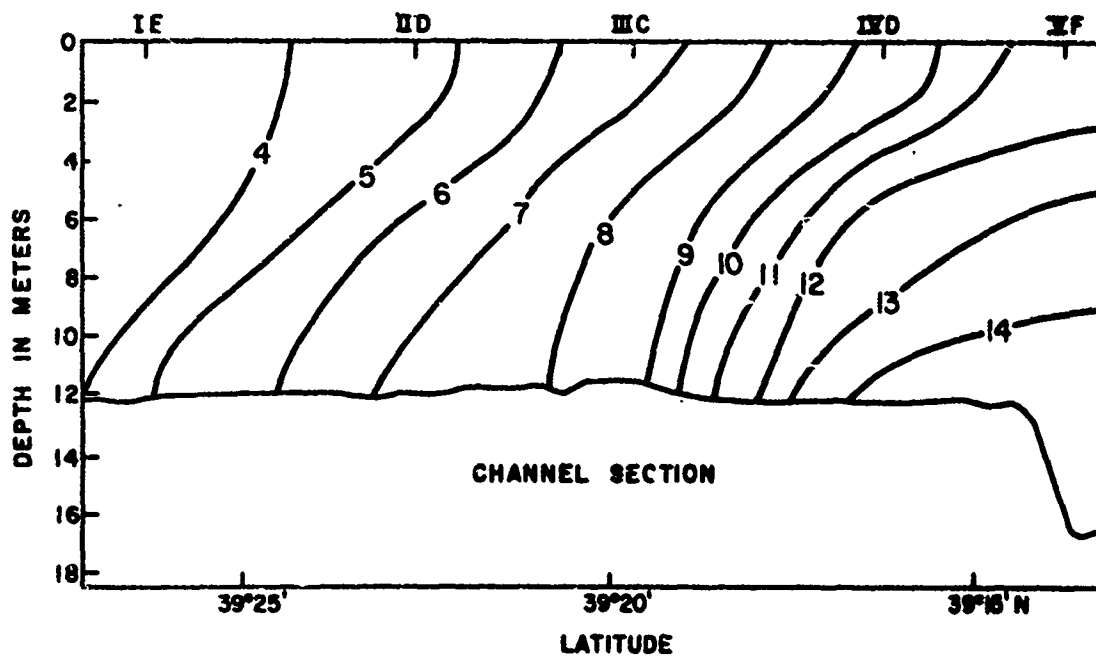


Fig. 6 Average temperature and salinity along the channel section in the upper Bay, Autumn 1966 (1 October - 15 December).

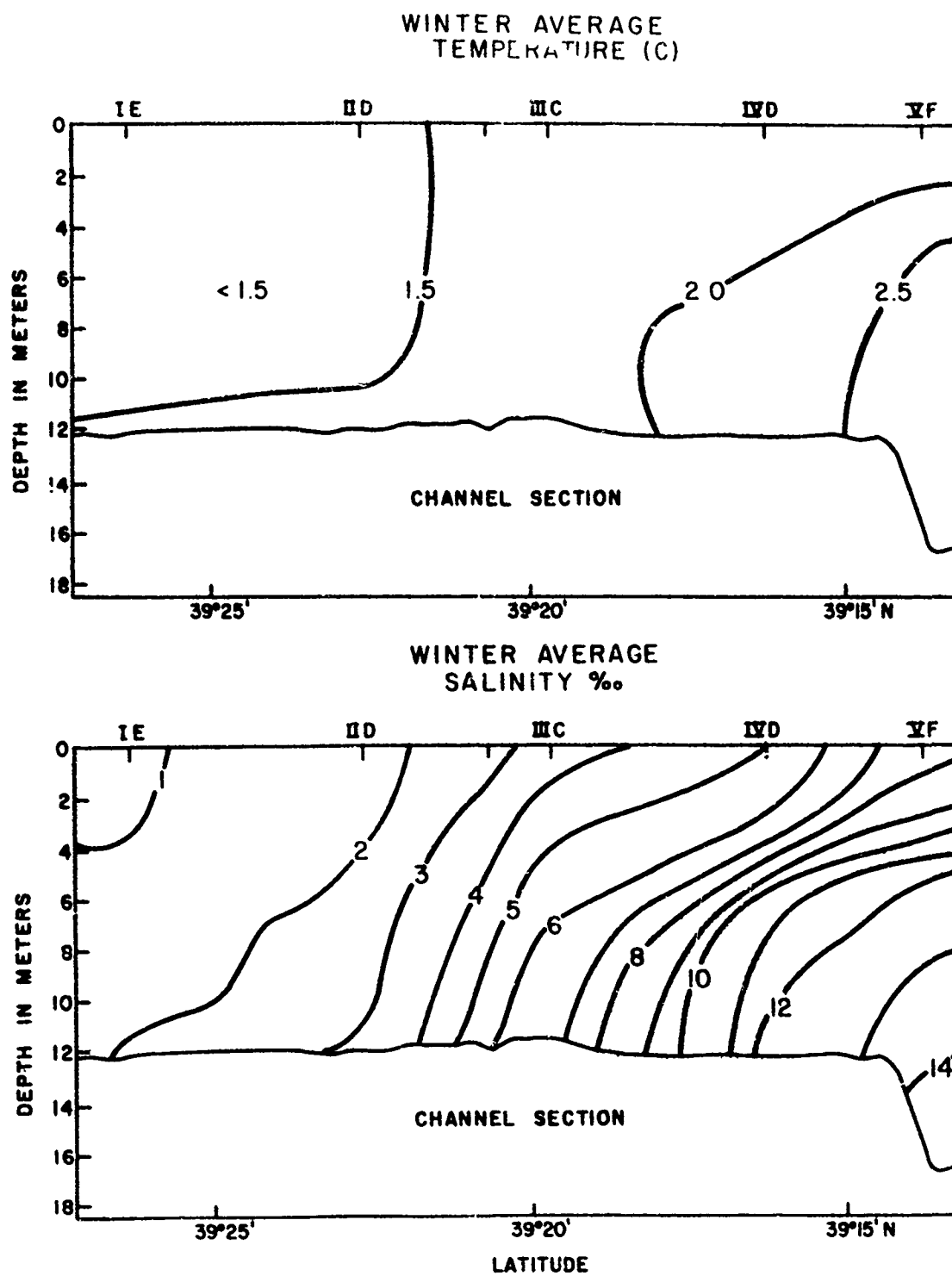


Fig. 7 Average temperature and salinity along the channel section in the upper Bay, Winter 1966 - 1967 (16 December - 14 March).

basin of the Susquehanna has been far below normal.

The rivers which flow into the Bay north of  $39^{\circ}12'N$ , and their estimated mean flows are presented in Table 1. The flow data, except that for the Susquehanna River, were provided by Carl Seitz (personal communication). The mean flow of the Susquehanna was determined by averaging daily discharge records for a 38 year period from the Conowingo Hydroelectric Plant. Only a portion of the drainage areas for tributary streams entering the Susquehanna River and the Bay below Conowingo is gauged. However, from these gauged areas the average runoff in cfs per square mile of drainage area was determined. The product of this average runoff factor times the total drainage area for each tributary provides the values of discharge for the tributary streams given in Table 1.

#### CONCENTRATION OF SUSPENDED SOLIDS

Substances are present in natural waters in true solution,

TABLE 1

Average Discharge of Rivers Flowing into the Northern Chesapeake Bay.

River	Mean Flow (cfs)
Susquehanna (at Conowingo)	34,800
Streams tributary to Susquehanna between Conowingo and Havre de Grace	406
Northeast	86
Elk	292
Bohemia	60
Sassafras	100
Back	58
Middle	10
Gunpowder	135
Bush	154

in colloidal suspension, and in true suspension. The boundaries between these three states are determined largely by particle size, but are transitional and cannot be precisely defined. Both colloidal suspensions and true suspensions are two phase systems consisting of a disperse phase (particles) and a dispersion medium. In each, a definite surface of separation exists between each particle and the dispersion medium. True solutions, on the other hand, are single phase systems in which true surfaces of separation are not found between the molecular particles of solute and solvent.

Colloidal behavior is commonly associated with particles in the  $5 \mu$  to  $0.2 \mu$  range--"...particles larger than molecules but not large enough to be seen in the (light) microscope (Glasstone, 1946, p. 557)." Some authors (e.g., Daniels, and Alberty, 1961) ascribe colloidal behavior to particles in the size range from  $1 \mu$  to  $1 \mu$ . Nearly all other investigators put colloidal particles somewhere within this latter range.

Lisitsin (1961) in his studies of oceanic suspended sediment set the boundary between colloidal and suspended particles at  $10 \mu$ . He states that his choice of boundary was dictated by the difficulty of obtaining and analyzing particles less than  $10 \mu$  in size. Although there is some freedom in the selection of this boundary, Lisitsin's choice is much too high.

In many environments the particles less than 10  $\mu$  in "diameter" account for more than 75 percent of the total volume and mass of suspended matter. Lisitsin's choice of boundary is not as serious as it might seem however, since many of his samples were collected with membrane filters of 0.7  $\mu$  APD.

This paper is concerned with the suspended particles of the upper Chesapeake Bay, and the author has set the boundary between suspended and colloidal particles at about 0.5  $\mu$ .

The particles in suspension are of both organic and inorganic origin. The organic component consists of organisms and their degradation products. The inorganic component consists of inorganically precipitated solids and particles produced by rock erosion.

The concentrations of the total suspended solids<sup>5</sup> can be determined directly by weighing the material which has been recovered by either filtration or centrifugation. They can be estimated indirectly by measuring the light scattered by the suspended particles. In this study, filtration was the basic method for the direct determination of the concentrations of the suspended solids. In addition, the suspended solids were removed from some large water samples by combinations of settling and filtering, and by settling and centrifuging with a continuous flow centrifuge. Optical measurements were made with

---

<sup>5</sup> Also referred to as suspended sediment, suspended matter, and seston.

a Clarke submarine photometer, a Beckman DU spectrophotometer, and a Secchi disc in an attempt to relate the optical properties to the concentration of suspended matter. These will be reported on elsewhere.

Filtration requires little equipment and the analyses of samples of 2 liters or less can be made easily and quickly, thus allowing the investigator to process a large number of samples in a relatively short time. In well mixed, turbid areas such as the upper Chesapeake Bay, the suspended solids of small (0.5-1ℓ) volumes of water are representative of those of much larger ( $\geq 50\ell$ ) volumes of water. In such areas, filtration of a large number of small water samples provides more information than can be obtained from the few large water samples which can be centrifuged in a comparable time. In addition, centrifugation has limited success in removing particles, such as phytoplankton and some organic aggregates, with specific gravities close to that of the surrounding water. A further drawback of the centrifuge method is that any losses of the small amounts of sediment during the transfers required by the technique can become critical. In regions where suspended matter is very inhomogeneously distributed, either very large water samples or integrated water samples must be analyzed to ascertain average conditions. In such situations, continuous flow centrifuges provide the best means of determining the

concentrations of the suspended solids.

To determine whether the concentrations of suspended matter in small volumes were representative of those of much larger volumes of water, the concentrations of suspended matter of 15 large (18-50ℓ) water samples were compared with those of a paired set of smaller (0.5 - 1ℓ) water samples. The large samples were pumped into carboys from various depths at several stations. At each of these sample depths, five small water samples were filtered through 47 mm, 0.45  $\mu$  APD metal membrane filters. The filters were washed with distilled water to remove any sea salt, and were stored in individual dessicators until they were weighed approximately 72 hours later. The carboys were returned to the laboratory and left undisturbed for 21 days, at which time the overlying water was carefully decanted. The settled solids were carefully transferred to a weighed beaker and placed in a dessicator for approximately 96 hours. The decanted water was filtered through 0.45  $\mu$  metal membrane filters which were then dessicated and weighed. This set of weights was added to the appropriate weights of settled solids, and the concentrations in mg/ℓ were calculated. The results are summarized in Table 2. In later tests the non-settled solids were extracted from the decanted water with a continuous flow centrifuge.

A glance at the table shows that the agreement and

TABLE 2

Comparison of Large (18-50 liter) and Small (0.5-1 liter) Samples

Station and Date	Sample Depth (m)	Small Sample Volume (ℓ)	Total Suspended Solids (mg/ℓ)	Large Sample Volume (ℓ)	Total Suspended Solids (mg/ℓ)
VF 21 Mar. 1966	Surface	0.5	13.28	50.4	13.87
		0.5	13.75	18.6	13.02
		0.5	12.98		
		0.5	13.82		
		0.5	14.01		
VE 21 Mar. 1966	Surface	0.5	17.16	18.5	17.20
		0.5	17.91	18.8	17.98
		0.5	17.20		
		0.5	17.87		
		0.5	16.91		
VC 21 Mar. 1966	2	0.5	47.88	49.4	47.32
		1.0	45.74	18.1	45.88
		0.5	46.78		
		0.5	47.23		

Table 2 Continued

Station and Date	Sample Depth (m)	Small Sample Volume (ℓ)	Total Suspended Solids (mg/ℓ)	Large Sample Volume (ℓ)	Total Suspended Solids (mg/ℓ)
IV E 21 Mar. 1966	Surface	0.5	24.34	19.2	24.78
		0.5	24.79		
		0.5	23.28		
		0.5	25.00		
IV D 21 Mar. 1966	6	0.5	37.18	18.2	36.83
		0.5	35.95		
		0.5	36.78		
		0.5	35.26		
		0.5	34.84		
II D 21 Mar. 1966	Surface	1.0	15.80	47.2	15.74
		0.5	15.88		
		1.0	15.75		
		0.5	15.92		
		0.5	14.76		

Table 2 Continued

Station and Date	Sample Depth (m)	Small Sample Volume (ℓ)	Total Suspended Solids (mg/ℓ)	Large Sample Volume (ℓ)	Total Suspended Solids (mg/ℓ)
SAS 22 Mar. 1966	Surface	0.5	18.53	18.2	18.98
		0.5	17.16	49.2	17.35
		0.5	18.21		
		0.5	17.99		
		0.5	18.34		
IA 22 Mar. 1966	Surface	0.5	23.76	18.0	23.90
		0.5	24.71		
		0.5	24.26		
		0.5	22.97		
		0.5	23.84		
IE 22 Mar. 1966	6	0.5	26.16	18.0	27.20
		0.5	26.92	18.4	25.33
		0.5	26.74		
		0.5	27.01		

stability of the suspended sediment concentrations determined from both large and small samples is very good. The maximum difference among the small samples of a single set never exceeded 9 percent, the maximum difference between a pair of large samples never exceeded 10 percent, and the maximum difference between any of the small samples and one of its paired large samples never exceeded 8 percent. Heeding John Gay's admonition, "Lest men suspect your tale untrue, keep probability in view," the author applied the F-test to each set of suspended sediment samples. In no case did the samples differ at the 1 percent level.

In selecting a filter pore size for mass determinations it was desirable, because of the higher filtration rate, to select the largest pore size which still retained "all of the suspended mass." It is well known that membranes retain a significant amount of material with sizes less than the APD of the membrane so it was suspected that a pore size larger than  $0.5 \mu$  could be used. In accordance with this,  $0.8 \mu$  APD membranes were tested. Fifteen one liter water samples were collected, and each sample was filtered through an  $0.8 \mu$  filter. The filtrate from each of the samples was then passed through an  $0.2 \mu$  metal membrane filter. All of the membranes were dessicated in individual dessicators for 72 hours and weighed. The data are given in Table 3. It is obvious from

TABLE 3

Suspended Sediment Retention Characteristic of 0.8  $\mu$  APD

Metal Membranes.

Sample No.	Mass of Sediment Retained by 0.8 $\mu$ Membrane. (mg)	Mass of Sediment passed by 0.8 $\mu$ Membrane, but retained by 0.2 $\mu$ Membrane. (mg)
1	10.51	- 0.01
2	8.36	- 0.01
3	11.65	+ 0.02
4	9.20	+ 0.03
5	6.47	+ 0.02
6	5.88	+ 0.02
7	3.62	- 0.02
8	6.99	+ 0.04
9	12.67	+ 0.02
10	7.73	- 0.02
11	6.68	+ 0.01
12	8.53	+ 0.02
13	7.21	- 0.01
14	9.62	+ 0.05
15	6.84	- 0.02

the data in Table 3 that the 0.8  $\mu$  membranes remove virtually all of the mass of suspended solids. In only three cases did the mass of filter passing material exceed the precision ( $\pm 0.02$  mg) of the balance.

Later tests on 1.2  $\mu$  membranes indicated that these could also be safely used to determine the concentrations of suspended matter, but it was decided to continue using the 0.8  $\mu$  membranes. Foolish consistency may be the hobgoblin of little minds, but the author had nearly a thousand 0.8  $\mu$  reasons to be consistent.

Metal membrane filters<sup>6</sup> were chosen over the more commonly used cellulose membrane filters. The metal membranes currently available are made of pure silver, and come in most of the same pore sizes as do cellulose filters. They are superior to cellulose filters for mass determination in several respects (Schubel, 1967). They do not contain any soluble material as do cellulose filters and hence require no pre-soaking. Unlike cellulose membranes, they are not hygroscopic, so they can be weighed without preliminary dessication. They are much less susceptible to electrostatic charges than cellulose membranes, but they should still be weighed under an

---

<sup>6</sup> Available from Selas Flotronics, Box 300, Spring House, Pa. 19477.

alpha-emitting source<sup>7</sup>. The metal membranes have no tendency to curl as do presoaked and dessicated cellulose membranes, and are consequently much easier to handle--an important consideration if field work aboard a rolling and pitching vessel is to remain tolerable. The metal membrane filters have the disadvantage of costing nearly three times as much as cellulose filters. They can however, be backwashed and reused if they have not been heated above 370 C.

Before each cruise the required number of metal membrane filters were weighed on a Mettler H16 balance, and placed in individual dessicators similar to those described by Winneberger et. al., 1963. Each dessicator carried the filter identification number, and the initial filter weight. The use of individual dessicators greatly facilitates identification of samples and helps reduce mistakes in logging results. It also speeds up the final weighing process since there is no waiting time between weighings. Because suspended matter is generally hygroscopic, it must be dessicated before its mass is determined. If a number of filters and their sediment loads are placed

---

<sup>7</sup> The Staticmaster Ionizing Unit, Model No. 2U500 mounted on a Flexible Arm Staticmaster Positioner BFL available from Nuclear Products Co., 10173 E. Rush St., El Monte, California has been found to be most useful.

together in a large dessicator, approximately 15-30 minutes are required between weighings--the time necessary for the re-equilibration of the water content of the dessicant with the filters and their suspended matter.

The individual dessicators are made from 4-ounce, squat-form jars. The jars are filled with about three-quarters of an inch of dessicant (active silica gel in this case) into which is stuck a short, about 30 mm, length of glass tubing or plastic pipe of about 40 mm O.D. The weighed filter rests on top of the tubing.

The following sampling procedure was used by the author. Water samples were pumped into one gallon jugs on deck by lowering a submersible pump to the desired sampling depths. Within 5 minutes after collection, each jug was swirled vigorously, two 500 to 1000 ml samples were measured out with a graduated cylinder, and filtered through 0.8  $\mu$  metal membrane filters. The filters were washed several times with distilled water to remove any sea salt, and were then placed in their individual dessicators. A small strip of aluminum foil was placed under the edge of each membrane on the filter support to facilitate removal of the membranes after filtration (Banse, Falls, and Hobson, 1963).

The filters and their suspended solids were dessicated at ambient temperature for at least 72 hours before weighing.

At the beginning of the study a network of 17 stations was established, Fig. 8. Except for the deletion of station IA after the ninth cruise, the original station pattern was maintained for the entire study. Sampling was done monthly for the first four months, and approximately every two weeks for the next eight months. The sampling interval was shortened to five days during the period of high runoff in March of 1967.

At stations deeper than 4 m samples were collected from at least three depths--surface, mid-depth, and 1 m off the bottom. At stations deeper than 8 m additional samples were collected from intermediate depths. At the three stations shallower than 4 m (IIB, IIIE, SAS), samples were collected only from the surface and 1 m off the bottom. Generally two 500 to 1000 ml water samples were filtered from each sample depth.

It was not always possible to occupy all of the stations on each cruise because of bad weather or other complications, but the program was followed as closely as possible. The dates of the cruises and other pertinent sampling data are summarized in Table 4.

The concentrations of the total suspended solids are summarized in Figs. 9 through 45. The data from each cruise are presented as vertical sections in Figs. 9 through 30. In figures 31 through 37 the surface and mid-depth concentrations

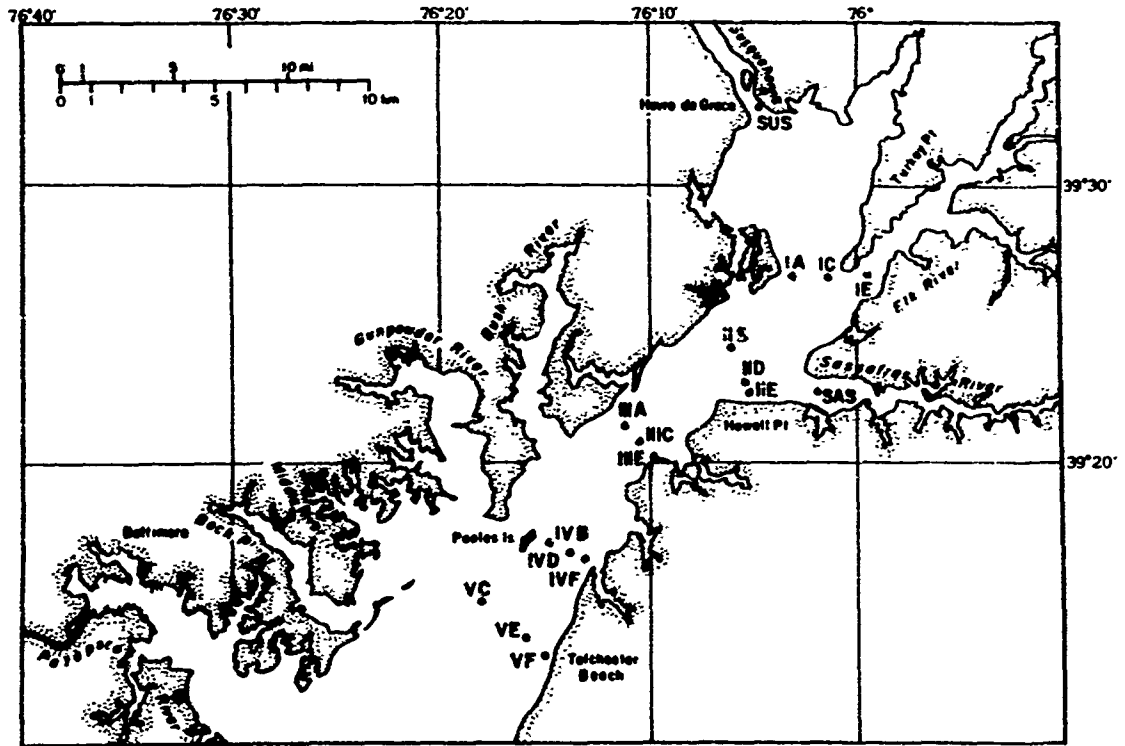


Fig. 8 Station Location Map

TABLE 4

Cruise No.	Cruise Dates	No. of Stations Occupied	No. of Depths Sampled	No. of Mass Determinations	No. of Determinations of Combustible Organic Matter
<u>1966</u>					
1	21-22 Mar.	17	48	73	47
2	5-6 May	11	32	58	29
3	31 May-1 June	15	42	91	41
4	27-28 June	17	47	92	47
5	11-12 July	17	48	94	45
6	25-26 July	17	46	88	46
7	8-9 Aug.	17	48	88	48
8	22-23 Aug.	17	42	89	56
9	6-7 Sept.	17	57	73	70
10	19-20 Sept.	16	52	97	59
11	3-4 Oct.	16	52	85	49
12	17-18 Oct.	16	53	81	58
13	1 Nov.	16	53	74	58
14	14 Nov.	16	54	76	60
15	30 Nov.-1 Dec.	16	56	79	59
16	13-14 Dec.	14	56	65	60
17	28-29 Dec.	15	49	68	55

Table 4 Continued

Cruise No.	Cruise Dates	No. of Stations Occupied	No. of Depths Sampled	No. of Mass Determinations	No. of Determinations of Combustible Organic Matter
<u>1967</u>					
18	12-13 Jan.	12	58	77	60
19	25 Jan.	1 <sup>(24)*</sup>	5 x (24)	172	49
20	14-15 Feb.	1 <sup>(16)**</sup> +4	5 x (16)+28	154	78
21	9-10 Mar.	18	75	127	51
22	15 Mar.	6	41	66	21
23	20 Mar.	8	60	103	36
<b>TOTALS</b>		358	1297	2070	1182

\* Anchor station, observed 24 times

\*\* Anchor station, observed 16 times

of the total suspended solids at the channel stations (SUS, IE, IID, IIIC, and VF) are plotted against distance to show the relationship between the suspended sediment concentrations in the Susquehanna River and those in the adjacent Bay. Samples collected from below mid-depth have not been included in Figs. 31 through 37 because they are too strongly influenced by tidal scour<sup>8</sup>. Seasonal averages of the total suspended solids are presented in vertical channel sections in Figs. 38 and 39.

Several significant features of the suspended sediment distribution emerge from these figures. These features will be enumerated here, but discussion will be deferred until the section on sedimentation processes.

(1) The concentrations of suspended solids in the Bay proper were greater than 5 mg/l throughout the year with the maxima, greater than 110 mg/l, occurring during the time of spring thaw and high river flow.

(2) The concentrations of suspended solids in the Bay proper were higher than those in the Susquehanna River at all times except during the spring period of high river flow.

(3) At any location the concentration of suspended solids generally increased with depth with the maximum occurring near

---

<sup>8</sup> At stations in depths of about 10 m, fluctuations in the suspended sediment concentrations which were clearly related to tidal currents were observed below 6 m.

the bottom. The only time when marked departures from this pattern occurred was during a brief period of peak spring runoff when at several stations very high concentrations were observed near the surface and near the bottom, with lower values at intermediate depths. This feature is going to be investigated further in the spring of 1968.

(4) The concentrations of suspended solids at any depth were more frequently higher on the western side of the Bay than on the eastern side.

(5) At depths below about 2 m the concentration of suspended solids generally dropped quite sharply between stations IVD and VF.

(6) The seasonal averages, Figs. 38 and 39, show that during the summer and fall the sediment distribution patterns were very similar, and that during this time the concentrations of suspended sediment were considerably lower than during the winter and spring.

The surface and mid-depth concentrations of suspended sediment at each station are plotted against the date when each sample was collected in Figs. 40 through 45. We are interested in seasonal patterns of suspended sediment concentration. Of the data available, only the samples from the upper part of the water column can be expected to reflect seasonal patterns clearly. Samples taken near the bottom are too strongly

influenced by tidal currents and the phase of the tide at which they were collected.

During periods of moderate river flow the sampling interval was usually two weeks, and the concentrations generally showed relatively small variations over this interval. During high river discharge when suspended sediment concentrations changed rapidly, the sampling interval was shortened. The data from Figures 40 through 45 are summarized in Table 5.

From Figs. 40 through 45 we conclude the following:

(1) The surface and mid-depth concentrations of suspended sediment at the Susquehanna River station were nearly equal throughout the year, and were quite low except during late February and March when river flow was very high. From mid-May 1966 through January 1967 concentrations averaged 5 mg/l, while values greater than 140 mg/l were recorded in March during peak river flow.

(2) At most of the stations within the Bay the maximum surface and mid-depth concentrations of suspended sediment occurred during the spring and were clearly determined by the Susquehanna River--the primary source of fluvial sediment in the region.

At four of the shallow, less than 6 m, stations (IIIE, IVE, VC, and VE), and at two stations located in about 6 m of water (IIA and IVB) the maximum concentrations were recorded

during periods of high winds and rough seas. Observations were not made at any of these stations on the day when peak suspended sediment concentrations associated with high spring runoff were recorded at the channel station of the corresponding section. However, from observed lateral gradients in suspended sediment concentration it seems probable that peak spring values would not have exceeded previously recorded maxima except at stations IVB and IVE, and perhaps at IIIE.

(3) In eighteen of the twenty-eight sets of data presented in Figs. 40 through 45, the fractional mean deviation of the suspended sediment concentration was less than 27 percent, and in only one case (IIIA-surface) did it exceed 50 percent. In general, the fluctuations in the suspended sediment concentration were less at the deeper stations than at the shallower stations, and the fluctuations on the eastern side of the Bay were less than those on the western side at the same cross-section.

#### Combustible Organic Matter

The total particulate organic matter was estimated in over half of the samples by determining the loss of weight of the total solids on ignition. The samples were combusted on the silver filters in Vycor crucibles at 475 C for thirty

minutes. Seasonal averages of the percent of the total suspended solids accounted for by combustible organic matter are presented as vertical channel sections in Figs. 46 and 47. The seasons are defined as before: spring, 15 March-15 June; summer, 16 June-30 September; autumn, 1 October-15 December; winter, 16 December-14 March.

During the summer and autumn when the concentrations of total suspended solids were relatively low, the combustible organic matter accounted for a greater percent of the total solids than it did during the winter and spring when the concentrations of total suspended solids were higher. At stations within the Bay the concentrations of combustible organic matter were highest during the spring and summer averaging nearly 5 mg/l, and lowest in the winter when they averaged only about 3 mg/l. The autumn mean concentration of combustible organic matter was less than 4 mg/l.

TABLE 5

Statistics Based on Data Presented in Figs. 40 Through 45.

Station and Depth	15 May 1966 - 1 February 1967				21 March 1966- 20 March 1967	
	Concentration of Suspended Solids			Fractional Mean Deviation	Maximum Concentration	
	Mean (mg/l)	Range (mg/l)	Mean Deviation (mg/l)	Mean Deviation (%)	Value (mg/l)	Date of Obs.
SUS (13.5m)						
surface	4.3	2.4-11.7	1.8	42	141.0	9 III 67
mid-depth	5.2	2.4-13.7	1.8	35	136.2	9 III 67
IC (6.5m)						
surface	11.5	6.9-20.0	3.0	20	113.4	10 III 67
mid-depth	12.9	7.7-19.0	3.4	26	117.4	10 III 67
IE (12.5m)						
surface	12.8	8.0-17.8	2.6	20	53.6	10 III 67
mid-depth	18.0	9.5-22.6	3.7	21	43.6	10 III 67
IIB (3.0m)						
surface	13.9	7.6-22.2	3.6	26	51.6	9 III 67
IID (12.0m)						
surface	12.0	6.7-37.5	4.0	33	58.7	9 III 67
mid-depth	14.3	8.2-32.5	4.1	29	52.4	15 II 67
IIE (6.5m)						
surface	10.3	6.7-23.4	2.6	25	34.4	9 III 67
mid-depth	11.9	8.1-22.3	2.8	24	40.0	9 III 67
IIIA (8.0m)						
surface	18.3	8.3-84.8	10.5	57	84.8	14 XII 66
mid-depth	27.0	9.3-65.0	10.4	39	65.0	14 XII 66
IIIC (12.0m)						
surface	11.0	6.6-20.4	2.5	23	66.5	15 III 67
mid-depth	15.0	9.0-28.7	3.8	25	68.6	15 III 67
IIIE (3.5m)						
surface	13.6	6.9-32.2	4.6	34	53.5	21 III 66

TABLE 5 Continued

Station and Depth	15 May 1966 - 1 February 1967				21 March 1966- 20 March 1967	
	Concentration of Suspended Solids				Maximum Concentration	
	Mean (mg/l)	Range (mg/l)	Mean Deviation (mg/l)	Fractional Mean Deviation (%)	Value (mg/l)	Date of Obs.
IVB (8.0m)						
surface	13.6	7.1-31.0	4.0	29	39.7	21 III 66
mid-depth	18.6	11.0-30.8	4.7	25	55.4	21 III 66
IVD (12.0m)						
surface	9.9	6.0-15.6	1.8	18	70.2	15 III 67
mid-depth	16.8	10.9-28.4	4.2	25	38.0	15 III 67
IVE (5.5m)						
surface	10.0	6.3-16.0	1.7	17	24.3	21 III 66
mid-depth	11.0	7.0-18.1	2.2	20	28.3	21 III 66
VC (5.0m)						
surface	14.0	7.2-20.8	3.9	28	37.2	21 III 66
mid-depth	17.3	6.4-28.4	6.2	36	47.4	21 III 66
VE (5.5m)						
surface	9.7	6.0-18.7	1.9	20	18.7	30 XI 66
mid-depth	11.0	6.3-19.7	2.8	25	19.7	30 XI 66
VF (15.0m)						
surface	7.9	5.2-11.0	1.4	18	30.1	15 III 67
mid-depth	11.0	7.6-18.0	2.1	19	20.3	20 III 67

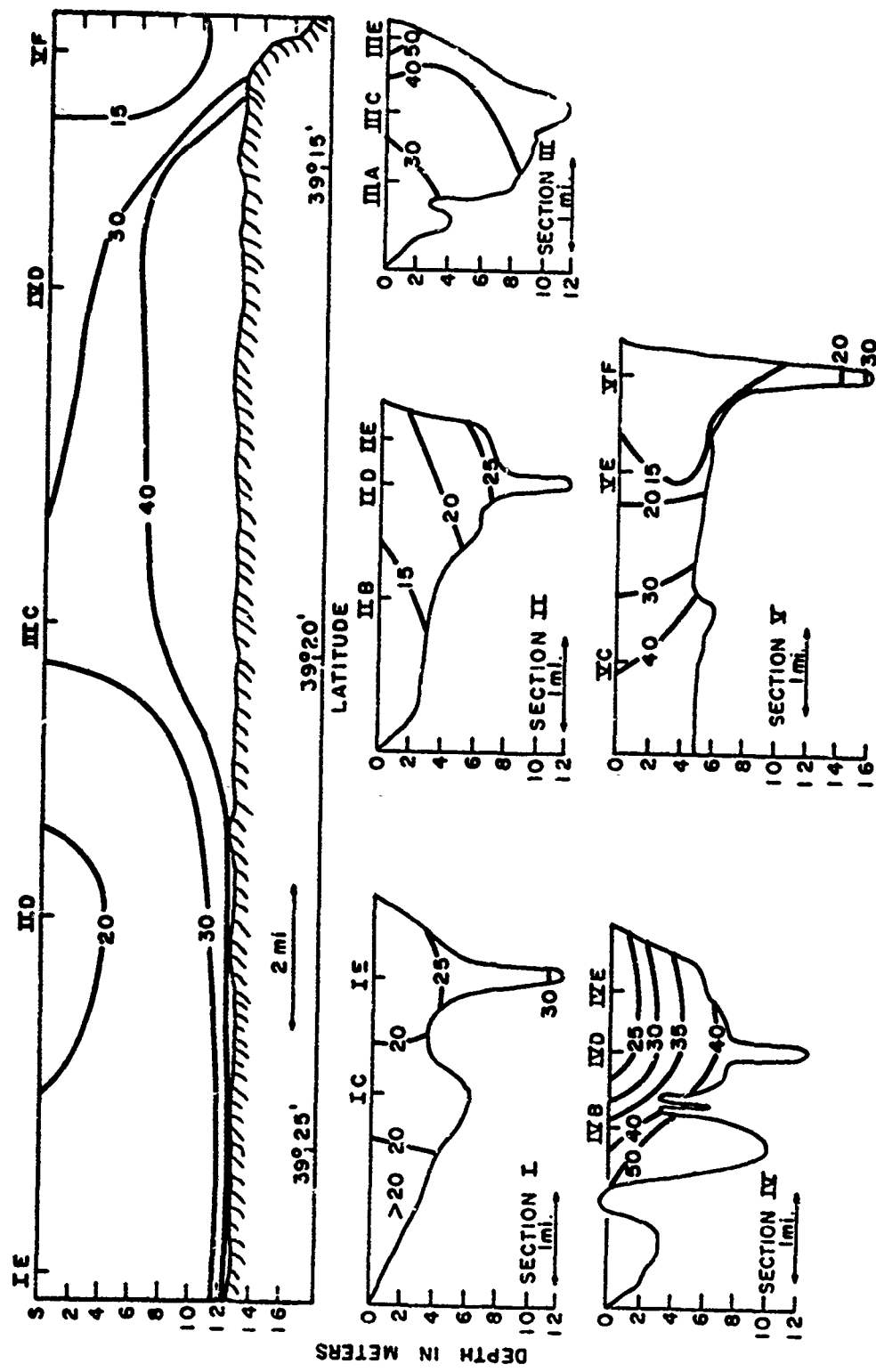


Fig. 9 Distribution of total suspended solids (mg/l) on 21-22 March 1966 (Cruise 1).

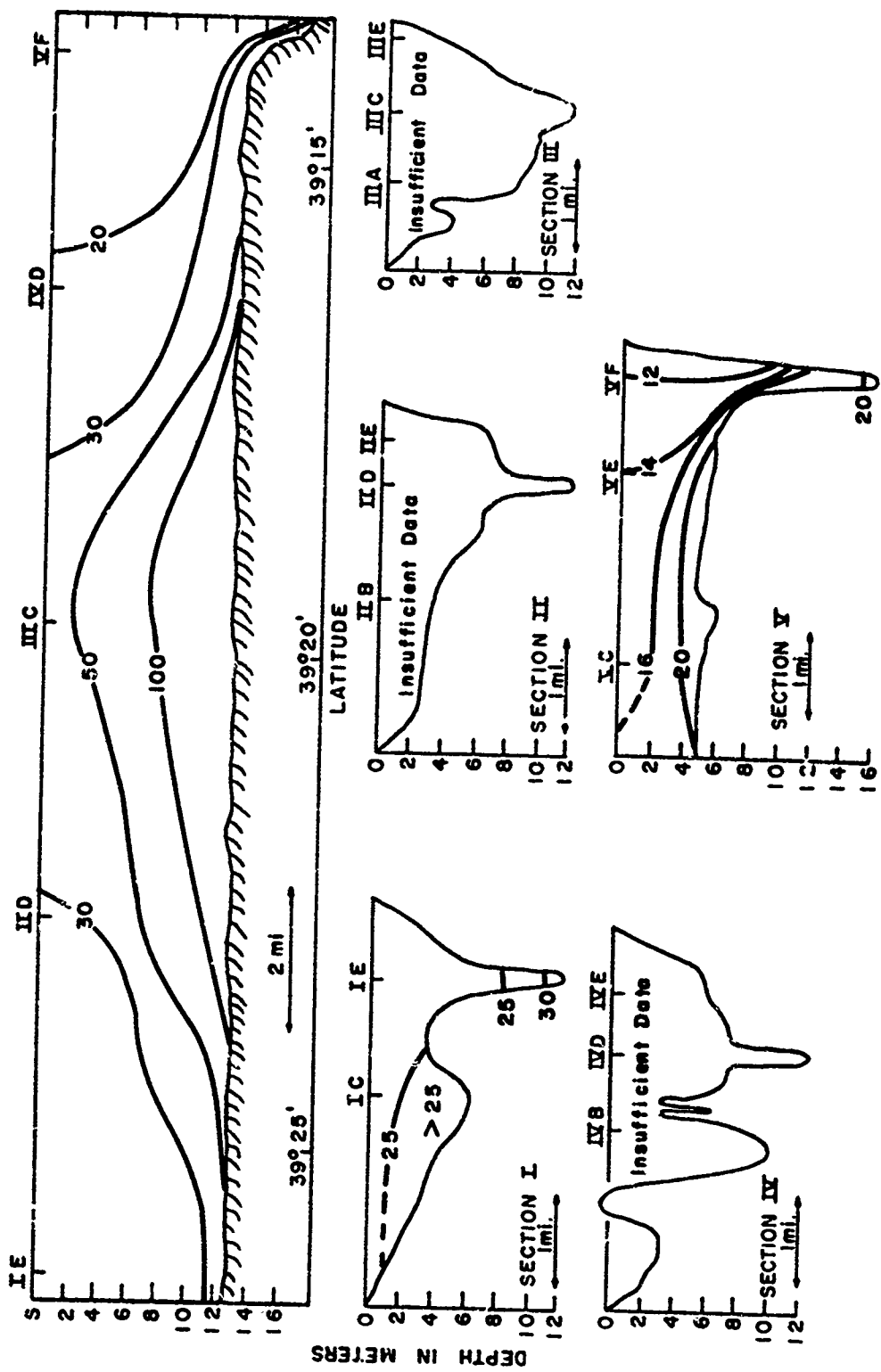


Fig. 10 Distribution of total suspended solids (mg/l) on 5-6 May 1966 (Cruise 2).

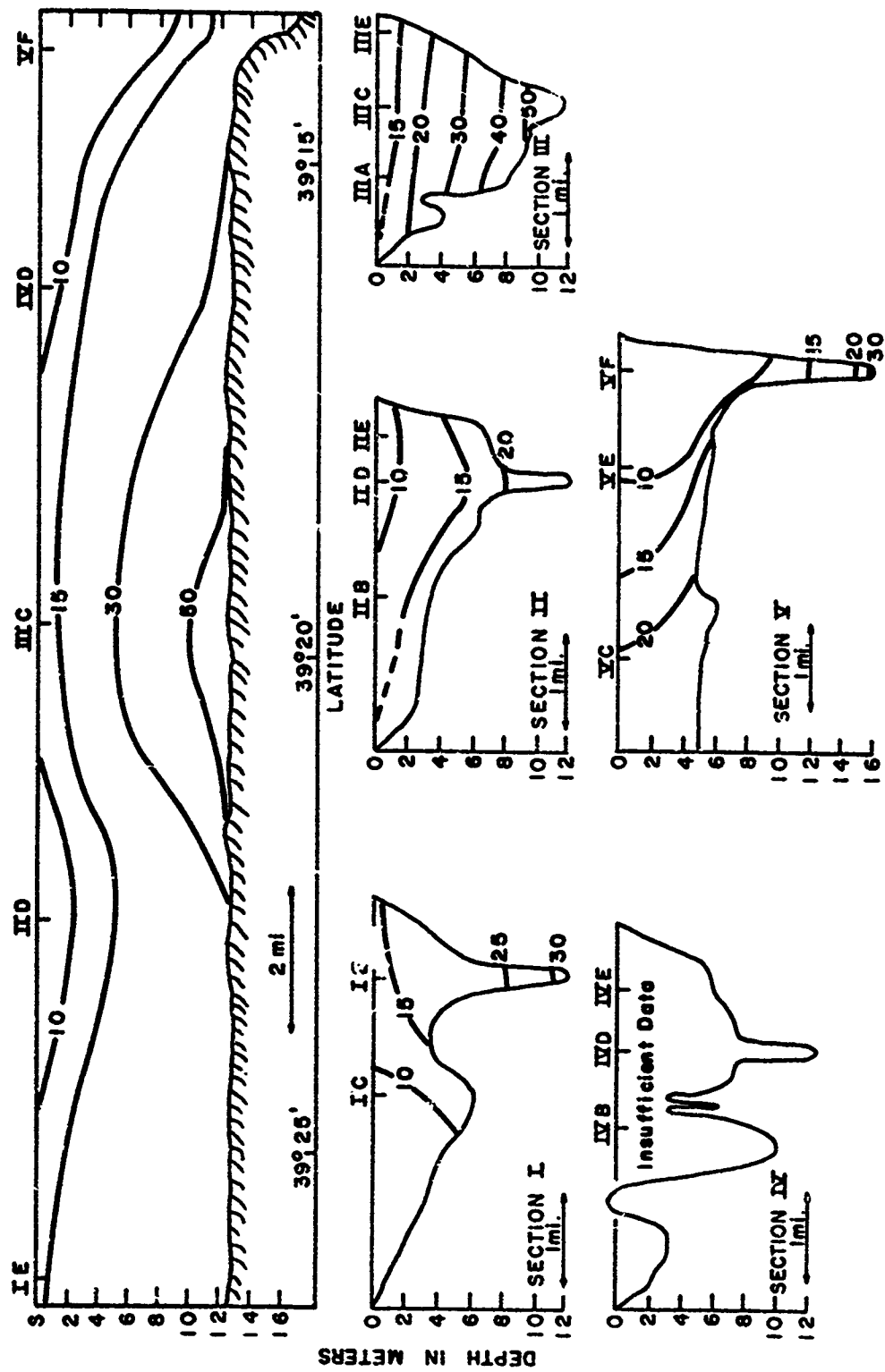


Fig. 11 Distribution of total suspended solids (mg/l) on 31 May - 1 June 1966 (Cruise 3).

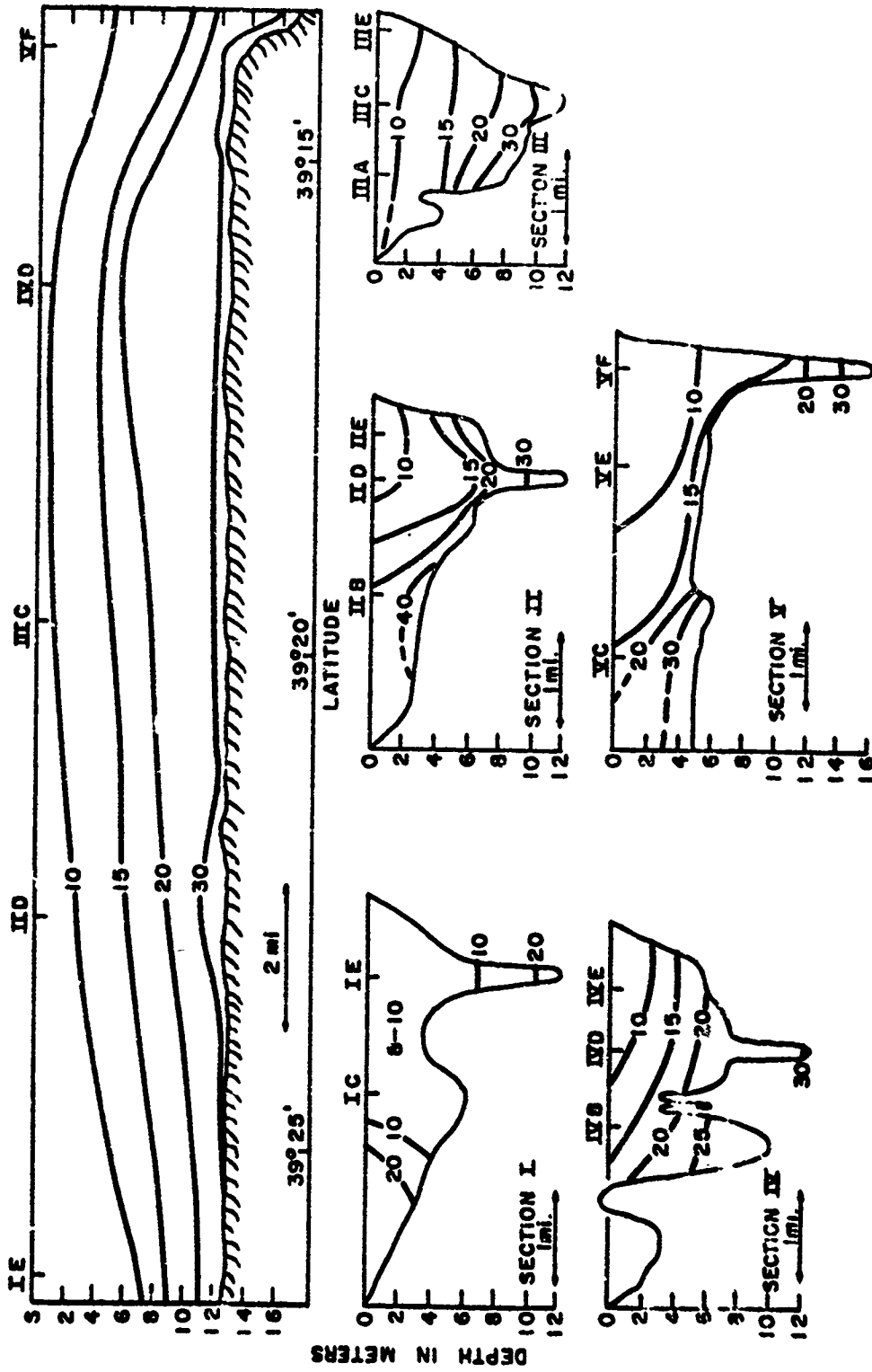


Fig. 12 Distribution of total suspended solids (mg/l) on 27-28 June 1966 (Cruise 4).

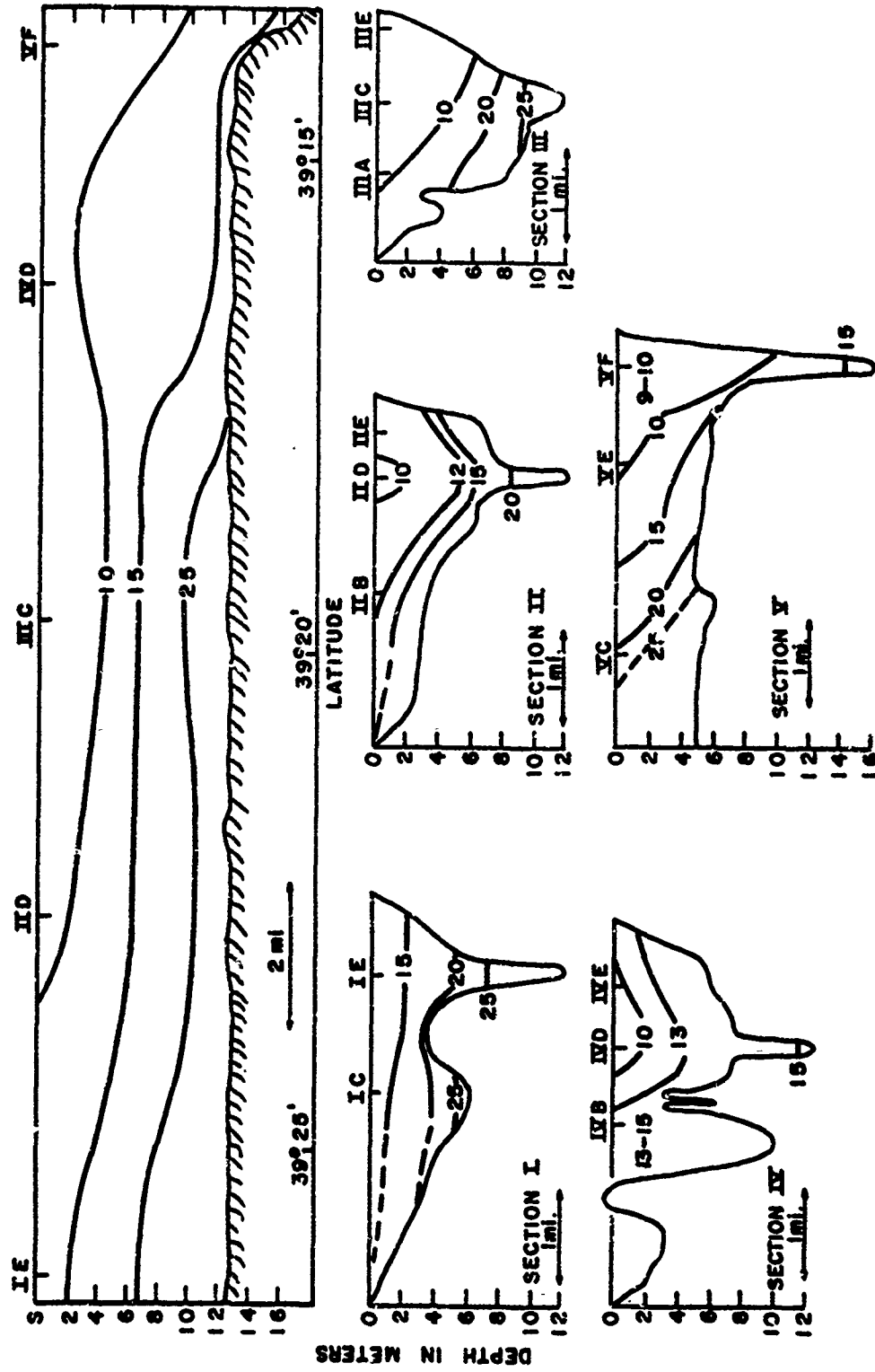


Fig. 13 Distribution of total suspended solids (mg/l) on 11-12 July 1966 (Cruise 5).

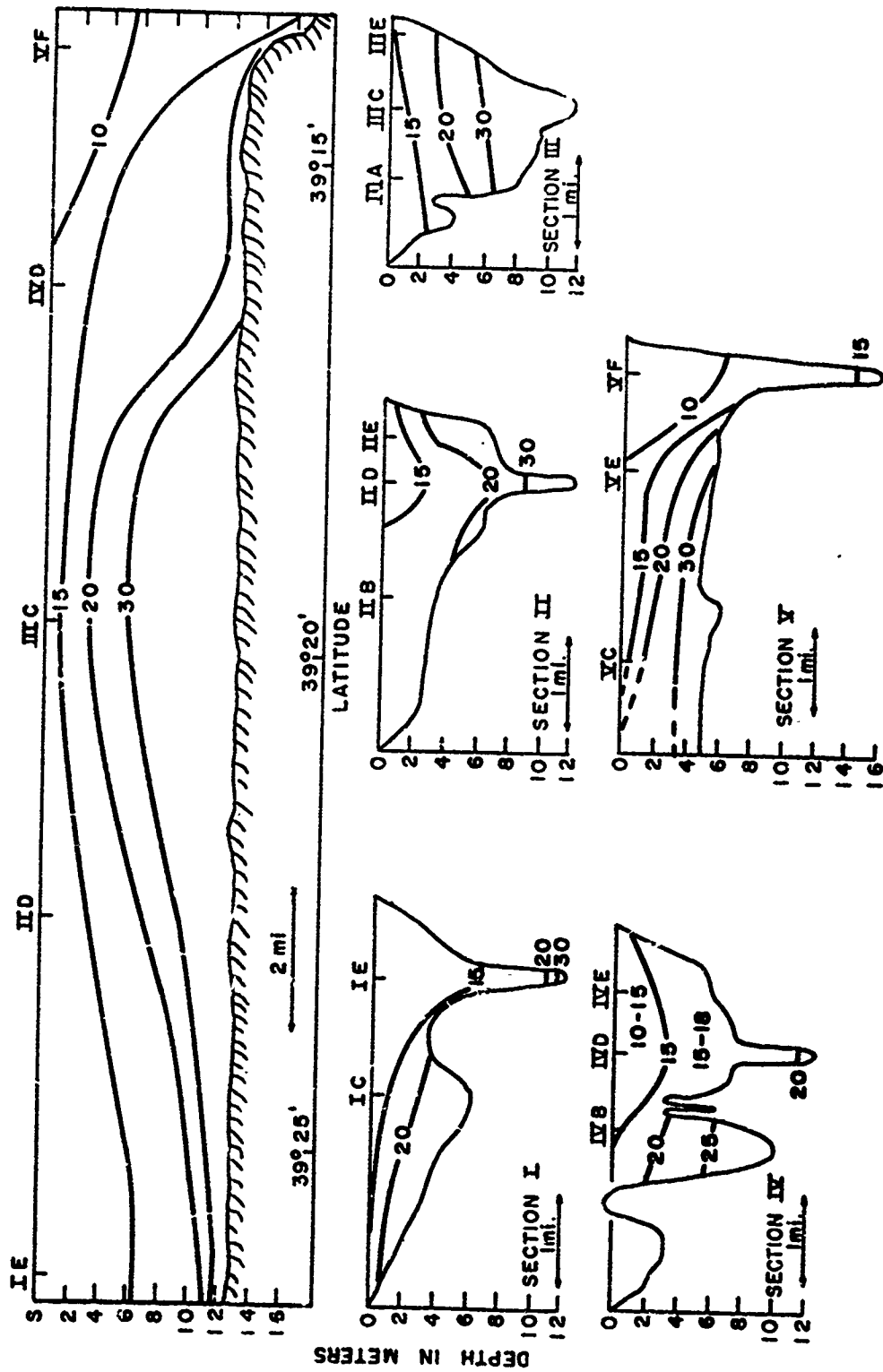


Fig. 14 Distribution of total suspended solids (mg/l) on 25-26 July 1966 (Cruise 6).

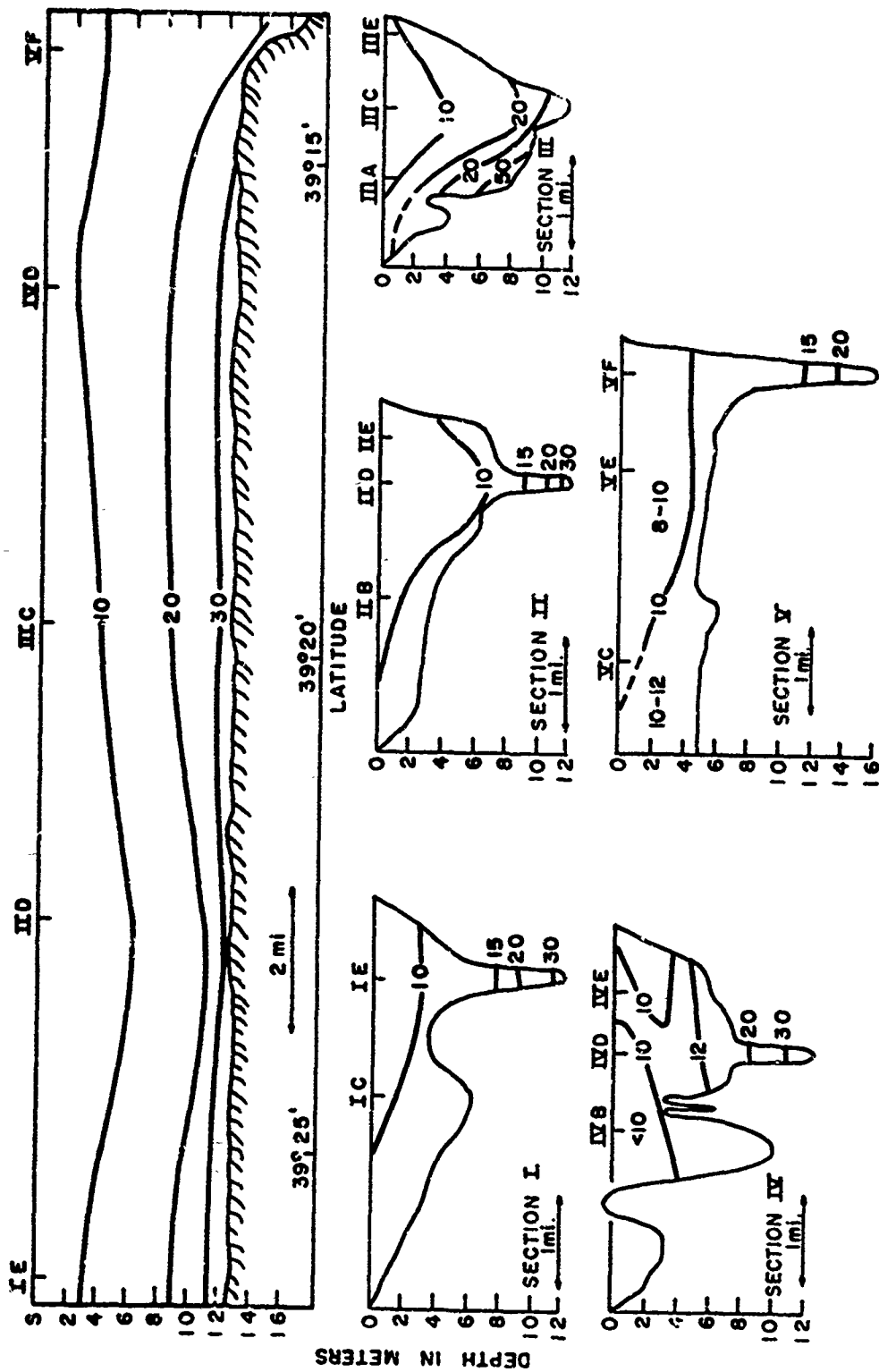


Fig. 15 Distribution of total suspended solids (mg/l) on 8-9 August 1966 (Cruise 7).

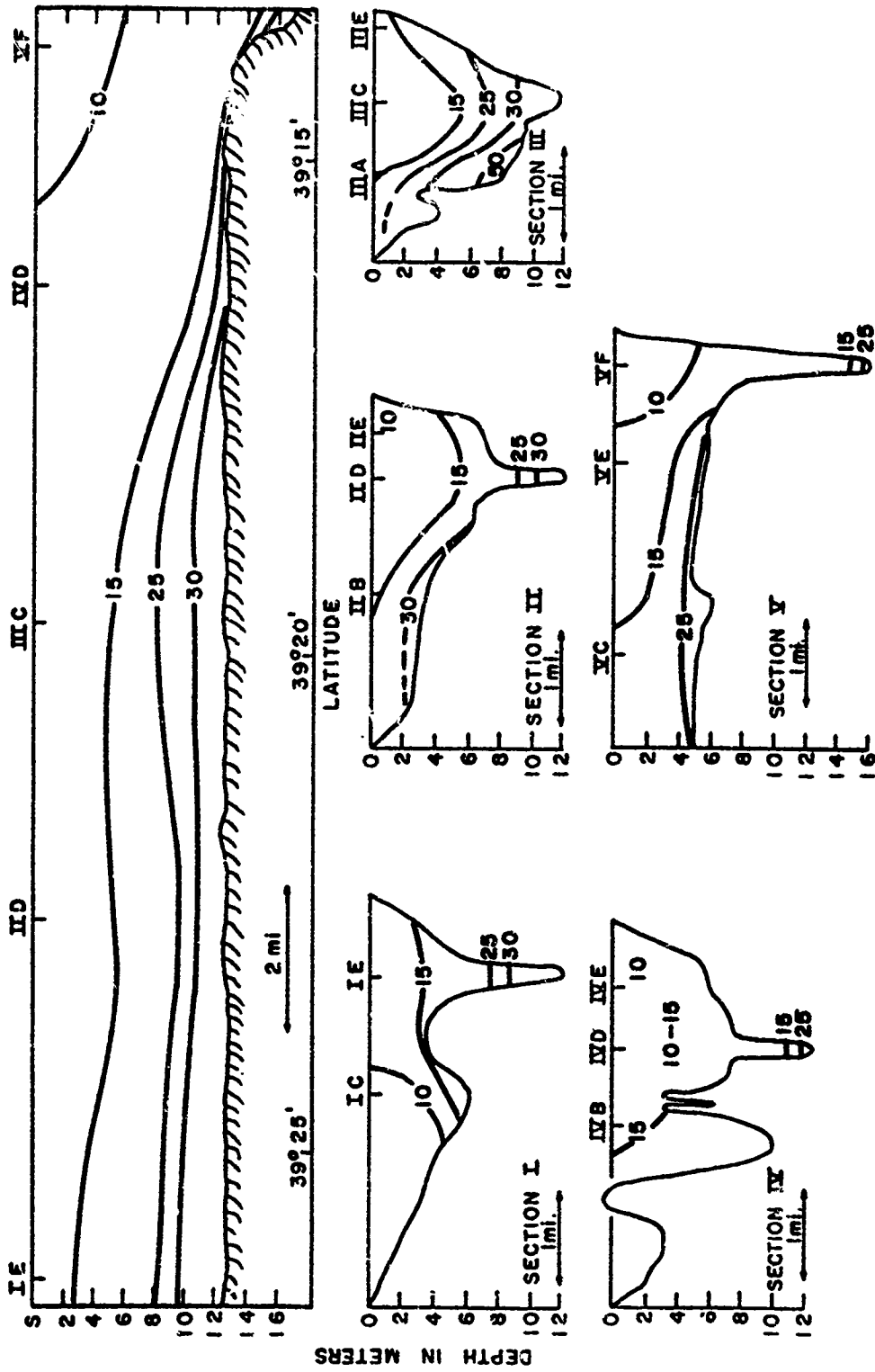


Fig. 16 Distribution of total suspended solids (mg/l) on 22-23 August 1966 (Cruise 8).

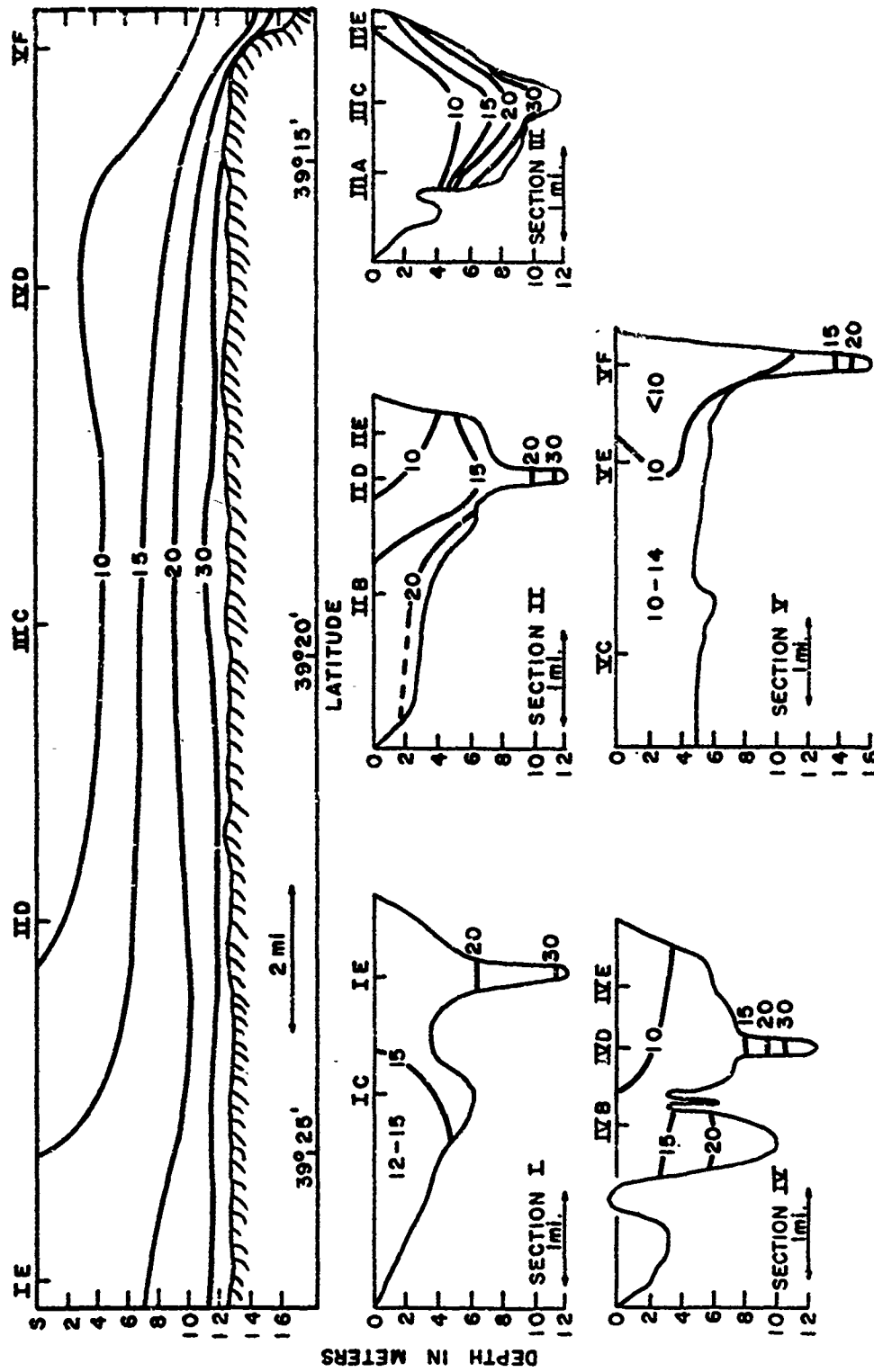


Fig 17 Distribution of total suspended solids (mg/l) on 6-7 September 1966 (Cruise 9).

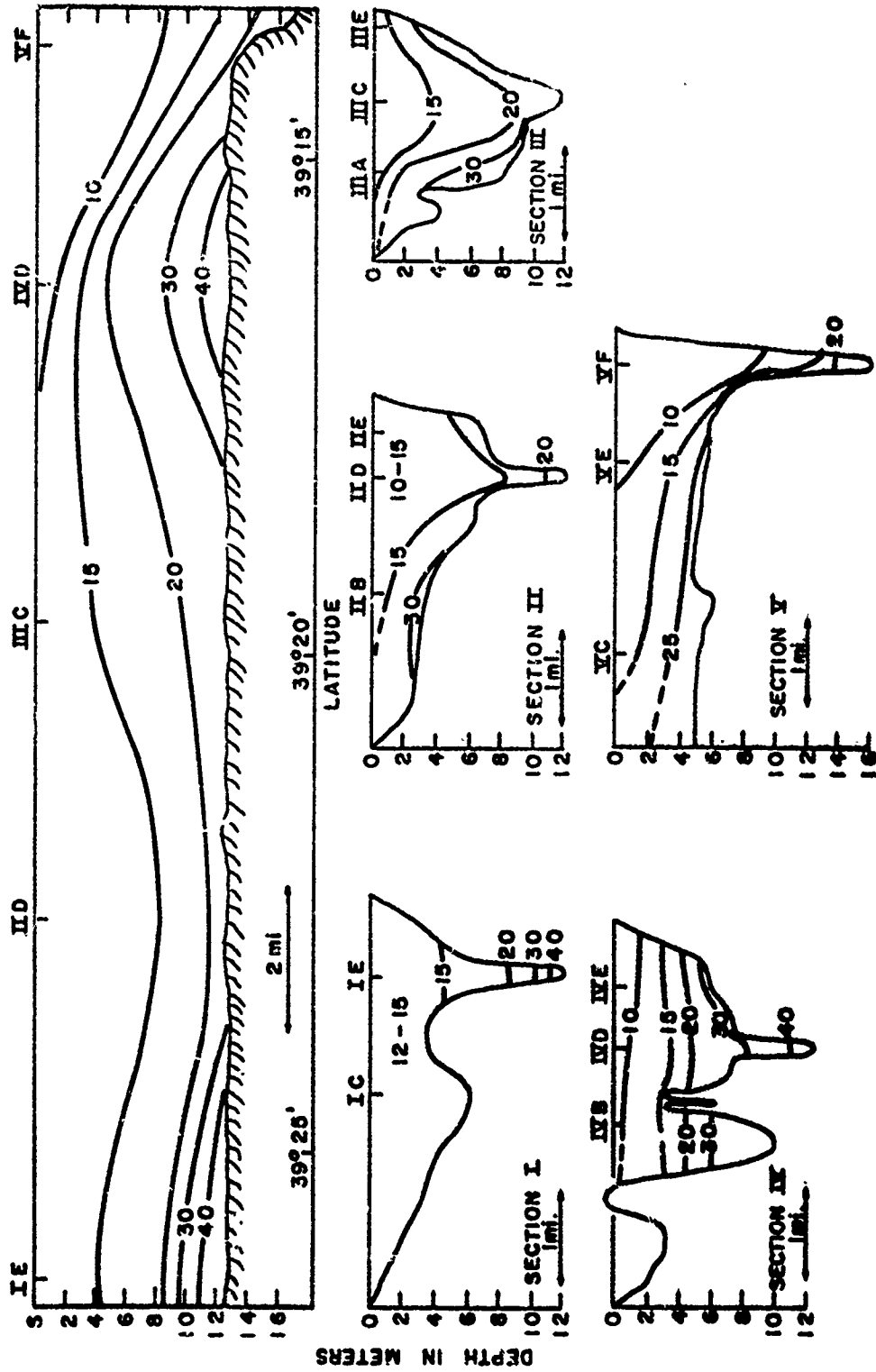


Fig. 18 Distribution of total suspended solids (mg/l) on 19-20 September 1966 (Cruise 10).

U.S. GOVERNMENT PRINTING OFFICE: 1966 O 348-100

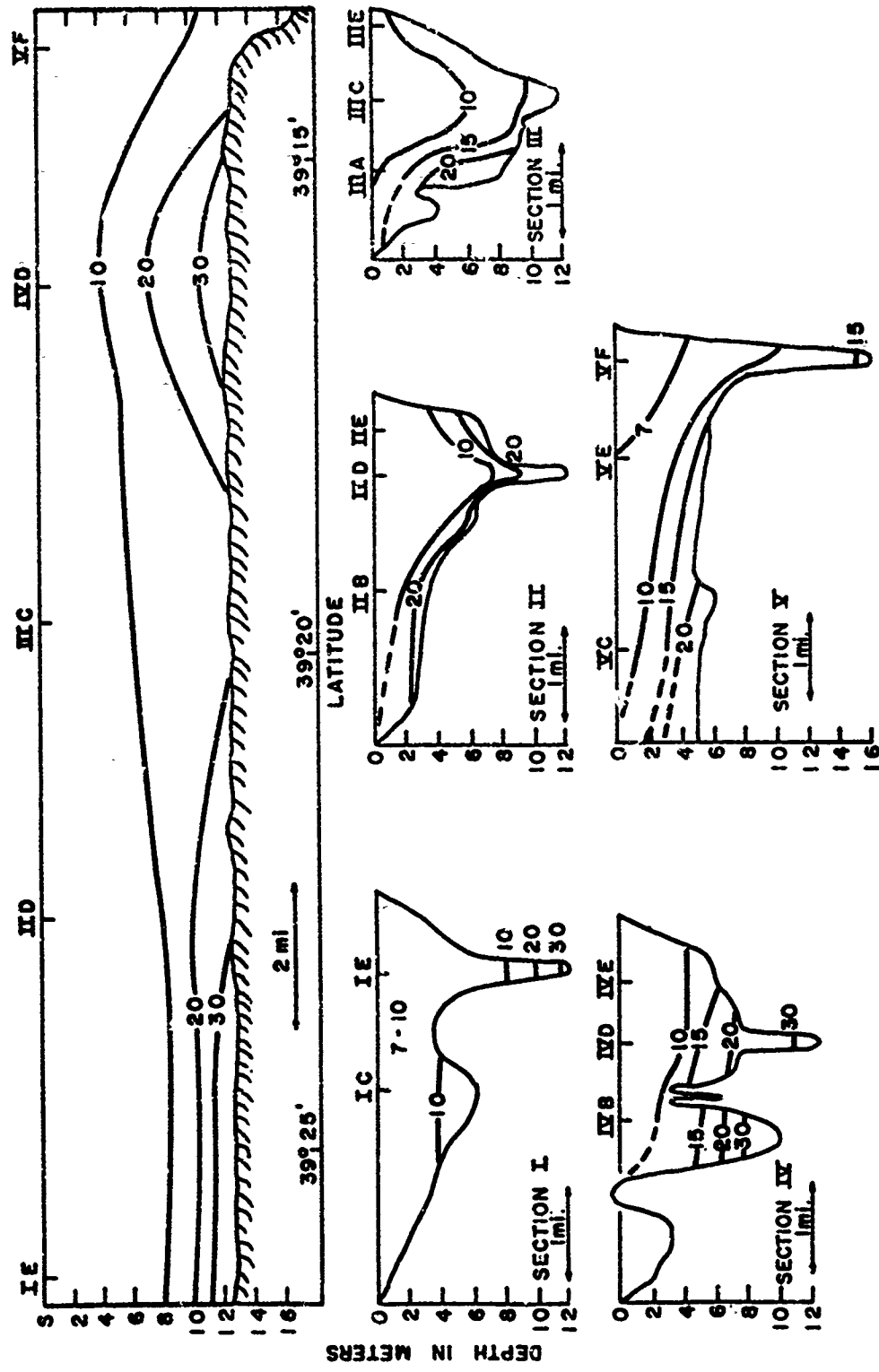


Fig. 19 Distribution of total suspended solids (mg/l) on 3-4 October 1966 (Cruise 11).

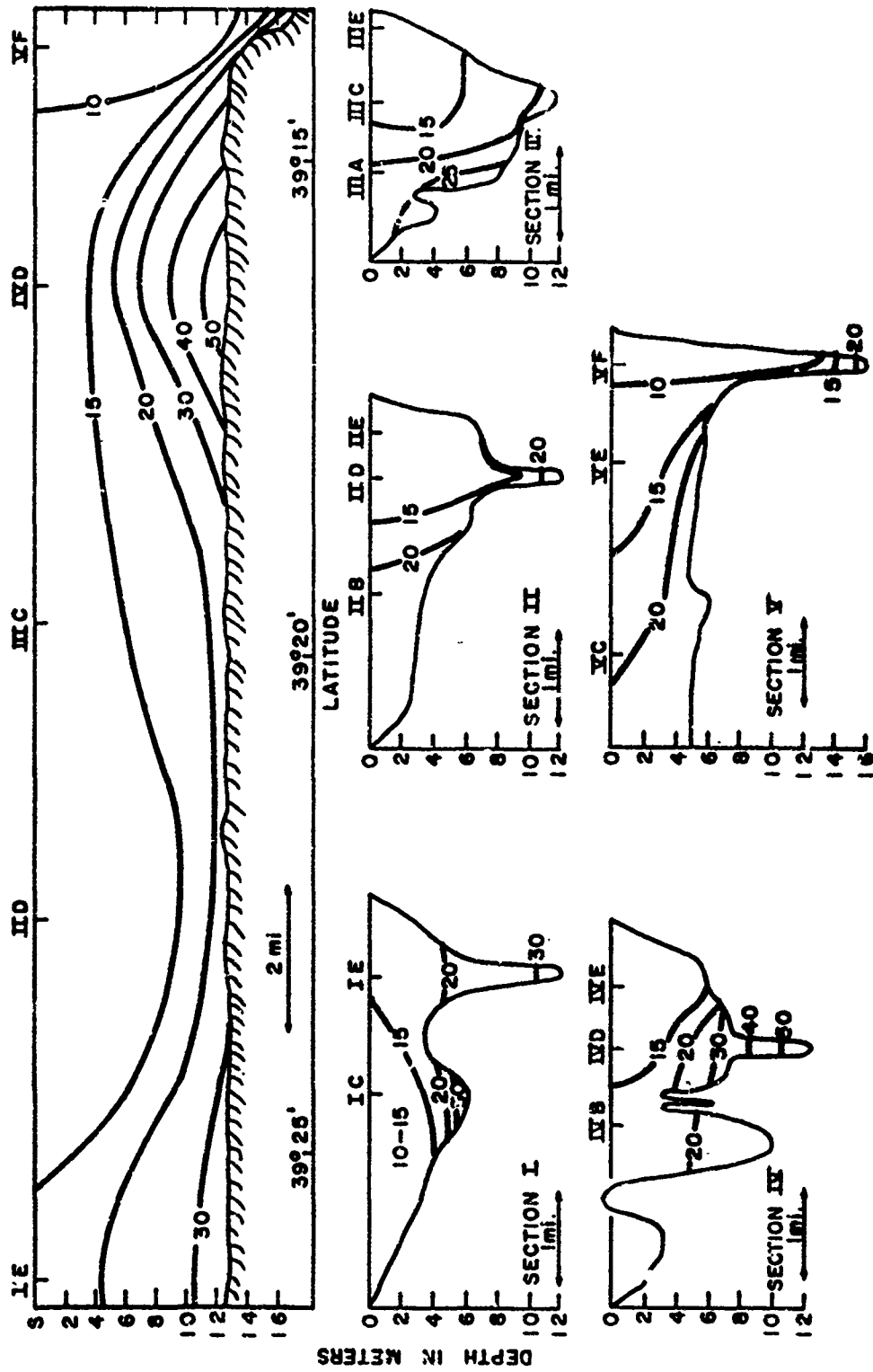


Fig. 20 Distribution of total suspended solids (mg/l) on 17-18 October 1966 (Cruise 12).

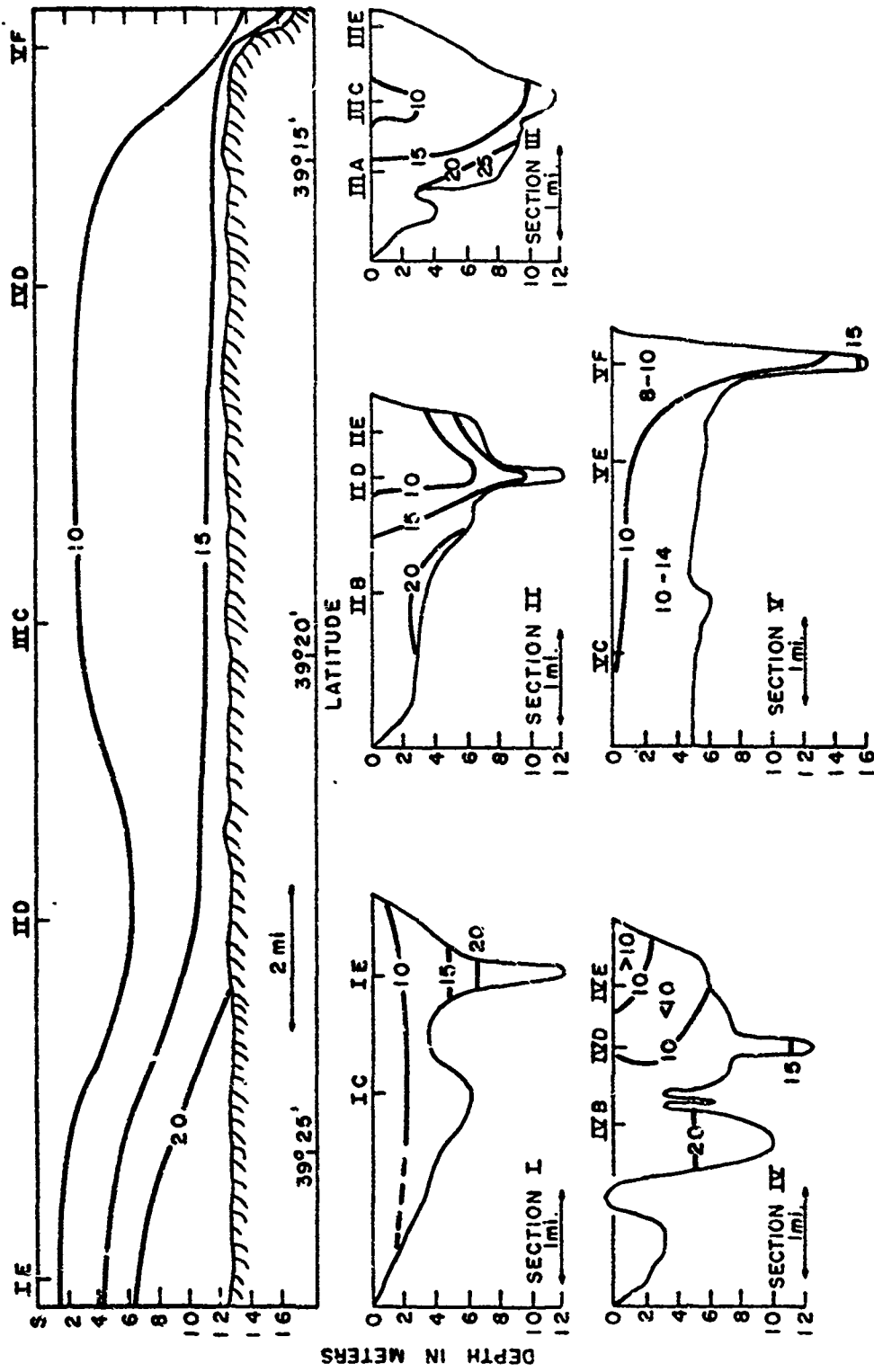


Fig. 21 Distribution of total suspended solids (mg/l) on 1 November 1966 (Cruise 13).

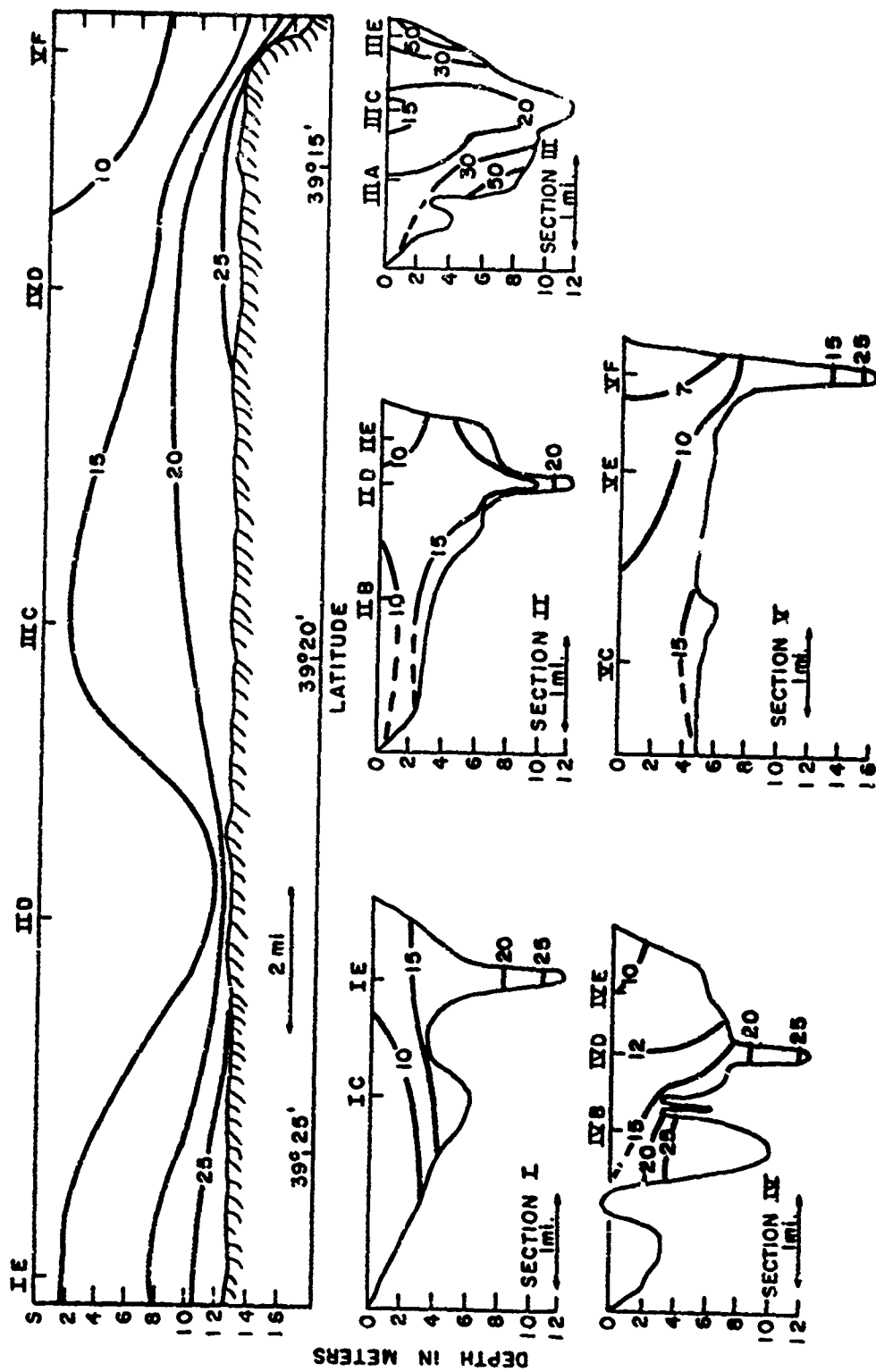


Fig. 22 Distribution of total suspended solids (mg/l) on 14 November 1966 (Cruise 14).

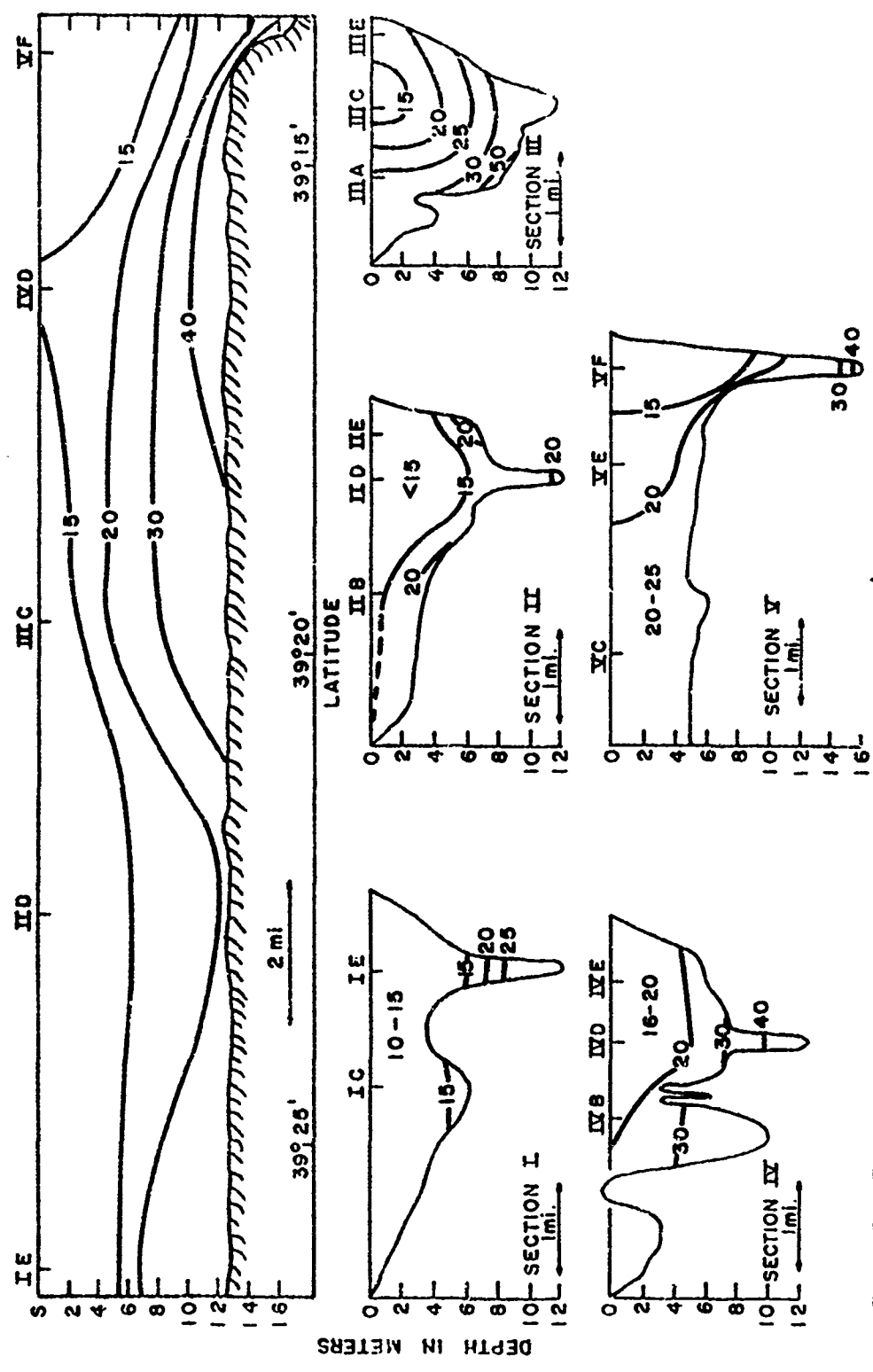


Fig. 23 Distribution of total suspended solids (mg/l) on 30-November - 1 December 1966 (Cruise 15).

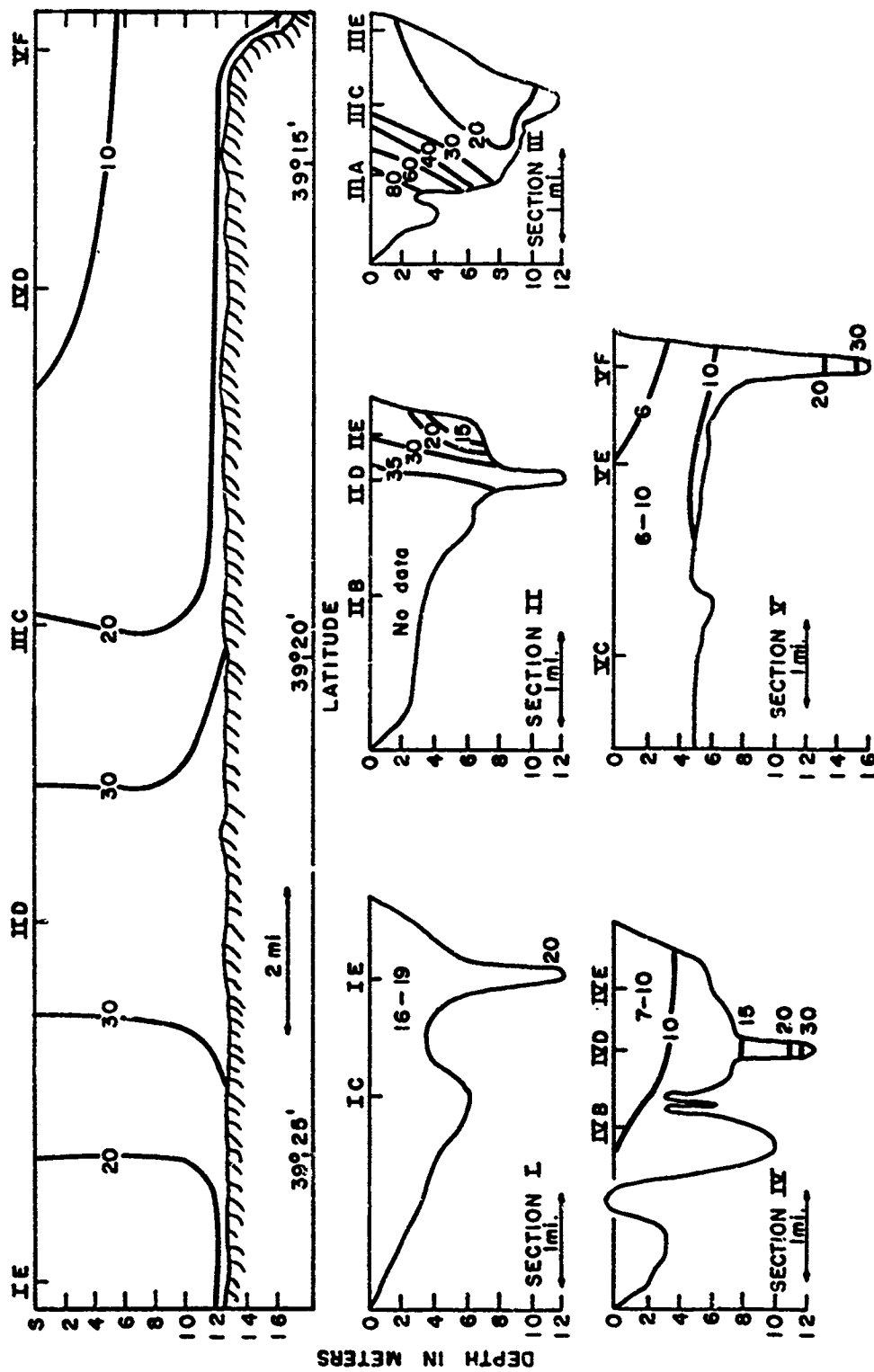


Fig. 24 Distribution of total suspended solids (mg/l) on 13-14 December 1966 (Cruise 16).

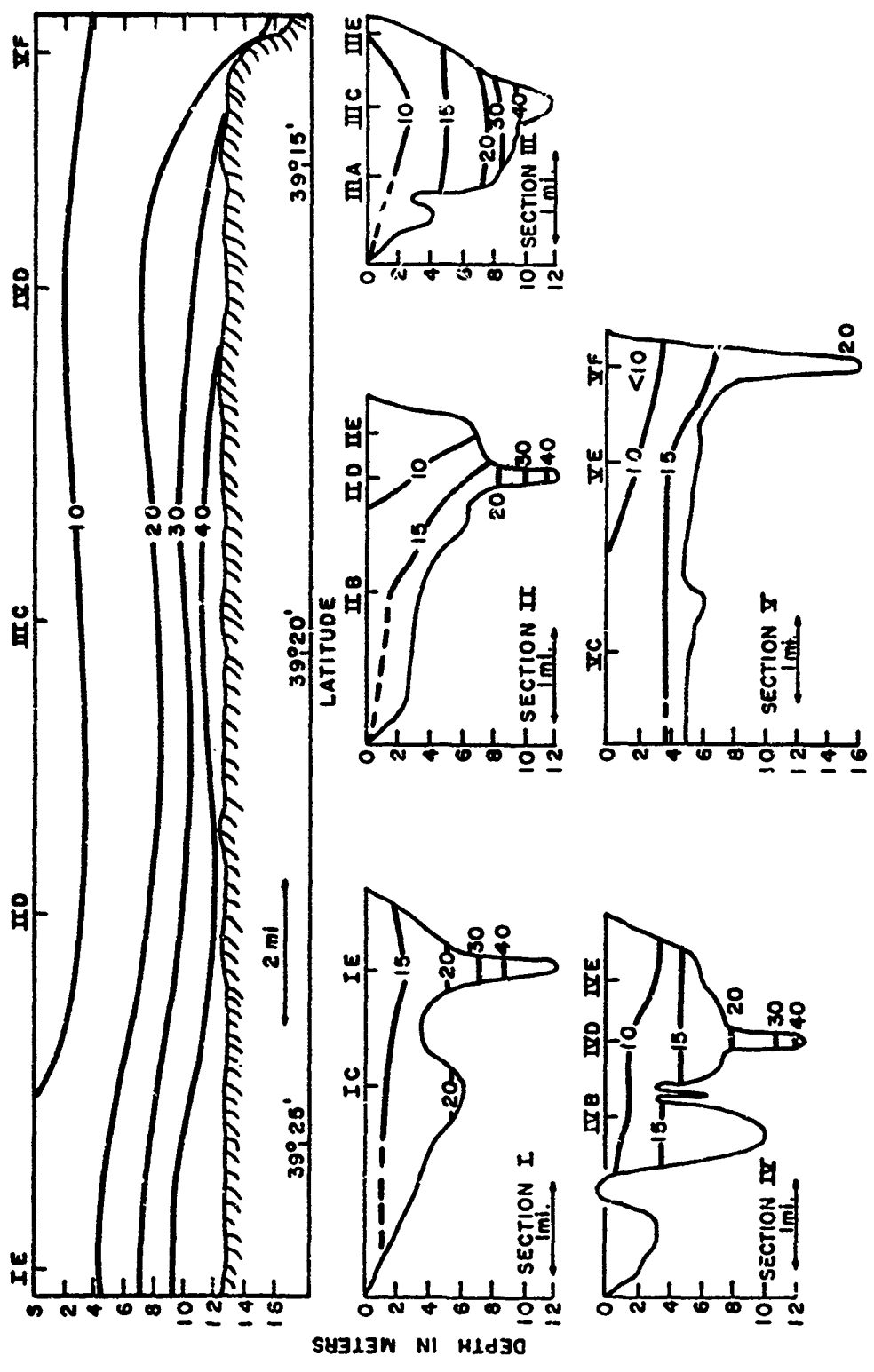


Fig. 25 Distribution of total suspended solids (mg/l) on 28-29 December 1966 (Cruise 17).

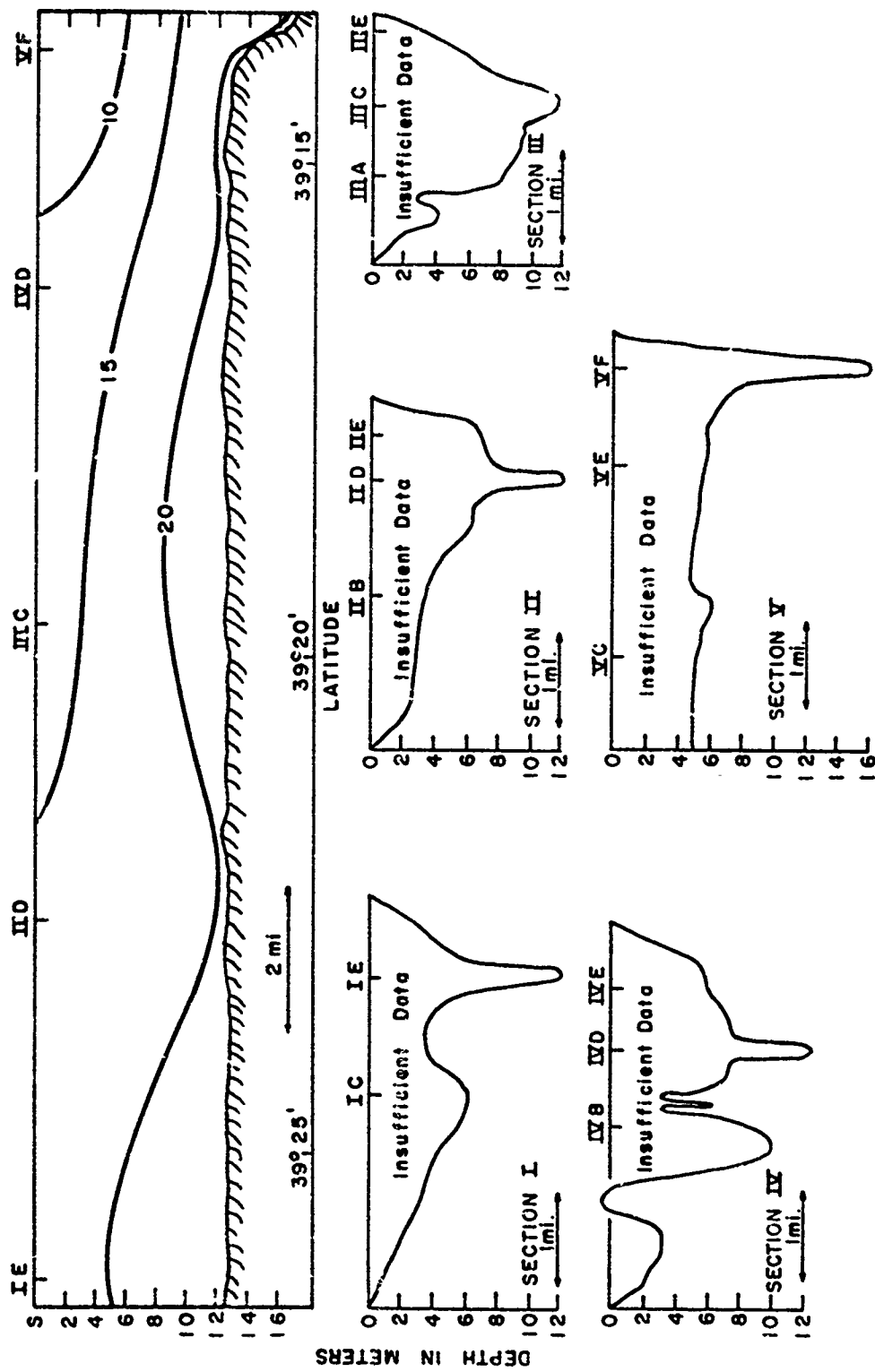


Fig. 26 Distribution of total suspended solids (mg/l) on 12-13 January 1967 (Cruise 18).

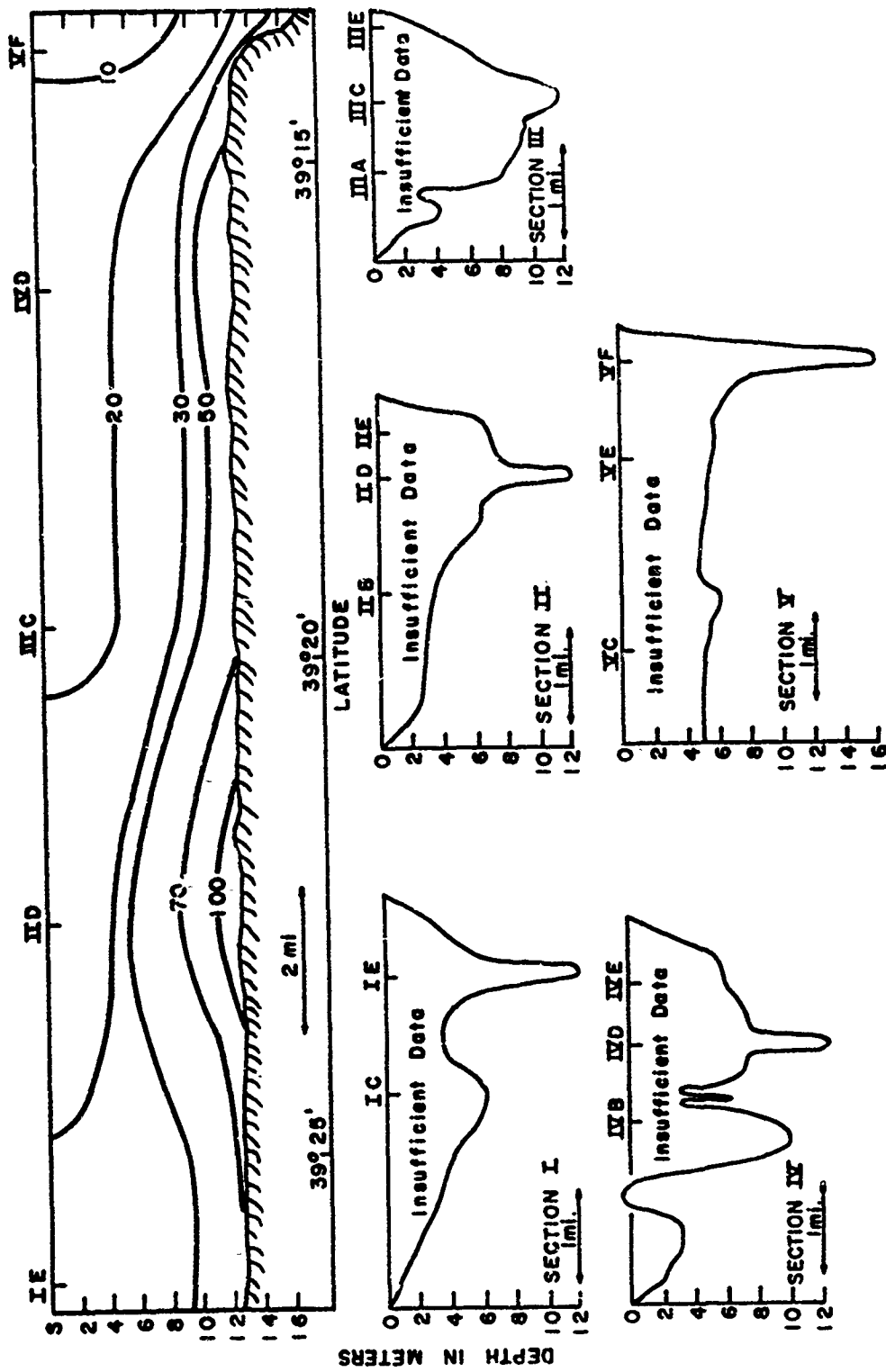


Fig. 27 Distribution of total suspended solids (mg/l) on 14-15 February 1967 (Cruise 20).

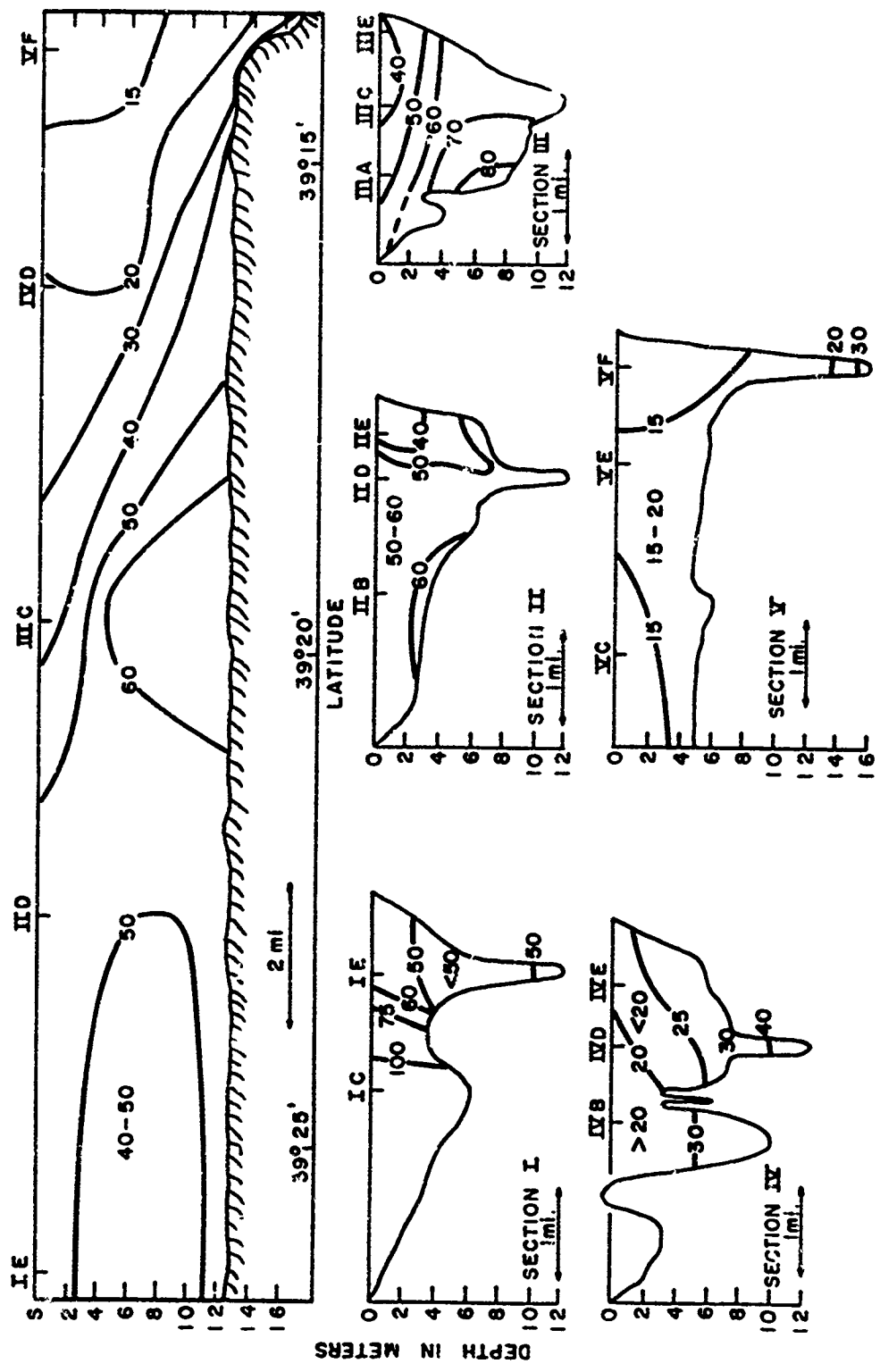


Fig. 28 Distribution of total suspended solids (mg/l) on 9-10 March 1967 (Cruise 21).

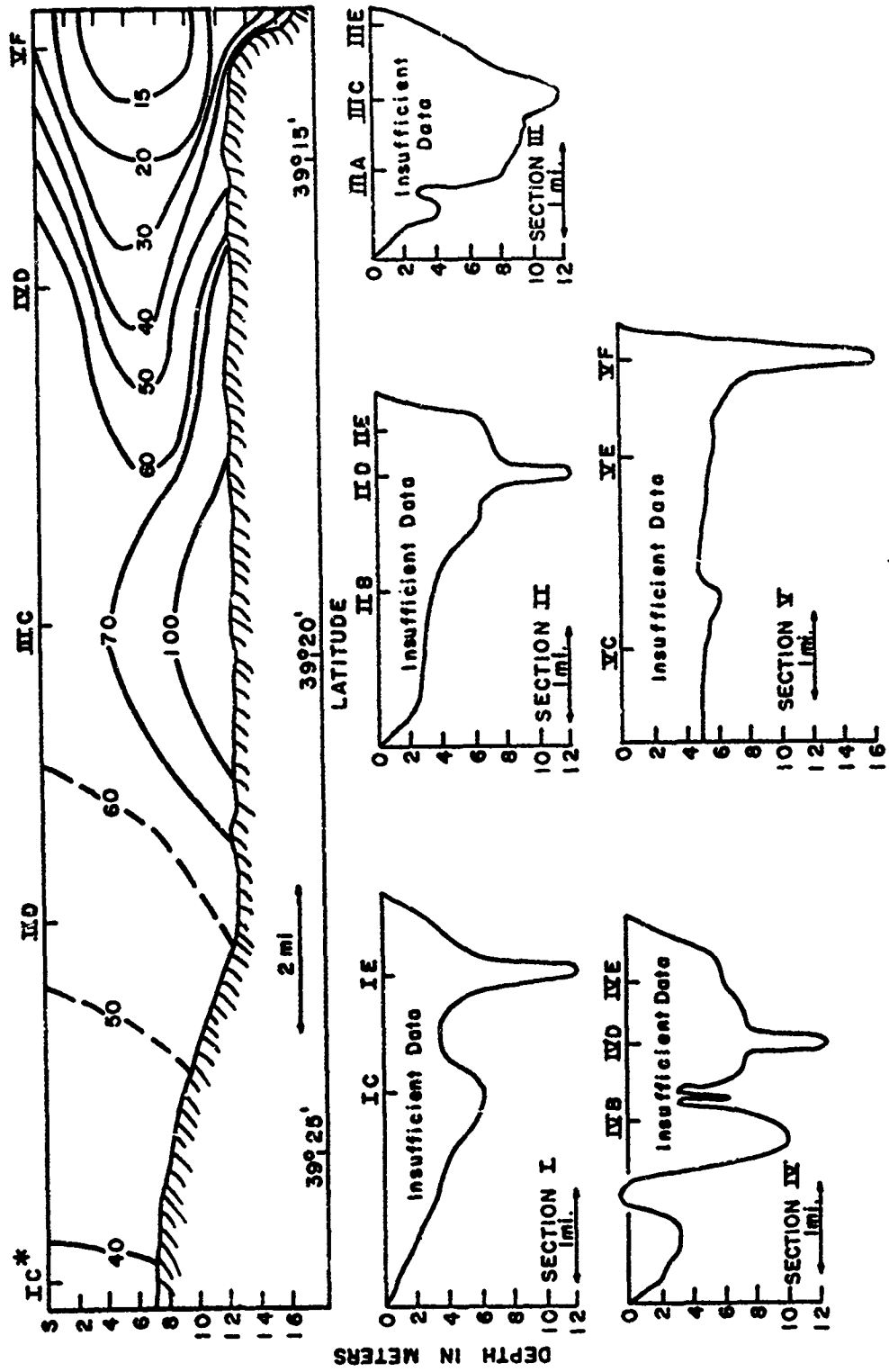


Fig. 29 Distribution of total suspended solids (mg/l) on 15 March 1967 (Cruise 22).

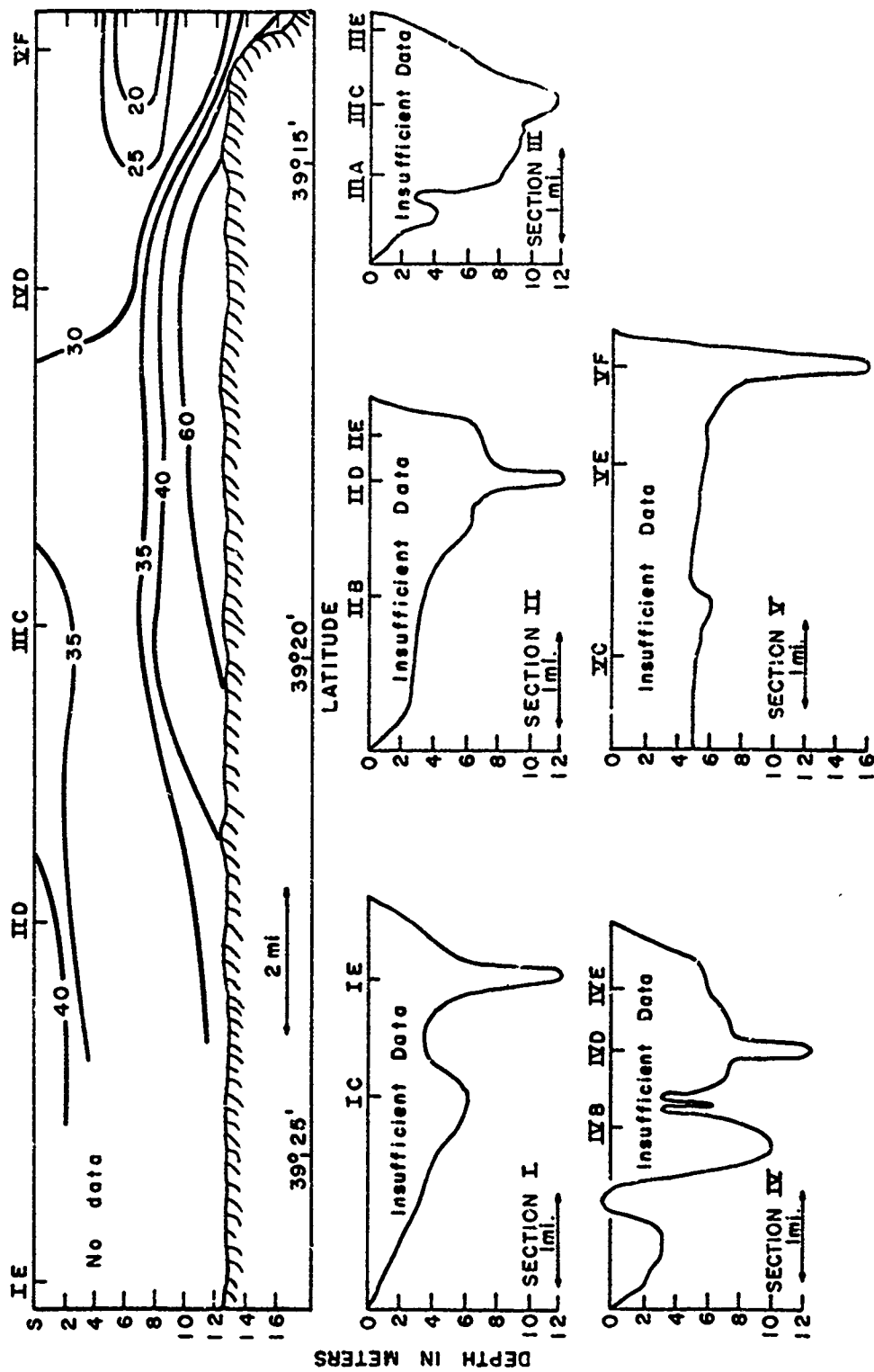


Fig. 30 Distribution of total suspended solids (mg/l) on 20 March 1967 (Cruise 23).

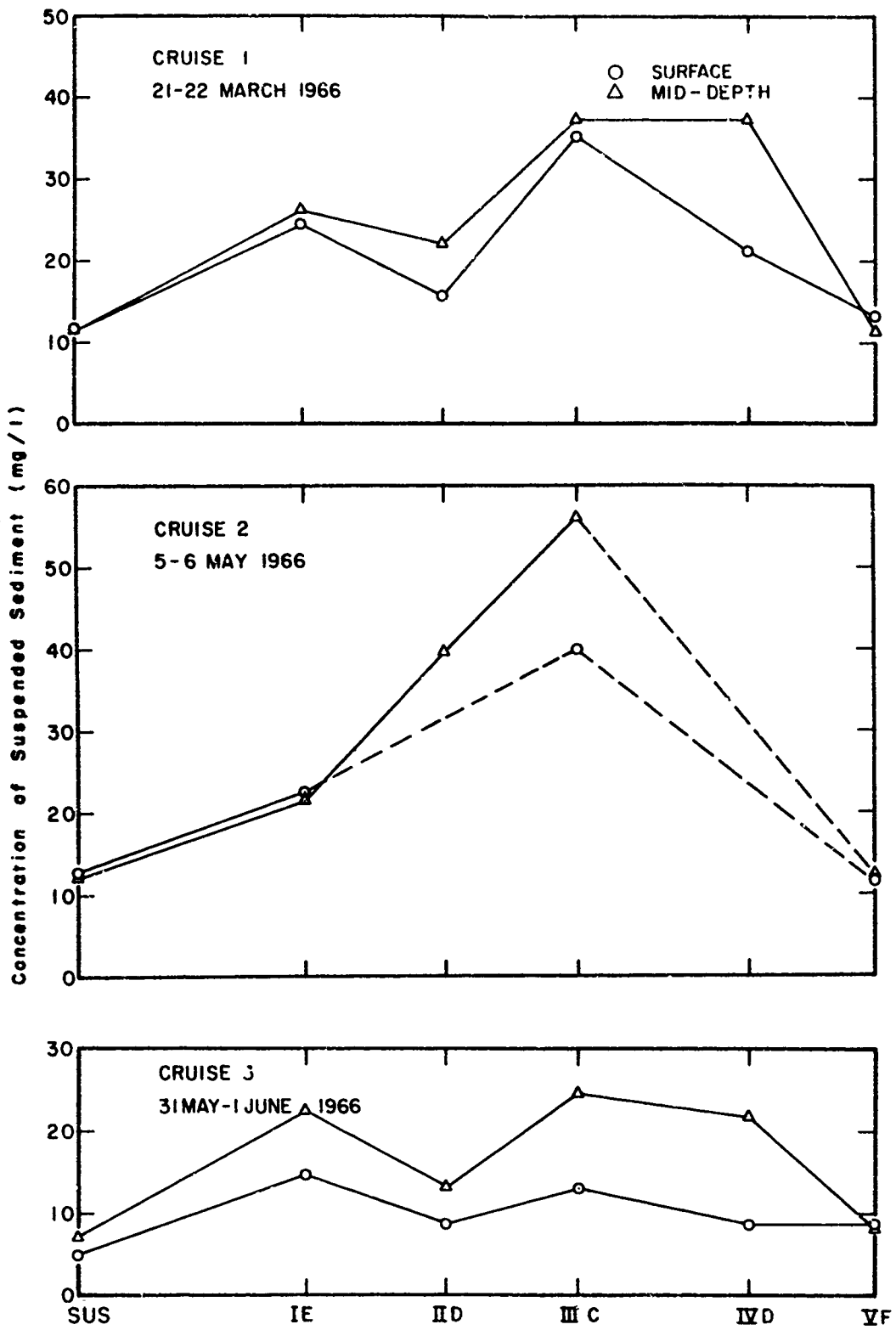


Fig. 31 Surface and Mid-Depth Concentrations of Suspended Sediment at the Susquehanna River Station and Channel Stations within the Bay.

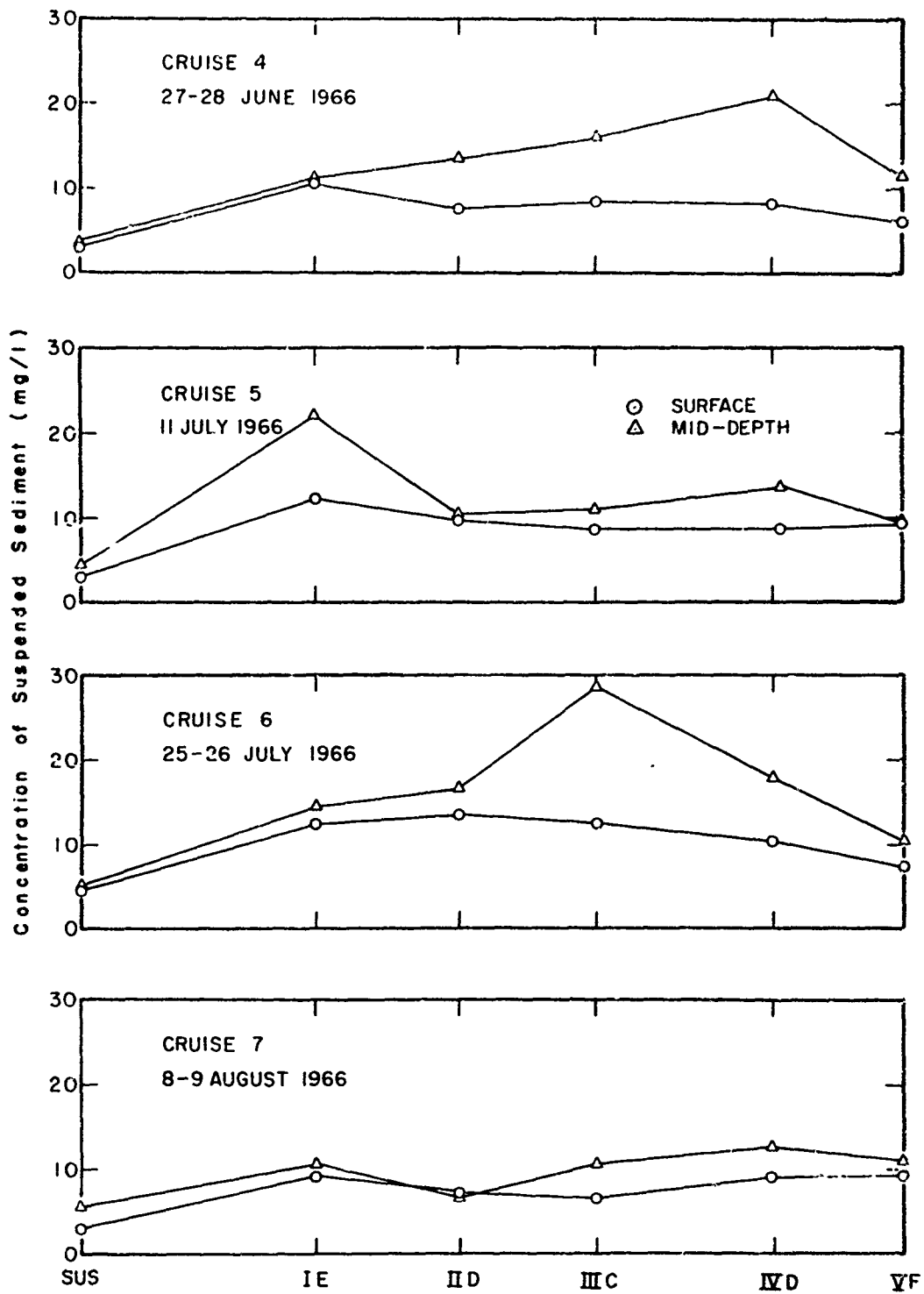


Fig. 32 Surface and Mid-Depth Concentrations of Suspended Sediment at the Susquehanna River Station and Channel Stations within the Bay.

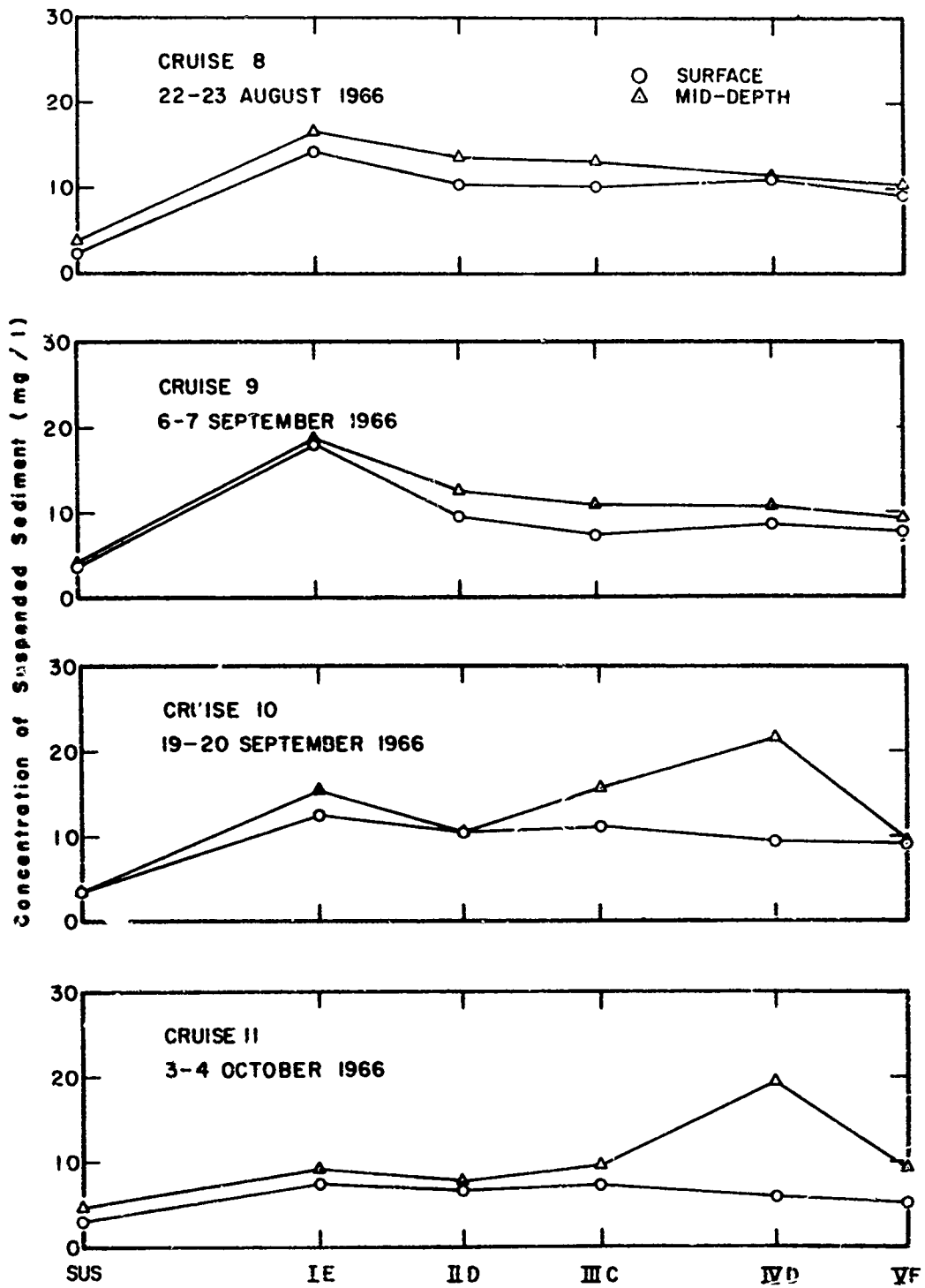


Fig. 33 Surface and Mid-Depth Concentrations of Suspended Sediment at the Susquehanna River Station and Channel Stations within the Bay.

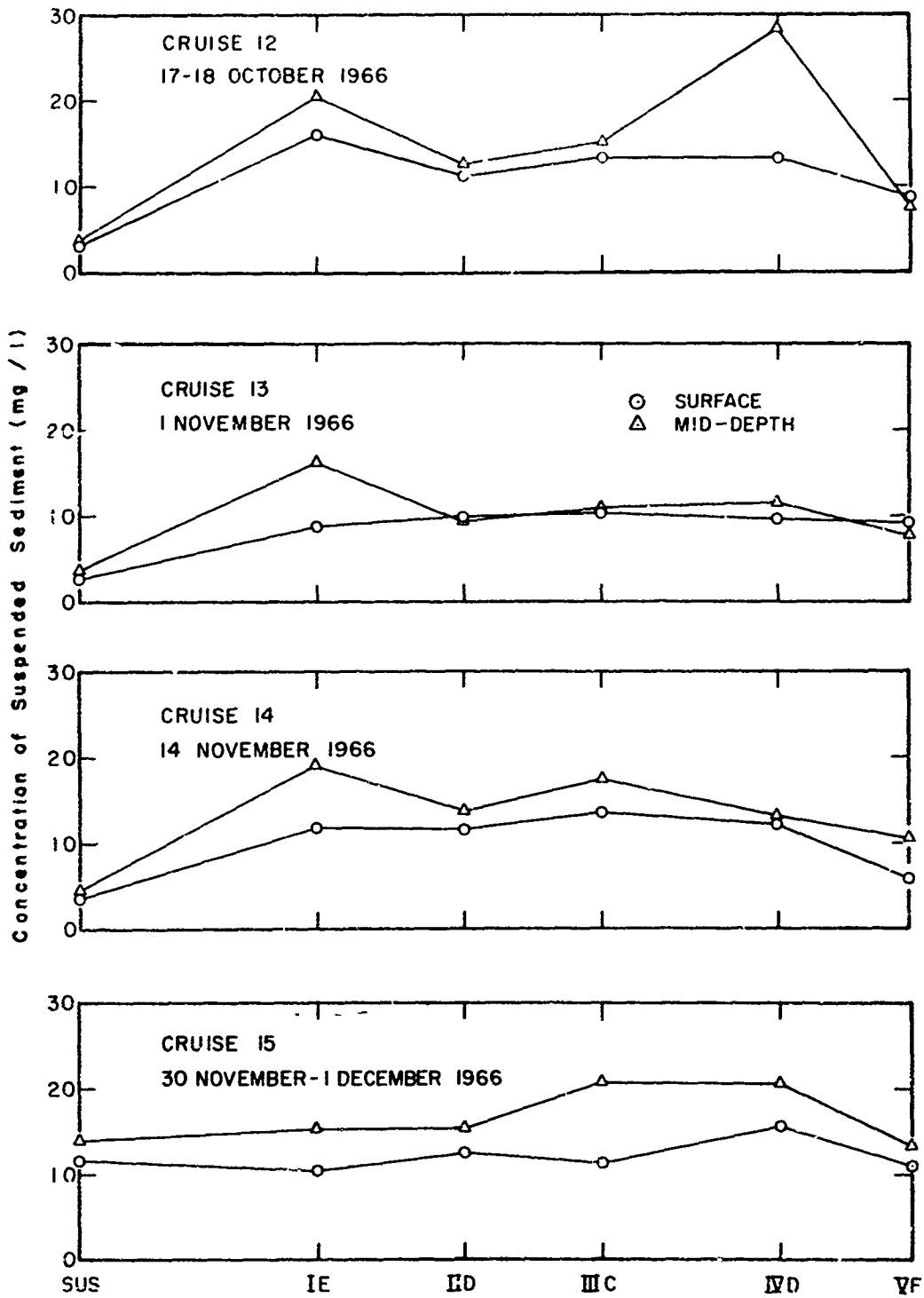


Fig. 34 Surface and Mid-Depth Concentrations of Suspended Sediment at the Susquehanna River Station and Channel Stations within the Bay.

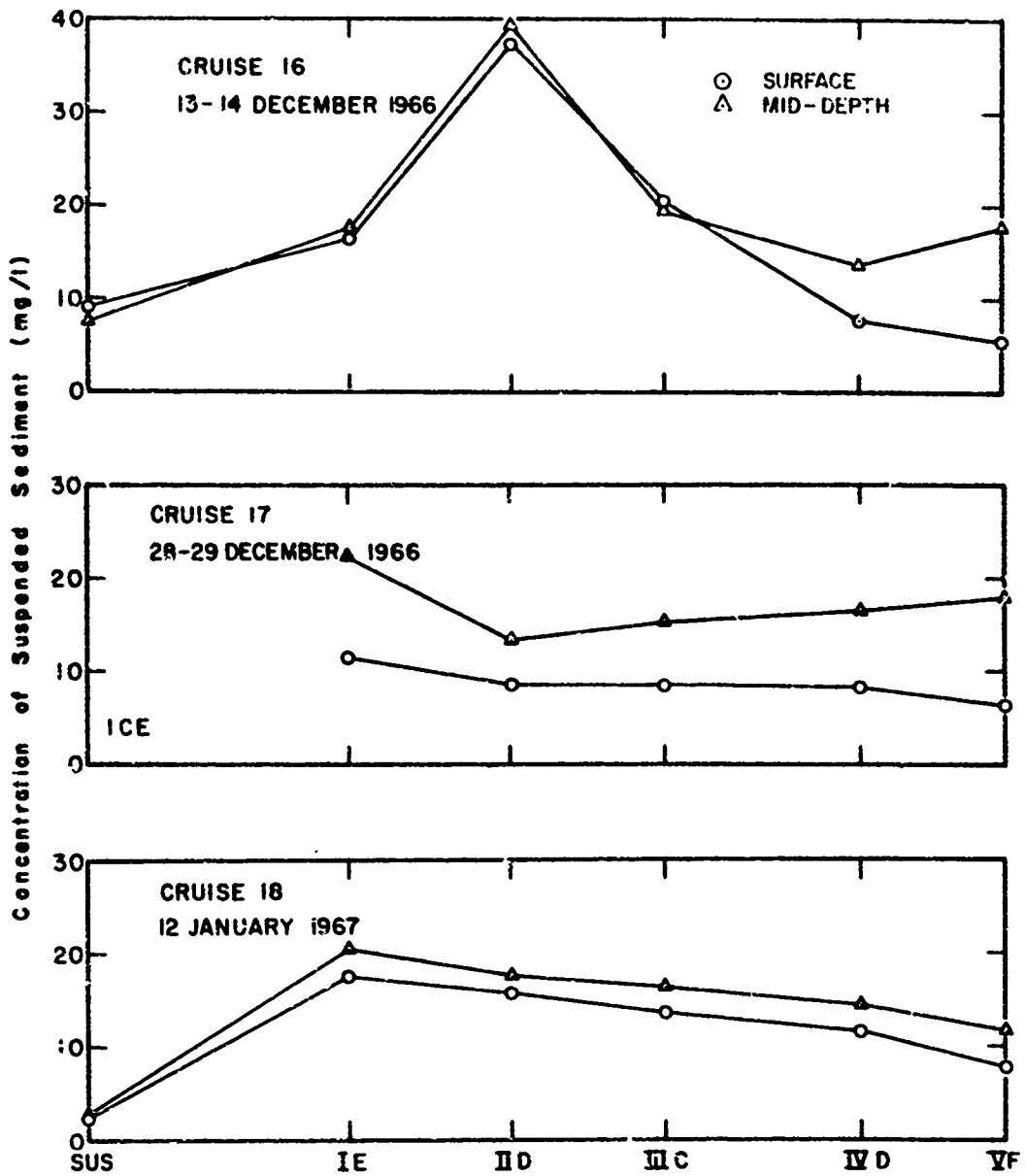


Fig. 35 Surface and Mid-Depth Concentrations of Suspended Sediment at the Susquehanna River Station and Channel Stations within the Bay.

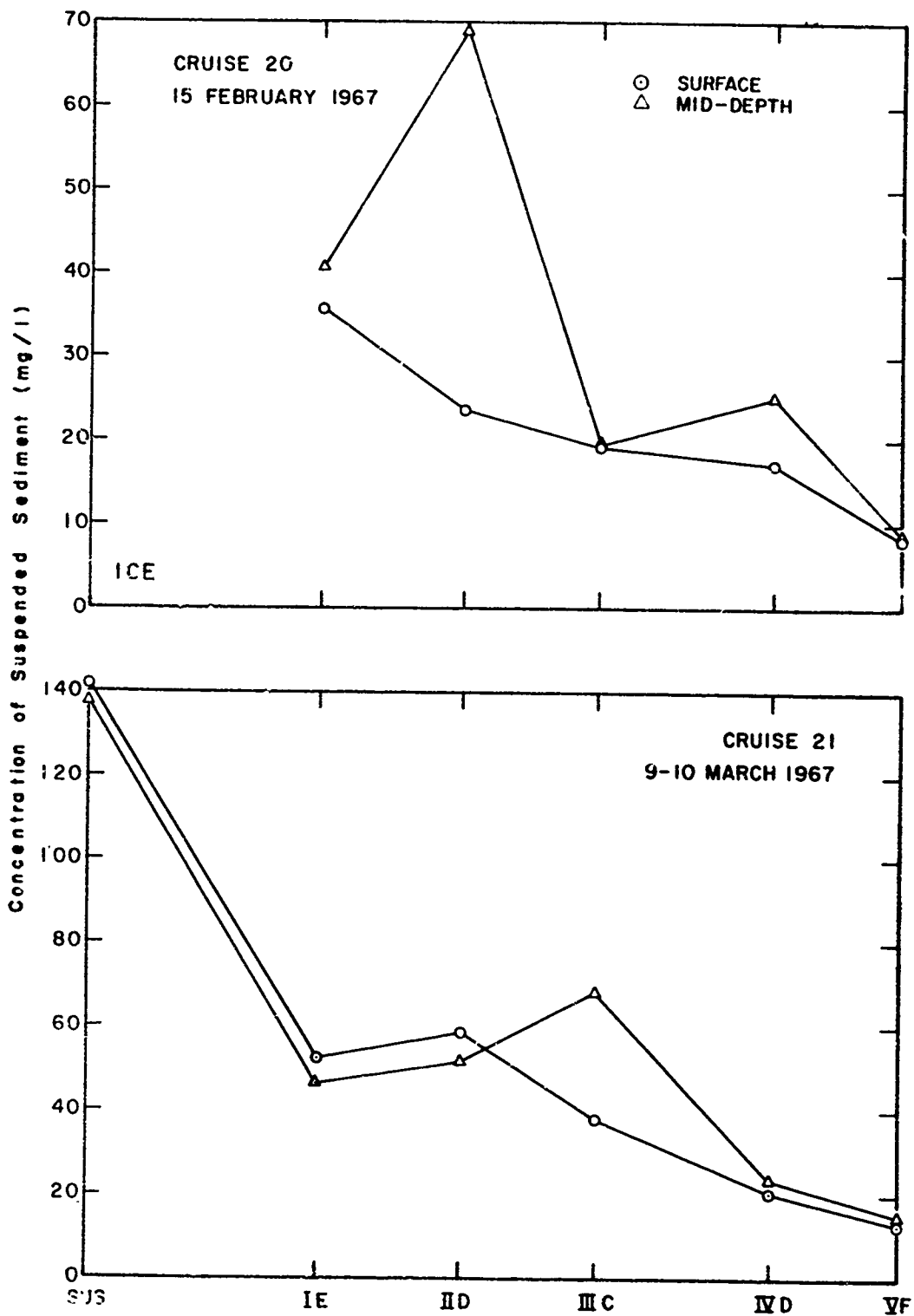


Fig. 36 Surface and Mid-Depth Concentrations of Suspended Sediment at the Susquehanna River Station and Channel Stations within the Bay.

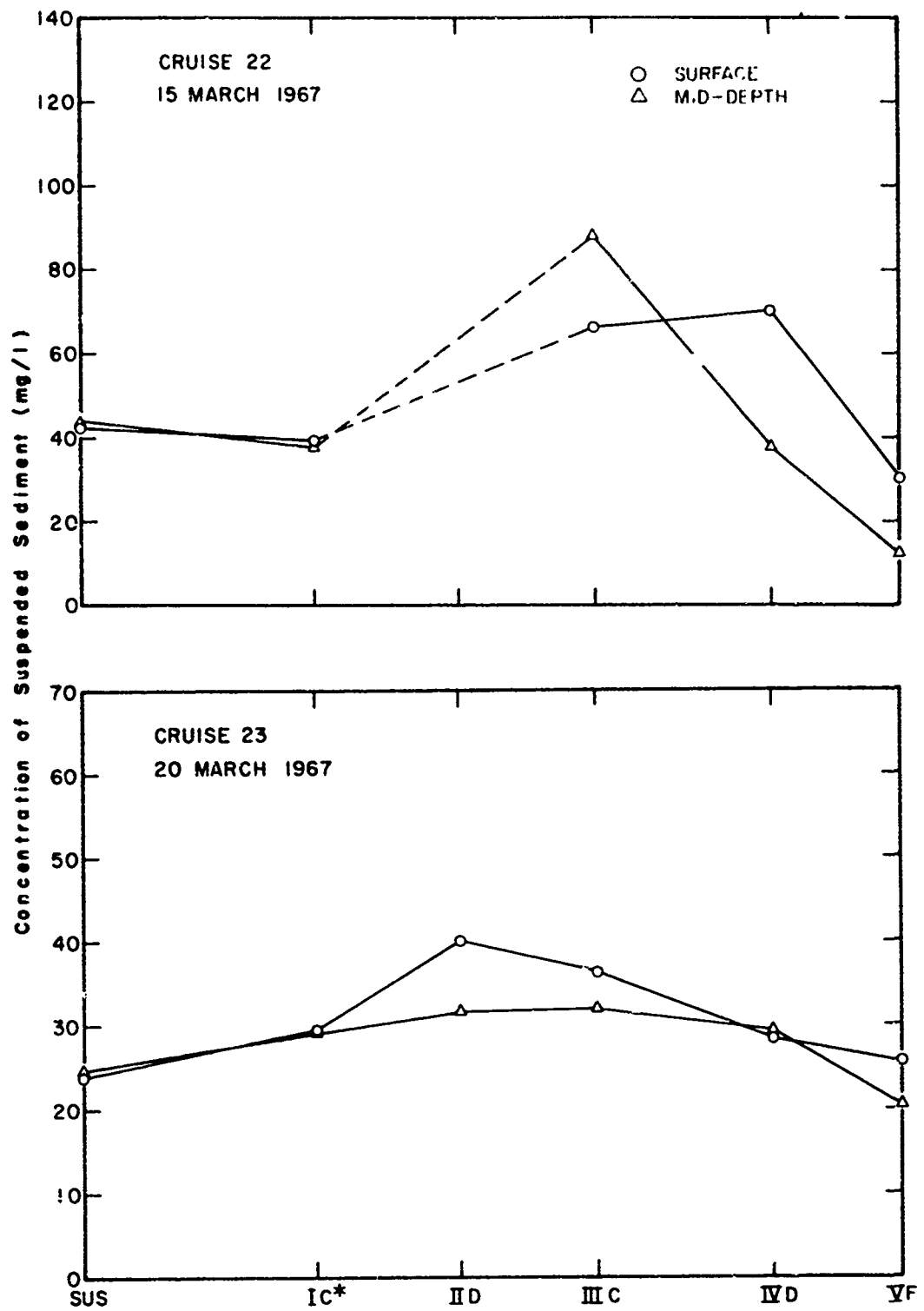


Fig. 37 Surface and Mid-Depth Concentrations of Suspended Sediment at the Susquehanna River Station and Channel Stations within the Bay.

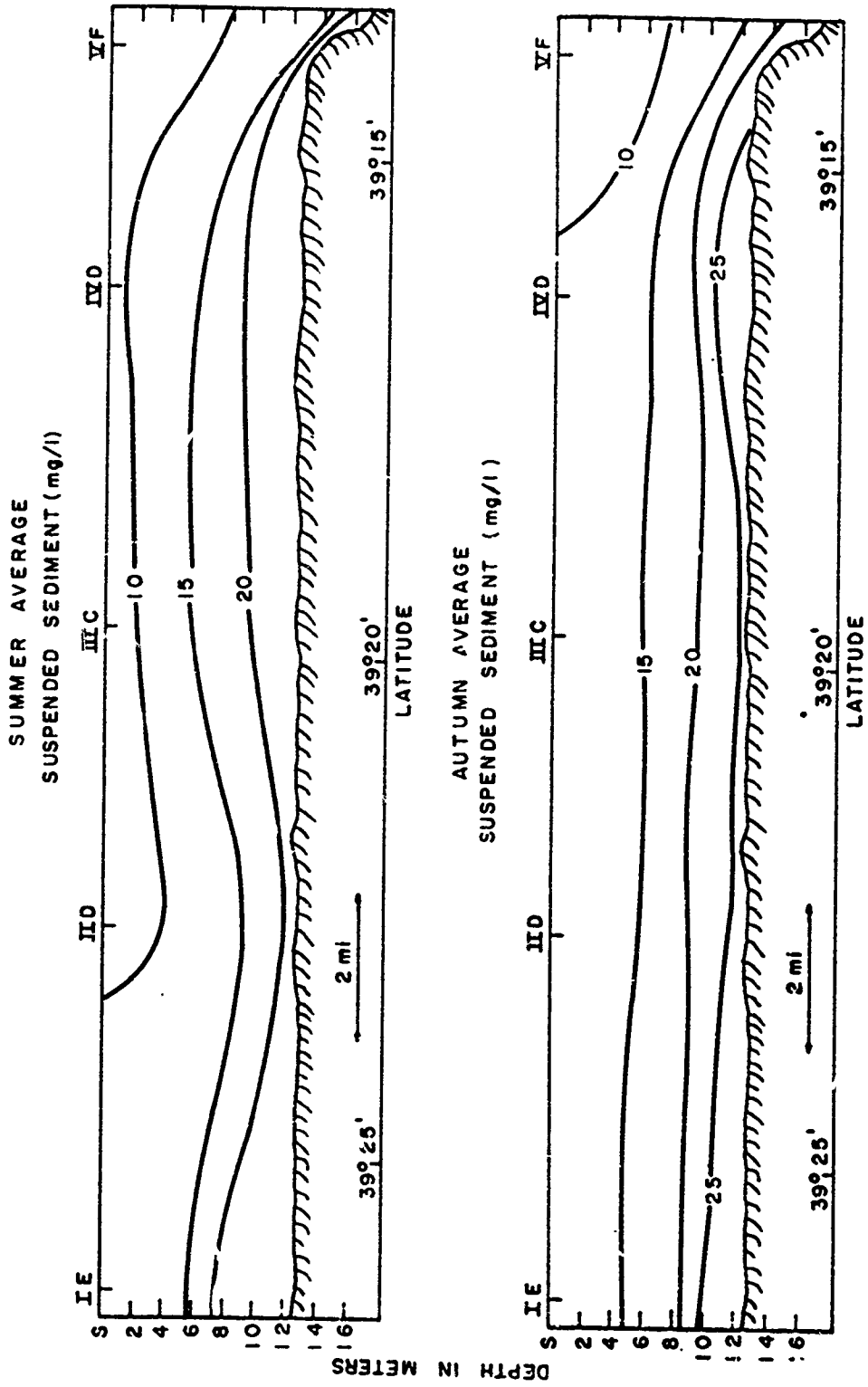


Fig. 38 Average Distributions of Total Suspended Solids (mg/l) during Summer 1966 (16 June - 30 September) and Autumn 1966 (1 October - 15 December).

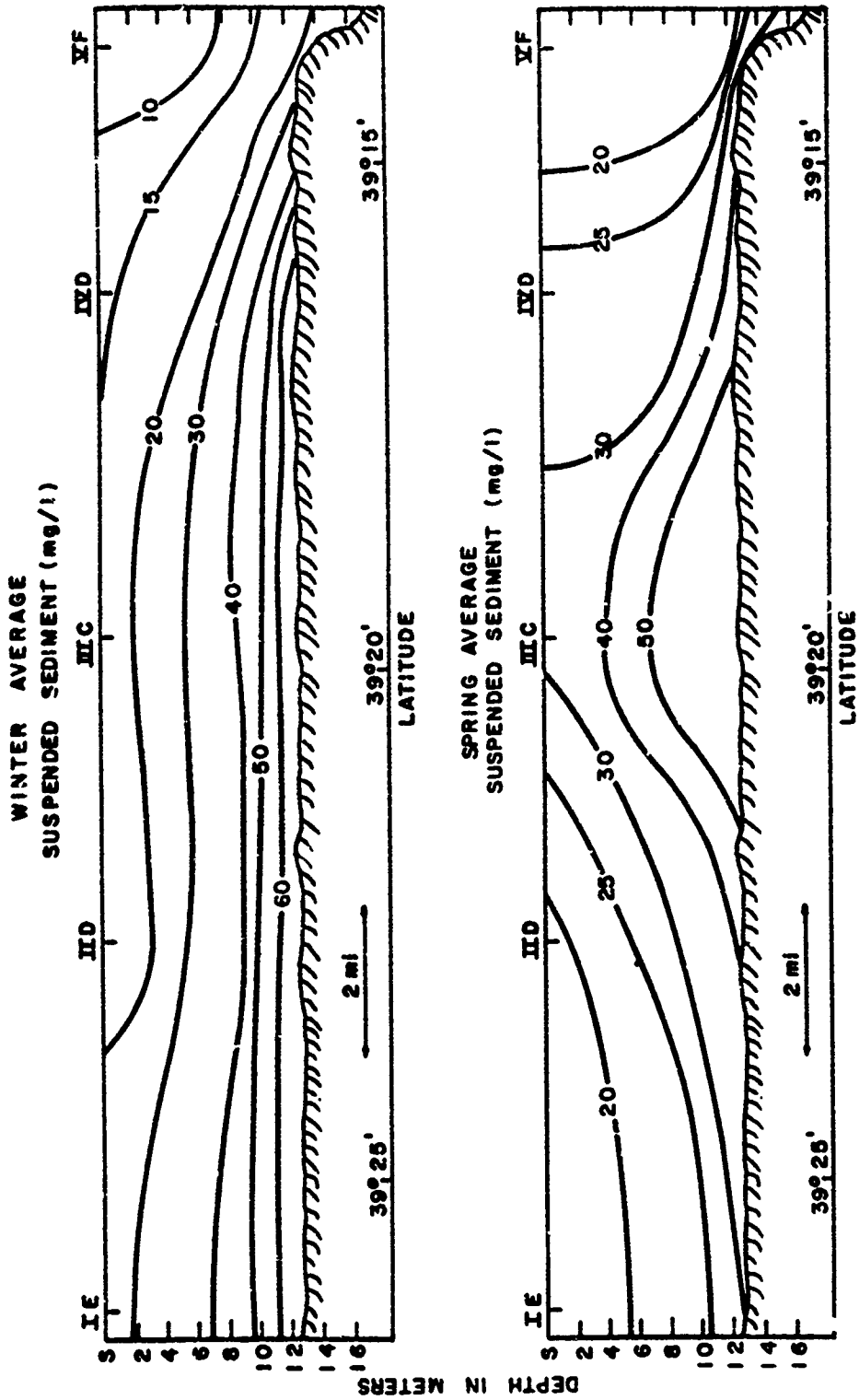


Fig. 39 Average Distributions of Total Suspended Solids (mg/l) during Winter 1966-1967 (16 December - 14 March) and Spring 1966 and 1967 (15 March - 15 June).

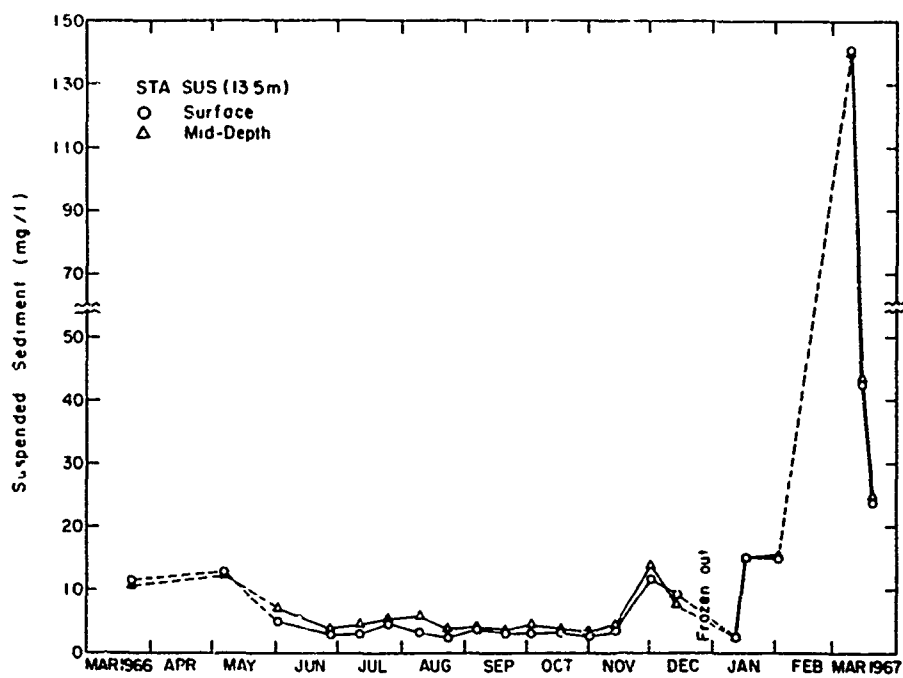


Fig. 40 Surface and Mid-Depth Concentrations of Suspended Sediment at Station SUS plotted against the Date of Sample Collection.

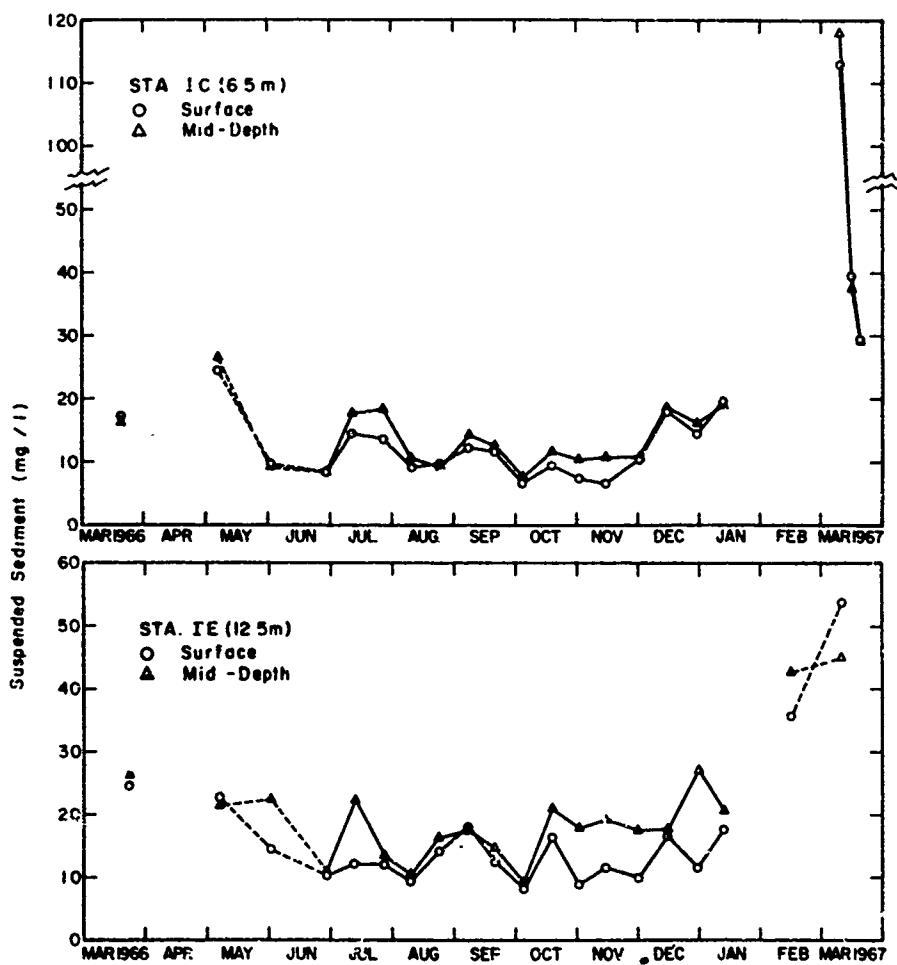


Fig. 41 Surface and Mid-Depth Concentrations of Suspended Sediment at Stations IC and IE plotted against the Date of Sample Collection.

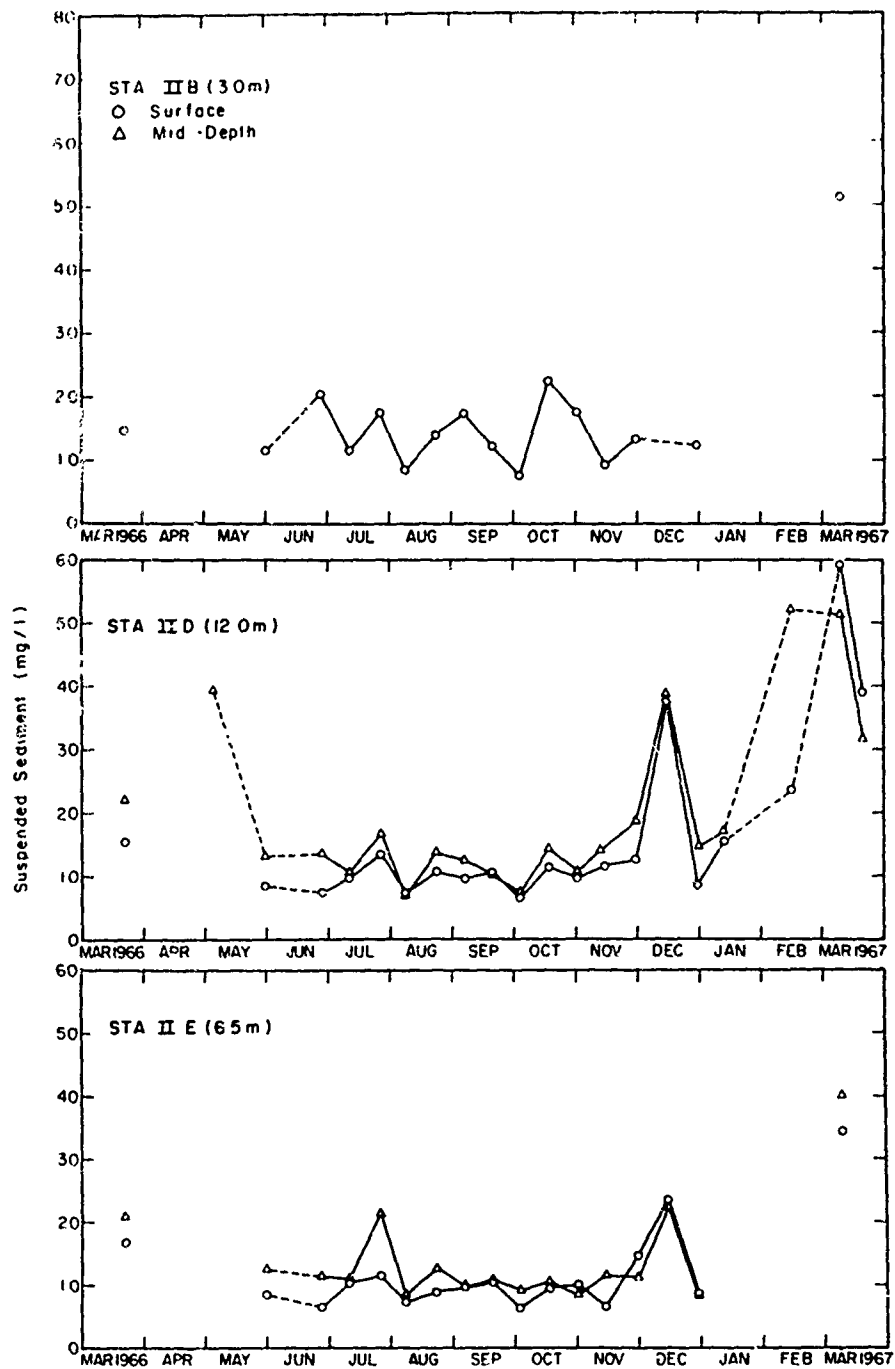


Fig. 42 Surface and Mid-Depth Concentrations of Suspended Sediment at Stations IIB, IID, and IIE, plotted against the Date of Sample Collection.

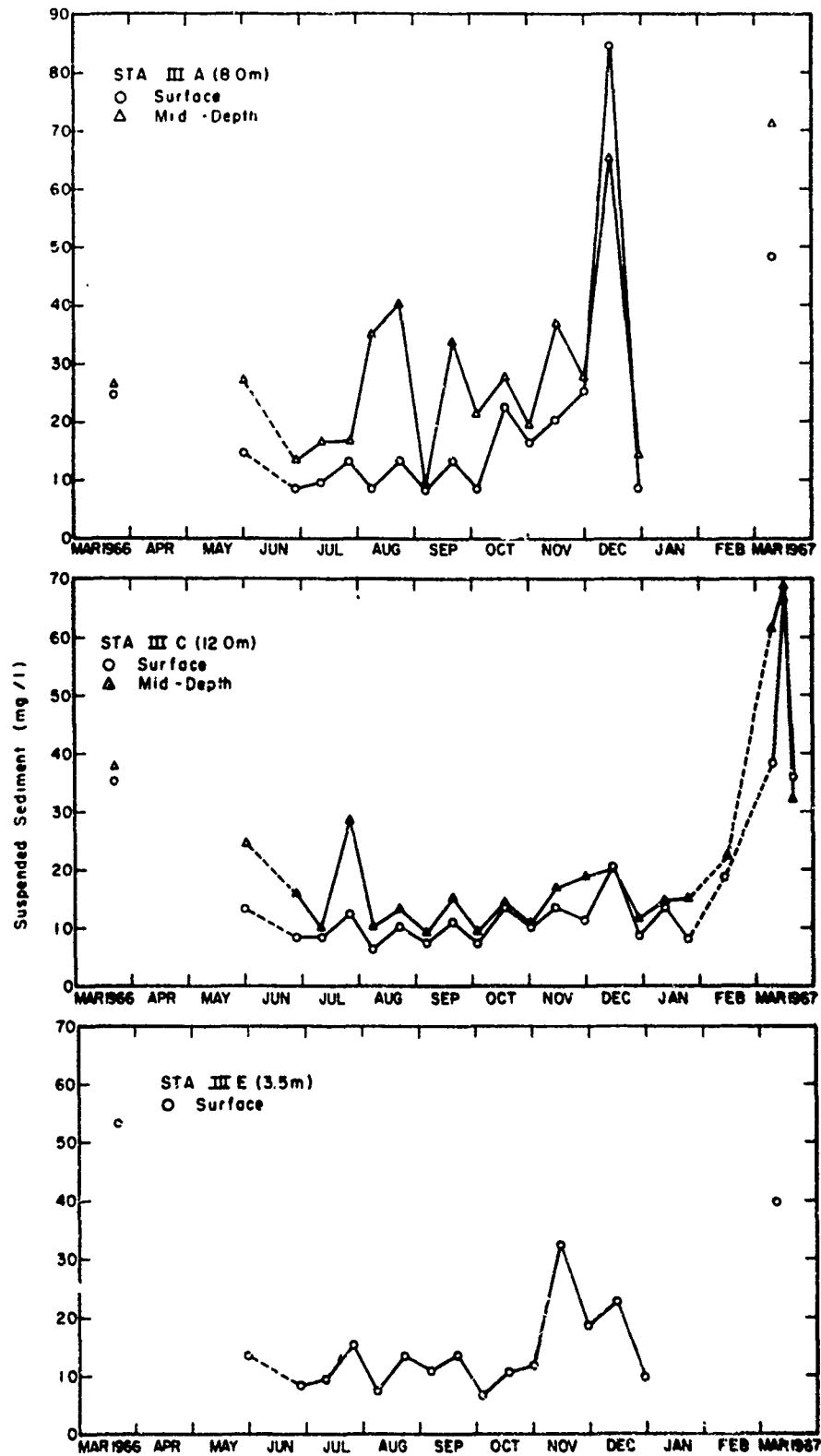


Fig. 43 Surface and Mid-Depth Concentrations of Suspended Sediment at Stations IIIA, IIIC, and IIIE, plotted against the Date of Sample Collection.

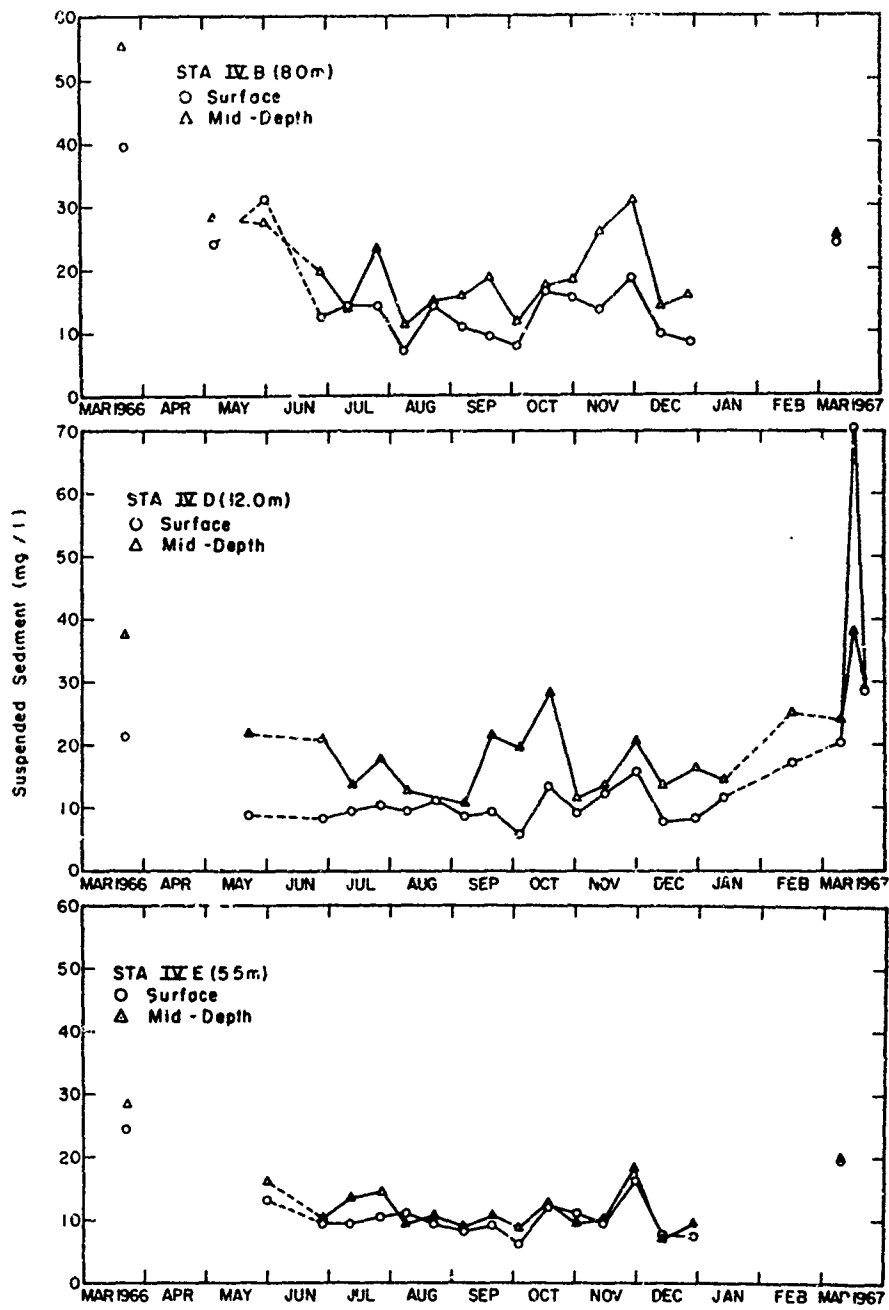


Fig. 44 Surface and Mid-Depth Concentrations of Suspended Sediment at Stations IVB, IVD, and IVE, plotted against Date of Sample Collection.

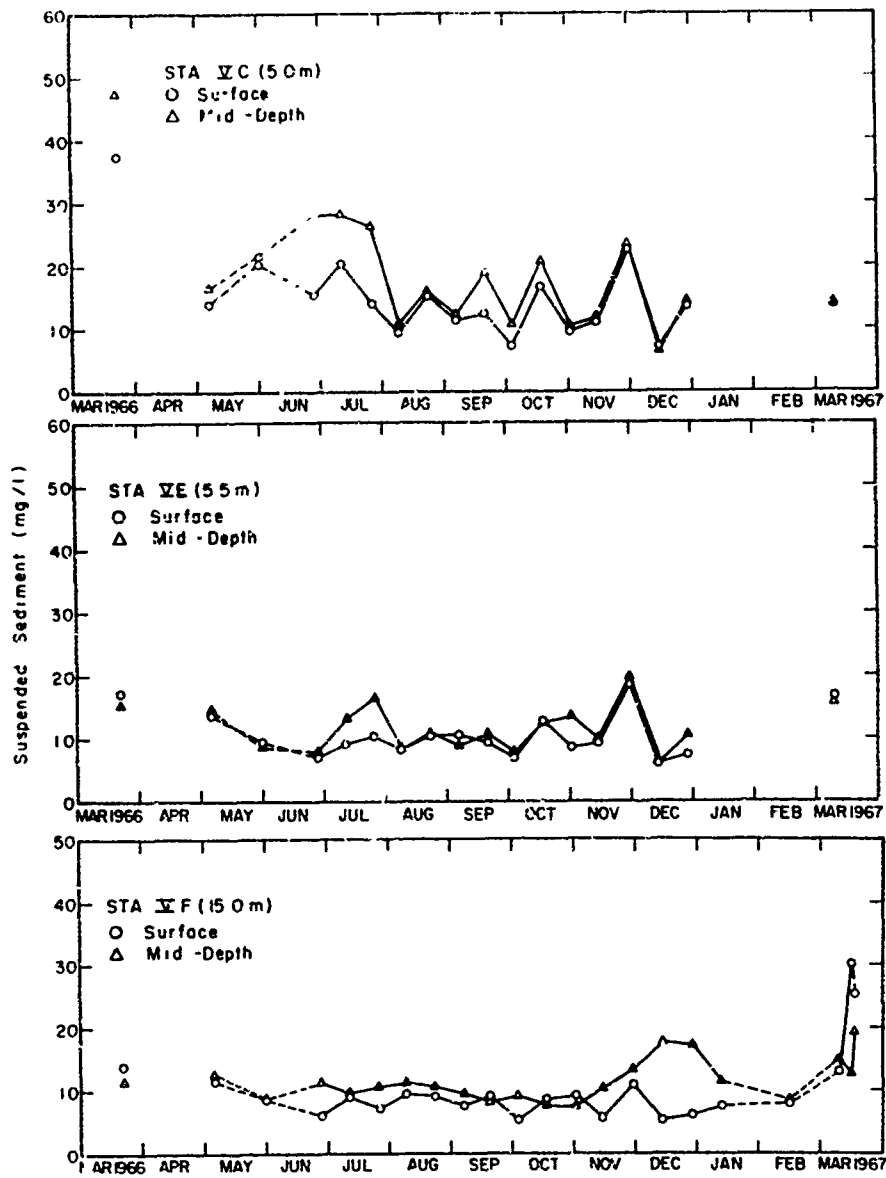


Fig. 45 Surface and Mid-Depth Concentrations of Suspended Sediment at Stations VC, VE, and VF, plotted against the Date of Sample Collection.

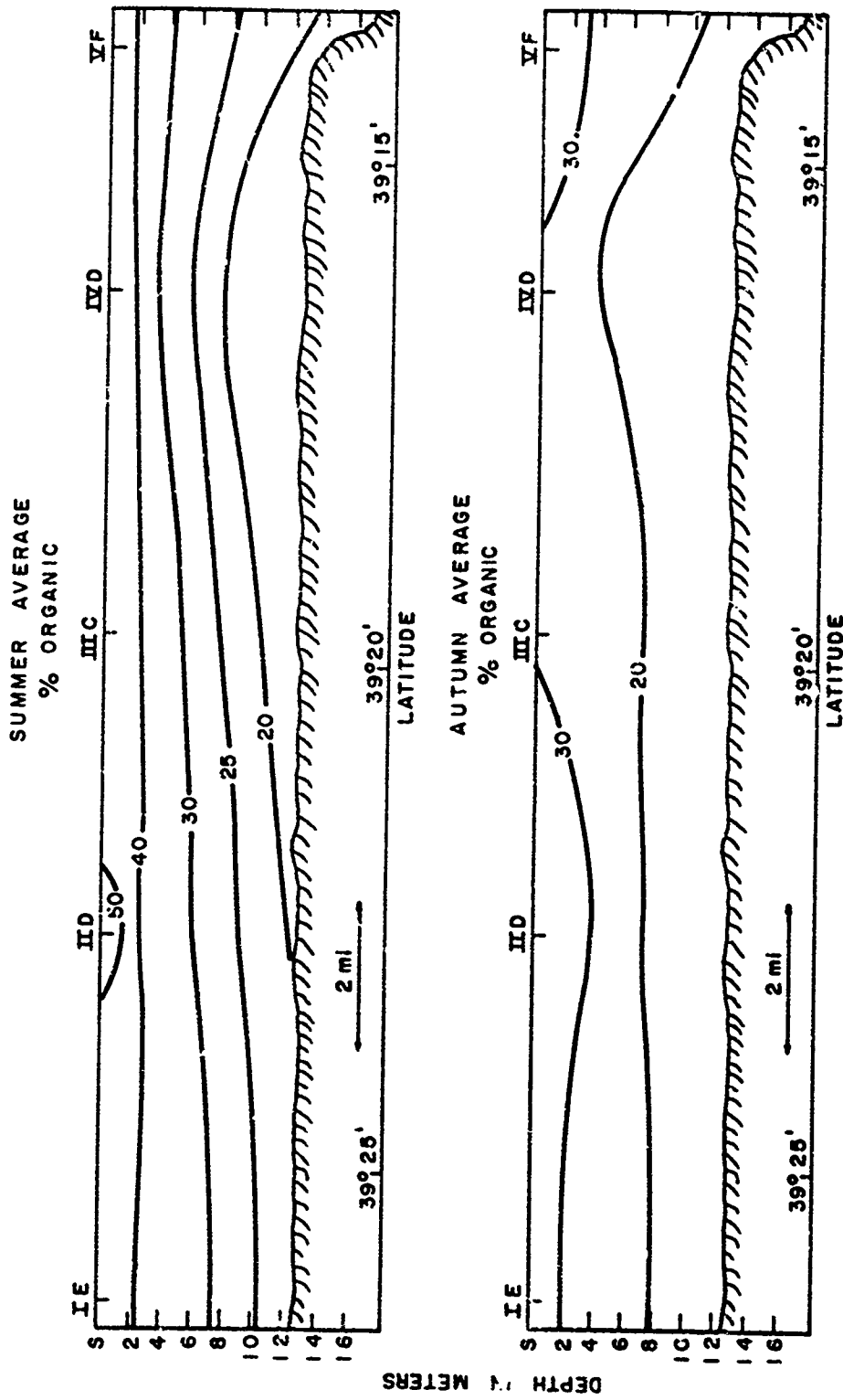


Fig. 46 Average Distributions of the Percent of the Total Suspended Solids Accounted for by Combustible Organic Matter during Summer 1966 (16 June - 30 September) and Autumn 1966 (1 October - 15 December).

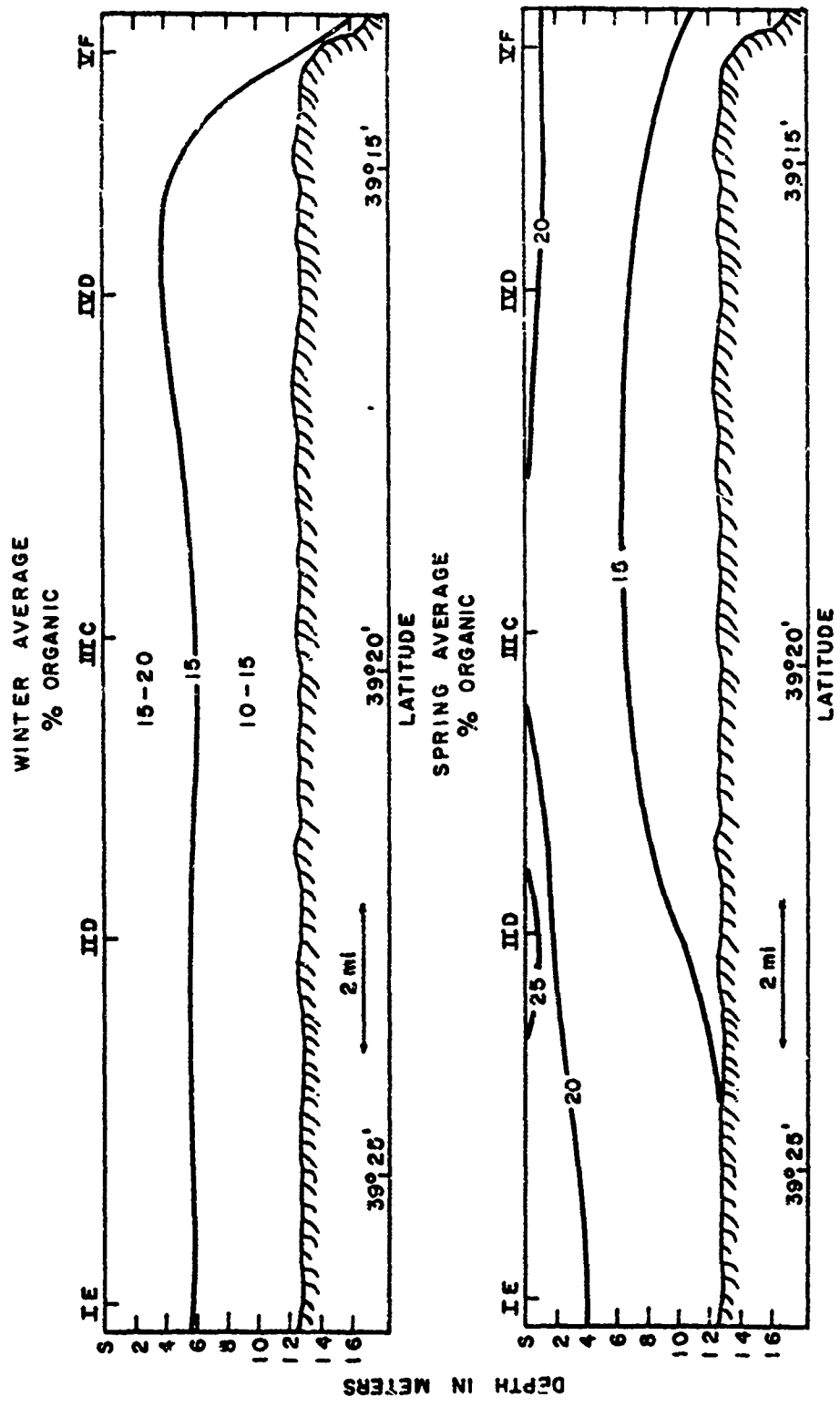


Fig. 47 Average Distributions of the Percent of the Total Suspended Solids Accounted for by Combustible Organic Matter during Winter 1966-1967 (16 December - 14 March) and Spring 1966 and 1967 (15 March - 15 June).

SIZE ANALYSIS

## INTRODUCTION

Only two methods of particle size analysis have been widely used for sizing particles in the subsieve range--microscopic analysis and sedimentation. In addition, optical methods based on light scattering have frequently been used to study one type of fine-grained particles--suspended sediment.

Microscopy is the most direct of all particle sizing methods, and is frequently used as a calibration technique for other methods. Microscopic examination can provide information on particle shape and composition as well as size. However, microscopic procedures are tedious, time consuming, and frequently inaccurate--particularly for broad size-distributions. The lower limit of the range of measurement is set by the limit of resolution of the microscopic set-up which is being used, Table 6. Although there is no corresponding upper limit imposed by the optical system, there is a practical limit. Large particles occur infrequently in natural populations of fine-grained sediments so that the probability of actually seeing them in the usual small sample is slight. In addition, it becomes increasingly more difficult to measure larger and larger particles because of their large thicknesses in relation to the depth of focus. The upper limit set by these conditions is not so definite

TABLE 6

Ranges of Applicability of Various Microscopic Techniques

Method	Normal Size Range (microns)
Transmitted white light	0.4 - 250
Transmitted green light	0.25 - 250
Transmitted ultraviolet light	0.10 - 100
Ultramicroscopy using ultraviolet scattered radiation	0.01 - 100
Electron microscopy	0.0005 - 5

as the lower limit set by the optical system, but it is just as real.

For many purposes the number statistics given by microscopic size analysis are not as valuable as other statistics such as area, volume, or weight. The transformation of number percentages into other statistics is generally not satisfactory except for very narrow size distributions because of the distorting effect of a few large particles.

Sedimentation methods have been widely used in the size analysis of fine-grained sediments. All sedimentation methods are based upon the relationship between particle size and settling velocity as derived from Stokes' Law. Stokes' Law applies reasonably well to particles in the size range from  $0.1 \mu$  to about  $50 \mu$ . However, particles as large as several thousand microns have been satisfactorily sized by sedimentation using one of the modifications of Stokes' Law such as those suggested by Oseen (1910), Goldstein (1929), or Rubey (1933). Stokes' Law was derived for a spherical particle of uniform density. Natural fine-grained sedimentary particles are seldom spherical, and populations are rarely of uniform density.<sup>1</sup>

---

<sup>1</sup> Industrial fine-grained materials are seldom spherical either, but if they are monomineralic, satisfy the condition of uniform density. Stokes' Law may thus be expected to be more exactly applicable to industrial particles than it is to natural sediments. The conditions under which Stokes' Law provides a satisfactory approximation are discussed later.

Sedimentation analyses measure the weight or volume distribution. The transformation of a weight or volume distribution to its number distribution, like the inverse transformation previously mentioned, is usually equivocal.

A number of investigators have used light scattering techniques to study suspended sediments in marine waters. The observations are relatively quick and easy to make, but are difficult to interpret usefully. An equation for light scattering by particles small compared with the wavelength of light ( $r \leq 0.1\lambda$ ) was derived by Rayleigh (1881). Rayleigh's Law was extended by Mie (1908) and Jobst (1925) for larger particles such as those characteristic of naturally occurring suspensions. The restrictive underlying conditions of isotropic spherical particles of known refractive index are seldom, if ever, realized in natural particle populations<sup>2</sup>. In addition, a particle size distribution must be assumed. The net result is that the average size value which is obtained is difficult to evaluate.

Even from our brief discussion of methods it is apparent

---

<sup>2</sup> Aerosols are a notable exception. Aerosols are suspensions of generally spherical and isotropic liquid droplets in a gaseous phase. In addition, they generally have a narrow size distribution. Because of these factors, light scattering techniques have been successfully used for sizing aerosols.

that no single method of size analysis is completely suitable for the measurement of suspended sediment. The information content of the three methods is in no case coextensive, and the underlying assumptions are very different. Most suspended sediment populations are characterized by broad size distributions composed almost entirely of nonspherical particles of widely varying densities. These considerations led to the author's determination of the size distributions of Chesapeake Bay suspended sediments both by microscopy and by sedimentation--the number frequency distribution by the former, and the volume distribution by the latter.

Since the validity of any size analysis and its usefulness for comparison with other analyses depends heavily upon the precise techniques used, the procedures employed by the author will be described in detail. However, we must first define our terms.

#### Some Definitions

"I hate definitions." Disraeli

Since the size of a particle is the object of a size analysis, we had better know what we mean by "particle." For our purposes a particle is any identifiable, naturally occurring object having a definite geometric figure. The stipulation that

it be identifiable distinguishes it from the conceptual fluid particle of fluid mechanics, and the requirement that it be naturally occurring tells us that we are concerned with the aggregates and agglomerates which occur in situ, and which survive the analysis, as well as with any homogenous single particles which we may encounter. Our interest is in the naturally occurring, in situ size distribution. To realize our definition it is essential that our methods of collection and analysis neither destroy those composite particles which occur in estuarine waters, nor artificially increase their number.

Aggregates and agglomerates are alike in being composite. They differ in the nature of the forces which bind their components and in the strengths of those forces. Aggregates are strongly bound by intermolecular, by intramolecular, or by atomic cohesive forces. They are stable under high speed mixing, ultrasonics, and, indeed, under all customary handling and dispersion techniques. Thus, they place no burden on the investigator. Agglomerates are bound by relatively weak forces including those arising from electrostatic fields, surface tension, and sticky organic matter. In reports of size analyses made for industrial purposes, the term flocculate has frequently been used as a synonym for the term agglomerate. In studies of sediment, however, most investigators have reserved, at least conceptually, the term flocculate for a subset of the

set of all agglomerates--those agglomerates bound by electrostatic forces. In practice, the discrimination between floculates and other agglomerates has nearly always been based on inadequate evidence. Just as to some men all geese are swans, to many "sedimentologists" all composite particles are floculates. On the basis of the available data, the importance of the flocculation of sediments in natural waters has, in this author's opinion, been greatly exaggerated. Since agglomerates are weakly held together, the investigator interested in in situ size distributions must exercise extreme care during sedimentation analysis or he will destroy them. He must be equally careful to see that his methods do not induce additional agglomeration. The risk of destroying natural agglomerates may be reduced by gentle treatment throughout the analysis. However, prevention of the formation of additional agglomerates requires vigorous dispersion. If the investigator is to steer safely between Scylla and Charybdis he must restrict himself to moderate dispersion, and to assure himself that the passage has been successfully made he can and should, after analysis, check his samples microscopically against untreated controls.

The size of a particle may be defined by any measure characteristic of the fineness of its subdivision. Since naturally occurring particles are usually irregular, and therefore have no unique diameter in the mathematical sense, it will be necessary for us to construct a "particle diameter" to describe its size. This diameter

is to be defined in two different ways corresponding to the two methods of size analysis used. For microscopic analysis the diameter of a particle,  $D_m$ , is the diameter of the circle with area equal to the projected area of the particle. For sedimentation analysis the diameter of a particle,  $D_s$ , is the diameter of an equivalent sphere having the same density as the particle and the same settling velocity as the particle in a fluid of the same density and viscosity.  $D_s$  and  $D_m$  for any given particle need not be equal, and seldom are.

The choice of a measure which best describes the size of a particle is a vexed question, and some brief defense of our selections must be made. Such measures are not limited to those with dimensions of length. Measures with dimensions of volume, velocity, and area have also been advocated.

The measure most commonly chosen is the "diameter" but the definitions of "diameter" offered have been myriad. The diameter of a particle may be any straight line drawn through its center of mass and terminating at its boundaries. The term diameter is unequivocally defined only for spheres and circles. For these shapes, and only for these, are the concepts of "diameter" and "size" equivalent. For any irregular particle there is an infinity of diameters whose distribution is continuous between some upper and lower bounds. If "the diameter" is to be a meaningful measure of the size of an irregular particle, it must be defined as some one of the possible statistics associated with the diameter distribution. The number

TABLE 7

## Some Definitions of Means

Mean	Definition
Arithmetic mean of diameters	$\frac{1}{n} \sum_{d_i=d_{\min}}^{d_{\max}} d_i$
Geometric mean of diameters	$\left( \prod_{d_i=d_{\min}}^{d_{\max}} d_i \right)^{\frac{1}{n}}$
Harmonic mean of diameters	$\left( \frac{1}{n} \sum_{d_i=d_{\min}}^{d_{\max}} \frac{1}{d_i} \right)^{-1}$

$n$  = number of diameters measured,  $d_{\min}$  = minimum diameter,  
 $d_{\max}$  = maximum diameter.

and variety of statistical measures that might be constructed is strictly unlimited. A few of them that have obvious appeal as being computationally simple are the geometric mean, the harmonic mean, and the arithmetic mean diameters, Table 7. At the simplest, the labor required to accumulate the diameter data and to calculate the statistical measure is inordinate. Attempts to size

sediments by following these definitions have been reduced to triviality by the inordinately small sample sizes forced on the investigator. Faced with the practical necessity of measuring large samples, the investigator, using microscopic techniques, is forced to adopt either highly simplified numerical approximations or graphical methods. Our definition for  $D_m$  is the most popular and lends itself to easy determination with available globe and circle gratitudes, such as those of Fairs (1943) and Patterson and Caswood (1936), or with the Zeiss Particle Size Analyzer TGZ 3 which the author used.

In contrast with the results of microscopic analysis, those of sedimentation analysis are generally expressed in terms of a Stokes' equivalent diameter, our  $D_s$ .  $D_s$  is called "diameter" but it is, in fact, a "velocity." Two particles having the same  $D_s$  will settle with the same speed in a fluid. Their shapes, surface areas, and volumes may differ markedly as may any of their orthodox statistical size measures. Only the equivalence of their settling rates is asserted. For this reason some investigators have reported the results of their sedimentation analyses in terms of velocities with dimensions  $L T^{-1}$  rather than in terms of diameters, dimension L, as conceptually more honest.

An attractive alternative measure which compensates for the shape effect of irregular particles was offered by Wadell (1932). He proposed a true nominal diameter which he defined as

the diameter of a sphere having the same volume as the particle in question. Although appealing and useful for describing some coarse-grained sediments, the volume measurements required by the definition makes it impossible to apply to fine-grained particles.

The author's choice of diameters,  $D_m$  and  $D_s$ , was guided by several considerations.  $D_m$  was chosen first because it has been shown that more reliable information can be obtained more rapidly from area comparison than from the comparison of linear dimensions (Hamilton, Holdsworth, and Walton, 1954), and second, the Zeiss Particle Size Analyzer is available to provide semi-automatic determinations of  $D_m$  from photomicrographs. For  $D_s$  there is hardly a choice. It is the only practical definition of diameter for sedimentation size analysis. Sedimentation analysis is a necessity since it provides the only practical way of determining the volume size distribution of the suspended sediment which is very important geologically.

It is apparent even from this brief discussion that the determination of the size distribution of irregular, fine-grained particles is not only an extremely difficult task, but that the results may be misleading unless the size terms are precisely defined. In addition, particle size data determined by different methods must be compared with extreme caution.

## Photomicrographic Size Analysis

Of all the available methods of size analysis, microscopy is the most direct, and in many ways, the most amenable to the determination of the in situ size distribution of fine-grained suspended matter. Microscopic sizing consists of the actual measurement of the particle images rather than some physical property more or less remotely connected with size, and it requires no sample dispersion or pretreatment which might alter the original size distribution. Since one must look at individual particles, microscopy also provides information on particle shape, degree of agglomeration, and on the composition of the suspended matter. Microscopic size analysis supplies a primary direct check on all indirect methods of size analysis including the volume size analysis using the MSA Particle Size Analyzer employed by the author.

The appealingly simple direct observation of the particles themselves with optical micrometers or gratitudes was abandoned in favor of the Zeiss Particle Size Analyzer TGZ-3, a semi-automatic instrument that gives reliable results rapidly. To secure these advantages, photography must intervene and direct observation be removed one step. However, introduction of photography provides a permanent record, gives precise control of the magnification, and permits the manipulation of photographic

contrast ( $\gamma$ ) to make the particles clearly visible against the background of the mounting medium.

A serious disadvantage of photomicrography is that the focus must be fixed at the time of exposure and some particles may be badly out of focus. In samples where particles differ greatly in thickness, it may be necessary to make several exposures of the same field at different focal settings. A single exposure, however, was found to be satisfactory for nearly all of the samples analyzed in this study.

The photomicrographic sizing technique involves four steps: (1) sample collection, (2) slide preparation, (3) photography of sample, and (4) sizing the images of the particles with the Zeiss Particle Size Analyzer.

#### (1) Sample Collection

In most instances, each sample was collected by pumping water from a fixed depth with a submersible pump. The pump was reliable, fast, and easy to operate. Further, and most important, it preserved the in situ size distribution of the suspended matter. This last feature was established by collecting twelve duplicate samples, one with the pump and one with a Van Dorn bottle. The size distributions of the samples were determined. In none of the twelve pairs of samples could any significant difference be detected.

The water was pumped into one gallon jugs, swirled vigorously, and three to five subsamples of 15 to 100 ml were filtered immediately through millipore GS (0.22  $\mu$ ) filters of 47 mm diameter using a manifold. The subsamples must be filtered with the least possible delay because the flocculation which occurs on storage renders any attempt to determine the in situ size distribution of the suspended matter almost worthless. The filter pressure was maintained above 400 mm of Hg at all times to minimize the disruption of flocculates and fragile organisms. After filtration of each sample, the filter and filtrate were thoroughly washed with distilled water to remove soluble salts. They were then removed from the filter support, inserted in a small plastic holder, and stored in a desiccated box.

The volume of water filtered at each depth was dictated by the concentration of the suspended matter. For size analysis the ideal sample is a single-particle layer with no particle touching another. For mass determination the sample should be as large as possible. These requirements on sample size are in direct conflict. The usual procedure of obtaining a single large sample and using it for both analyses is totally unsatisfactory. Although it provides adequately for mass determination, for microscopic examination the material is piled too thickly on the filter, thus obscuring many of the particles, causing agglomeration, and masking the true size distribution. On the other hand, the small

samples amenable to size analysis are not suitable for mass determination. No compromise is possible. The only solution is to collect separate samples, large samples for mass determinations and small samples for size analyses.

## 2. Slide Preparation

The primary reason for selecting cellulose membrane filters is that they can be made transparent, thus allowing the filtrate to be examined microscopically in transmitted light. Cellulose membrane filters become transparent when their pores are filled with a liquid whose index of refraction is very close to that of the cellulose ( $n = 1.510$  for Millipore GS filters). Suitable clearing liquids include cedar oil, Karo syrup, Tween 80<sup>3</sup>, and Permout<sup>4</sup>. The most transparent membrane results from drawing serial dilutions of either cedar oil in alcohol or Karo syrup in water through the filter as suggested by Goldberg, et. al. (1952). The cleared membrane, or a portion of it, can then be put on a slide and covered with a cover slip or it can be mounted in balsam. For most purposes a membrane can be satisfactorily cleared and mounted by the following simpler and faster method. Put several drops of cedar oil or Permout on a glass microscope

<sup>3</sup> Atlas Powder Co., Wilmington, Delaware.

<sup>4</sup> Fisher Scientific, Washington, D.C.

slide and carefully lay the membrane, or a section of it, face up, on top. Next, cover the membrane with a cover slip and tap it gently being careful to avoid any relative motion between the cover slip and the membrane. Using this method the author prepared three slides for each depth at which the size distribution was to be determined. Each slide was made from a pie-shaped section cut from a different membrane. There was no bias at this stage because the "data" were invisible to the naked eye.

The most important optical property of a mounting medium is its index of refraction. If the difference in refractive index of the mounting medium and the particles is too great, excessive contrast results, edge detail is lost, and the details of flocculates may be impossible to determine. If, on the other hand, this difference in refractive index is too small, the contrast will be very low, many particles may be overlooked, and it may be difficult to determine their edges. Under ordinary light microscope conditions colorless transparent particles are visible only in outline and only then when they differ in refractive index from the mounting medium. A large percentage of the suspended particles in the Chesapeake Bay are very nearly colorless, have indices of refraction very close to 1.51, and are hence nearly invisible when mounted in one of the media suitable for clearing Millipore filters. The particles were most clearly visible when

the membranes were examined under phase microscopy. The phase microscope transforms small changes of phase produced by small differences in optical path into changes of amplitude (brightness) which can then be detected by the eye or by a photographic plate. The optical path is the product of the thickness of the transmitting medium and its index of refraction, and the differences in optical path are due to differences in either of these factors, or both. When light traverses materials with different optical paths, phase differences are produced. These phase differences, which cannot be detected by the human eye, are converted to amplitude differences by the phase microscope, and thus become visible. A good discussion of phase microscopy can be found in Bennett, et. al. (1951).

### 3. Photography of Sample

The microscopic system and the photographic procedures are given in detail because of their effects on the apparent size distribution (Loveland, 1959). The cleared membranes were photographed on Kodak Pan X film with a 35 mm Zeiss Ikon camera mounted on a Zeiss Standard Universal Pol microscope. The film was developed in Kodak Microdol-X developer under strict time and temperature controls. The microscope was equipped with an Achromatic-aplanatic Bright-Field Phase-contrast Dark-field Condenser VZ (Zeiss catalog number 485276) with a numerical aperture of 1.4.

The light source was a 6V-15W lamp built into the base of the microscope. It was adjusted in accordance with the Kohler principle before each picture taking session, or whenever objectives were changed. The light was filtered with a green interference filter (max. transmission at  $546 \text{ m}\mu$ ) to increase resolving power. Two objectives were used, a Neofluar Ph 40/0.75 and a Planachromat 100/1.25 (Zeiss catalog numbers 46 07 21 and 46 19 11). The former was the working objective. The latter was used primarily as a check to get an idea of the number of particles below the resolving power of the 40X objective. For photography, both objectives were used in conjunction with an 8X eyepiece, and with the Optovar set at 1.25. The approximate observed magnification using the 40X objective was  $40 \times 8 \times 1.25 \approx 480$ . The camera factor is 0.5X, hence the image magnification was approximately 240. The 40X objective has a theoretical useful magnification of approximately 1500 and the 100X objective of approximately 2500. The negatives taken with the 40X objective were enlarged to 2000X thus producing some empty magnification. Parallel analyses with the 100X objective indicated however, that the empty magnification did not falsify the determination of the size distributions. The upper limit of useful magnification is a theoretical limit, and not a practical one. The additional "empty" magnification in this case proved to be valuable since our interest was in the particle size distribution, and the further magnification made measurement

of the finer particles much easier. The smallest particle image which can be measured with the Zeiss Particle Size Analyzer on the standard range used in this study is 1.2  $\mu$ m. The method of determination of the final magnification of the enlarged photographs is explained below.

The fields which were photographed were selected without prior observation according to a previously chosen area pattern based upon mechanical stage graduations. The area pattern insured a reasonable coverage of the filter segment, and since the author never saw the appearance of the sample before the area was finally fixed, he was guarded against being biased in his selection by his visual impressions. The total number of fields which was photographed per sample depended on the number of particles per field. Generally six to nine fields were photographed from each of the three filter segments for a total of eighteen to thirty-six fields per sample. The resulting photographs represent a composite of portions of three subsamples from which the size distribution at that particular depth was determined for that cruise.

Each photograph was identified by the station number, sample depth, and cruise number. This information was written on an identification film strip which was inserted into a slot provided in the camera back, and was registered on the film at the time of exposure.

To determine and set the magnification of the enlargements a stage micrometer was photographed at the beginning of each roll of film. It was photographed under the same optical conditions as used for the remainder of the film and thus served as a reference for all other photographs on that roll. At the time of printing, the final magnification, generally 2000X, was selected by carefully adjusting the position of the enlarger head until the desired magnification of the micrometer scale negative was attained. A print of the scale was then made and processed with the other prints of that sample. After drying, the magnification of the micrometer scale was checked to evaluate shrinkage. The negatives were printed on Kodak Kodagraph P1 Projection Paper, a high contrast paper on ultra-thin stock. This paper was chosen because of the necessity of having a translucent photographic paper for analysis with the Zeiss Particle Size Analyzer TGZ-3.

#### 4. Photomicrographic Measurement with the Zeiss Particle Size Analyzer

The images of the particles on the photomicrographs were sized with a Zeiss Particle Size Analyzer TGZ-3, a semi-automatic device in which the eye and judgement of the operator participate in the measuring process. The instrument is shown diagrammatically in Fig. 48. The principal components of the instrument

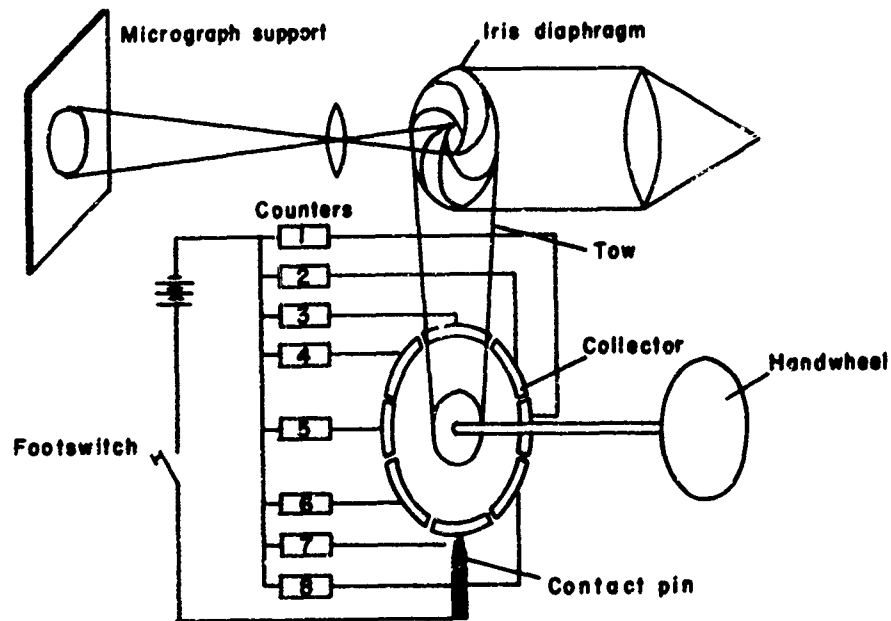


Fig. 48 Diagrammatic sketch of Zeiss Particle Size Analyzer TGZ-3.

are a light source, a lens system, and an adjustable iris diaphragm which is correlated via a commutator with 48 telephone counters, each counter corresponding to a certain aperture interval of the iris diaphragm. The instrument is also equipped with a cumulative counter which registers the total number of particles measured. The iris diaphragm is illuminated from below and is imaged as a sharply defined circular light spot in the plane of the plexiglass plate which supports a photomicrograph. The photomicrograph is moved by hand until the center of gravity of the image of a particle lies approximately at the center of the measuring mark. The particle image is then measured by adjusting the diaphragm until the light spot has an area equal to that of the particle image. For irregular particles the total area of the portions of the particle protruding beyond the measuring mark must be made equal to the re-entrant areas. Once the diaphragm is adjusted the foot-switch is depressed, the proper counter is activated, a hole is punched in the image of the particle, and the total registered on the cumulative counter is increased by one. The photomicrograph is then shifted until another particle is above the stationary measuring mark and the same procedure is followed. An experienced operator can size approximately 1000 particles in thirty minutes.

The instrument can be used to determine either frequency

or cumulative size distribution and the forty eight counters can be switched into either a linear or logarithmic sequence. The instrument is provided with two measuring ranges--a reduced range for measuring particle images of 1.0 - 9.2 mm diameter, and a standard range for measuring particle images with diameters in the range 1.2 - 27.7 mm. In situations where particle diameters fluctuate by more than a factor of 23, either two or more sets of photomicrographs of different enlargements, or a templet, is necessary.

The standard measuring range and exponentially increasing size classes were used in this study to determine the size distributions of Chesapeake Bay suspended sediment. The choices of measuring range and size classes were dictated by the broad size distribution of the suspended matter. The 2000X magnification used by the author together with the standard range of the instrument fixes the particle size diameter ( $D_m$ ) range at 0.6 - 13.85  $\mu$  (1.2 - 27.7 mm on the photomicrographs). Suspended particles with diameters greater than 13.85  $\mu$  are found in the Bay so that it was necessary to extend the upper limit of the range. The upper limit was extended with a templet overlay. This method was the most convenient since there were relatively few particles with diameters greater than 13.85  $\mu$ . The templet consisted of a series of circles with exponentially increasing diameters drawn on tracing paper. The diameters of

the circles were determined by extending the exponentially increasing size classes beyond the 48 intervals of the Zeiss Particle Size Analyzer.

Although particles with diameters less than  $0.6 \mu$  are also found in the Bay, this lower limit was not extended. Sizing below approximately  $0.6 \mu$  requires the use of an oil immersion lens, and below  $0.25 \mu$  an ultraviolet microscope must be used, Table 6. When several magnifications are used for a single sample, extreme caution must be used in combining the results.

For each group of three slides taken from a single sample at least 1500 particles, but most commonly 2000 particles were sized. The minimum number of particles to be counted was determined by a commonly accepted counting technique. Two hundred and fifty particles were sized from a sample and the first four moments of the resulting size distributions were calculated. An additional two hundred and fifty particles were then measured and the moments recalculated for the 500 measurements. The procedure of doubling the sample size and calculating the moments was continued until the moments showed no substantial change between successive cycles. This was done for fifteen samples, and in each a sample size of 1000 particles was found to be adequate to secure agreement between the moments on successive cycles to within 10 percent of the mean of each pair

of moments.

Although a sample size of 1000 is entirely satisfactory for the stability of the moments, the author was particularly interested in the frequencies of the rarely occurring large particles because of their overwhelming effect on the volume size distribution. In order to form a better idea of these, he elected to size an additional 500 to 1000 particles in most samples.

#### Results and Discussion

One hundred and sixty-one size analyses of suspended sediment from different space-time positions in the upper Bay were made with the Zeiss Particle Size Analyzer. In addition, sixty-one replicate analyses were made, making a total of 222 particle size analyses. Those statistics descriptive of the distribution of suspended sediment in the upper Bay are formed entirely from the set of 161 essentially different samples. The replicate analyses are involved only when questions of the stability of the statistics are discussed.

The number-size distributions of 12 of these samples are presented in Figures 49 and 50. The mean, the standard deviation, the skewness, and the kurtosis of each of these samples is

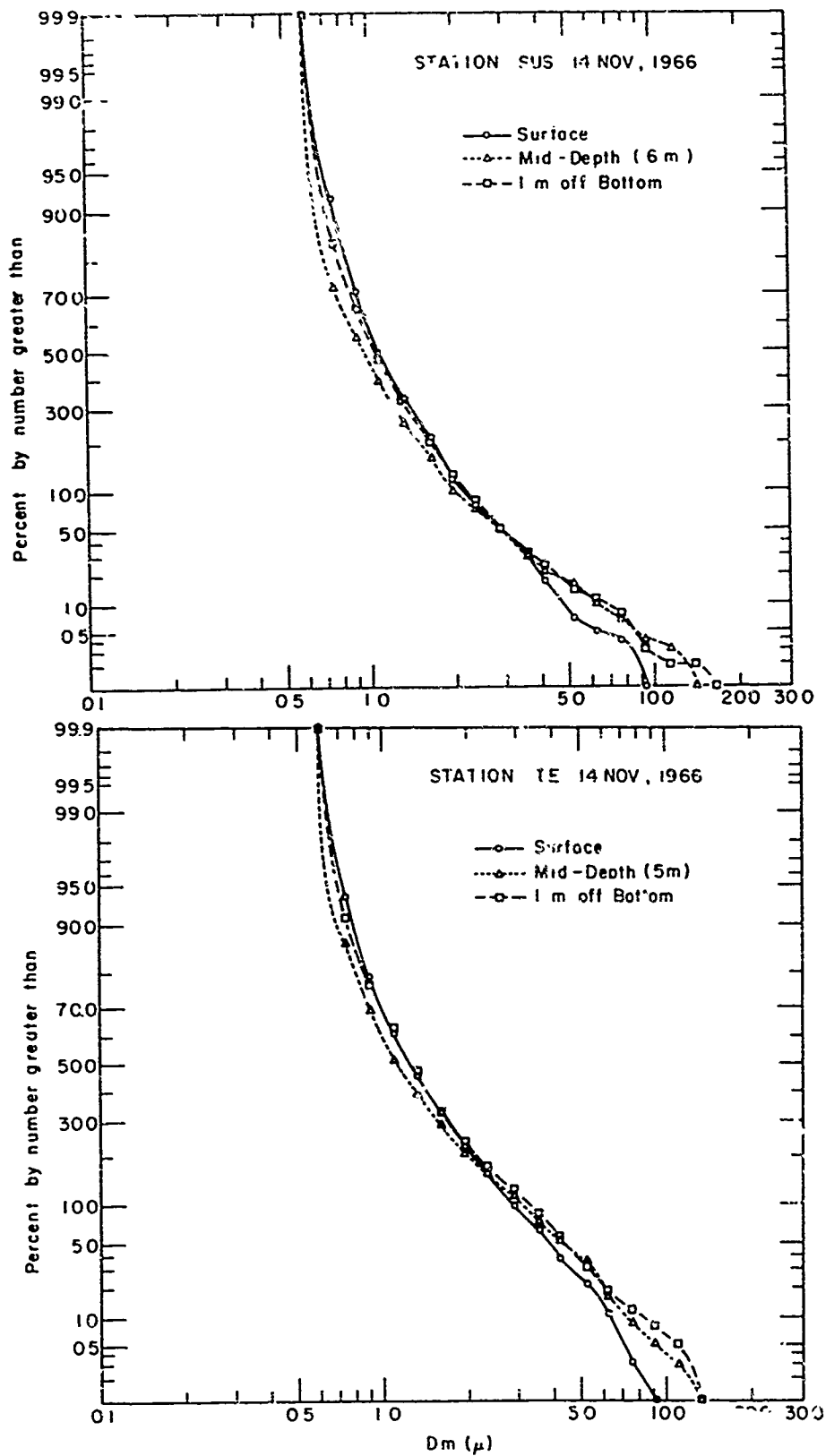


Fig. 49 Particle Size Distribution Curves of Suspended Sediment Samples from Selected Space-Time Positions in the Upper Bay

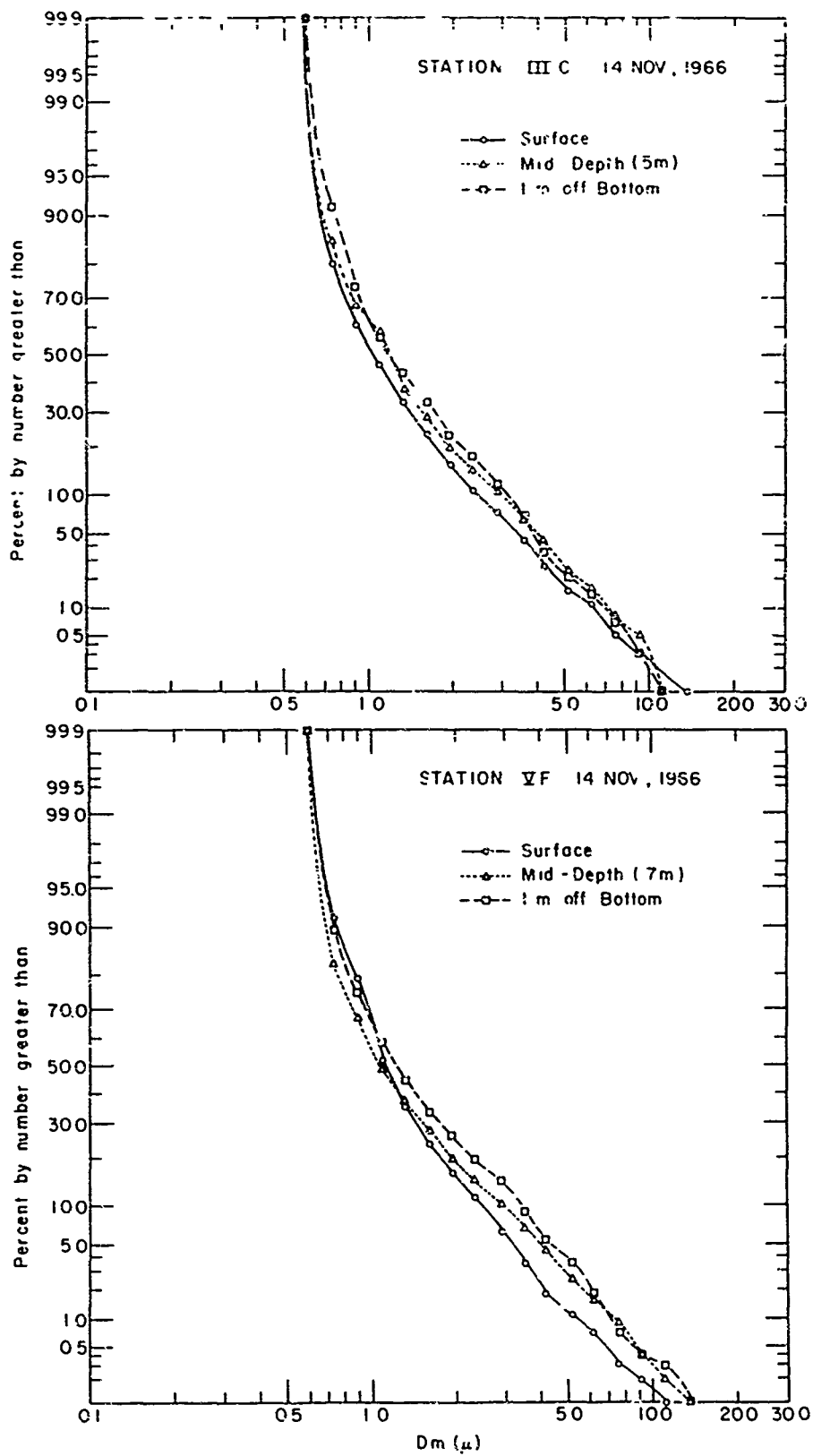


Fig. 50 Particle Size Distribution Curves of Suspended Sediment Samples from Selected Space-Time Positions in the Upper Bay.

presented in Table 8. In addition, the results of 33 other analyses are given in Appendix A.

The presentation of the entire set of 161 size analyses in this paper would require an inordinate amount of space and therefore only a representative subset of the analyses is presented. Presented here are typical analyses which depict the consistency and variability of the particle size distributions both spatially and temporally within the area.

The forty-eight size classes of the Zeiss Particle Size Analyzer and the twelve classes which were added with a template were grouped by threes to form twenty classes. The statistics which were calculated are standard moment measures. The mean is the first moment about zero, and the standard deviation the square root of the second moment about the mean. The skewness and kurtosis are defined in terms of the second ( $\mu_2$ ), third ( $\mu_3$ ), and fourth ( $\mu_4$ ) moments by

$$\text{Skewness} \equiv \frac{1}{2} \frac{\mu_3}{\mu_2^{3/2}}$$

$$\text{Kurtosis} \equiv \frac{\mu_4}{\mu_2^2} - 3$$

The twenty class midpoints,  $x_v$ , used in the calculations were defined by

$$x_v \equiv \frac{\xi_{3v-2} f_{3v-2} + \xi_{3v-1} f_{3v-1} + \xi_{3v} f_{3v}}{f_{3v-2} + f_{3v-1} + f_{3v}}$$

which reduces to

$$x_v \equiv \frac{\sum_{i=3v-2}^{3v} \xi_i f_i}{\sum_{i=3v-2}^{3v} f_i}$$

where  $\xi_i$  are the midpoints of the sixty subclasses,  $f_i$  the frequency of observations in each subclass, and  $v=1, \dots, 20$ .

The mean diameter,  $\overline{D}_m$ , showed little variability either seasonally or geographically. It generally increased with depth at each station, but the increase was usually small. The increase of  $\overline{D}_m$  with depth was attributed primarily to the resuspension of slightly coarser and pelleted bottom sediment. At most stations an increase in the concentration of aggregate particles was observed near the bottom. This increase is to be expected because much of the sediment suspended near the bottom is material derived from the bottom which is pelleted.<sup>5</sup>

$\overline{D}_m$  ranged in value from 1.1 to 2.8  $\mu$ , and in nearly 80 percent of the samples analyzed it was between 1.4 and 2.0  $\mu$ . Histograms of  $\overline{D}_m$  for the samples from the surface, from mid-depth, from one meter off the bottom, and for the entire set of

<sup>5</sup> Resuspension of bottom sediment by tidal currents is discussed in a later section.

TABLE 8

Statistical Properties of Particle Size Distributions Shown in  
Figures 49 and 50

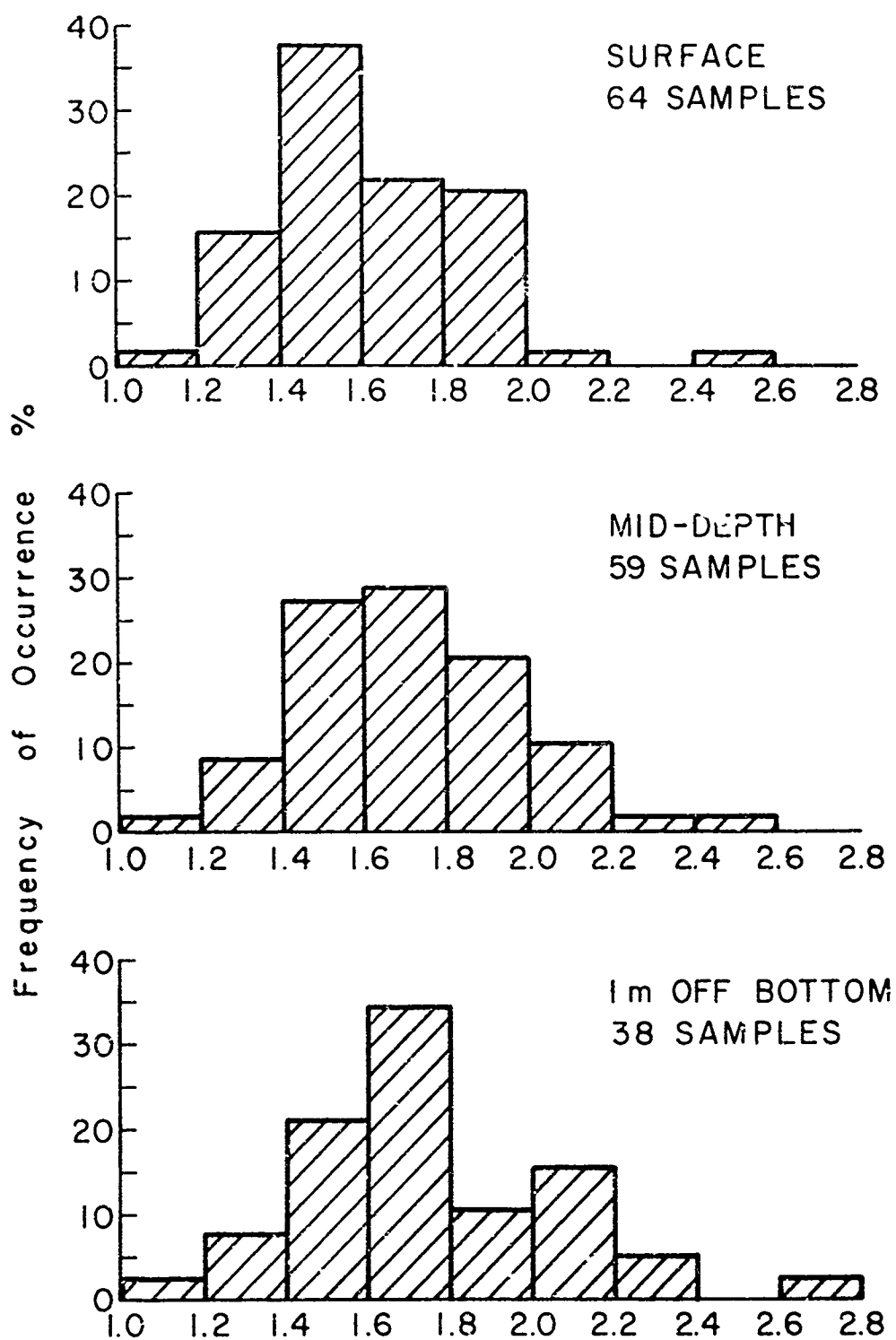
Station, Date, and Depth	Mean ( $\mu$ )	Standard Deviation ( $\mu$ )	Skewness	Kurtosis
SUS (14 XI 66)				
surface	1.4	1.0	3.4	80.0
mid-depth	1.3	1.2	4.0	107.4
1 m off bot.	1.4	1.2	3.2	62.7
IE (14 XI 66)				
surface	1.6	1.1	1.4	10.2
mid-depth	1.6	1.5	2.2	32.6
1 m off bot.	1.7	1.6	2.1	25.5
IIC (14 XI 66)				
surface	1.4	1.2	2.4	40.4
mid-depth	1.6	1.3	1.8	17.4
1 m off bot.	1.6	1.3	1.6	15.5
VF (14 XI 66)				
surface	1.4	1.0	2.1	28.8
mid-depth	1.6	1.5	3.2	76.4
1 m off bot.	1.7	1.5	1.8	22.9

161 samples are shown in Figs. 51 and 52. The uniformity of the suspended sediment particle size distribution indicates that there is considerable transport and shifting of the sediment within this segment of the Bay.

No systematic downstream decrease in  $\overline{D}_m$  was observed within this segment of the Bay. During much of the year the mean size,  $\overline{D}_m$ , was slightly greater at stations in the Bay than at the Susquehanna River station. This increase in  $\overline{D}_m$  was most apparent in the mid-depth and near bottom samples, and again was attributed to resuspension.

There was no evidence that flocculation plays an important role in the sedimentation in the region. The composite particles which were observed were organically bound agglomerates and not flocculates. The tidal currents and turbulence are apparently sufficient to overcome any flocculation forces that may exist.

There was a tendency for the mean size and the modal class to shift toward smaller values in late winter and spring. This was most marked at the Susquehanna River station where masking of the newly introduced suspended sediment by resuspended material is minimal. Histograms of the modal class, presented in Figs. 53 and 54 for various periods of the year, clearly show this shift. This change in the particle size distribution is apparently related to weathering and will be investigated.



Mean Projected Diameter,  $D_m$ , in Microns  
 Fig. 51 Frequency Distributions of Mean Projected Suspended  
 Sediment Particle Diameters for Three Depths.

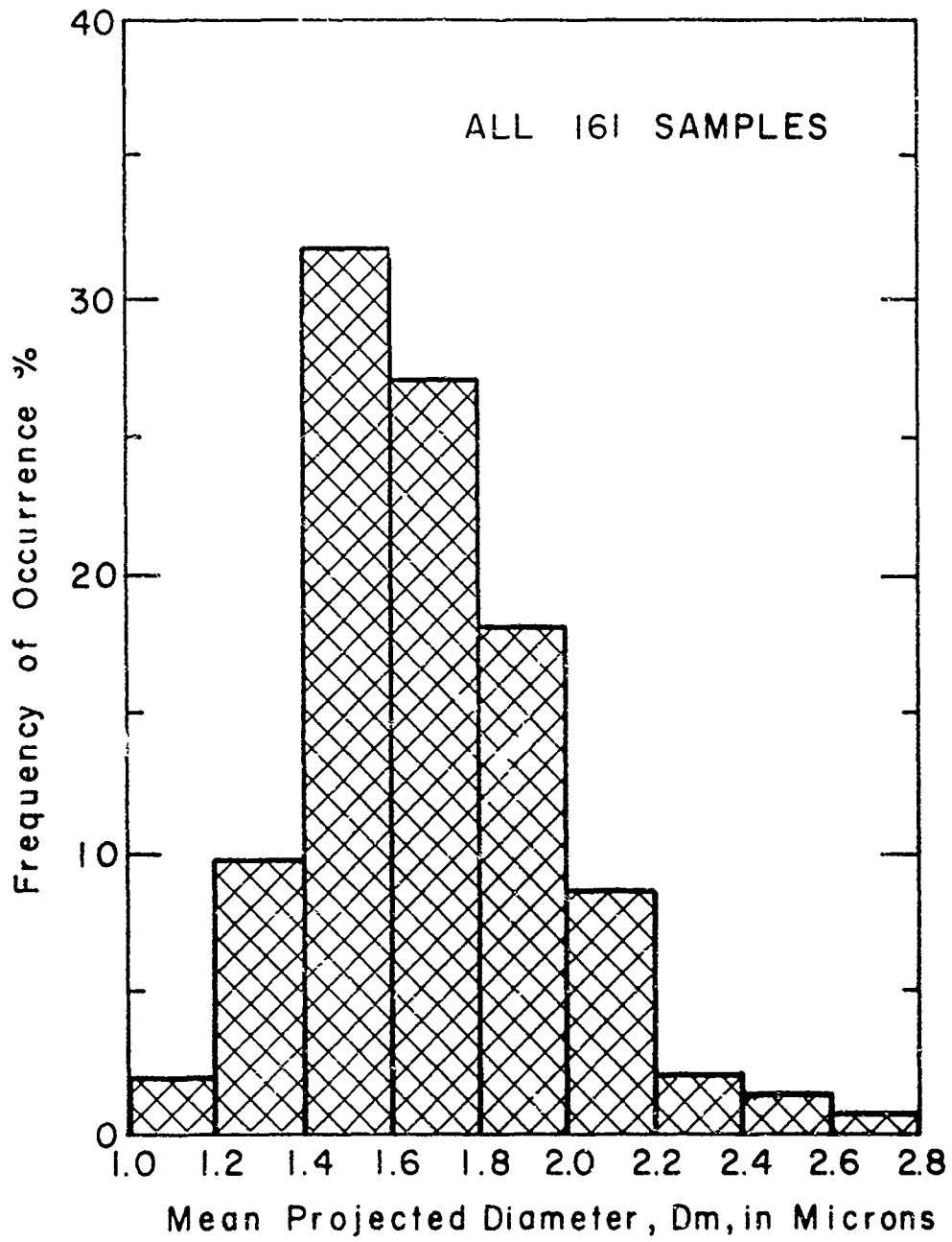


Fig. 52 Frequency Distribution of Mean Projected Suspended Sediment Particle Diameters for All 161 Samples.

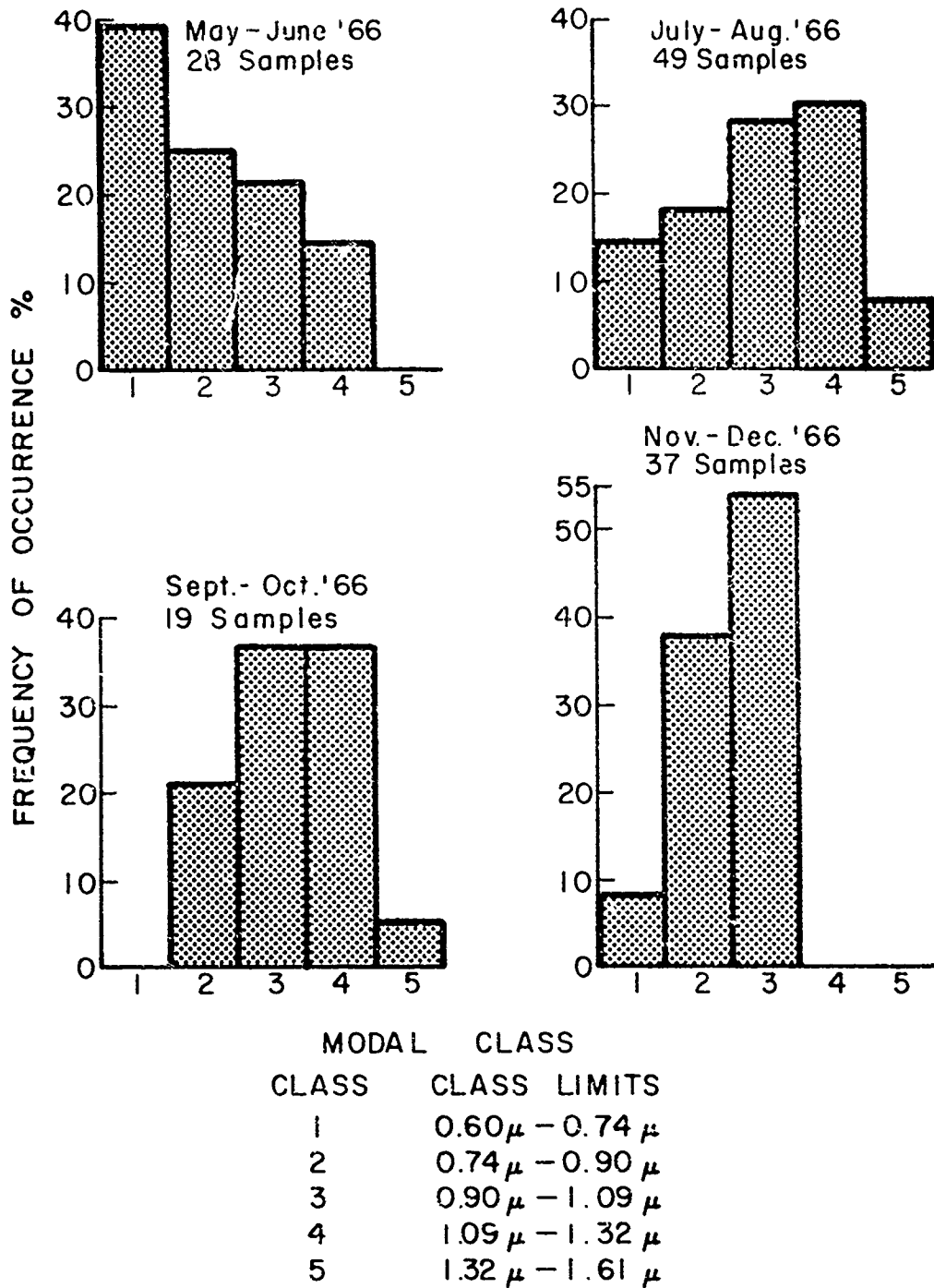
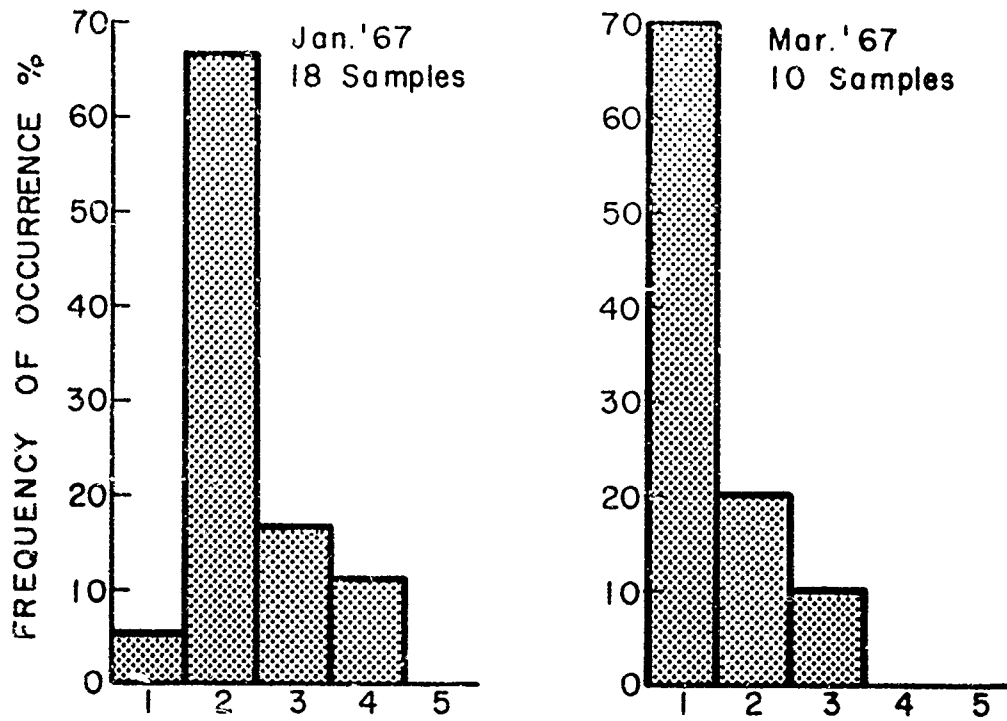


Fig. 53 Frequency Distributions of the Modal Class of Equivalent Projected Diameters ( $D_m$ ) for Samples from various Periods of the Year.



MODAL CLASS

CLASS	CLASS LIMITS
1	$0.60\mu - 0.74\mu$
2	$0.74\mu - 0.90\mu$
3	$0.90\mu - 1.09\mu$
4	$1.09\mu - 1.32\mu$
5	$1.32\mu - 1.61\mu$

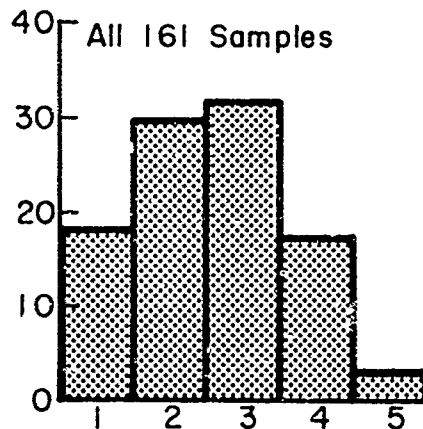


Fig. 54 Frequency Distributions of the Modal Class of Equivalent Projected Diameters ( $D_m$ ) for Samples from January and February 1967, and for All 161 Samples.

The number of suspended colloidal ( $D_m < 0.5\mu$ ) particles increased sharply during the period of maximum runoff, March and early April. These particles, however, are below the limit of resolution of the microscopic system used by the author and therefore were not sized. Even during this period, the colloidal particles account for at most a few percent of the total mass and volume of suspended sediment. In spite of their small mass and volume however, colloidal particles have a very profound effect on the optical properties of the water during this period. The large increases in extinction coefficients resulting from the large numbers of colloidal particles render optical methods of estimating suspended sediment concentrations questionable under such conditions.

The skewness and kurtosis are of unknown significance and are much less stable than the mean and the standard deviation. Their instability results because they are defined in terms of higher moments, and the higher the moment, the greater the relative weighting of the large deviations. It follows that the kurtosis, which is defined in terms of the fourth moment, is less stable than the skewness which is defined in terms of the third moment. Because of their high degree of sensitivity to fluctuations in the tail regions of the distribution, both measures are restricted in their usefulness unless a very large number of measurements have been made. The skewness ranged from

1.5 to 4.5, and the kurtosis from 2.6 to 150.1. In all of the samples, the skewness was positive which means that more than half of the deviations were on the left (negative) side of the mean, but that the majority of the large deviations were on the right (positive) side. It should be remembered that the particle size distributions were truncated at the lower end at about  $0.5 \mu$ .

The volume transformations of the number-size distributions are shown in Figs. 55 and 56, and in Appendix A. To effect the transformations the conventional assumption was made that each particle population was made up of a polydisperse system of spheres, and consequently no shape factors were employed. This assumption of course is not true, and its implications must be examined.

Particle shape is an important factor in transforming number distributions into volume distributions because the projected diameters,  $D_m$ , are converted into volume diameters,  $D_v$ , where  $D_v$  is defined as the diameter of a sphere with the same volume as the particle in question. If the volume diameters obtained by this transformation are to provide a useful measure of the true volume diameters, either the particles should be approximately spherical, or shape factors should be employed in making the transformation. Shape factors must be determined by the direct measurement of two or more dimensions of a large

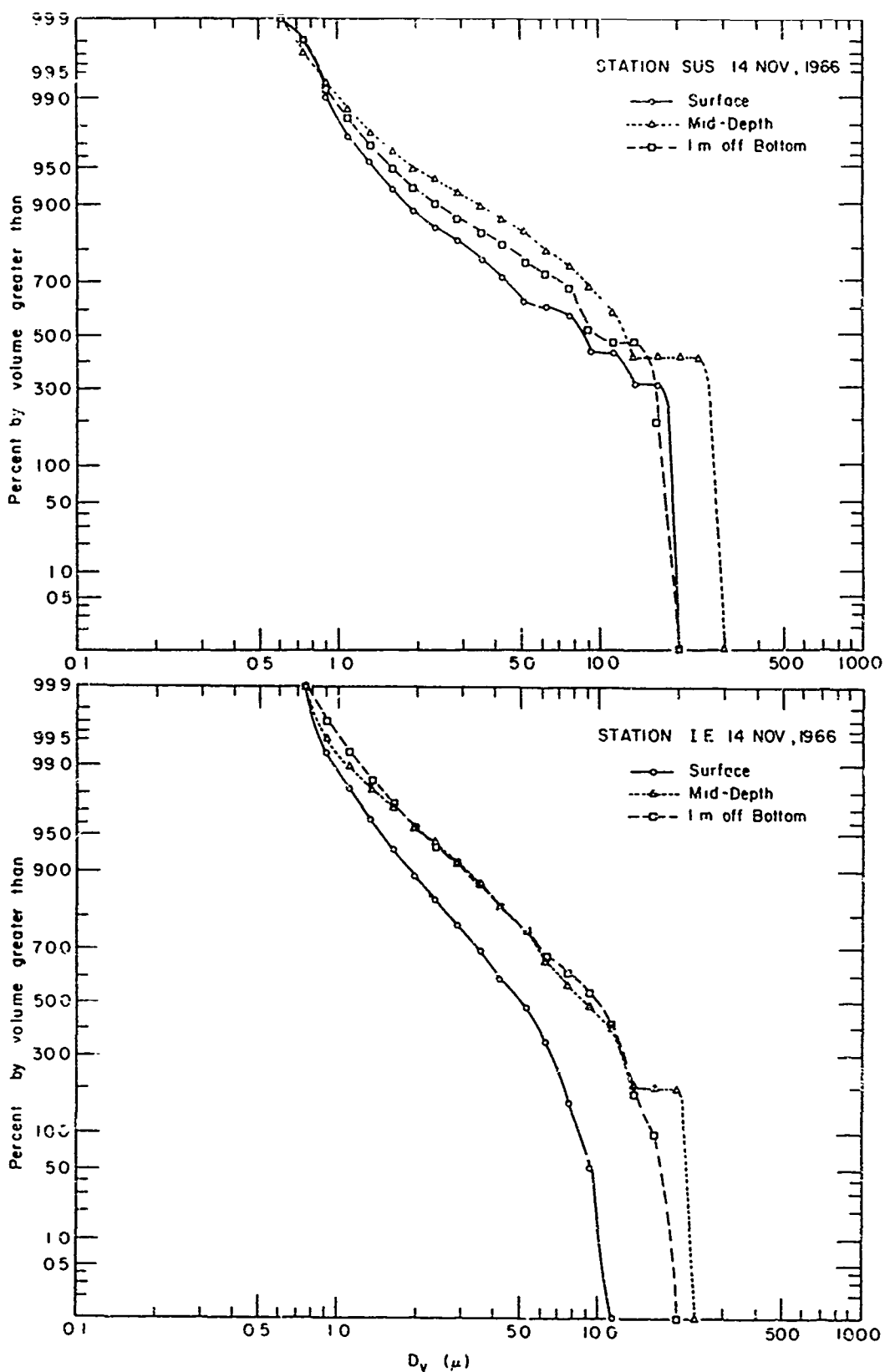


Fig. 55 Volume-Size Distribution Curves obtained by Transformation of Number-Size Data.

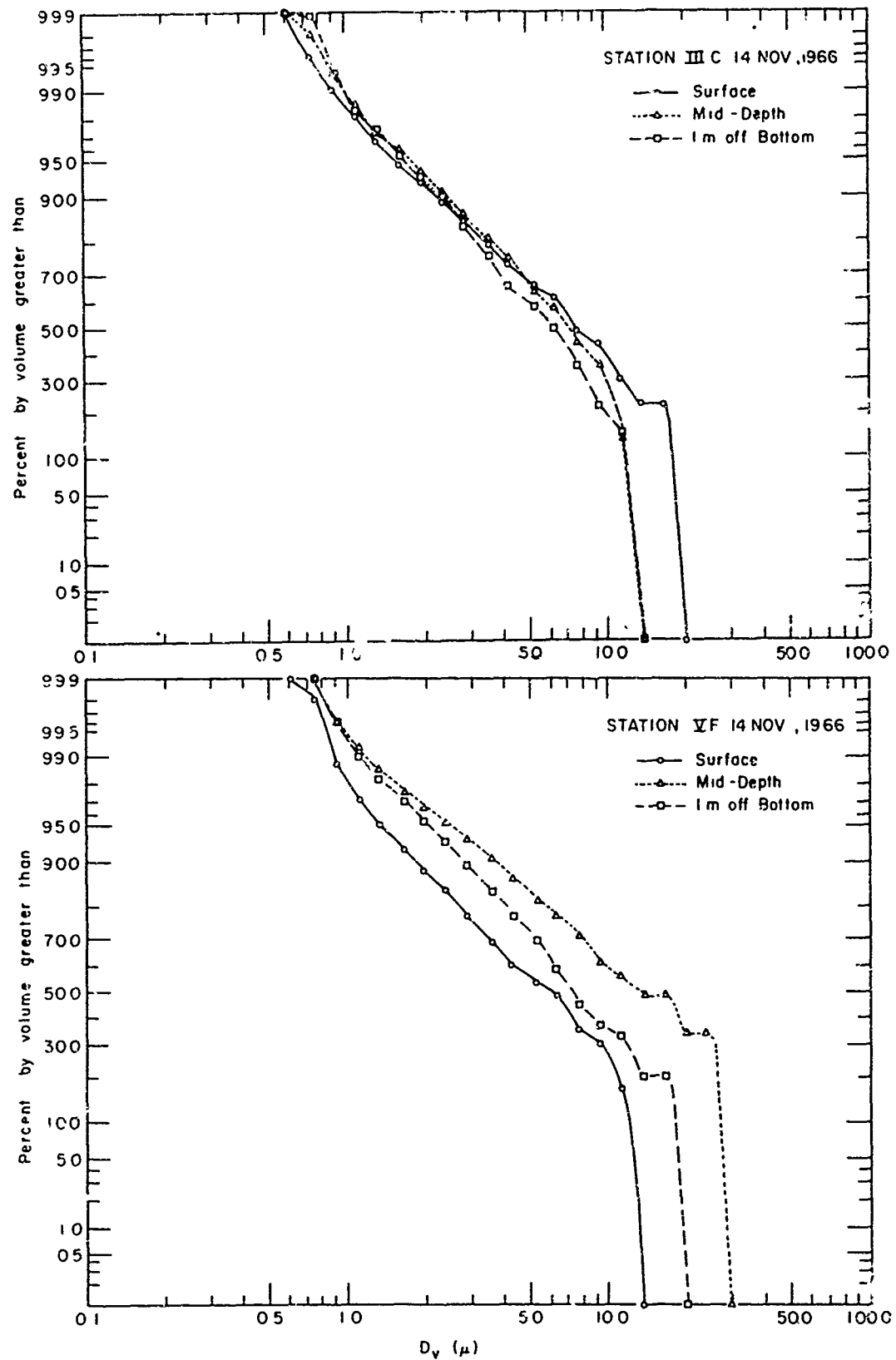


Fig. 56 Volume-Size Distribution Curves obtained by Transformation of Number-Size Data.

number of particles. Generally, since shape is not constant for all sizes of particles which make up a population, different shape factors must be used for different size ranges of a distribution. However, the direct measurement of particles in the sub-sieve range is an extremely difficult and arduous task. In the rare instances where shape factors have been determined, the procedure has been to assign an average shape factor to the entire population. Such shape factors have generally been defined as the ratio of two mean particle dimensions. The use of an average shape factor to characterize an entire particle population is acceptable for many industrial materials where the particles are of uniform composition and where particle shapes have been determined by a common and uniform comminution process. The use of an average shape factor may also be acceptable for some natural populations of fine-grained particles which are monomineralic, or nearly so. However, in the case of the suspended sediment population of the Chesapeake Bay, the assumption is entirely unjustified. As pointed out in the introduction, the particle population consists of both organic and inorganic particles, and of composite particles, all displaying a wide range of shapes from "spheres" to flakes.

A series of shape factors would have to be determined to cover various ranges of this size distribution. The determina-

tion of particle thickness, which would be required for the calculation of meaningful shape factors, is almost impossible for particles in the size and shape ranges encountered here. Because of these reasons, shape factors were not determined, and this fact must be kept in mind when examining the volume transformations.

A few general comments will be of use in interpreting and evaluating the volume transformations. During filtration the particles settle with their largest surfaces in the plane of the filter, and many of the composite particles "flatten out" when they hit the filter. Both of these factors result in an overestimate of the true volume diameters when the projected diameters,  $D_m$ , are cubed to obtain the volume-size distribution. From microscopic examination it is apparent that the smaller particles are more nearly equidimensional than the larger particles. Most of the particles greater than about  $10 \mu$  across are either thin flakes or composite particles. This change in average shape with particle size results in a displacement of the volume size distribution curve toward larger sizes when the volume transformation is made. In summary, the volume transformations of the number-size data result in an overestimate of the true volume diameters, and of the statistics associated with the volume size distribution. As pointed out in the next section, sedimentation size analyses of

a parallel set of samples provided an underestimate of the true volume-size distributions. This underestimate results from the fact that all irregular particles fall more slowly than spheres of the same mass and volume. The true volume distribution curve then, lies somewhere between these two estimates. We shall return to this topic after we have dealt with the sedimentation analyses.

An additional factor to consider when interpreting the volume-size transformations is the distorting effect which a few large particles can have. From the data in Table 8 and in the appendix, it is obvious that particles with diameters,  $D_m$ , greater than about 15  $\mu$  are rare. However, a single particle with a diameter,  $D_m$ , of 20  $\mu$  has a volume equivalent to that of 8000 particles 1  $\mu$  in diameter--assuming, as we have, that both have the same shape. Since we usually sized only 1500-2000 particles, in a few samples a single large composite particle accounted for more than fifty percent of the total sediment volume.

For these reasons, the volume statistics are much less stable than the number statistics. This is shown clearly by the data in Table 9 which summarizes the results of photomicrographic size analyses of seven suspended sediment samples. Each of the sediment samples was extracted by filtration from subsamples of a 10 l water sample collected from mid-depth at

station III C on 8 August 1966 at 1215 hours. The maximum difference between any of the number-mean diameters,  $\overline{D}_n$ , was about 11 percent, while the maximum difference between the volume-mean diameters was greater than 100 percent. It would be necessary, therefore, to size many more particles to attain a precision of the volume-statistics comparable to the precision of the number-statistics obtained by sizing one thousand particles.

The volume mean diameter of the suspended particles of the upper Chesapeake Bay ranged from 4 to 28  $\mu$  and generally increased with depth. No systematic seasonal or geographic patterns were observed. A value of 10-15  $\mu$  for  $\overline{D}_v$  would probably be a good estimate of the average volume-mean diameter for this section of the Bay.

TABLE 9

STABILITY OF PHOTOMICROGRAPHIC SIZE ANALYSIS. Subsamples of a mid-depth sample collected at Station IIIC on 8 August 1966.

Sample No.	Vol. of Water Filtered (m <sup>3</sup> )	Number of Particles Sized	$\bar{D}_m$ ( $\mu$ )	$\sigma_m$ ( $\mu$ )	$\bar{D}_v$ ( $\mu$ )	$\sigma_v$ ( $\mu$ )
IIIC <sub>1</sub>	10	1000	1.8	1.5	8.5	4.6
IIIC <sub>2</sub>	10	1000	1.9	1.7	12.6	6.8
IIIC <sub>3</sub>	10	1000	2.0	1.6	9.1	4.9
IIIC <sub>4</sub>	25	1000	2.1	2.2	16.9	8.8
IIIC <sub>5</sub>	25	1000	2.0	1.8	9.0	3.8
IIIC <sub>6</sub>	25	1000	2.0	2.2	18.0	8.8
IIIC <sub>7</sub>	25	1000	1.9	1.6	8.1	4.3

SIZE ANALYSIS BY SEDIMENTATION USING THE MSA PARTICLE SIZE  
ANALYZER

Of all available methods of size analysis, sedimentation techniques provide the most satisfactory means of determining both the weight distribution and the volume distribution of particles in the sub-sieve range. Among the sedimentation techniques, the Mine Safety Appliance Particle Size Analyzer provides the most satisfactory method of sedimentation analysis for fine-grained suspended sediment. It can work effectively with small ( $< 1 \text{ mg}$ ) sediment samples, and it can work rapidly because it combines gravity and centrifugal settling.

All sedimentation methods of size analysis are based upon a relationship between particle size and terminal settling velocity. The classic relationship was derived by Stokes (1850) for a rigid sphere. Since Stokes' law is invoked, often tacitly, in almost all sedimentation size analyses, we will do well to make explicit what it says, and more importantly, what it does not say.

Consider the case of a small, rigid, sphere settling in a viscous fluid at rest. As the sphere settles, it is acted upon by body forces and by surface forces. The body forces arise from gravity, buoyancy, and inertia. The surface forces arise from the viscosity of the fluid.

Stokes (1850) found that the viscous drag on a sphere may be expressed by

$$F = 3\pi\mu vD \quad (1)$$

where  $\mu$  is the dynamic viscosity of the fluid,  $v$  is the velocity of the sphere, and  $D$  its diameter. Equation (1) was derived by Stokes as the limiting case of the resistance to a ball pendulum, and was stated by him to be applicable to a falling sphere when the velocity of the sphere is low enough that the part of the resistance dependent upon the square of the velocity is negligible.

The buoyant force of the fluid on the particle is given by Archimedes' principle as

$$B = \frac{1}{6} \pi D^3 \rho_0 g \quad (2)$$

where  $\rho_0$  is the density of the fluid,  $g$  is the acceleration due to gravity, and  $D$  is the diameter of the sphere. The weight of the sphere is given by

$$W = mg = \frac{1}{6} \pi D^3 \rho g \quad (3)$$

where  $\rho$  is the density of the sphere,  $m$  is the mass of the sphere, and  $D$  and  $g$  are defined as before.

If the sphere were released from rest, initially  $F = 0$ , since  $v = 0$ . As the sphere accelerates, it experiences a

retarding force,  $F$ , which increases as  $v$  increases. Eventually a velocity is reached at which the downward force and the retarding force are equal, and acceleration ceases. This final constant velocity is called the terminal velocity of the sphere. It can be determined by equating the downward force due to gravity, the upward buoyant force, and the upward force due to frictional resistance. The form of  $F$  given in (1), according to Stokes (1850) ... "may be employed to determine the terminal velocity of a sphere ascending or descending in a fluid, provided the motion be so slow that the square of the velocity may be neglected." What this means is that if  $v$  is sufficiently small the inertial forces are so much smaller than the viscous drag forces that they may be neglected in the balance of forces.

Equating those forces which are not negligible we obtain

$$\frac{1}{6} \pi D^3 \rho g = \frac{1}{6} \pi D^3 \rho_0 g + 3 \pi \mu v D \quad (4)$$

weight	buoyant force	viscous drag	
--------	------------------	-----------------	--

where  $v$  is positive downward. Solving for  $v$  we obtain

$$v = \frac{1}{18} \frac{D^2 g}{\mu} (\rho - \rho_0) \quad (5)$$

Equations (1) and (5) are both referred to as Stokes' law.

From (5) we can determine the time for a sphere of diameter,  $D$ , to settle a distance,  $h$ , under the influence of gravity.

We have

$$t_g = \frac{18 \mu h}{(\rho - \rho_0) g D^2} \quad (6)$$

Since Stokes' law forms the basis of most sedimentation particle size analyses, it is extremely important to point out its underlying assumptions and to establish the conditions under which it can be expected to hold. Stokes' law (1) was derived for a single, smooth, rigid, sphere settling in a homogeneous and continuous fluid of infinite extent with a uniform velocity which is slow enough that the viscous drag is the only important restraining force on the particle.

When one or more of these conditions are not met, modifications of Stokes' law may be required. The modifications demanded by various degrees of departure from the conditions assumed by Stokes make up a voluminous literature. It is neither the author's intent to summarize this literature, nor to attempt to evaluate it in depth. This Aegean stable shall remain uncleaned. Its contents shall merely be put into different piles to allow enough of the oxen to be removed so that we can resume the race. We shall briefly examine the range of conditions under which Stokes' law can be expected to hold, see how closely the suspended particles of the upper Chesapeake Bay and the methods used by the author fulfill these conditions, and finally, we shall establish what modifications, if any, of Stokes'

law are required.

Stokes' law was derived for a single sphere. In sedimentation size analysis a cloud of particles is in suspension, and if Stokes' law is to apply strictly, each particle must settle unhindered. When the particle concentration becomes sufficiently great, there is appreciable particle interference. Below some critical concentration the interaction is small, and Stokes' law can be expected to hold.

The general problem of the hydrodynamic interference between particles in a moving fluid has not been solved. Theoretical studies of the effects of concentration on settling have been restricted to suspensions of mono-sized spheres (monodisperse systems). In such systems there is no relative motion between the particles, so the problem is greatly simplified. There have been no investigations of the interference occurring in polydisperse systems, of which suspended sediment populations are an example. The tendency in polydisperse systems is for all of the particles to settle together. The finer particles are apparently carried down by the coarser particles, but the presence of the finer particles, on the other hand, tends to retard the settling of the larger particles. The net result is that the size distribution at any level of a settled slurry is broader (the sediment is less well sorted) than would be expected by considering that essentially a single size particle is settling out at any given time.

According to Hawksley (1951), particle interference is probably appreciable for concentrations greater than 0.5 percent by volume, and probably cannot be neglected until the concentration is less than 0.05 percent by volume. Jarrett and Heywood (1954), on the other hand, found in a series of careful comparative tests that interference was negligible for concentrations less than 1 percent by volume. Irani and Callis (1963) state that volume concentrations should be kept between 0.2 and 0.5 percent by volume. The author found in a series of comparative tests run on natural suspended sediment populations that particle interference was negligible below about 0.75 - 1.0 percent by volume. In all suspensions analyzed by the author all of the concentrations were kept below the 1 percent by volume level and nearly all were kept well below 0.5 percent.

Stokes' law was derived for a homogeneous continuous fluid. Real fluids, however, are molecular in nature and this condition is not strictly fulfilled. For most sedimentation size analyses, the slippage which occurs because of the molecular character of the fluid is unimportant. The slippage, of course, is greater the smaller the particles, and is more serious in gaseous sedimentation analyses because of the greater mean free path. The effects of slippage in liquids for particles equal to or greater than  $0.5 \mu$  across are very small and have been neglected by the author.

Stokes' law assumes that the viscous drag is the only restraining force acting on the sphere. This assumption is not fulfilled if the sphere is so large or has a settling velocity so great that a turbulent wake develops. The assumption is valid only when the ratio of the inertial forces to the viscous forces is very small. The Reynolds number is a measure of this ratio. For a sphere settling in an undisturbed fluid we can write the Reynolds number as

$$\text{Re} = \frac{\rho_0 v D}{\nu} \quad (7)$$

where  $v$  is the velocity of the sphere,  $D$  its diameter,  $\rho_0$  is the density of the fluid, and  $\nu$  is the kinematic viscosity of the fluid.

The upper limit of the Reynolds number for which Stokes' law still holds has not been unanimously agreed upon. Hawksley (1951) states that the error in using the Stokes drag (1) does not exceed 1 percent until the Reynolds number is larger than about 0.05. According to Rose (1954), the Stokes drag is valid to within  $\pm 1$  percent for Reynolds numbers less than 0.1. Lamb (1932) sets the upper limit at a Reynolds number of one. Arnold (1911) found experimentally that the inertial effects of the fluid on the settling velocity were negligible for Reynolds numbers less than 1.2. Davies (1947), cited by Cadle (1965), estimated that errors of 1, 5, and 10 percent in settling velocity

correspond to Reynolds numbers of 0.074, 0.38, and 0.82, respectively.

For virtually all size analyses a choice of 0.1 as the critical Reynolds number should be low enough to ensure satisfactory results. The use of Stokes' law above some critical Reynolds number results in an underestimate of the particle diameter from the observed settling velocity. Above this critical Reynolds number the inertial terms must be included in the balance of forces. The inertial terms have been partially accounted for in theoretical solutions by Goldstein (1929, 1938). The upper limit on the Reynolds number for size analysis by settling has been extended to about 10 in theoretical solutions, and to more than  $10^5$  empirically.

The importance of a critical Reynolds number for size analysis is what it means in terms of a limiting particle diameter. It is apparent from (5) and (7) that a limiting particle diameter depends upon the effective density of the particle, and the viscosity of the fluid. If we take the critical Reynolds number to be 0.1, then from (5) and (7) we find a limiting diameter of about 50  $\mu$  for spherical particles with a density of 2.5 gm/cm<sup>3</sup> settling in water at 25 C. Since the suspended particles of the upper Chesapeake Bay have about this density, and since almost no particles with "diameters" greater than 50  $\mu$  were observed, the inertial forces could be safely

neglected and the Stokes drag (1) could be used.

There is also a lower size limit to the applicability of Stokes' law. Stokes' law fails to hold for particles which are so small that the bombardment of them by the fluid particles becomes an effective force. The lower limit for centrifugal settling is, according to Irani and Callis (1963), about  $0.01 \mu$ . Some other investigators place it somewhat higher, but it is always within the colloidal range. The lower limit for gravity settling is, of course, higher than for centrifugal settling. Since the author used centrifugal settling for particles less than  $10 \mu$  in diameter, no modifications of Stokes' law were required.

Stokes' drag was derived for a sphere settling in a fluid of infinite extent. Since all sedimentation analyses are carried out in vessels of finite extent, it is important to determine the conditions under which the retarding influence of the walls must be taken into consideration. Theoretical drag relationships have been derived for a sphere moving with an infinitely low velocity parallel to an infinite plane, between two parallel infinite planes, and along the axis of an infinitely long cylinder (see Hawksley, 1951). All of the theories have been derived for infinitely slow motion and in all cases, the drag increases as the ratio of the particle diameter to the distance from the wall(s) increases. The wall effects

decrease as the Reynolds number increases, and are probably negligible for Reynolds numbers greater than 1 according to Hawksley (1951).

The experimental evidence is not conclusive, and there is no detailed published evaluation of the available data. Experiments by Arnold (1911) using various sized spheres and a long cylinder, indicated that the drag on an axially falling sphere is not appreciably affected until the diameter of the particle equals 1/10 of the diameter of the cylinder. According to data from Landerburg (1907) as given by Hawksley (1951), for Reynolds numbers equal to or less than 0.05, the Stokes drag should be divided by about 0.95 for a 10  $\mu$  sphere settling along the axis of a cylinder whose diameter is 1000  $\mu$ . The capillaries of the two types of MSA centrifuge tubes which were used by the author have diameters of 750 and 1000  $\mu$ .

It is clear that the drag is increased by the presence of the walls and the base of the sedimentation vessel, however, because of the lack of agreement as to what corrective factors should be used, no modifications of the Stokes drag have been made by the author.

Stokes' law was derived for a smooth, rigid sphere. The suspended particles which the author is interested in are essentially rigid so this condition is sufficiently satisfied. The particles are probably not smooth however, and they are rarely

spherical. There is very little information concerning the effects of surface roughness on settling velocity. Arnold (1911) found that minor surface irregularities did not appreciably affect the settling velocity of small spheres. Because of the lack of data, the author has not applied any corrections for surface roughness.

The condition of spherical particles is rarely, if ever, satisfied by natural fine-grained sediment populations. Generally, a wide range of shapes is present. The settling characteristics of non-spherical particles can be most conveniently discussed by considering two settling ranges--settling which is within the Stokes range, and settling which occurs at Reynolds numbers outside of the Stokes range. Since the particles in which we are interested settle at Reynolds numbers within the Stokes range, we shall limit our discussion to these.

There is a great deal of confusion in the literature concerning the alleged departures from Stokes' law arising from the shapes of non-spherical particles. Much of this confusion apparently stems from a failure to understand the meaning of the term, Stokes diameter. A Stokes diameter is defined as the diameter of a sphere having the same density and the same terminal settling velocity as the particle in question in a fluid of the same density and viscosity. Neither a volume, nor a mass equivalence is asserted, only an equivalence in settling

velocity. If the investigator's interest in the particle population is to characterize a sedimentary process, then the Stokes diameter is a useful measure, and Stokes' law can be applied directly. If, on the other hand, the investigator is interested in the particles primarily as a product, then he is probably more interested in their masses or volumes, and accordingly in a volume diameter<sup>5</sup>. A volume diameter,  $D_v$ , is defined as the diameter of a sphere having the same volume as the particle in question. The determination of the volume diameters of non-spherical particles by settling may require modifications of Stokes' law. The modifications will depend, of course, on the shape factors of the particles. The Stokes and volume diameters will be equal only for spheres. According to Irani and Callis (1963) Stokes' law can be safely used for particles whose maximum-to-minimum diameter ratio does not exceed 4. This means that under these conditions the Stokes diameter,  $D_s$ , is a "good" estimator of the volume diameter,  $D_v$ . The exact relationship between the Stokes diameter, the volume diameter, and the sphericity is not known (Hawksley, 1951). As pointed out later however, there is good reason to believe that the Stokes diameter is always less than the volume diameter, except for spheres.

<sup>5</sup> Also known as a spherical diameter and a true nominal diameter.

Theoretical investigations of the settling of non-spherical particles within the Stokes range have been limited to ellipsoids, infinitely long cylinders, flat blades, and infinitely thin discs (Lamb, 1932). For a discussion of the theoretical work the reader is referred to Gans (1928), Davies (1947), and Lamb (1932).

Kunkel (1948) found in an experimental study that all shapes fall more slowly than the sphere of the same mass and volume. His study included aggregates of particles as well as single particles of various shapes. He found that aggregates fell in such a way as to offer the greatest possible resistance. In general, Kunkel concluded that all shapes fall more slowly than the equivalent spheres, and that ... "the deviation from Stokes' law increases with the deviation from spherical shape and it is always in the sense of causing slower fall than the sphere of the same mass so that size estimates would always yield a radius which is too small." The radius is too small only if the investigator is interpreting the results in terms of a volume diameter. Once again it must be pointed out that the investigator must decide whether he is interested in Stokes diameters or volume diameters. Results obtained with Stokes' law are expressed in terms of a Stokes diameter. These "diameters" will be equivalent to volume diameters only if the particles are spheres. In all other cases,

the Stokes diameters will be less than the corresponding volume diameters, and the degree of departure between the two measures depends upon the shapes (sphericities) of the particles. If the investigator is interested in volume diameters it may be necessary for him to employ shape factors. It is not clear however, from the available literature how Stokes' law should be modified for various shapes of particles to determine volume diameters. The modifications must, of course, be based upon shape factors and these are extremely difficult to determine for small particles.

Wadell (1936) quoted by Krumbein and Pettijohn (1938) derived a modified form of Stokes' law by developing a resistance formula for a particle intermediate in shape between a sphere and a disc. He obtained the following expression for the drag

$$R = 9.44 \pi r \mu v \quad (8)$$

Comparison of (8) with (1) shows that Wadell's drag differs from the Stokes drag only in the value of the numerical constant. Using (8) to obtain an expression for the terminal settling velocity, Wadell found

$$v_p = \frac{1}{28} \frac{\rho - \rho_0}{\mu} g D_p^2 \quad (9)$$

where  $v_p$  is called a practical settling velocity,  $D_p$  a practical

sedimentation diameter, and the rest of the terms are defined as before. If we divide (2) by (1) we obtain  $v/v_p = 0.64$  and have a convenient way of modifying results obtained with Stokes' law to account for shape variations. It can be easily shown that a practical sedimentation diameter is 1.25 times as large as the corresponding Stokes diameter.

The author has used Wadell's equation in some instances to get a better idea of the volume diameters of the suspended particles of the Chesapeake Bay. In cases where it has been used, both the Stokes diameters and the Wadell estimates of the volume diameters have been plotted.

One of the largest uncertainties in all sedimentation analyses arises from the necessity of assuming a mean density for the entire particle population. In most industrial samples, and in natural sediment populations in which there is little density variation, this does not present a serious problem if the sample size is large enough so that the mean density can be determined. The error in a calculated Stokes diameter due to a difference in the assumed and true densities will be approximately

$$\text{percent error in } D_s = 100 \left( 1 - \frac{\rho_{\text{true}} - \rho_0}{\rho_{\text{assumed}} - \rho_0} \right)$$

where  $\rho_0$  is the density of the sedimentation fluid. For example, if  $\rho_{\text{true}} = 2.5$ ,  $\rho_{\text{assumed}} = 2.2$ , and  $\rho_0 = 1.0$ , the percent error

in  $D_s$  is about 12 percent.

For populations whose particles have a wide range in density, it is nearly impossible to determine what effect the assumption of a mean density has on the observed distribution. The suspended particles of the Chesapeake Bay have a range in density from about  $1 \text{ gm/cm}^3$  for organic detritus and plankton to about  $2.8 \text{ gm/cm}^3$  for some clay particles. The densities of seven samples were determined with a pycnometer, and were found to range from 2.24 to  $2.60 \text{ gm/cm}^3$ .

For particles smaller than approximately  $10 \mu$  the analysis may be accomplished in a shorter time if centrifugal settling is substituted for gravitational settling. Additional advantages are a lessening of the effects of convection currents, Brownian movements, and flocculation. These effects all introduce increasingly serious distortions of the results as the particles become smaller. Centrifugal settling is identical in principle with gravitational settling. It differs only in the force which causes the settling. The constant force of gravity is replaced by the variable centrifugal force which depends on the angular velocity and the radius of rotation.

To understand sedimentation in a centrifugal field, let's consider the case of a small sphere of density,  $\rho$ , being sedimented in a fluid of density,  $\rho_0$ , where  $\rho$  is greater than  $\rho_0$ . At any time the sphere is acted upon by the effective centrifugal

force and an opposing viscous drag force. The effective centrifugal force may be expressed as

$$\frac{\pi D^3}{6} (\rho - \rho_0) \omega^2 r \quad (10)$$

where  $D$  is the diameter of the sphere,  $\rho$  its density,  $\rho_0$  the density of the sedimenting fluid,  $\omega$  is the angular velocity, and  $r$  is the distance of the sphere from the axis of rotation. The viscous drag force is the same as in the case of gravity settling, namely  $3\pi\mu vD$ .

Locally these forces are nearly balanced for very small particles (less than, say,  $10 \mu$  in diameter) and we can write

$$\frac{\pi D^3}{6} (\rho - \rho_0) \omega^2 r = 3 \pi \mu v D \quad (11)$$

Effective centri-	Viscous
fugal force	drag force

Solving for  $v$ , we obtain

$$v = \frac{(\rho - \rho_0) \omega^2 r D^2}{18\mu} \quad (12)$$

Equation (12) shows that with centrifugal sedimentation  $v$  is a function of  $r$ , the radius of rotation of the sphere, and a constant terminal velocity is not reached as in gravity settling. This means that the time for the sphere to settle a given distance must be determined by integration. Since  $v = dr/dt$ , we can write (12) as

$$\frac{dr}{dt} = \frac{(\rho - \rho_0) \omega^2 r D^2}{18\mu}$$

or

$$\frac{dr}{r} = \frac{(\rho - \rho_0)\omega^2 D^2}{18\mu} dt \quad (13)$$

Integrating between the limits  $r_1$  and  $r_2$  at times  $t=0$

and  $t=t_1$  gives

$$\int_{r_1}^{r_2} \frac{dr}{r} = \frac{(\rho - \rho_0)\omega^2 D^2}{18\mu} \int_{t=0}^{t=t_1} dt$$

and

$$t_1 = \frac{18\mu}{(\rho - \rho_0)\omega^2 D^2} \ln \frac{r_2}{r_1} \quad (14)$$

where  $t_1$  is the time for a sphere of diameter,  $D$ , to settle from  $r_1$  to  $r_2$  while being centrifuged at an angular velocity  $\omega$ .

If the particles are started from the surface of the sedimentation liquid, as in the layer sedimentation method, and if the sample is centrifuged immediately, then (14) can be applied directly to obtain the time necessary for a sphere of diameter,  $D$ , to arrive at the bottom of the centrifuge tube. In this case  $r_1$  would be the distance from the axis of rotation to the surface of the sedimentation liquid and  $r_2$  would be the distance from the axis to the bottom of the tube. In the method used by the author, which combines gravity and centrifugal settling, we cannot apply (14) directly since  $r_1$  can no longer be taken as the distance from the axis to the surface of the sedimentation liquid. The reason for this is that during the period

of gravity settling the particles become sorted throughout the column of liquid because of differences in size<sup>6</sup>. Therefore, at any time  $t$  greater than zero, different size particles will have different  $r_1$  values. The appropriate value of  $r_1$  to assign to a particular sphere will depend upon the diameter of the sphere, and the duration of the gravity settling period. We can determine the  $r_1$  appropriate to a particular size of sphere from an equation of the form

$$r_1 = r_0 + r_g \quad (15)$$

where  $r_0$  is the distance from the axis of rotation to the surface of the sedimentation liquid, and  $r_g$  is the distance below the surface to which the sphere will have settled during the period of gravity settling  $T_g$ .

During the gravity settling period,  $T_g$ , all spheres with diameters equal to or greater than some diameter,  $D_g$ , will have settled to the bottom of the tube, a distance we shall call  $h$  ( $h \equiv r_2 - r_1$ ). All spheres with diameters less than  $D_g$  will have

---

<sup>6</sup> The sorting is actually due to differences in settling velocity which may, or may not, be closely associated with differences in size. However, for convenience we shall consider that we are dealing with a polydisperse population of spheres of uniform density.

settled a lesser distance. Consider a sphere of diameter  $D$  less than  $D_g$  which has settled a distance  $r_g$ . From (6)

$$T_g = \frac{Kh}{D_g^2} = \frac{Kr_g}{D^2}$$

or

$$r_g = \frac{hD^2}{D_g^2} \quad (16)$$

Hence, from (15)

$$r_1 = r_0 + \frac{hD^2}{D_g^2} \quad (17)$$

which says that  $r_1$  for a sphere of diameter,  $D$ , depends upon the diameter,  $D_g$ , of the sphere which was just settled in the time,  $T_g$ . If we substitute (17) into (14) we obtain

$$t = \frac{18\mu}{(\rho - \rho_0)\omega^2 D^2} \ln \frac{r_2}{\left(r_0 + \frac{hD^2}{D_g^2}\right)} \quad (18)$$

which can be used to calculate the centrifuging times corresponding to the sedimenting times of spheres of designated diameters.

The MSA Particle Size Analyzer combines gravity settling with centrifugal settling in a cumulative sedimentation technique for the determination of the volume-size distribution. The MSA procedure calls for the determination of the amount of sedimented material at times precalculated from Stokes' law.

The amount of material is determined by measuring the height of the column of settled particles which have accumulated in the capillary of one of the special centrifuge tubes.

The volume distribution is then calculated from the ratio of the sediment height observed at times corresponding to certain Stokes diameters ( $D_s$ ) to the sediment height after "all" particles have settled. It is assumed that the sediment height is proportional to sediment volume.

A complete analysis consists of the following steps: (1) sample collection, (2) calculation of a reading schedule, (3) sample dispersion, (4) transfer of the suspension to one of the special centrifuge tubes, (5) reading the sediment height at times precalculated from Stokes' law for the gravity settling period, (6) transfer of the centrifuge tube to the lowest speed centrifuge, running for a precalculated time, removing the tube and determining the sediment height, (7) continuing centrifuging for predetermined combinations of times and speeds until the reading schedule has been completed, and (8) calculating the volume-size distribution from the measured sediment heights.

Before discussing these steps we will take a closer look at the components of the MSA Particle Size Analyzer. The complete MSA Particle Size Analyzer consists of four special centrifuges (300, 600-1200, 1800, and 3600 r.p.m.), the MSA

Optical Projector, and special centrifuge tubes. Miscellaneous accessories include a feeding chamber, measuring rods, cleaning wires, and a tube rack. The major components have been designed as separate units, and for most analyses two of the centrifuges are sufficient. The specially designed centrifuges have the following characteristics: (1) Speeds constant to within  $\pm 1$  percent of their stated values. (2) Maximum acceleration rates of less than  $5 \text{ rad sec}^{-2}$  during starting and stopping. (3) Stable starting and stopping characteristics. The speed versus time curves during starting and stopping are known and constant enough that corrections do not vary more than  $\pm 0.5$  sec. (4) Built-in 1 sec to 1 hour timers allowing the centrifuges to be started and stopped without adjusting any speed control device.

The centrifuges are powered by hysteresis type synchronous motors. The starting and stopping characteristics are controlled by a combination of an inertia disk on the motor shaft and a variable resistor in series with one winding of the motor. The centrifuges are equipped with small, two-place, commercial heads. The speed stability and the controlled acceleration rates of the MSA centrifuges remove two of the serious drawbacks to size analysis by centrifugation. Most ordinary laboratory centrifuges lack speed stability, and their acceleration rates are too low at low speeds, and too high at high

speeds for reliable size analysis.

The special centrifuge tubes designed to fit standard 15 ml centrifuge shields, are available with three different capillary bore diameters--1 mm, 0.75 mm, and 0.5 mm.

The MSA projector projects a magnified ( $\sim 5X$ ) image of the capillary and its sediment column onto a graduated screen for easy and convenient measurement. The magnification also allows the investigator to check on the dispersion of the sample, and to get an idea of the shapes of the large particles. The projector is used to hold the sedimentation tube during the gravity settling period. The projector is equipped with a cam operated tapper which is used during the gravity settling period to prevent particles from sticking to the walls of the tube. The tapper gently strikes the tip of the tube at the rate of 40 times per minute.

Using a 600-1200 r.p.m. centrifuge, an 1800 r.p.m. centrifuge, 0.5 mm and 0.75 mm capillary centrifuge tubes, and a tube projector, Chesapeake Bay suspended sediment samples were successfully sized. The procedures which were followed are described below.

#### 1. Sample Collection

Suspended solids for MSA size analysis were extracted from subsamples of the pumped water samples described earlier.

The samples for MSA analysis were obtained from at least three depths--surface, mid-depth, and 1 m off the bottom, at all channel stations, the Susquehanna River station, and at other selected stations. At each sample depth generally three samples of the suspended solids were collected by filtration--one sample of approximately 1 mg on a 0.22  $\mu$  Millipore filter, 1 sample of 2 to 5 mg on a 0.45  $\mu$  silver filter, and a third sample consisting of the suspended solids from 500 ml of water on a 0.45  $\mu$  silver filter. In addition, some raw water samples of 1 to 2 liters were collected and stored in bottles.

## 2. Calculation of The Reading Schedule

Except in the case of extremely fine-grained material, a complete MSA analysis involves both gravity and centrifugal settling, and it is convenient to calculate a complete reading schedule before a run is initiated. Generally a series of diameters are chosen which cover the size range of the sample, and the corresponding settling times are calculated. The gravity portion of the schedule is calculated from Stokes' law, (5). Equation (5) gave the terminal velocity of a sphere as

$$v = \frac{D_g^2(\rho - \rho_0)}{18\mu}$$

and (6) gave the time,  $t_g$ , for a sphere to settle a distance  $h$  under the influence of gravity as

$$t_g = \frac{18\mu h}{(\rho - \rho_0)gD^2}$$

If the units of  $D$  are microns, and if the other terms are expressed in c.g.s. units, then  $t_g$ , in seconds, is given by

$$t_g = \frac{18 \times 10^8 \mu h}{(\rho - \rho_0)gD^2} \quad (19)$$

If we let

$$K_g = \frac{18 \times 10^8 \mu h}{(\rho - \rho_0)g} \quad (20)$$

then (19) can be expressed by

$$t_g = \frac{K_g}{D^2} \quad (21)$$

Since  $K_g$  is a constant for a given material in a given sedimentation liquid, a complete reading schedule for the gravity period can be readily calculated from (21) for any sizes desired.

It is generally convenient to change from gravity settling to centrifuge settling about 10 to 15 minutes after the beginning of a run. Although it is desirable to keep the gravity portion of the run as short as possible to speed up the analysis, there is a lower limit since the centrifuge timer settings must be at least as long as the times necessary for them to reach constant speed.

The centrifuge portion of the reading schedule can be

calculated from a modified form of (18). Equation (18) can be simplified in the same manner as (19) by the use of a constant.

We can define a  $K_\omega$  for each centrifuge.

$$K_\omega = \frac{18 \times 10^8 \mu}{(\rho - \rho_0) \omega^2} \quad (22)$$

Comparing (22) to (20) we see that

$$K_\omega = \frac{g}{h\omega^2} K_g \quad (23)$$

and we can write (18) as

$$t = \frac{K_\omega}{D^2} \ln \frac{r_2}{\left(r_0 + \frac{hD^2}{D_g}\right)} \quad (24)$$

Equations (18) and (24) cannot be used directly to calculate centrifuging times since they are based on the assumption that  $\omega$  is constant for the entire centrifuging period. This, of course, in practice is not true because the centrifuges must be started and stopped. Consequently a corrective time factor,  $\tau_\omega$ , must be added to the times calculated from (24) to obtain the correct centrifuge timer settings. The determination of starting-and-stopping corrections is discussed in Appendix B. The time calculated from (24) plus  $\tau_\omega$  gives the initial centrifuge timer setting. Subsequent times calculated from (24) must also be corrected to account for previous centrifuging time, as well as for starting and stopping. We can express

the initial timer setting,  $t$ , in the form

$$t = t' + \tau_{\omega} \quad (25)$$

where  $t'$  is the time calculated from (24) and  $\tau_{\omega}$  is the starting-stopping correction factor. Subsequent timer settings for the same  $\omega$  can be determined from

$$t_n = t_n' - t_{n-1}' + \tau_{\omega} \quad (26)$$

where  $t_n$  is the  $n$ th timer setting,  $t_n'$  is the  $n$ th-time calculated from (24),  $t_{n-1}'$  is the constant-speed time equivalent of previous centrifuging also calculated from (24), and  $\tau_{\omega}$  is the starting-stopping correction factor.

When  $\omega$  is increased, the  $t_{n-1}'$  term in (26) must be multiplied by  $(\frac{\omega_1}{\omega_2})^2$  to determine the first timer setting at the new speed. This is true since an interval  $t_n$  at  $\omega_1$  is equivalent in terms of sedimentation to an interval  $(\frac{\omega_1}{\omega_2})^2 t_n$  at speed  $\omega_2$  as can be seen from (14).

In summary then, we have the following equations for the calculation of settling times:

For gravity settling times

$$t = \frac{18 \times 10^8 h \mu}{(\rho - \rho_0) g D^2} = \frac{K_g}{D^2}$$

For centrifuge settling times

$$t = \frac{18 \times 10^8 \mu}{(\rho - \rho_0) \omega^2 D^2} \ln \frac{r_2}{\left(r_0 + \frac{hD^2}{D_g}\right)} = \frac{K_\omega}{D^2} \ln \frac{r_2}{r_0 + \frac{hD^2}{D_g}}$$

For the initial centrifuge timer setting

$$t' = \frac{K_\omega}{D^2} \ln \frac{r_2}{r_0 + \frac{hD^2}{D_g}} + \tau_\omega$$

For successive timer settings at the same speed,

$$t_n = t_n' - t_{n-1}' + \tau_\omega$$

Initial timer setting after changing speed from  $\omega_1$  to  $\omega_2$

$$t_n = t_n' - t_{n-1}' \left(\frac{\omega_1}{\omega_2}\right)^2 + \tau_{\omega_2}$$

A sample reading schedule is worked out in Appendix C.

For further discussion the reader is referred to the MSA manual and to Cartwright and Gregg (1958).

### 3. Sample Dispersion

Proper sample dispersion is one of the most important factors in any sedimentation analysis, and is one of the most difficult conditions to fulfill--particularly when the determination of the naturally occurring particle size distribution is the aim

of the analysis. As pointed out previously, choosing the proper intensity of dispersion is akin to steering a course between Scylla and Charybdis. If the dispersion is too vigorous, naturally occurring flocculates may be destroyed, while if the dispersion is too weak additional flocculates may be produced during the analysis. The only course open is to use moderate dispersion and to include a number of checks in the analysis.

The MSA method is probably more sensitive to the state of sample dispersion than any other size analysis technique. The primary reason for this is that if dispersion is not adequate, the void spaces between the settled particles will be greater than for the monodisperse system which is assumed to be settling out at any given time. This increased void space will result in a reorientation of the particles at high centrifuge speeds and a compaction of the sediment column, which, if appreciable, will invalidate the analysis.

A number of criteria have been established for determining whether or not adequate dispersion has been achieved. A good discussion can be found in Herdan (1960). It is important to remember that the phrase "adequate dispersion" has a much different meaning in most industrial applications than it does in this study. Industrial size analyses are generally concerned

with the size distribution of the primary particles<sup>7</sup> and an effort is made to destroy all flocculates. In industrial applications the most powerful criterion of adequate dispersion is that repeated analyses of a sample should give the same results regardless of the dispersive procedures employed. This criterion is obviously less useful when the investigator is interested in preserving the naturally occurring composite particles.

The procedures and criteria which the author found to be most useful for establishing adequate dispersion were:

- (1) Microscopic examination of a drop of suspension just prior to analysis. If the particles less than 2  $\mu$  were more or less evenly dispersed, and if they exhibited Brownian movement, the sample was considered to be adequately dispersed at this stage.
- (2) The direct observation with the projector of the particles in the capillary of the centrifuge tube. If there was no visible flocculation, or sticking of particles to walls of the capillary, the sample was assumed to be adequately dispersed.
- (3) Determination of the degree of compaction of the sediment

---

<sup>7</sup> A primary particle is an individual particle or any true aggregate of individual particles which are so firmly held together that it is not possible to distinguish the individual particles making up the group. (American Society for Testing and Materials, ASTM E 20 - 51 T, 1951).

column during analysis. If the height of the sediment column did not decrease as the centrifuge speed was increased, the sample was assumed to be adequately dispersed.

(4) Filtration and microscopic size analysis of a portion of the suspension prepared for MSA analysis. The subsample was filtered through a 0.22  $\mu$  Millipore filter, photographed, and sized with the Zeiss Particle Size Analyzer. The results were compared with the results of the Zeiss analysis of a sample collected at the same time and from the same depth as the first sample, but which was filtered immediately after collection without any pretreatment. The methods of collection and analysis of this set of samples were explained in the section on microscopic size analysis. Since this second sample was not dispersed in any way, its size distribution is presumably representative of the in situ size distribution of the suspended matter. This comparison provided the most powerful criterion in assessing the state of dispersion.

All of these criteria were used for each sample, and if at any step the sample failed to meet these specifications, it was either resuspended, redispersed and the analysis rerun, or the sample was discarded.

The MSA samples were dispersed in standard 50 ml centrifuge tubes with a small stirrer attached to a variable speed motor. The suspensions were prepared in one of several ways depending

upon the mode of sediment collection. Sediment samples on silver filters were removed from the membranes either by brushing lightly or by the use of an ultrasonicator. Sediment samples on Millipore filters were removed either by brushing or by dissolving the membrane in acetone. The sediment contained in raw water samples was first concentrated and washed by centrifugation, and then resuspended and dispersed in distilled water. Since the author used the homogeneous sedimentation technique for most of the samples, the dispersive liquid generally served as the sedimentation liquid. Distilled water was used in all cases except for the Millipore filters which were dissolved in acetone. These samples were analyzed with acetone as the sedimentation liquid. The effects of the dissolution of the Millipore membrane on the density and the viscosity of the acetone had to be determined and the new values were used in the calculation of the reading schedule. The new values of  $\rho$  and  $\mu$ , although higher than those for pure acetone, were still lower than the corresponding values for water and consequently speeded up the analyses.

For many samples physical agitation must be supplemented by dispersing and wetting agents to achieve proper dispersion. A fairly complete discussion of wetting and dispersing agents with recommendations for use with specific materials is given by Hendan (1960).

The use of wetting and dispersing agents was kept at a minimum in this study. Only Tween 80<sup>8</sup>, and sodium hexametaphosphate were used, and these were used sparingly, and only after mechanical agitation alone was found to be inadequate.

In many instances it was impossible to adequately disperse the samples for MSA analysis because of the sticky organic matter which was present both as amorphous clots and as coatings surrounding many of the particles. The organic matter was removed from some of these samples by combustion or by adding H<sub>2</sub>O<sub>2</sub>, or by ultraviolet radiation. The samples were then sized with the MSA analyzer to determine the size distribution of the remaining inorganic and non-combustible organic particles. The size distributions thus determined do not represent the in situ size distributions of these constituents since many of these particles originally formed organically bound agglomerates. These size distributions are however representative of the volume-size distributions of the primary noncombustible particles.

After dispersion the sample is transferred to one of the special centrifuge tubes which is placed in the reading projector and the sediment height is recorded at times calculated from Stokes' law for gravity settling. At the end of the gravity settling period, the centrifuge tube is transferred from the projector to the lowest speed centrifuge, and run for a predetermined

---

<sup>8</sup> Available from Atlas Powder Co., Wilmington, Delaware.

time. The sediment height is again determined, and centrifuging is continued according to a predetermined plan until the reading schedule has been completed.

The volume-size distribution is calculated from the measured sediment heights by determining the ratios between sediment heights recorded at the predetermined times and the total sediment height at the end of the run. Each such ratio gives the volume fraction of the sample accounted for by particles with Stokes' diameters,  $D_s$ , greater than the  $D_s$  which corresponds to that particular sediment height. These ratios are converted to percentages and plotted as a cumulative size distribution.

#### Results and Discussion:

Fifty suspended sediment samples from various space-time positions in the upper Bay were sized by sedimentation using the Mine Safety Appliance Particle Size Analyzer. Each of these samples was split and two parallel analyses were made.

The volume-size distributions of eight of these samples are presented in Figs. 57 and 58. The mean, the standard deviation, the skewness, and the kurtosis of each sample are presented in Table 10. In addition, the results of 14 other analyses are presented in Appendix D.

The reproducibility of the MSA method was usually very

good. Table 11 summarizes the results of three replicate runs on a single small (about 5 mg) sample of suspended sediment. The maximum deviation of the individual volume percentages for a particular size class from the mean volume percentage for that class was only 1.3 volume percent. These results are typical of what can be expected from careful analyses of fine-grained suspended sediment.

It will be necessary to size many more samples, to definitely establish the existence or absence of any significant seasonal or geographic patterns of the volume-size distribution, but from the data at our disposal the variation of the volume-size distribution with depth appears to be the only persistent feature. At nearly all of the stations for which MSA size analyses were made, the mean Stokes' diameter,  $\bar{D}_s$ , increased with depth, and at most of these stations the standard deviation also increased with depth. It was pointed out in the previous section that the mean projected diameter,  $\bar{D}_m$ , also increased with depth at most stations. It is significant that the mean volume diameter,  $\bar{D}_v$ , calculated from the volume transformations of the projected diameter data, did not show this characteristic increase with depth. This supports the statement made earlier that the common practice of transforming number-size data to volume-size data by assuming spherical particles is frequently unsatisfactory.

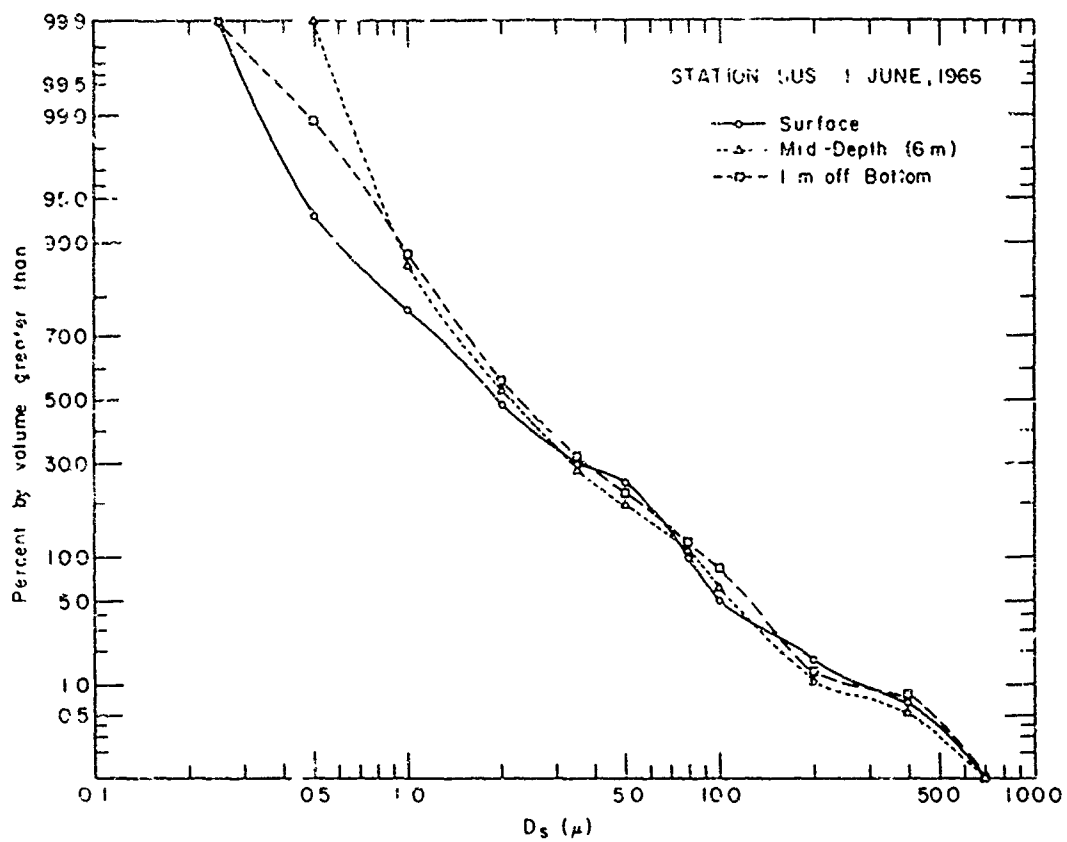


Fig. 57 MSA Centrifuge determined Volume- size Distributions of Selected Samples of Suspended Sediment from the Upper Bay.

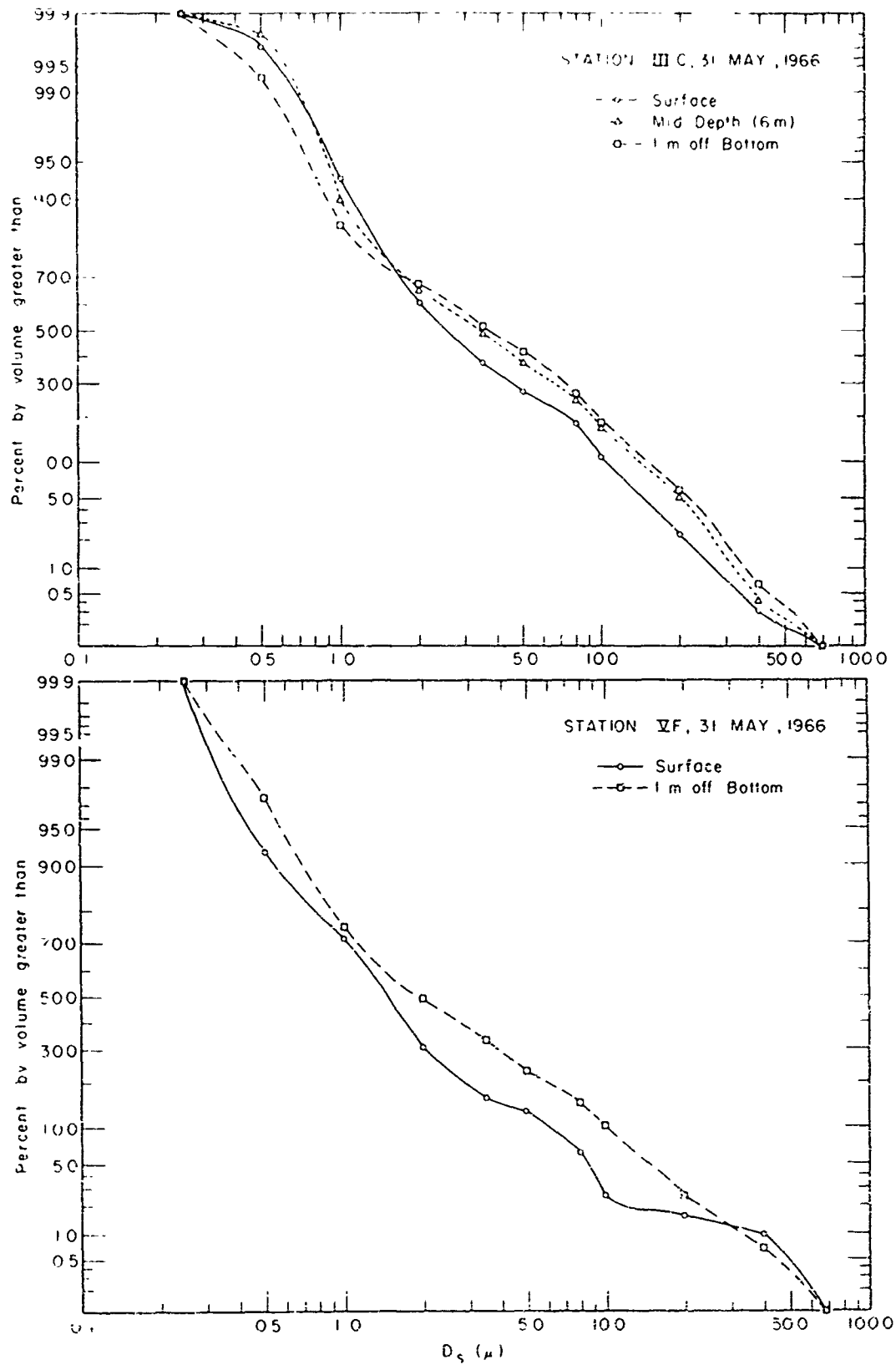


Fig. 58 MSA Centrifuge determined Volume-Size Distributions of Selected Samples of Suspended Sediment from the Upper Bay.

TABLE 10

Statistical Properties of Particle Size Distributions Shown in Figures 57 and 58.

Station, Date, and Depth	Mean $D_s$ ( $\mu$ )	Standard Deviation ( $\mu$ )	Skewness	Kurtosis
SUS (1 VI 66)				
surface	3.9	6.3	2.9	44.3
mid-depth	3.9	5.7	2.9	48.8
1 m off bot.	4.3	6.5	2.8	42.1
IIIC (31 V 66)				
surface	4.9	6.2	1.9	22.3
mid-depth	6.3	7.7	1.4	10.9
1 m off bot.	6.6	8.2	1.4	11.5
VF (31 V 66)				
surface	3.0	6.6	3.5	55.8
1 m off bot.	4.5	7.1	2.2	27.0

TABLE 11

Replicate MSA Analyses of A Suspended Sediment Sample From the  
Upper Bay.

Stokes Diameter ( $\mu$ )	Percent by volume greater than size			Mean
	Run 1 Operator A	Run 2 Operator B	Run 3 Operator A	
30.0	0	0	0	0
40.0	0.5	0.7	0.2	0.5
20.0	4.9	5.2	3.6	4.6
10.0	7.3	8.0	5.9	7.1
5.0	30.5	31.8	29.3	30.5
2.0	67.1	66.2	65.5	66.3
1.0	85.4	86.0	84.0	85.1
0.5	93.7	95.0	94.1	94.3
0.2	100.0	100.0	100.0	100.0

At the surface,  $\bar{D}_s$  ranged from 2.3 to 6.0  $\mu$ , and in more than 75 percent of the samples analyzed it was between 2.3  $\mu$  and 4.0  $\mu$ . The mean Stokes diameter,  $\bar{D}_s$ , at mid-depth ranged from 3.4  $\mu$  to 6.8  $\mu$  and in over 75 percent of the samples it was between 3.4  $\mu$  and 6.0  $\mu$ . Near the bottom  $\bar{D}_s$  ranged from 4.2  $\mu$  to 12.2  $\mu$ , and was between 4.2  $\mu$  and 8.0  $\mu$  in more than 75 percent of the samples analyzed.

Serial observations of current velocity and suspended sediment concentration show that near the bottom there are marked fluctuations in the concentration of suspended sediment which are clearly related to current velocity and tidal period. Maximum concentrations recorded near times of maximum flood and ebb velocities exceeded minimum concentration recorded shortly after slack water by as much as a factor of 18. These large variations of the concentration of suspended sediment must be accompanied by marked changes of the weight (and volume) size distributions. This would explain why the range of  $\bar{D}_s$  is greater near the bottom than at mid-depth or at the surface.

Current measurements were not made at the times of collection of the samples whose MSA size analyses are presented here. Recently however, a size investigation was undertaken of a set of suspended sediment samples collected simultaneously with current velocity determinations at hourly intervals over a

---

See section on Sedimentation Processes.

complete tidal cycle.

The results of these analyses should provide an important contribution to our understanding of the sedimentation processes in the upper Bay. A knowledge of the settling characteristics of the particles of a suspended sediment population is a prerequisite to the understanding and interpretation of that population.

## MINERALOGY OF THE SUSPENDED SEDIMENT

The mineralogy of selected mid-depth samples of suspended sediment was determined by X-ray diffraction, Table 12. The suspended sediment was removed from the 18 to 100 liter water samples by settling and centrifugation. The organic solids were decomposed with hydrogen peroxide, and the sediment samples were centrifuged several times with distilled water to remove salts and soluble organics. A size separation of each sample into a greater than two micron fraction and a less than two micron fraction was made by settling in distilled water. Each of the size fractions was concentrated by centrifugation, water-sedimented onto glass slides, and dried at room temperature.

It was impossible to obtain useful X-ray diffraction patterns from samples in which the organic matter had not been destroyed. A few samples were given the following additional treatment before X-raying. The amorphous iron was removed by the citrate-bicarbonate-dithionite method, and the amorphous silica and alumina were removed by boiling the sample in 0.4 N  $\text{NaCO}_3$  (Jackson, 1956). These procedures were not found to be necessary however, for identification purposes.

Each slide was X-rayed from  $3$  or  $4^\circ 2\theta$  to at least  $49^\circ 2\theta$  at a scanning speed of  $1^\circ 2\theta$  per minute using copper  $K\alpha$  radiation and 35-45 kV, and 20-25 ma. Typical X-ray diffraction patterns are presented in Figs. 59 and 60.

TABLE 12

## Mineralogy Samples

Station	Date of Collection
Susquehanna	Feb. 17, 1966
Susquehanna	June 28, 1966
Susquehanna	July 25, 1966
Susquehanna	Aug. 9, 1966
Susquehanna	Sept. 20, 1966
Susquehanna	Oct. 3, 1966
Sassafras	Sept. 19, 1966
IC	Oct. 4, 1966
IE	July 26, 1966
IID	Sept. 19, 1966
IIIC	Sept. 19, 1966
IIIC	Oct. 17, 1966
IVD	Sept. 6, 1966
IVD	Sept. 19, 1966
VF	Sept. 6, 1966
VF	Sept. 19, 1966
VF	Oct. 3, 1966
VF	Oct. 17, 1966
VF	Nov. 30, 1966

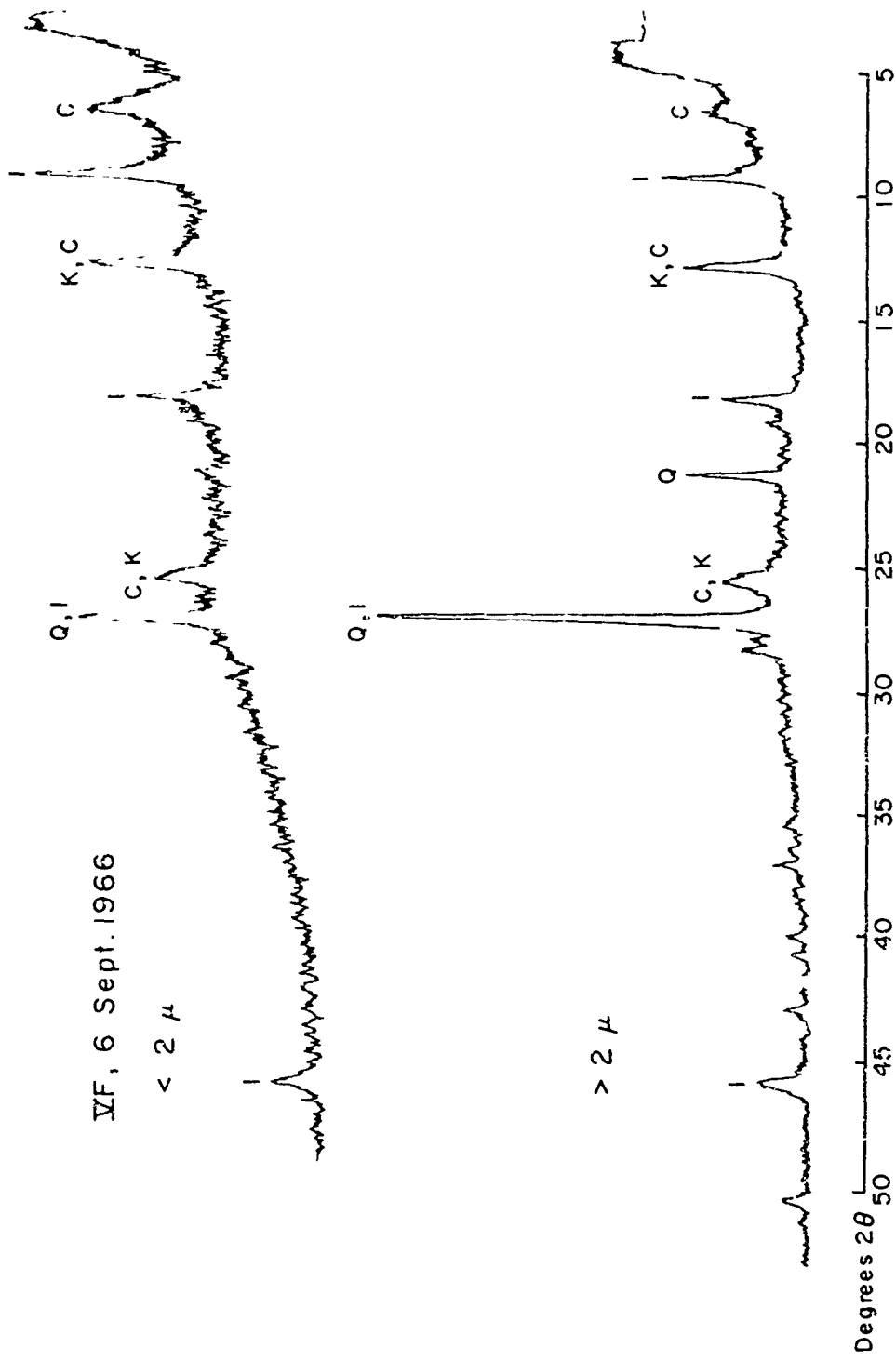


Fig. 59 X-ray Diffraction Patterns of the less than  $2 \mu$  and greater than  $2 \mu$  Fractions of the Mid-Depth Mineral Assemblage at Station VF on 6 September 1966.

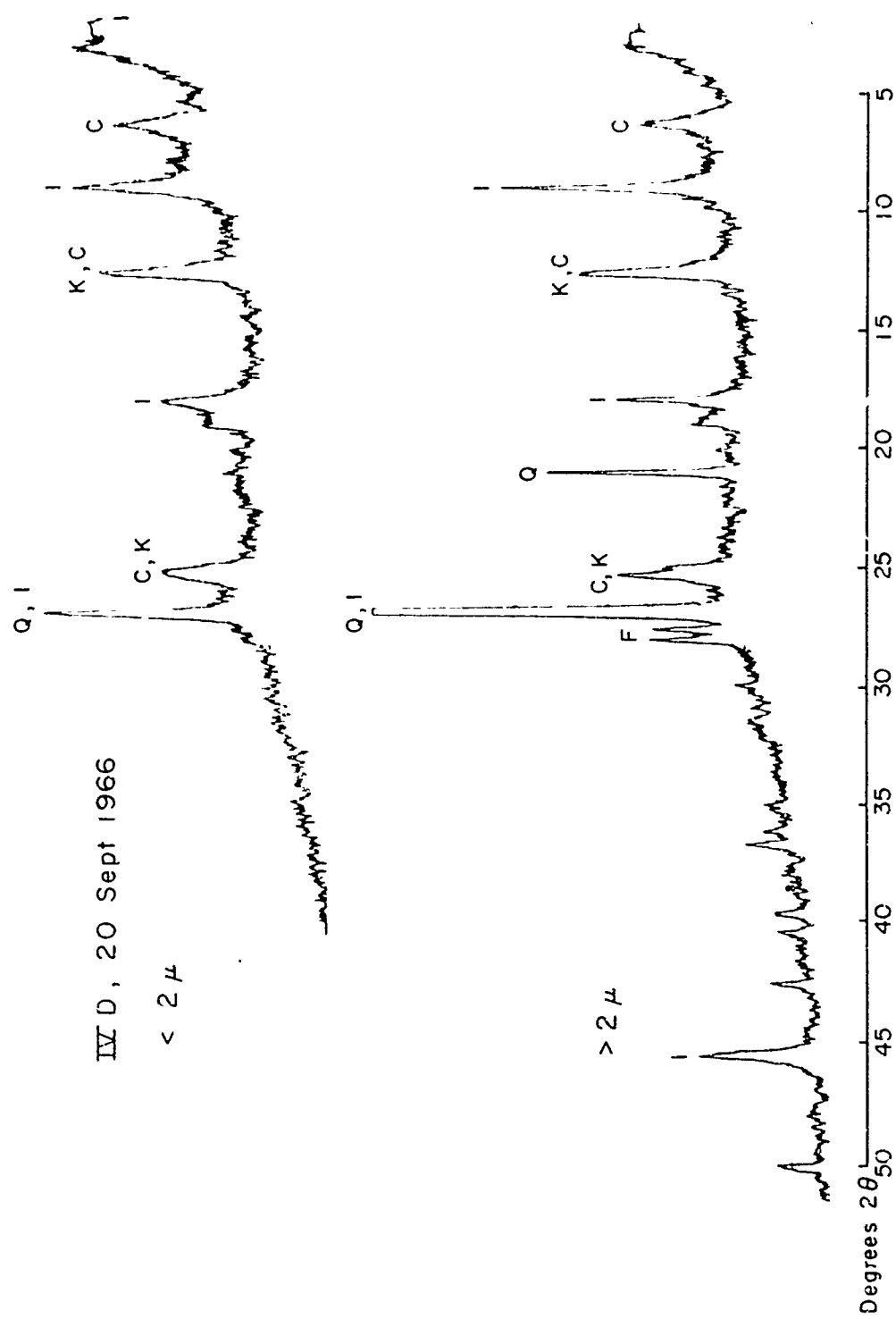


Fig. 60 X-ray Diffraction Patterns of the less than  $2 \mu$  and greater than  $2 \mu$  reactions of the Mid-Depth Mineral Assemblage at Station IVD on 20 September 1966.

The illite, chlorite, and kaolinite "groups" were the only clay minerals identified, and these were present in all of the samples. No attempt was made at intra-group identification. Illite was probably the most abundant constituent of the clay mineral assemblage. Quartz and feldspar were the only non-clay minerals identified. Quartz was present in all of the samples and was more abundant in the greater than two micron fraction than in the less than two micron fraction. During high spring runoff, the X-ray patterns were very poor. This was probably due to the abundance of colloidal amorphous iron particles.

Illite was defined by its 10, 5, 3.3, and 2.5 Å sequence of basal diffraction maxima (peaks). Chlorite was defined by its 14, 7.1, 4.7, and 3.5 Å basal sequence, and kaolinite was defined by its 7.2, 3.5, and 2.38 Å peaks. Quartz was defined by its 3.34 and 4.26 Å peaks, and feldspar by its 3.24 and 3.20 Å peaks.

Quantitative interpretations of the X-ray diffraction patterns of clay mineral assemblages are usually equivocal. Peak intensities cannot be used directly as absolute quantitative indicators of the abundance of clay minerals. In addition to mineral abundance, peak intensity depends upon X-ray machine settings, thickness of sample mount, and the degree of preferred orientation of the mineral particles. Peak intensity also depends upon the mineral's ability to diffract X-rays,

and this ability varies not only with different minerals, but also with different samples of the same mineral. The latter variability is due to differences in chemical composition and crystallinity. These factors preclude the direct use of peak intensities as indicators of absolute abundance.

Various intrasample ratios of peak intensities can sometimes however, be used to provide useful intersample comparisons. In making such comparisons the assumption is made that between samples the variations in the crystallinity, and chemical composition of each mineral are small and that variations in the degree of particle orientation are small. If these conditions are fulfilled, then variations in peak intensity are due to variations in abundance.

The following peak height ratios were determined: kaolinite/chlorite ( $3.58 \text{ \AA} / 3.54 \text{ \AA}$ ), kaolinite/illite ( $7.2 \text{ \AA} / 10 \text{ \AA}$ ), and chlorite/illite ( $7.1 \text{ \AA} / 10 \text{ \AA}$ ). Peak height was used as a measure of peak intensity. Peak area is a better measure of peak intensity, but it requires a slower scanning speed, and involves considerably more work. It was expected that the relative abundances of the various clay minerals would be nearly constant, and that the additional work required to determine peak areas was unjustified. No systematic variations in the ratios were detected--either geographically or seasonally.

In summary, the suspended sediment mineral assemblage

consisted of illite, chlorite, kaolinite, quartz, and occasionally feldspar. No patterns of peak height ratios were found. The intersample variations of the ratios were usually no greater than the precision of the individual ratios indicating that fluctuations in the relative abundances of the clay minerals were small.

## SEDIMENTATION PROCESSES

The causes of events are even more interesting than the events themselves. Cicero

Will your answer serve fit to all questions?  
Shakespeare

It is not every question that deserves an answer.  
Publilius

The sediments of the Chesapeake Bay are composed of an inorganic and an organic fraction. The inorganic portion is comprised almost entirely of terrigenous sediments which have been delivered to the Bay by the rivers tributary to it, and by erosion of the Bay's margins which are poorly consolidated. The organic fraction consists primarily of planktonic organisms and their degradation products. The Bay's suspended sediment, a subpopulation of its total sediment population, is made up of newly introduced inorganic sediment which has not been deposited; of living plankton; of organic detritus which has not settled out; and of previously deposited sediments, both organic and inorganic, which have been resuspended from the Bay floor, Fig. 61. At a given time all of these components are present, but their relative abundances vary temporally and spatially.

In discussing the suspended sediment population we shall first consider the external sediment source, upland discharge.

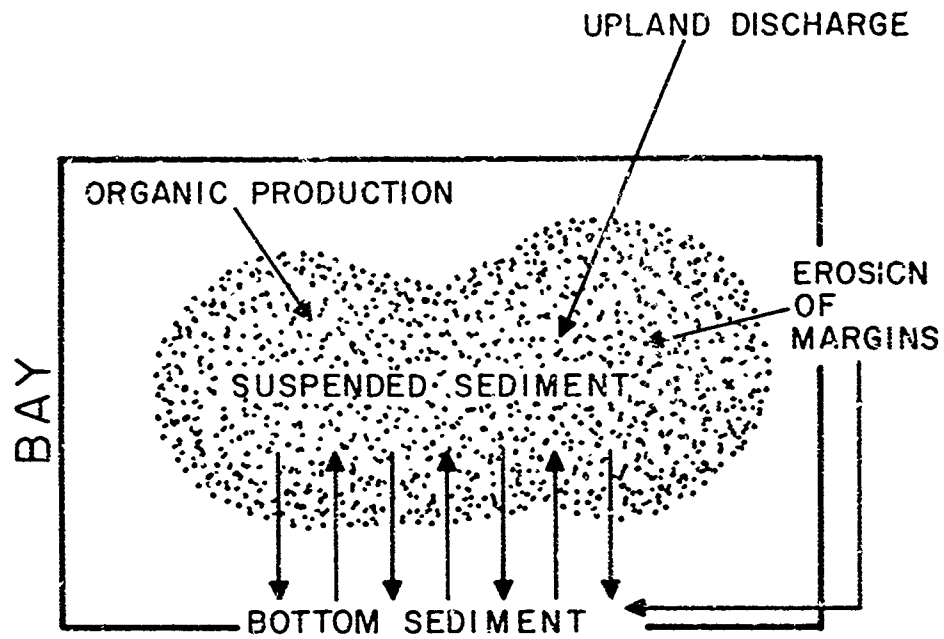


Fig. 61 Diagram of the Sources of the Suspended Sediment of the Chesapeake Bay.

Next we shall consider the marginal source, cliff and shore erosion; and finally we shall briefly consider the internal sources, organic production and resuspension of bottom sediment. A detailed discussion of the resuspension of bottom sediment by tidal scour is to be presented in another report now in preparation. This subject will be treated here only to the extent necessary to place this source of suspended material in proper perspective with the other sources.

#### SUSPENDED SEDIMENT DISCHARGE OF THE SUSQUEHANNA

The Susquehanna River, which provides more than 97 percent of the fresh water inflow into the upper Bay, is the source of nearly all of the fluvial sediment introduced into the region. The fluvial sediment being introduced into the Bay is almost entirely silt and clay sized material. The lower reaches of the rivers tributary to the Bay have very low gradients as a result of drowning caused by the post-glacial rise in sea level, and these low gradients have decreased the competency of the rivers to the extent that very little gravel and sand reach the main body of the estuary. In addition, the reservoirs of the Susquehanna have virtually eliminated the introduction of any sand into the Bay by the Susquehanna.

Cores taken by Ryan (1953) and by the author show that

the bottom sediments are predominantly clay and silt. The sand which is present is derived almost entirely from shore erosion and is largely restricted to a narrow band along the shore. Ryan's analyses show an increase in the total silt and clay content at channel stations from about 88 percent by weight at  $76^{\circ}02'20''\text{W}$ ,  $39^{\circ}24'20''\text{N}$  (about 0.8 mile north of Grove Point) to more than 98 percent by weight at  $76^{\circ}04'15''\text{W}$ ,  $39^{\circ}14'36''\text{N}$  (about 2.5 miles southeast of Pooles Island). Cores taken outside the channel show an increase in sand, but only close to shore is the total sand content greater than the total silt and clay content. Ryan (1953) presents a reconnaissance map of the bottom sediments of the Chesapeake Bay.

During the year from 1 April 1966 through 31 March 1967 the Susquehanna River discharged an estimated  $0.60 \times 10^6$  metric tons of sediment into the Bay at Havre de Grace<sup>1</sup>. This figure was determined from daily river discharge records and direct determinations of the suspended sediment concentration made approximately every one to two weeks in the Susquehanna River off Havre de Grace, Fig. 62. The discharge records were provided

---

<sup>1</sup> This is equivalent to approximately  $1.60 \times 10^6 \text{ m}^3$  or  $2.08 \times 10^6 \text{ yds}^3$  of in-place sediment. The upper meter of in-place sediment in the Bay is composed of approximately 30 percent (by weight) solids and 70 percent water, with a consequent in-place density of about  $1.25 \text{ gm cm}^{-3}$ .

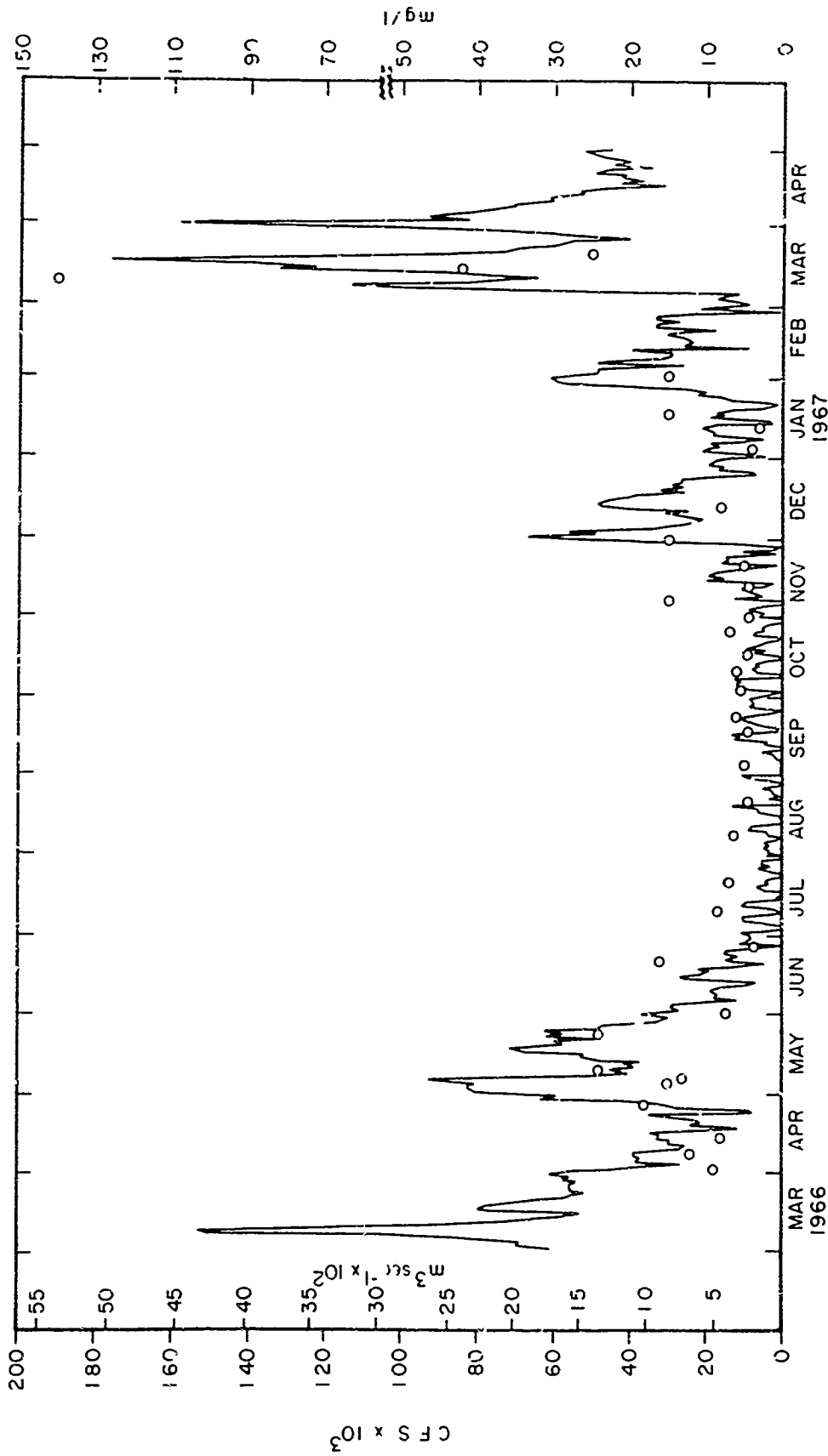


Fig. 62. Discharge of the Susquehanna River at Conowingo ( $\text{cfs} \times 10^3$ ,  $\text{m}^3 \text{sec}^{-1} \times 10^2$ ) and mean suspended concentrations ( $\text{mg/l}$ ) at Havre de Grace used in calculating the suspended sediment discharge of the Susquehanna.

by the Conowingo Hydroelectric Plant. Twenty of the 34 sets of suspended sediment concentrations were determined by the author, 3 were provided by J.H. Carpenter, and 11 were provided by R. B. Biggs of the Chesapeake Biological Laboratory. The estimate of sediment discharged was made in the following way.

First, a mean concentration of suspended sediment was determined for the entire water column for each of the days on which suspended sediment samples were taken. Second, these mean values were assumed to represent the average concentration of suspended sediment over the time intervals defined by the midpoints between sample dates. Third, each of these suspended sediment concentrations was multiplied by the average daily discharge rate averaged over the same period, and by the length of the time interval to get the total sediment discharged during the period. Fourth, these discharges were summed to obtain the total sediment discharged during the sampling year.

The value,  $0.60 \times 10^6$  metric tons, is only an estimate of the sediment discharged. In making the calculation it was assumed that the mean concentration with depth at a single station was representative of the entire river cross section. The few pertinent data which we have, and the fineness of the suspended sediment indicate that this assumption is probably reasonable. It was also assumed that these mean suspended sediment concentrations were representative of time intervals varying from 3 to as long as 25 days with nearly all intervals

from 6 to 14 days. The other assumptions are tied up in the averaging implicit in the calculation. To evaluate these assumptions, let's look at the calculation more closely.

We define the following terms:

$D_i$   $\equiv$  the sediment discharge during a time interval  $\Delta t_i$ .

$\Delta t_i$   $\equiv$  the time interval defined by the midpoints between sample dates.

$C$   $\equiv$  the instantaneous sediment concentration averaged over the cross section.

$R$   $\equiv$  the instantaneous river discharge

$(C_t)_i$   $\equiv$  the mean of the measured instantaneous sediment concentrations at the specific time  $t$  within the time interval  $\Delta t_i$ .

$\bar{C}_i$   $\equiv$  the average suspended sediment concentration over the time interval  $\Delta t_i$ .

$\bar{R}_i$   $\equiv$  the average river discharge over the time interval  $\Delta t_i$ .

The suspended sediment discharged over a time interval  $T$ , where

$$T = \sum_{i=1}^n \Delta t_i,$$

was estimated by

$$D_E = \sum_{i=1}^n D_i = \sum_{i=1}^n (C_t)_i \bar{R}_i \Delta t_i$$

which may also be written as

$$D_E = \sum_{i=1}^n \bar{C}_i \bar{R}_i \Delta t_i + \sum_{i=1}^n \left\{ (C_t)_i - \bar{C}_i \right\} \bar{R}_i \Delta t_i \quad (27)$$

The true value of the sediment discharge over the time interval T may be expressed by

$$D_T = \sum_{i=1}^n \overline{(CR)}_i \Delta t_i \quad (28)$$

where

$$\overline{(CR)}_i = \frac{1}{\Delta t_i} \int_{\Delta t_i} CR dt$$

The instantaneous values of C and R can be expressed as the sum of a mean value and a deviation term. Thus, for the time interval  $\Delta t_i$

$$\begin{aligned} C &= \bar{C}_i + C_i' \\ R &= \bar{R}_i + R_i' \end{aligned} \quad (29)$$

If we take the product of these and average, we obtain

$$\overline{(CR)}_i = \overline{\bar{C}_i \bar{R}_i} + \overline{C_i' \bar{R}_i} + \overline{\bar{C}_i R_i'} + \overline{C_i' R_i'}$$

which reduces to

$$\overline{(CR)}_i = \bar{C}_i \bar{R}_i + \overline{C_i' R_i'} \quad (30)$$

The terms  $\overline{C_i' \bar{R}_i}$  and  $\overline{\bar{C}_i R_i'}$  both equal zero since  $\bar{R}_i' = \bar{C}_i' = 0$ .

And it is obvious that  $\overline{\overline{C_i R_i}} = \overline{C_i} \overline{R_i}$  if we average over the same time interval originally used to define  $\overline{C_i}$  and  $\overline{R_i}$ . The term  $\overline{C_i' R_i'}$  does not equal zero however, except under very special circumstances or unless the variables are uncorrelated, which is not the case here.

Equation (28) can therefore be written

$$D_T = \sum_{i=1}^n \overline{C_i R_i} \Delta t_i + \sum_{i=1}^n \overline{C_i' R_i'} \Delta t_i \quad (31)$$

The difference between the true sediment discharge and the estimate given here is then

$$D_T - D_E = \sum_{i=1}^n \overline{C_i' R_i'} \Delta t_i - \sum_{i=1}^n \left\{ (C_t)_i - \overline{C_i} \right\} \overline{R_i} \Delta t_i \quad (32)$$

The error in the estimate (27) of the suspended sediment discharge over the time interval, T, then is given by the difference between two terms. The first term on the right side of Equation (32) depends on the correlation between the fluctuations of the suspended sediment concentration and the river discharge during the time intervals  $\Delta t_i$ . The suspended sediment concentrations were usually measured at intervals of one to several weeks, and thus one assumption implicit in the calculations used here is that the correlation of the fluctuations of river discharge and suspended sediment concentration

at frequencies higher than one per week may be ignored. In general, suspended sediment concentration increases with river discharge and therefore the correlation between them is probably positive. The first term on the right side of (32) then is positive, and our estimate of the suspended sediment discharge,  $D_E$ , tends to be less than the true value,  $D_T$ .

The second term on the right side of Equation (32) depends on the difference between the average of the single set of measurements of the suspended sediment concentration in the section during the time interval  $\Delta t_1$  and the mean value of the suspended sediment concentration over the time interval  $\Delta t_1$ . This term may be either positive or negative, and hence may either add or subtract from the bias introduced into the estimate by the first term. Since there are  $3^4$  sets of suspended sediment concentration determinations (i.e.,  $n = 3^4$  in Equation 32), and since there is equal probability that  $\{(C_t)_1 - \bar{C}_1\}$  for any single set will be either positive or negative, the effect of this term on the estimate of the suspended sediment discharge is probably quite small.

Thus our estimate of the total suspended sediment discharge is probably an underestimate, but we can not say by how much. An indication of this bias is given by the zero-order estimate obtained by taking the product  $\bar{C}_T \bar{R}_T T$ , where  $\bar{C}_T$  and  $\bar{R}_T$  are the average values of the suspended sediment concentration and the river discharge over the time period,  $T$ ,

of one year. The zero-order estimate was found to be  $0.31 \times 10^6$  metric tons, as compared to our first order estimate of  $0.60 \times 10^6$  metric tons found by summing over the  $3\frac{1}{4}$  sub-intervals.

Daily suspended sediment samples are now being taken at the Conowingo Hydroelectric Plant and sampling will continue through at least one calendar year. This set of data will allow us to evaluate the daily correlation of river discharge and suspended sediment concentration.

A cumulative curve and histogram of the suspended sediment discharged by the Susquehanna River at Havre de Grace from 1 April 1966 through 31 March 1967 are presented in Fig. 63. Nearly 20 percent of the total suspended sediment discharged during this period was introduced between 1 April 1966 and 24 May 1966, whereas over the next eight months the additional discharge was less than 10 percent of the total. In less than two months, 19 February 1967 through 31 March 1967, the Susquehanna discharged over 70 percent of its total suspended sediment discharge of  $0.60 \times 10^6$  metric tons for the year 1 April 1966 through 31 March 1967. Most of this was probably discharged in a period of less than three weeks during March, but the suspended sediment observations are not closely enough spaced to show this.

During the period of peak sediment discharge the

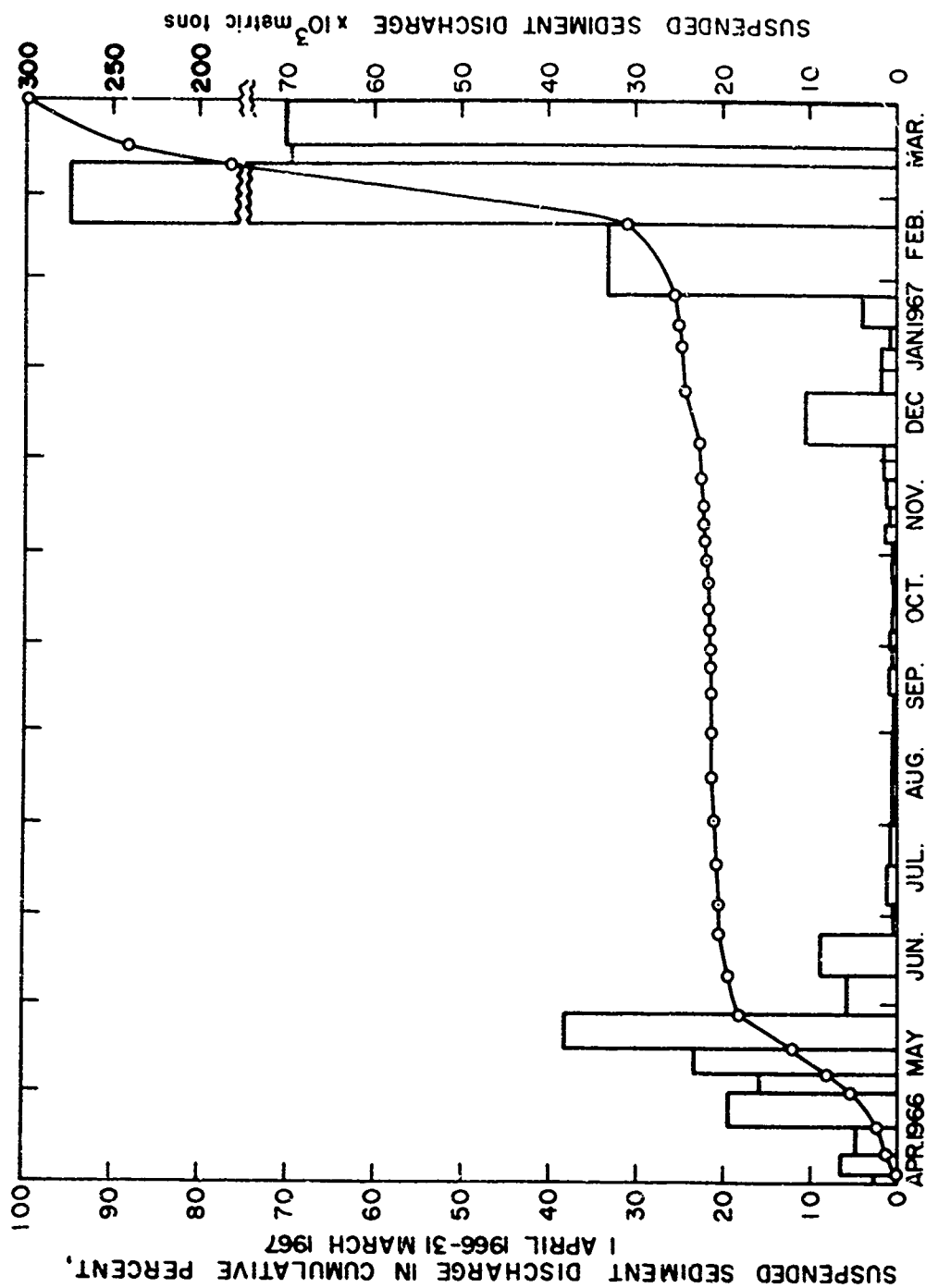


Fig. 63 Suspended Sediment Discharge of the Susquehanna River at Havre de Grace from 1 April 1966 through 31 March 1967 Plotted as Cumulative Percent, and as the Mass of Sediment Discharged during Consecutive Periods of Varying Lengths.

Susquehanna River clearly dominated the distribution of suspended sediment within the upper Bay (see Figs. 40 through 45). The maximum suspended sediment concentrations of the Susquehanna were reflected in the high concentrations recorded at each of the channel stations within the Bay. Although these values were lower than those recorded in the Susquehanna off Havre de Grace, they were in each case the maximum values recorded in the upper layer at that station over the sampling year.

In Fig. 6<sup>4</sup> the maximum surface concentrations of suspended sediment measured at each of the channel stations is plotted as the percentage of the maximum surface concentration measured in the mouth of the Susquehanna at Havre de Grace. Plotted as percentages in the same figure are the fresh water fractions of the surface waters at the same stations<sup>2</sup>.

<sup>2</sup> These fractional volumes were determined from  $S = nS_B + (1-n) S_R$ , where  $n$  is the fraction of a unit volume of water accounted for by Bay water of salinity,  $S_B = 15 \text{‰}$ ;  $(1-n)$  is the fraction of a unit volume of water accounted for by river water of salinity,  $S_R = 0.1 \text{‰}$ ; and  $S$  is the salinity of the unit volume of a mixture of river water and Bay water.

Solving for  $n$

$$n = \frac{S - S_R}{S_B - S_R}$$

and from this we obtain  $(1-n)$ .

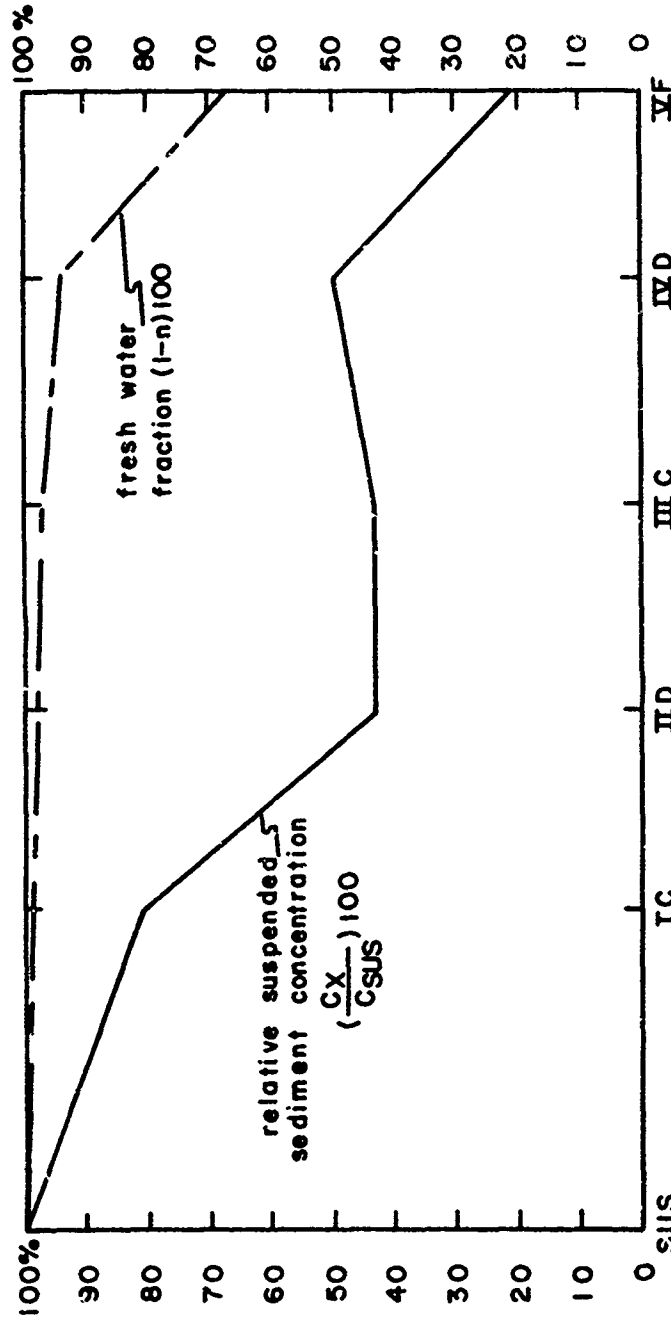


Fig. 64 The maximum surface concentrations of suspended sediment ( $C_x$ ) at each of the channel stations plotted as the percentage of the maximum surface concentration of suspended sediment at Station SUS ( $C_{SUS}$ ). The fresh water fractions (1-n) of the surface waters at the same stations are also plotted as percentages.

Figure 64 clearly show that the downstream decrease in the concentration of suspended sediment resulted primarily from the loss of material by settling; the dilution of river water by Bay water could not have produced the longitudinal gradient of suspended sediment. At station VF the concentration of suspended sediment dropped to 20 percent of the suspended sediment concentration in the mouth of the Susquehanna off Havre de Grace, whereas the volume percent of Susquehanna water in a unit volume of surface water only decreased to 67 percent. If one assumes that no material was added to the upper layer from other sources, then about 80 percent of the material introduced by the Susquehanna at Havre de Grace during maximum runoff was deposited above the seaward end of the study area. This amounts to about  $0.33 \times 10^6$  metric tons of suspended sediment, or to  $0.92 \times 10^6 \text{ m}^3$  of in-place sediment which if deposited uniformly over the Bay portion of the study area ( $370 \times 10^6 \text{ m}^2$ ) would form a deposit 2.5 mm thick. Since resuspended sediment is added to the upper layer and therefore contributes to the concentrations within the Bay, it is obvious that less than 20 percent of the sediment discharged by the Susquehanna during peak runoff in 1967 was directly transported through the study area.

At all times of the year other than during peak runoff, the concentrations of suspended sediment were higher within the

Bay than in the mouth of the Susquehanna at Havre de Grace, indicating the importance of another source or sources.

#### COASTAL EROSION OF THE UPPER BAY

Using the shore erosion data of Singewald and Slaughter (1949) in conjunction with relief data obtained from topographic maps and from field measurements of cliff heights, an estimate was made of the mass of sediment derived annually by erosion of the coast of the main body of the Bay north of Tolchester ( $30^{\circ}12'N$ ). Singewald and Slaughter report the mean annual losses of acres of coast per mile of coastline for the Maryland counties bordering the Bay. Their data are based on the comparisons of charts covering a period of about 90 years, and are reported by coastline segments. The author combined each of their annual areal losses with relief data for the same coastline segment to calculate the volume of sediment removed annually from that section of coastline. Along the eastern, northern, and along parts of the western shore, the elevations obtained from topographic maps were supplemented with field measurements. This was not possible, however, in the restricted zone of the Aberdeen Proving Grounds.

The mass of sediment removed from each coastline segment was calculated from the volume by using a mean sediment density of  $2.65 \text{ gm/cm}^3$ . The percent of each of these masses

of eroded material accounted for by silt and clay was estimated in the following way. Cliff face sections were measured and sediment samples were collected from each of the exposed facies. These samples were then split by wet-sieving into two size fractions--sand, and silt plus clay. The percent of silt plus clay in each sample was then determined by weighing. These percentages were then weighted by the thicknesses of the parent beds to determine the percent of the total exposed cliff accounted for by silt and clay-sized material. The length of coastline over which each such determination was considered to be representative was dictated by the lateral and vertical uniformity of the exposed beds. For most coastline segments at least three sets of measurements were made. It was not possible to obtain samples along the shoreline of the Aberdeen Proving Grounds. For this stretch of coast, silt and clay were assumed, on the basis of samples from adjacent areas, to account for 35 percent of the eroded sediment. The measurement sites are indicated in Fig. 65.

The results of the analysis show that approximately 37,466 m<sup>2</sup> (9.26 acres) of coast are lost annually by coastal erosion. This amounts to more than 125,000 m<sup>3</sup> of sediment or more than 0.33 × 10<sup>6</sup> tons. Of this, about 0.12 × 10<sup>6</sup> tons are silt and clay. This contribution of silt and clay is equivalent to about 20 percent of the sediment discharged by the Susquehanna River from 1 April 1966 through 31 March 1967. The

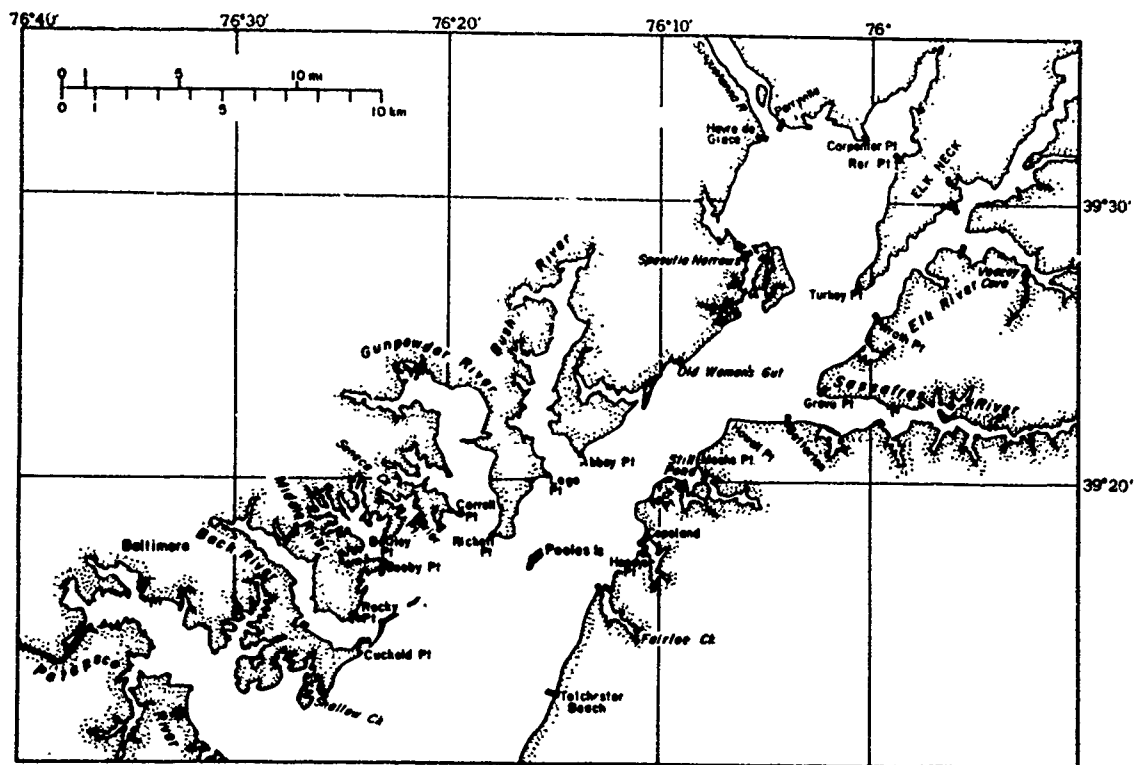


**Fig. 65** Map of the Upper Bay showing Shoreline Segments used in Calculating Annual Losses due to Erosion.

data are summarized in Table 13. The highest rates of areal loss were found along low-lying stretches of the western shore from Old Woman's Gut to Abbey Point, and from Cuckold Point to Shallow Creek. The highest rates of volume loss however, were found in areas of relatively high relief along the eastern shore from Grove Point to Wroth Point, and at the head of the Bay from Turkey Point to Red Point. The weighted mean annual rates of areal and volume loss of coast were found to be  $328 \text{ m}^2/\text{km}$ , and  $1095 \text{ m}^3/\text{km}$ , respectively. The weighting factors used in the calculation were the lengths of coastline over which the erosion rates given in Table 13 were derived. In other words, the mean annual rate of erosion per kilometer of coastline is given by

$$E = \frac{\sum_{i=1}^n E_i l_i}{\sum_{i=1}^n l_i}$$

where  $E_i$  is the erosion rate (either areal or volume) for a particular coastline segment of length  $l_i$ .

Ryan's (1953) sediment map and the author's own observations show that very little of the eroded sand and gravel escape the littoral zone. Most of the silt and clay however, is winnowed out of the littoral zone.

The rates of coastal erosion are highest during periods of rough seas and would therefore be higher during the late

TABLE 13  
Coastal Erosion Data

Coastline Segment	Length of Segment (km)	Annual Area Rate of Loss of Coastline per km of Coastline ( $m^2/km$ )	Area of Coastline Lost Annually ( $m^2$ )	Annual Volume Rate of Loss of Sediment per km of Coastline ( $m^3/km$ )	Mass of Sediment Lost Annually ( $10^3 tons$ )	Mass % Silt plus clay ( $\%$ )	Mass of Silt and Clay lost Annually ( $10^3 tons$ )
Tolchester to Fairlee Ck.	6.6	277	1828	8039	21.3	52	11.1
Fairlee Ck. to Handy's Pt.	3.6	75	270	821	2.2	52	1.1
Copeland to Rocky Pt.	7.0	427	2989	12884	34.1	53	18.1
Still Pond to Betterton	8.7	226	1966	18766	49.7	39	19.4
Grove Pt. to Wroth Pt.	6.6	503	3320	19139	50.7	33	16.7
Wroth Pt. to Veszey Cove	4.5	151	680	1036	2.8	26	0.7
Hyland's Pt. to Turkey Pt.	5.6	176	986	7252	19.2	33	6.3
Turkey Pt. to Red Pt.	9.0	277	2493	24559	65.1	33	21.5
Carpenter Pt. to Perryville	6.4	176	1126	3929	10.4	25	2.6
Havre de Grace to Spesuti Narrows	10.8	+ 5	+ 54	+ 207	+ 0.6	35	+ 0.2
Spesuti Narrows to Old Woman's Gut	5.6	402	2251	2072	5.5	35 <sup>2</sup>	1.9
Old Woman's Gut to Abbey Pt.	10.0	729	7290	9050	24.0	35 <sup>2</sup>	8.4

TABLE 13 Continued

Coastline Segment	Length of Segment (km)	Annual Areal Rate of Loss of Coastline per km of Coastline (m <sup>2</sup> /km) <sup>1</sup>	Area of Coastline Lost Annually (m <sup>2</sup> )	Annual Volume Rate of Loss of Coastline per km of Coastline (m <sup>3</sup> /km)	Mass of Sediment Lost Annually (10 <sup>3</sup> tons)	Mass % Silt plus Clay (%)	Mass of Silt and Clay lost Annually (10 <sup>3</sup> tons)
Lego Pt. to Rickett Pt.	6.8	553	3760	5699	15.1	35 <sup>2</sup>	5.3
Carrroll Pt. to Brierr Pt.	7.7	427	3288	4026	10.7	35 <sup>2</sup>	3.7
Seneca Ck. to Bowley Pt.	2.6	151	393	592	1.6	35 <sup>2</sup>	0.6
Booby Pt. to Rocky Pt.	8.0	151	1208	1850	4.9	35 <sup>2</sup>	1.7
Cuckold Pt. to Shallow Ck	4.7	780	3666	5544	14.7	35 <sup>2</sup>	5.1
TOTALS	114.2	328 weighted average	37460	125051	331.4		124.0

<sup>1</sup> After Singewald and Slaughter (1949).

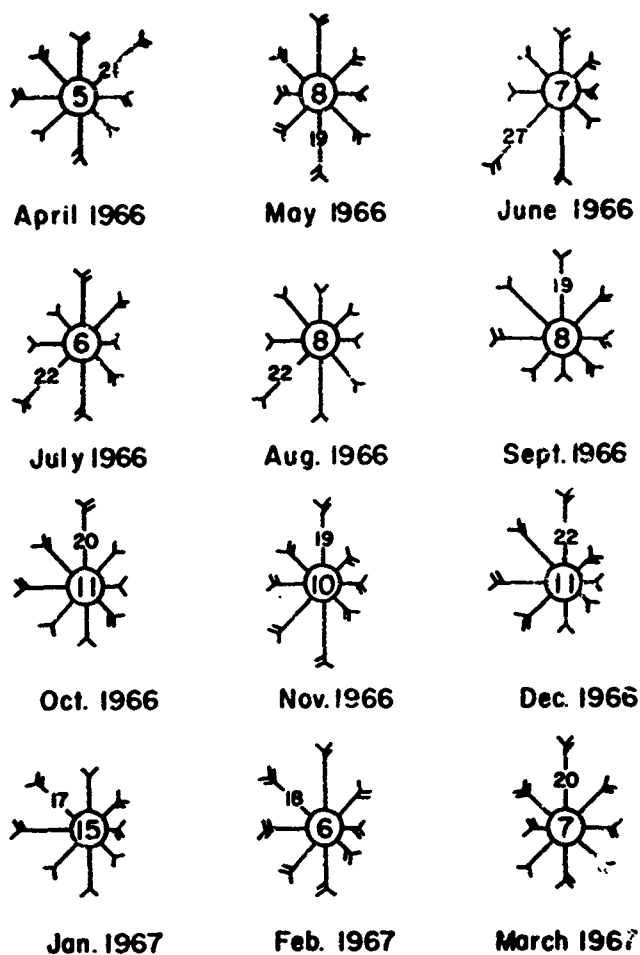
<sup>2</sup> Assumed.

fall, winter, and spring months than during the summer and early fall months. Wind data from the meteorological station at Aberdeen Proving Grounds are presented as monthly wind roses in Fig. 66.

#### RESUSPENSION OF BOTTOM SEDIMENT

It should be apparent from the discussion and from Figs. 31 through 45 that neither the mass of sediment introduced by the Susquehanna River during peak flow, nor the silt and clay derived annually by coastal erosion can directly account for the relatively high concentrations of suspended sediment found throughout the year in the upper Bay. The explanation emerges from serial measurements made at anchor stations of both current velocity and the concentration of suspended sediment. The results of one of these sets of observations are presented in Figs. 67 through 69. From 1200 hours on 10 July 1967 to 1600 hours on 11 July 1967, hourly measurements were made at the surface, and at depths of 2, 4, 6, 8, and 9 m at a station, IIIC\*, in 9.5 m of water just outside the channel opposite station IIIC.

Figs. 67 through 69 show that at the surface, at 2 m and at 4 m the concentrations of suspended sediment were relatively constant over the period of measurement. At 6 m fluctuations of the concentration of suspended sediment were appreciable,



0 10 20 30 40 50 60 70 80 90 100  
 SCALE OF WIND PERCENTAGES

Fig. 66 Monthly Wind Rose Diagrams for the Year 1 April 1966 through 31 March 1967. Based on Hourly Measurements made at Aberdeen Proving Grounds. The Wind Percentages are concentrated on 8 Points. The Arrows fly with the Wind. The length of Arrow measured from the Outside of the Circle on the Attached Scale gives the Percent of the Total Observations in which the Wind has blown from or near the given Point. The Number of Feathers shows the Average Speed of the Wind: 2 Feathers -- 2 to 5 m. p. h., 3 Feathers -- 6 to 10 m. p. h., 4 Feathers -- 11 to 15 m. p. h. The Figure in the Center of the Circle gives the Percentage of Calms.

varying by as much as a factor of three and one-half, but they were not strongly related to current speed. At 8 m the suspended sediment concentrations varied by nearly a factor of seven, and the fluctuations were clearly related to current speed and tidal period. Maximum concentrations were recorded near times of maximum ebb and flood velocities, and minimum concentrations were observed shortly after times of slack water. At 9 m there was an even stronger relationship between current speed and the concentration of suspended sediment. The concentration varied by more than a factor of eighteen, ranging from 15 to nearly 280 mg/l. It is apparent that the bottom sediment is being resuspended by tidal scour, and that the concentrations of suspended sediment in the lower part of the water column are determined by the events of the past few hours.

The upward flux density of sediment through a horizontal plane at 9 m was found to be about  $4 \times 10^4$  mg/m<sup>2</sup>/hr. This represents the rate at which bottom sediment is resuspended and transported through a horizontal plane 0.5 m above the bottom. The bulk of this is redeposited within a few hours, and the net movement over a tidal cycle must be small.

Resuspension results from both wind waves and tidal scour. Since most of the area is very shallow, resuspension by wind waves is an important factor during periods of high wind and rough sea. Resuspension by tidal scour is important

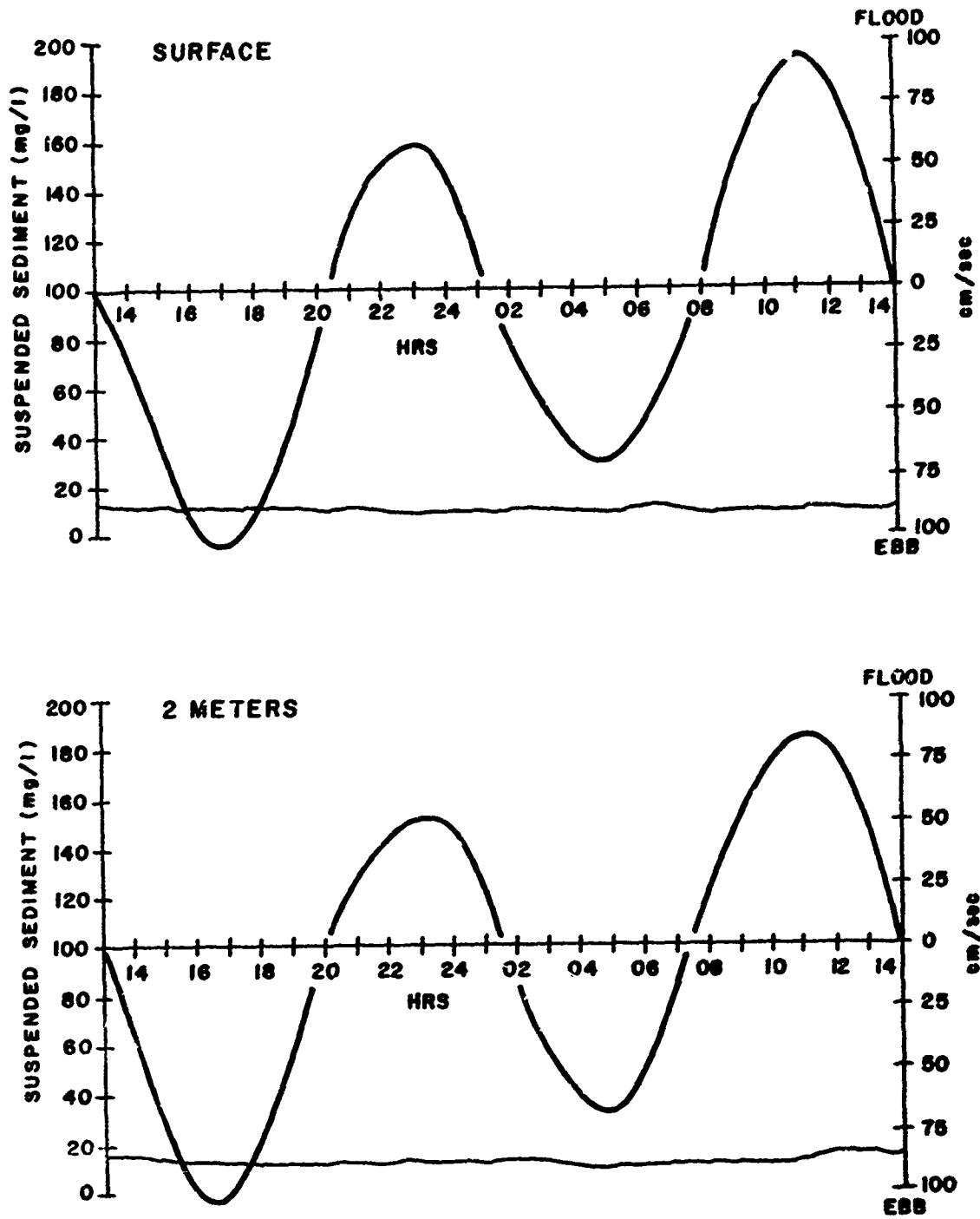


Fig. 67 Current Velocity and Suspended Sediment Concentration at the Surface and at 2m at Station IIC\* (9.5m) on 10-11 July 1967. Based on hourly measurements.

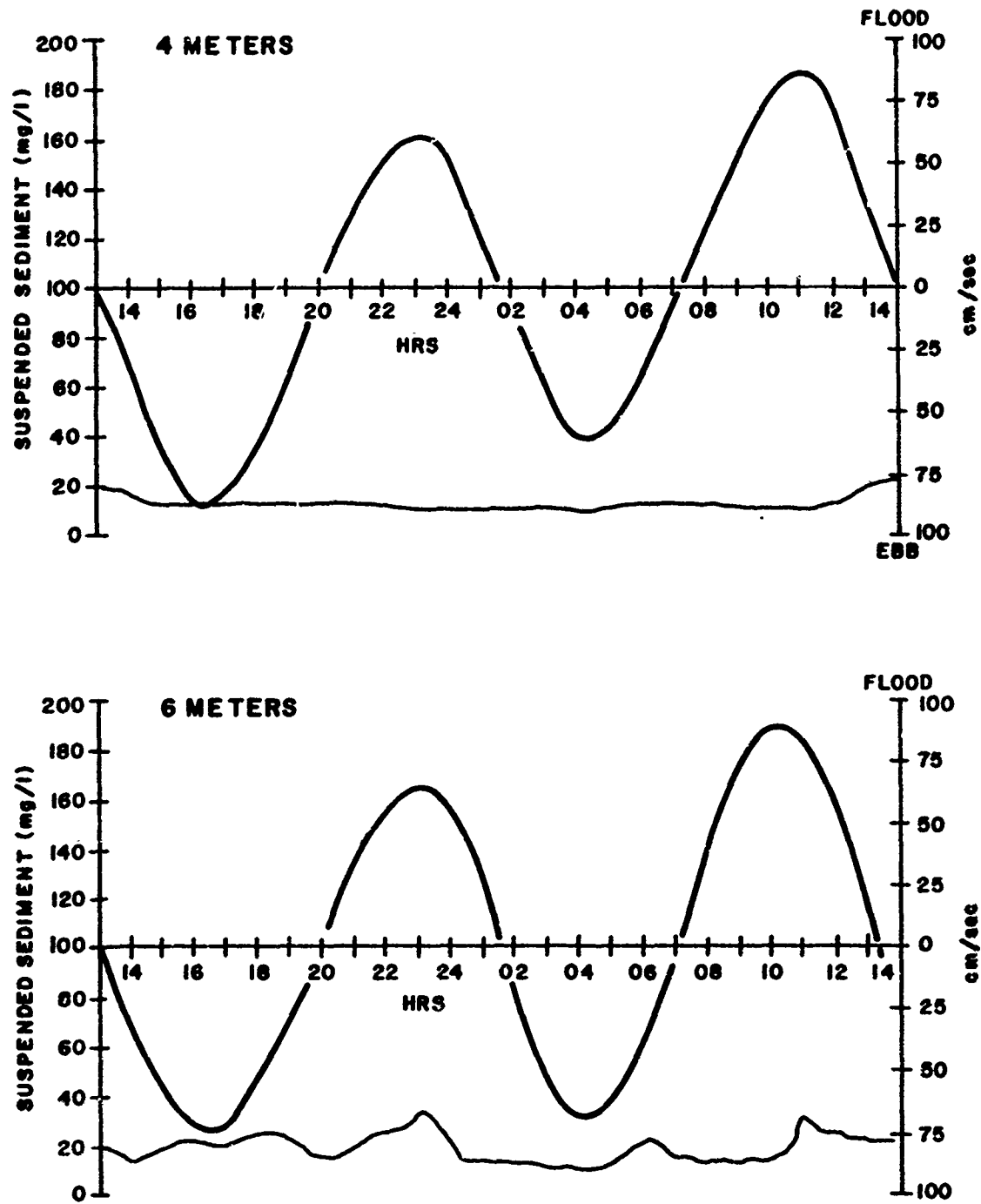


Fig 68 Current Velocity and Suspended Sediment Concentration at 4m and at 6m at Station IIC\* (9.5m) on 10-11 July 1967. Based on hourly measurements.

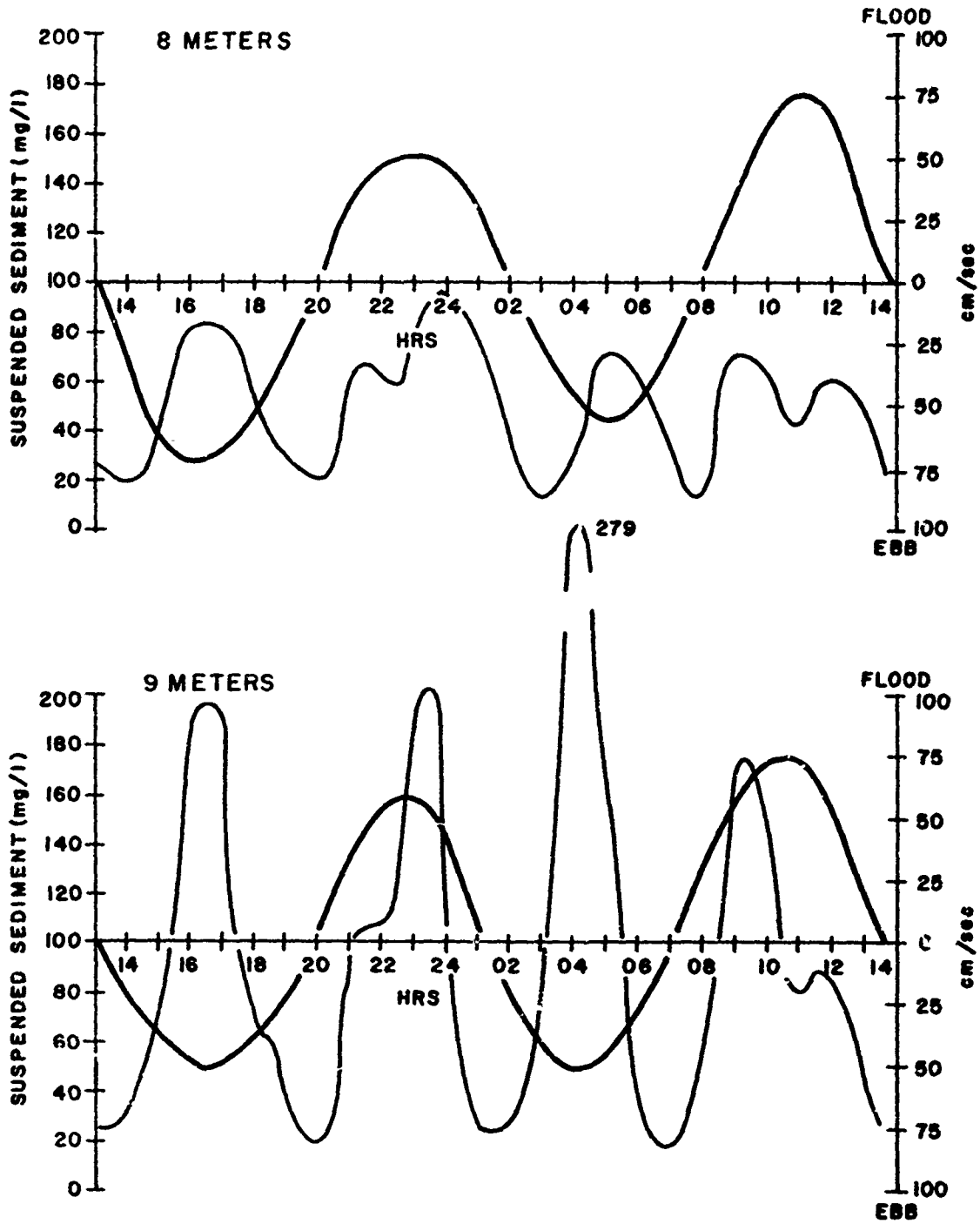


Fig. 69 Current Velocity and Suspended Sediment Concentration at 8m and at 9m at Station IIIC\* (9.5m) on 10-11 July 1967. Based on hourly measurements.

at all times of the year and probably accounts for most of the resuspended material. Observations made during rough weather show that the concentrations were higher than the background concentrations maintained by tidal scour, but the high "storm concentrations" dissipated within a few days.

The concentrations of total suspended solids were usually higher on the western side of the Bay than on the eastern side of the Bay at the same cross section (see section on total suspended solids). These higher concentrations are attributed to the greater area of shallow water found to the west of the channel. Because of the decreased depth, resuspension by both tidal scour and wind mixing is effective throughout a greater part of the water column.

#### Explanations explanatory of things explained. A. Lincoln

During the period of maximum runoff there was an obvious link between the upper Bay and its principal sediment source, the Susquehanna. At all other times of the year however, this association was missing and the upper Bay was more closely linked with its internal sources--organic production and particularly the bottom. Except for the period of peak runoff, the concentrations of suspended sediment were higher within the upper Bay than in the mouth of the Susquehanna despite the dilution of the fluvial sediment and the settling

out which occur within the Bay. The higher concentrations within the Bay are due in part to the fact that the concentrations of organic matter found in the upper Bay are higher than those in the Susquehanna, Fig. 70. But, Fig. 70 shows that the increased organic matter is not sufficient to account for the differences between the Susquehanna and the Bay. There are three possible explanations for the high concentrations of suspended sediment observed in the upper layer. First, the high concentrations may be due to the addition to the upper layer of sediment which has been locally (within the study area) resuspended from the bottom. Second, the high concentrations in the upper layer may result from the direct addition of sediment which has been resuspended downstream from the area and brought upstream in the lower layer. Third, the high concentrations in the upper layer may be the result of a combination of these two mechanisms.

At present we cannot distinguish among these possibilities. We can however, calculate the net flux of sediment through the surface separating the upper and lower layers. It will be more instructive if first we write an instantaneous total suspended sediment balance equation for both the upper and lower layers within the study area. We shall assume that at any time the suspended sediment population is derived from the Susquehanna River, from local resuspension, and from material brought up-

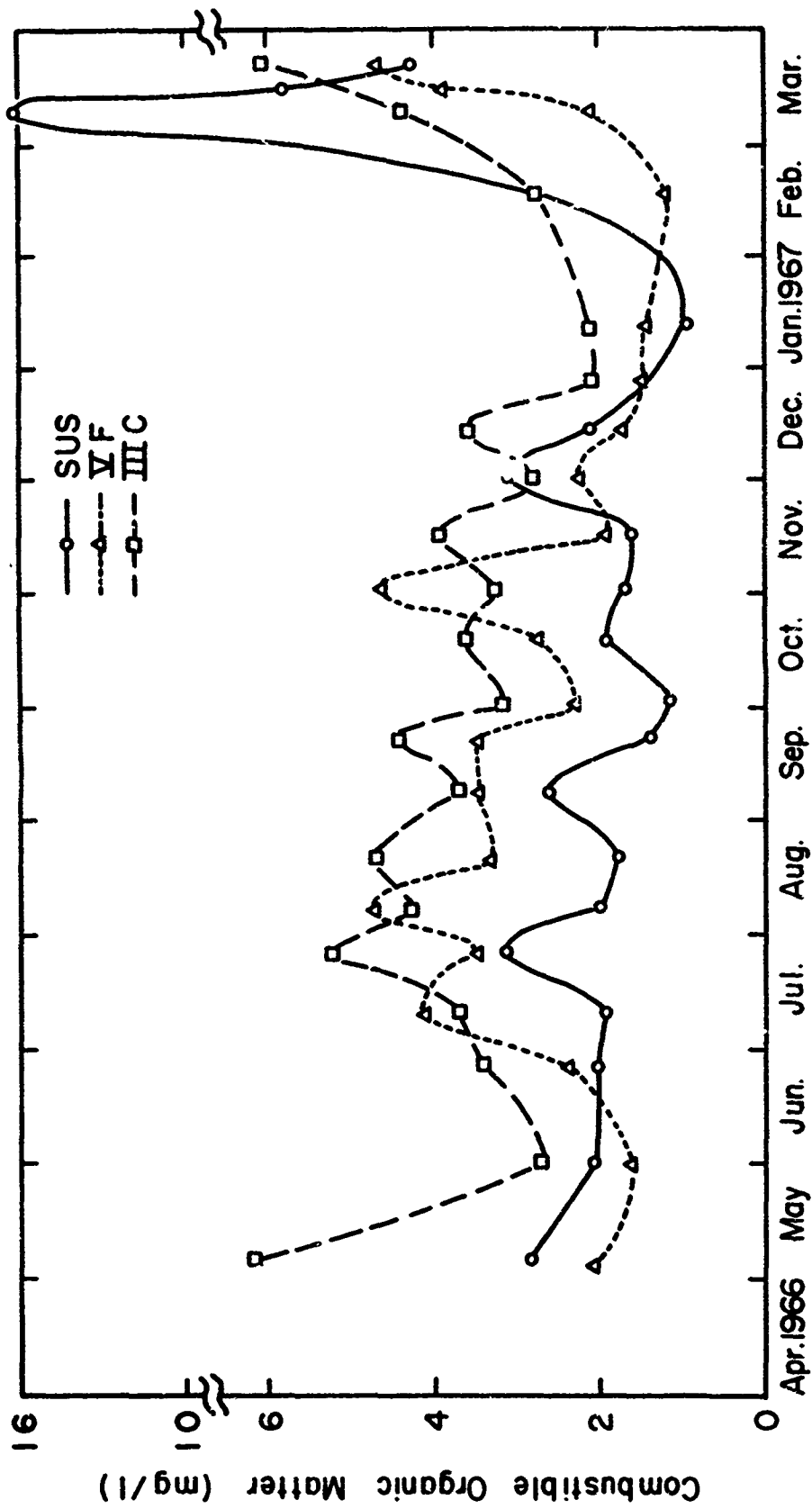


Fig. 70 Surface Concentrations (mg/l) of Combustible Organic Matter at Stations SUS, IIC, and VF Plotted against the Date of Sample Collection.

stream in the lower layer into the region. Making this assumption we can write the following instantaneous balance equation.

(33)

$$\frac{\partial}{\partial t} \int V C d\tau = \int_{S_R} C_R v_R d\sigma + \int_{S_l} C_l v_l d\sigma + G - \int_{S_u} C_u v_u d\sigma - \int_A w_s C_A d\sigma$$

rate of change of total mass of suspended sediment	rate of supply by Susquehanna	rate of supply to region by transport upstream in lower layer	rate of supply by re- sus- pension	rate of loss by transport out in up- per layer	rate of loss by settling
--	----------------------------------	---	---	--	--------------------------------

where  $C$  = the instantaneous concentrations of suspended sediment within the study area

$V$  = total volume of Bay within the study area

$S_R$  = the cross-sectional area of the Susquehanna River at Havre de Grace

$C_R$  = the instantaneous concentrations of suspended sediment at the cross section in the mouth of the Susquehanna River at Havre de Grace

$v_R$  = the instantaneous river velocities

$S_l$  = the cross-sectional area of the lower layer at the seaward end of the study area

$C_l$  = the instantaneous suspended sediment concentrations in the lower layer at the seaward end of the study area

$v_l$  = the instantaneous velocities in the lower layer at the

seaward end of the study area

$G$  = Rate of sediment supply from bottom of study area

$S_u$  = the cross-sectional area of the upper layer at the seaward end of the study area

$C_u$  = the instantaneous suspended sediment concentrations in the upper layer at the seaward end of the study area

$v_u$  = the instantaneous velocities in the upper layer at the seaward end of the study area

$A$  = the area of the study region just above the bottom

$w_s$  = the settling velocity of the suspended particles

$C_A$  = the concentration of suspended sediment just above the bottom

Returning now to our original problem, we can write a suspended sediment balance equation for the upper layer and calculate the net flux density of sediment through the surface separating the upper and lower layers. We shall assume that the suspended sediment population of the upper layer is derived entirely from the Susquehanna River and from the lower layer. Making this assumption, we can write the following

$$\frac{\partial}{\partial t} \int_{V_u} c_u d\tau = \int_{S_R} C_R v_R d\sigma + \int_A F d\sigma - \int_{S_u} C_u v_u d\sigma \quad (34)$$

$\frac{\partial}{\partial t} \int_{V_u} c_u d\tau$ rate of change of total mass of suspended sedi- ment in upper layer	$= \int_{S_R} C_R v_R d\sigma$ rate of supply by Sus- quehanna	$+ \int_A F d\sigma$ net flux of sediment thru surface separ- ating upper and lower layer	$- \int_{S_u} C_u v_u d\sigma$ rate of loss by transport in upper layer	(34)
---	--	--	---	------

where  $A'$  = the area of the surface separating the upper and lower layers

$F$  = the flux density of sediment through the surface separating the upper and lower layers

and the other terms are defined as before.

Assuming steady state and taking the time average of (34) over  $T$  we can write

$$0 = \overline{\int_{S_R} C_R v_R d\sigma} + \overline{\int_A F d\sigma} - \overline{\int_{S_u} C_u v_u d\sigma} \quad (35)$$

Each instantaneous value of  $C_u$ ,  $v_u$ ,  $C_R$ , and  $v_R$  can be expressed as the sum of a mean value over some time interval,  $T$ , and a corresponding mean deviation

$$\begin{aligned} C_u &= \bar{C}_u + C_u' \\ C_R &= \bar{C}_R + C_R' \\ v_u &= \bar{v}_u + v_u' \\ v_R &= \bar{v}_R + v_R' \end{aligned} \quad (36)$$

where  $\bar{C}_u$ ,  $\bar{C}_R$ ,  $\bar{v}_u$ , and  $\bar{v}_R$  represent the mean values over the time,  $T$ , and  $C_u'$ ,  $C_R'$ ,  $v_u'$ , and  $v_R'$  represent the fluctuations from the mean. If we substitute (36) into (35) and average over the time interval,  $T$ , we obtain

$$\overline{\int_A F d\sigma} \equiv A' \langle F \rangle = \int_{S_u} (\bar{C}_u + C_u') (\bar{v}_u + v_u') d\sigma - \int_{S_R} (\bar{C}_R + C_R') (\bar{v}_R + v_R') d\sigma \quad (37)$$

where  $\langle F \rangle$  is the space-time average of  $F$ . Multiplying yields

$$A' \langle F \rangle = \int_{S_u} (\bar{C}_u \bar{v}_u + C_u' \bar{v}_u + \bar{C}_u v_u' + C_u' v_u') d\sigma - \int_{S_R} (\bar{C}_R \bar{v}_R + C_R' \bar{v}_R + \bar{C}_R v_R' + C_R' v_R') d\sigma \quad (38)$$

which can be written as

$$A' \langle F \rangle = \int_{S_u} (\overline{C_u v_u} + \overline{C_u' v_u} + \overline{\bar{C}_u v_u'} + \overline{C_u' v_u'}) d\sigma - \int_{S_R} (\overline{C_R v_R} + \overline{C_R' v_R} + \overline{\bar{C}_R v_R'} + \overline{C_R' v_R'}) d\sigma \quad (39)$$

The terms  $\overline{C_u' v_u}$ ,  $\overline{\bar{C}_u v_u'}$ ,  $\overline{C_R' v_R}$ , and  $\overline{\bar{C}_R v_R'}$  all equal zero since  $\bar{C}_u' = \bar{v}_u' = \bar{C}_R' = \bar{v}_R' = 0$ . And  $\overline{C_u v_u} = \overline{\bar{C}_u \bar{v}_u}$ , and  $\overline{C_R v_R} = \overline{\bar{C}_R \bar{v}_R}$ , if we average over the same time interval used to define  $\bar{C}_u$ ,  $\bar{v}_u$ ,  $\bar{C}_R$ , and  $\bar{v}_R$ . The terms  $\overline{C_u' v_u'}$  and  $\overline{C_R' v_R'}$  do not equal zero, however, unless the variables are uncorrelated or except under very special circumstances. The variables are not uncorrelated. But, if we exclude the period of high runoff the term  $\overline{C_u' v_u'}$  is small compared with  $\overline{C_u v_u}$  because the fluctuations of  $C_u$  are generally less than 10 percent of the mean value. Therefore, we can neglect  $\overline{C_u' v_u'}$ . The term  $\overline{C_R' v_R'}$ , however, can not be neglected. Omitting the period of maximum runoff, (39) reduces to

$$A'\langle F \rangle \doteq \int_{S_u} \bar{C}_u \bar{v}_u d\sigma - \int_{S_R} \bar{C}_R \bar{v}_R d\sigma - \int_{S_R} \overline{C_R' v_R'} d\sigma \quad (40)$$

where  $\langle F \rangle$  is the spatial and temporal mean flux density of sediment through the surface separating the upper and lower layers.

Since our observations show that  $C_u$  and  $C_R$  are quite uniform with depth at any given time (except during maximum runoff), we can write (40) as

$$A'\langle F \rangle \doteq \bar{C}_u \int_{S_u} \bar{v}_u d\sigma - \bar{C}_R \int_{S_R} \bar{v}_R d\sigma - \overline{C_R' \int_{S_R} v_R' d\sigma} \quad (41)$$

which is equivalent to

$$A'\langle F \rangle \doteq \bar{C}_u \bar{V}_u - \bar{C}_R \bar{R} - \overline{C_R' R'} \quad (42)$$

where  $\bar{V}_u$  is the mean volume flow in the upper layer through the cross section at the seaward end of the study area,  $\bar{R}$  is the mean discharge of the Susquehanna River at Havre de Grace,  $R'$  is the mean deviation, and the other terms are defined as before.

The quantity  $\bar{C}_R \bar{R} + \overline{C_R' R'}$  was calculated for the period 1 April 1966 through 18 February 1967 and found to be about  $0.18 \times 10^6$  metric tons or approximately  $6.4 \times 10^3$  gm/sec.  $\bar{C}_u$  was approximately  $9$  gm/m<sup>3</sup> over the same period. Based on the average salinities in the upper and lower layers at the seaward

end of the study area,  $V_u$  was estimated to be about  $3R$  or  $20 \text{ m}^3/\text{sec}$ .  $A'$  is approximately  $3.7 \times 10^8 \text{ m}^2$ . Solving (42) for  $\langle F \rangle$  and substituting these values we obtain

$$\langle F \rangle = \frac{\bar{C}_u \bar{V}_u - \bar{C}_R \bar{R} - \bar{C}_R' \bar{R}'}{A'}$$

$$\langle F \rangle = \frac{\bar{C}_u 3R - \bar{C}_R \bar{R} - \bar{C}_R' \bar{R}'}{A'} = \frac{(9 \text{ gm/m}^3)3(680 \text{ m}^3/\text{sec}) - 6.4 \times 10^3 \text{ gm/sec}}{3.7 \times 10^8 \text{ m}^2}$$

$$\langle F \rangle = 3.2 \times 10^{-5} \text{ gm/m}^2 \text{ sec} = 0.03 \text{ mg/m}^2 \text{ sec}$$

Since  $\langle F \rangle$  is positive, the net flux density of sediment is upward through the surface separating the upper and lower layers.

We can also express  $\langle F \rangle$  as

$$\langle F \rangle = \langle F_s \rangle - \langle w_s C_{u*} \rangle \quad (43)$$

where  $\langle F_s \rangle$  is the space-time mean upward flux density of sediment into the upper layer,  $w_s$  are the instantaneous settling velocities,  $C_{u*}$  are the instantaneous concentrations of suspended sediment at the surface separating the upper and lower layers, and  $\langle w_s C_{u*} \rangle$  is the space-time mean downward flux density of sediment through the surface separating the upper and lower layers. Since the mean Stokes diameter,  $\bar{D}_s$ , of particles suspended in the upper layer is about  $3.8 \mu$ ,  $w_s$  is of the order  $1 \times 10^{-5} \text{ m sec}^{-1}$ , and

$$\langle w_s C_{u^*} \rangle \approx 10^{-5} \text{ m/sec} \times 10^4 \text{ mg/m}^3 \approx 10^{-1} \text{ mg/m}^2 \text{ sec}$$

Solving (43) for  $\langle F_s \rangle$ , we have

$$\langle F_s \rangle = \langle F \rangle + \langle w_s C_{u^*} \rangle$$

Substituting for  $\langle F \rangle$  and  $\langle w_s C_{u^*} \rangle$  yields

$$\langle F_s \rangle = 0.03 \text{ mg/m}^2 \text{ sec} + 10^{-1} \text{ mg/m}^2 \text{ sec}$$

Therefore,  $\langle F_s \rangle$  is also of the order  $10^{-1} \text{ mg/m}^2 \text{ sec}$ .

For a purely advective model, we can express  $\langle F_s \rangle$  as

$$\langle F_s \rangle = \langle w_{\text{up}} C_{\ell^*} \rangle \quad (44)$$

In (44)  $w_{\text{up}}$  are the instantaneous upward vertical velocities,  $C_{\ell^*}$  are the instantaneous concentrations of suspended sediment at the top of the lower layer, and  $\langle w_{\text{up}} C_{\ell^*} \rangle$  is the space-time mean upward advective flux density of sediment through the surface separating the upper and lower layers. Since  $C_{\ell^*}$  is approximately  $10^4 \text{ mg/m}^3$ ,  $w_{\text{up}}$  would be of the order  $10^{-5} \text{ m/sec}$  which is not unreasonable (Pritchard, 1956), and it appears that our estimate of  $\langle F \rangle$  is at least reasonable.

Using the same arguments as before, we can write the following suspended sediment balance equation for the entire study area.

$$A \langle F_B \rangle \doteq \bar{C}_u \bar{V}_u - \bar{C}_R \bar{R} - \bar{C}_R \bar{R}' - \int_{S_\ell} \overline{C_\ell v_\ell} d\sigma \quad (45)$$

In (45)  $\langle F_B \rangle$  is the space-time mean net flux density of sediment through a surface just above the bottom,  $C_l$  are the instantaneous concentrations of suspended sediment in the lower layer at the seaward end of the study area,  $v_l$  are the associated instantaneous velocities, and the other terms are defined as before. Since  $C_l$  varies considerably with depth at any time, we cannot remove  $C_l$  from the integrand. At the present time we have the data to evaluate the first two terms on the right side of Equation (45). If we could evaluate  $\int_{S_l} \overline{C_l v_l} d\sigma$ , we could calculate  $\langle F_B \rangle$ , and we would have made a major advance in understanding the sedimentation in the upper Bay.

Since we are interested in the total average transport of suspended sediment by the lower layer,  $\int_{S_l} \overline{C_l v_l} d\sigma$ , we want to define some space-time mean suspended sediment concentration ( $\langle C_l \rangle$ ) for the lower layer such that

$$\langle C_l \rangle \bar{V}_l = \int_{S_l} \overline{C_l v_l} d\sigma \quad (46)$$

where  $\bar{V}_l$  is the mean volume flow in the lower layer through the cross section at the seaward end of the study area, and the other terms are as previously defined. We can determine  $\langle C_l \rangle$  by making serial measurements of current velocity and suspended sediment concentration at different depths at two or more stations along a cross section at the seaward end of the study

area. If we take the products of these paired measurements of instantaneous velocity and suspended sediment concentration and sum them over the cross-sectional area of the lower layer over an integral multiple of tidal cycles, and then divide this quantity by the sum of the instantaneous velocities summed over the same area and time, we will obtain  $\langle C_{\ell} \rangle$ . We hope to make the measurements necessary for the calculation of  $\langle C_{\ell} \rangle$  in the near future.

From the data we have it appears that, except for the period of peak runoff, the upstream and downstream fluxes of suspended sediment through the seaward end of the study area may be nearly balanced. It is important however, to remember that we are looking at a small difference between two large numbers and it is difficult to determine even the sign of the difference, let alone the magnitude. Also, as has been pointed out, our knowledge of the mean concentration in the lower layer at the seaward end of the study area is very poor.

It appears that we have three choices. First, the net flux of sediment through the seaward end of the study area may be nearly zero except during maximum runoff, and the amount of sediment deposited in the upper Bay during this period may represent a net deposit. Second, there may be a small net upstream flux of sediment through the seaward end of the study area thereby supplementing the amount of

material deposited during high runoff with sediment from downstream. Third, over the year there may be a small net downstream flux of sediment through the seaward end of the study area thereby decreasing the amount of sediment deposited by the Susquehanna during the period of high runoff, and perhaps resulting in a net loss of sediment. All three conditions may produce net deposition over the year; the first two must.

As always the difficulty in life is the choice, and unlike choosing a horse or a wife, the choice must satisfy not only the chooser, but it also must be the best choice on the basis of the available information. From the data we have, it is very unlikely that there is a net annual loss of sediment from the study area. It is much more likely that there is a net annual accumulation of sediment. At present, we are not in a position to write a sediment budget for this segment of the Bay but we could pose a number of questions to demonstrate that accumulation is more probable than erosion. We shall ask one. If during the six weeks of peak runoff the Susquehanna deposited  $0.33 \times 10^6$  metric tons of sediment within the study area, could an equivalent amount of material have been resuspended and transported out of the area over the rest of the year? To obtain an answer consider the following advective model

$$(\bar{R}\bar{C}_u - 2\bar{R}\bar{C}_l) T = 0.33 \times 10^6 \text{ metric tons}$$

where  $\bar{R}$  is the average river flow,  $\bar{C}_u$  and  $\bar{C}_l$  are the mean con-

centrations of suspended sediment in the upper and lower layers at VF over the time,  $T$ , of 46 weeks, and  $0.35 \times 10^6$  metric tons is the amount of the sediment discharged by the Susquehanna which was deposited within the study area during the six weeks of peak runoff in February and March of 1967. Solving for  $(3\bar{C}_u - 2\bar{C}_l)$ , we obtain

$$3\bar{C}_u - 2\bar{C}_l \approx 17 \text{ mg/l}$$

Our observations show that a value of 9 mg/l is a good estimate of  $\bar{C}_u$ . If we use this value, then  $\bar{C}_l$  would have to be only about 5 mg/l which is clearly unreasonable in view of all the data we have. This simplified model indicates that all of the sediment deposited by the Susquehanna during maximum runoff could not have been removed over the rest of the year. If 20 percent of it were to be removed by this process,  $\bar{C}_l$  would have to be about 12 mg/l, which is still too small. It appears then that there is a net accumulation of sediment within the upper Bay. From data presented earlier, a deposition rate of 2 to 3 mm per year, averaged over the study area, seems reasonable.

Although we have made major strides in understanding the nature of the suspended sediment of the upper Bay, our knowledge of the sedimentation processes is still meager. It should be obvious that we need to sample more intensively, both temporally and spatially, during the period of maximum runoff. In

addition, we need supplementary time series data within the study area, at the seaward end of the study area, and at stations downstream from VF. Moreover, the paired measurements of current velocity and suspended sediment concentration must be supplemented by determinations of the size distribution of the sediment suspended near the bottom at different phases of the tide. Work along each of these lines is either in progress or is planned for the near future.

## SUMMARY

An intensive study was made of the northern (north of 39°13'N) Chesapeake Bay from 21 March 1966 through 31 March 1967. Samples were collected routinely at sixteen stations for determinations of both the concentrations of total suspended solids and the concentrations of combustible organic matter. Additional samples were collected at selected stations for mineral identification by X-ray diffraction and size analysis by a photomicrographic technique (Zeiss Particle Size Analyzer) and by a sedimentation technique (Mine Safety Appliance Particle Size Analyzer).

The concentrations of suspended sediment in the Bay proper were greater than 5 mg/l throughout the year with maximum concentrations greater than 110 mg/l occurring in March during the period of peak river flow. The concentrations of suspended sediment in the mouth of the Susquehanna River, the principal source of fluvial sediment of the study area, exceeded 140 mg/l during this period of maximum runoff. Excluding the period of peak river flow and short periods of very rough seas, the surface and mid-depth suspended sediment concentrations were relatively constant throughout the year at each of the stations deeper than about 5 m. In shallower water larger fluctuations resulting from the resuspension of bottom sediment by both tidal scour and wind waves were observed. Excluding the

period of high river discharge, the mean concentration of suspended sediment in the upper layer, averaged over the entire study area, was about 13 mg/l and the mean deviation less than 4 mg/l.

Near the bottom, where the suspended sediment concentrations are determined primarily by tidal scour, large (as much as 18 X) fluctuations of the suspended sediment concentration were observed which were clearly related to current velocity and the phase of the tide at which the samples were collected.

The concentrations of combustible organic matter were highest in the spring and summer months averaging nearly 5 mg/l and lowest during the winter months when they averaged about 3 mg/l.

The mean equivalent projected diameter of the suspended particles ranged from 1.1 to 2.8  $\mu$  and in nearly 80 percent of the samples analyzed it was between 1.4 and 2.0  $\mu$ . The mean projected diameter decreased slightly during the period of high river flow. The mean Stokes diameter of the suspended particles ranged from 2.3 to 12.2  $\mu$  and in nearly 70 percent of the samples it was between 3 and 6  $\mu$ . At nearly all of the stations both the mean equivalent projected diameter and the mean Stokes diameter increased near the bottom. An important factor which remains to be investigated is the tidal induced variation

of the particle size distribution near the bottom.

The mineral assemblage of the suspended sediment consisted of the illite, chlorite, and kaolinite clay mineral "groups" and of quartz and feldspar. Illite appears to be the most abundant mineral. The seasonal and geographic variations of the relative abundances of the clay minerals were small.

During the year 1 April 1966 through 31 March 1967 the Susquehanna River, which provides nearly all of the fluvial sediment introduced into the region, discharged  $0.61 \times 10^6$  metric tons of suspended sediment into the Bay at Havre de Grace. Nearly 70 percent of this  $0.61 \times 10^6$  tons was discharged during peak runoff in late February and March and about 80 percent of this 70 percent was deposited within the study area. Approximately  $0.1 \times 10^6$  metric tons of silt and clay are introduced annually into the study area from coastal erosion.

During the period of peak runoff the upper Bay's suspended sediment population was closely linked to its major source of new sediment--the Susquehanna River. The maximum suspended sediment concentrations of the Susquehanna were reflected in the high concentrations found in the Bay. Although these values were lower than those recorded in the Susquehanna, they were the maximum concentrations recorded in the Bay. Except for the period of maximum river flow, the concentrations of suspended sediment were higher in the Bay than in the mouth of the

Susquehanna River despite the dilution of the Susquehanna discharge and the settling out which occur within the Bay. Excluding the period of maximum runoff, the concentrations of suspended sediment in the Bay were largely determined by local (within the study area) resuspension and by the upstream transport of sediment into the study area by the lower layer. It is not possible to assess the relative contributions by these two mechanisms with the data we now have. It was possible however, to calculate the net flux density of sediment through the surface separating the upper and lower layers. Omitting the period of peak river flow, this was calculated to be  $0.03 \text{ mg/m}^2/\text{sec}$ .

Although we do not have sufficient information to write a sediment budget for this segment of the Chesapeake Bay, there can be little doubt that this is an area of net deposition. The data indicate an average deposition rate of about 2 to 3 mm per year.

The sedimentation pattern of the northern Chesapeake Bay then, is one of fluvial domination during the period of thaw and high runoff, and cannibalism (resedimentation) throughout the remainder of the year.

APPENDIX A--Number-Size Distributions and their Statistical Properties of Suspended Sediment Samples from Selected Space-time Positions in the Upper Chesapeake Bay. Data obtained with a Zeiss Particle Size Analyzer TGZ-3.

Volume-Size Distributions and their Statistical Properties of the Same Set of Samples Obtained by Transformation of the Number Data by Assuming Spherical Particles.

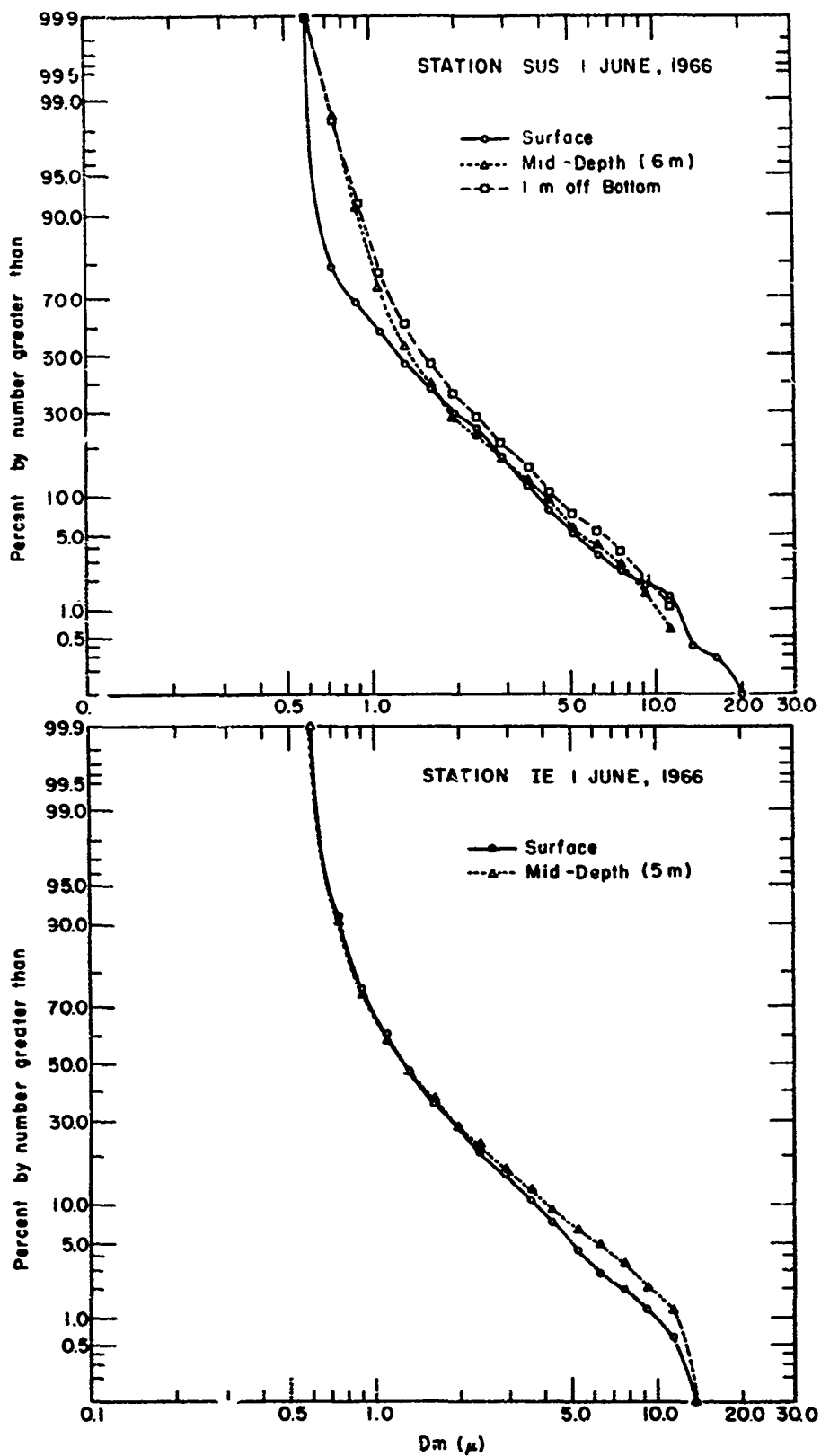


**Fig. A1 Particle Size Distribution Curves of Suspended Sediment Samples from Selected Space-Time Positions in the Upper Bay.**

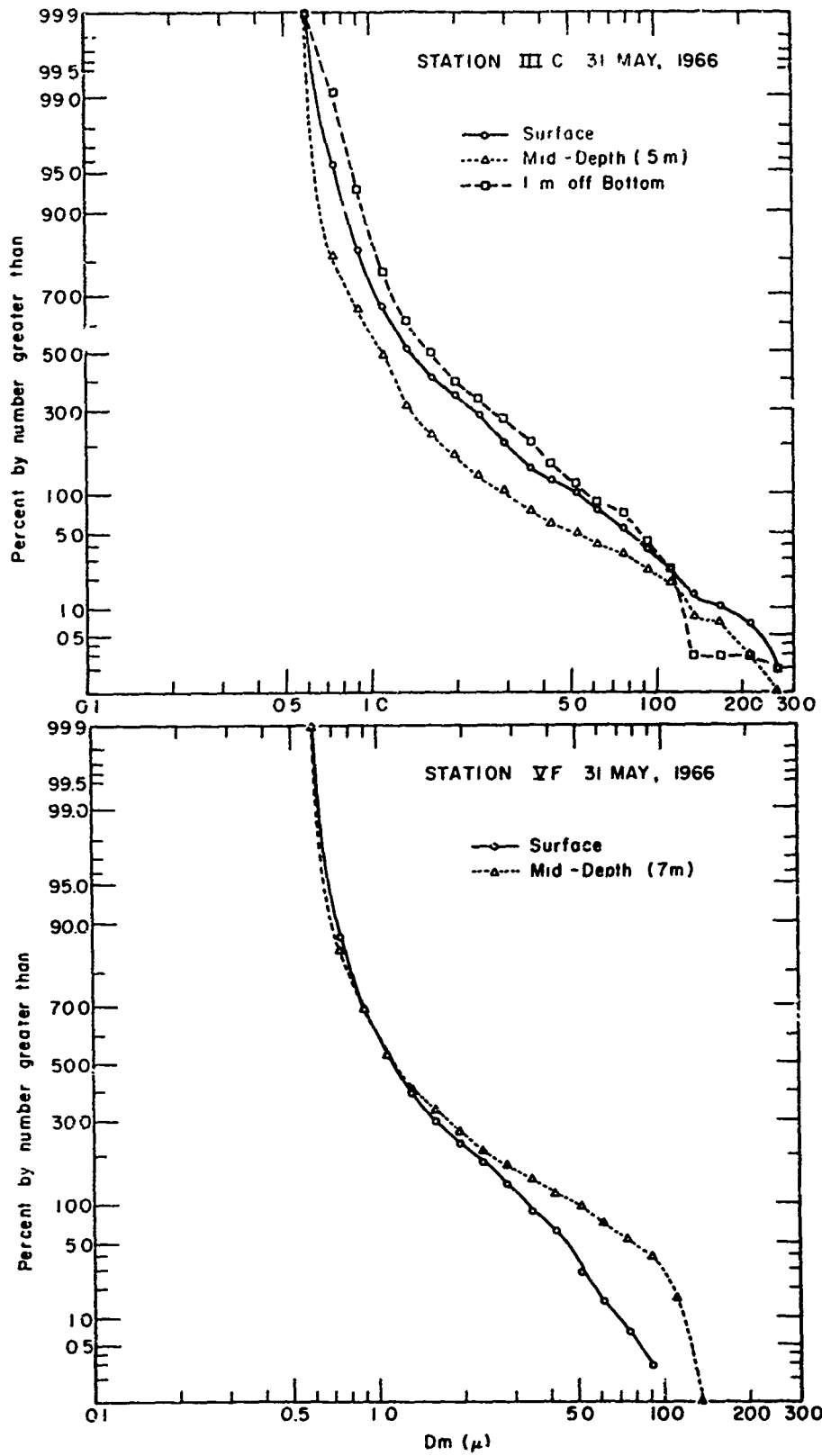


Fig. A2 Particle Size Distribution Curves of Suspended Sediment Samples from Selected Space-Time Positions in the Upper Bay.

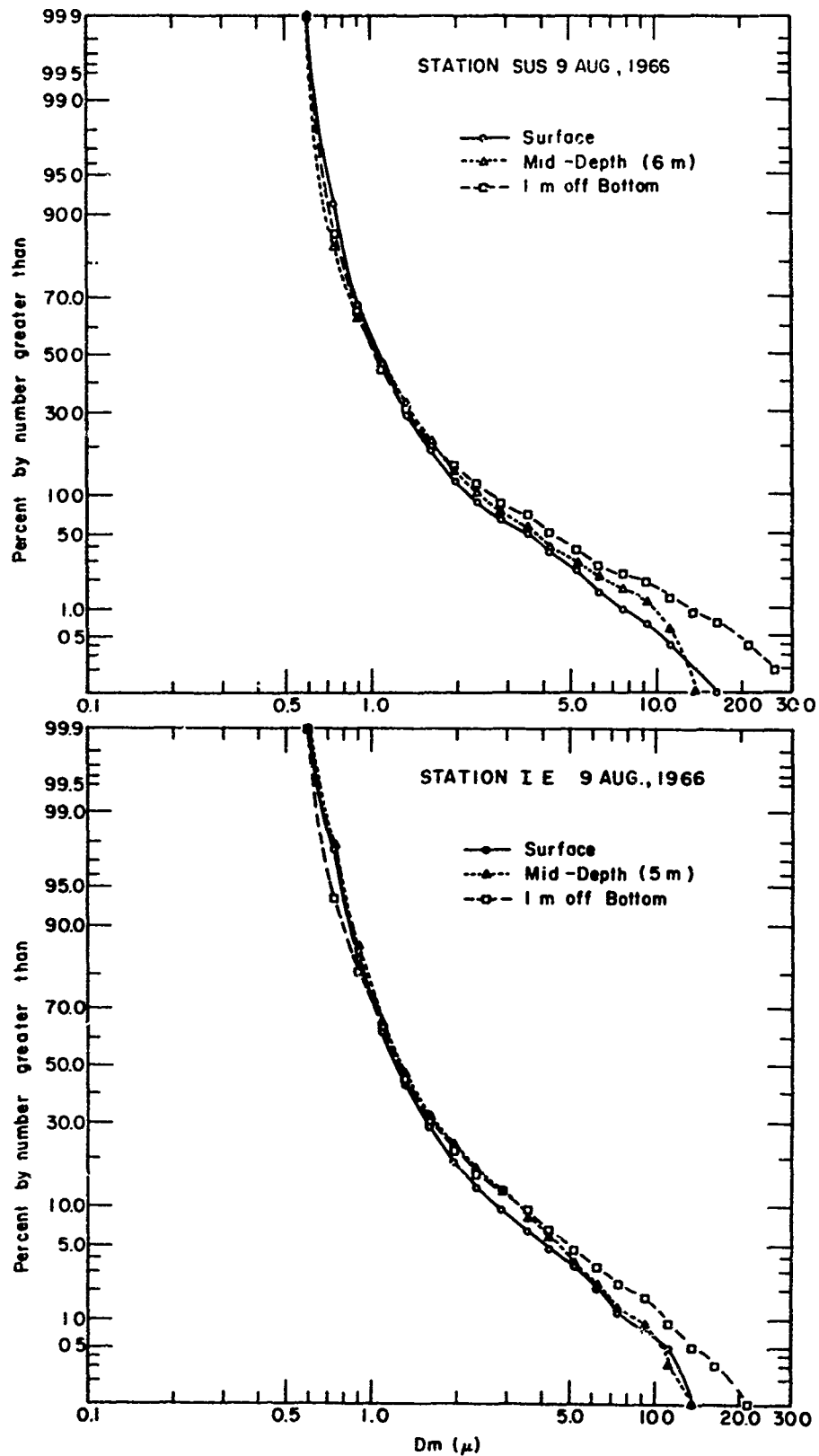
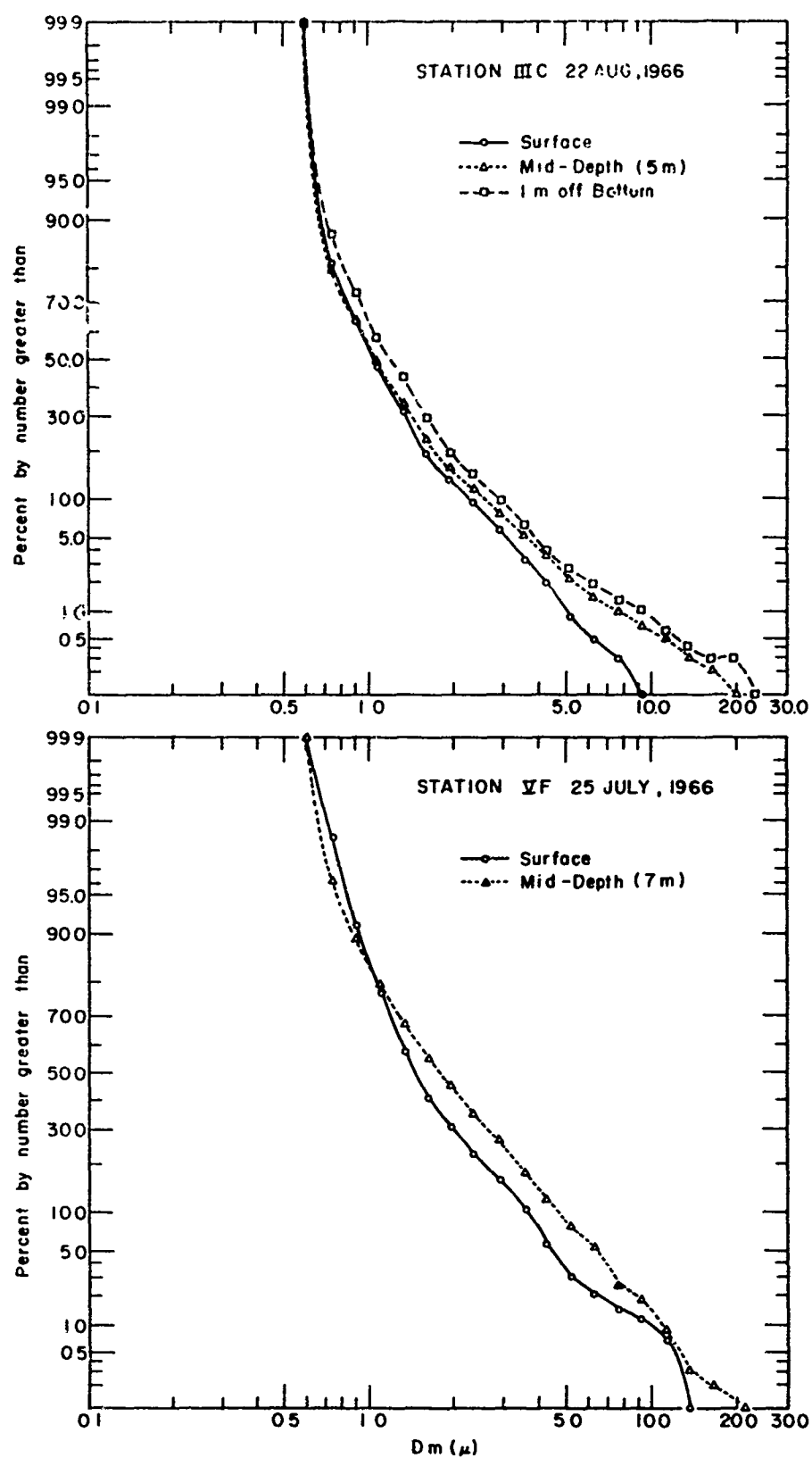


Fig. A3 Particle Size Distribution Curves of Suspended Sediment Samples from Selected Space-Time Positions in the Upper Bay.



**Fig. A4 Particle Size Distribution Curves of Suspended Sediment Samples from Selected Space-Time Positions in the Upper Bay.**

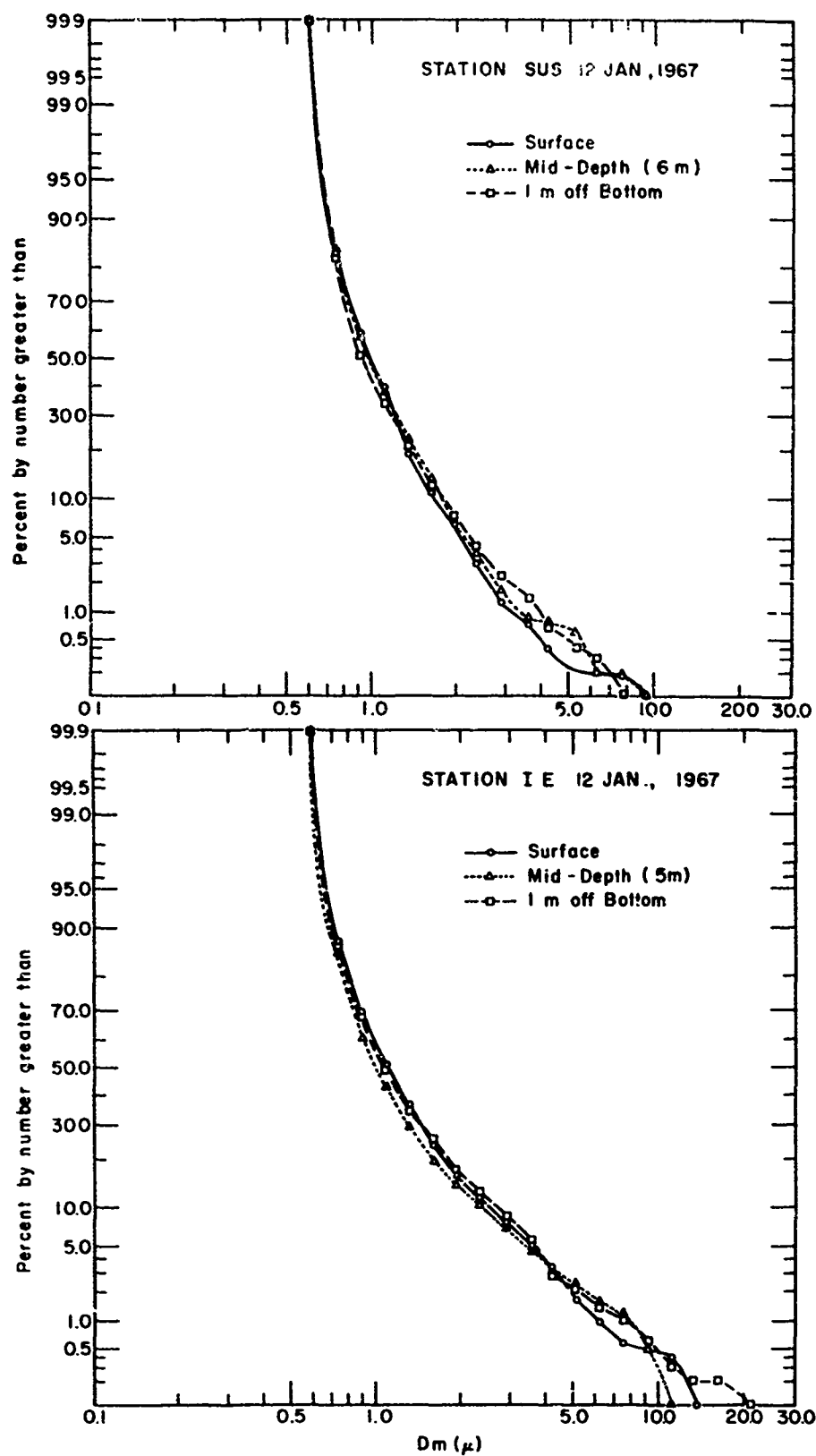


Fig. A5 Particle Size Distribution Curves of Suspended Sediment Samples from Selected Space-Time Positions in the Upper Bay.

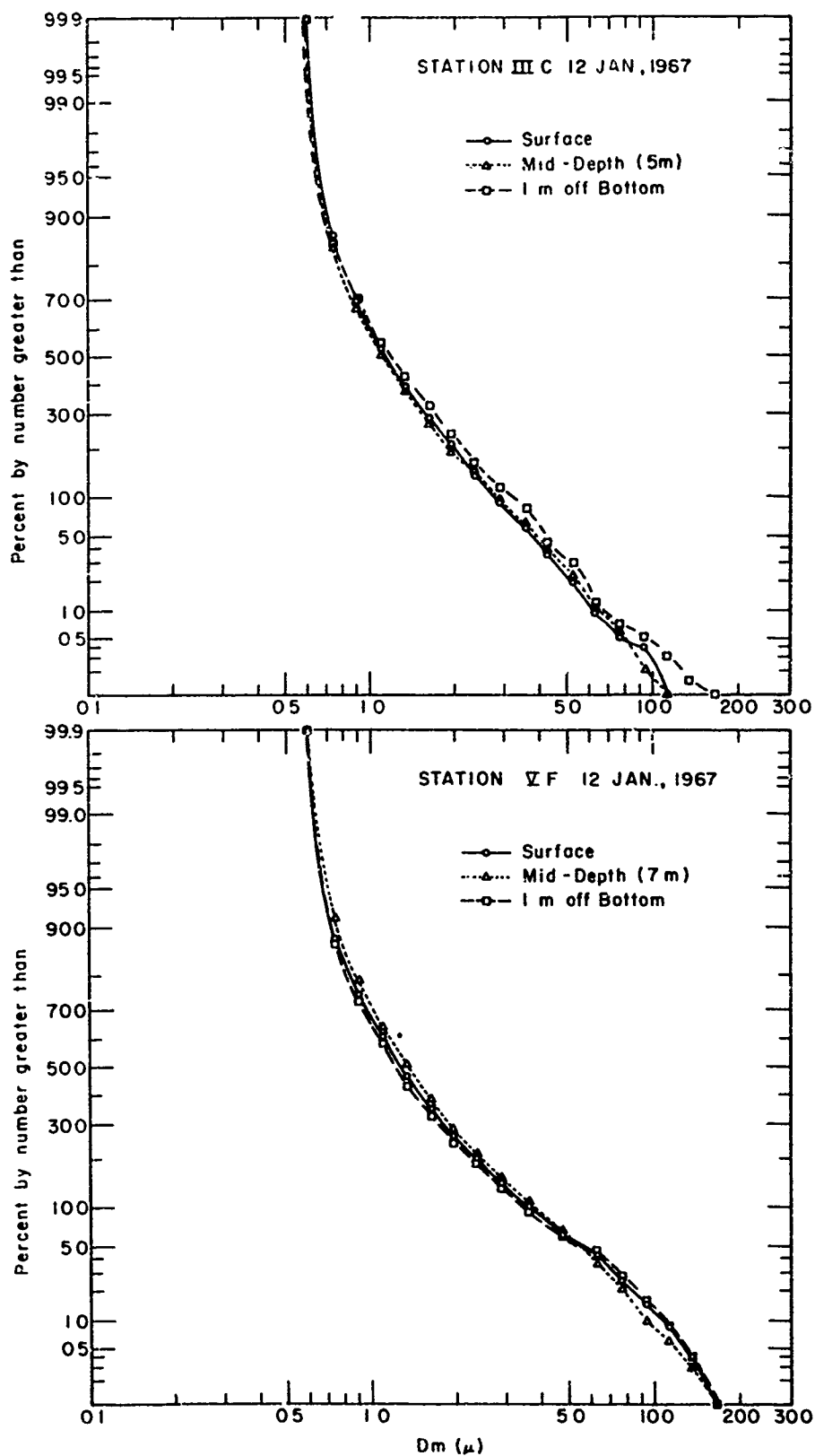


Fig. A6 Particle Size Distribution Curves of Suspended Sediment Samples from Selected Space-Time Positions in the Upper Bay.

TABLE A-1

Statistical Properties of Particle Size Distributions Shown in  
Figures A1 through A6.

Station, Date, and Depth	Mean ( $\mu$ )	Standard Deviation ( $\mu$ )	Skewness	Kurtosis
SUS (1 VI 66)				
surface	2.0	2.2	2.4	34.6
mid-depth	2.1	1.8	1.5	10.9
1 m off bot.	2.3	2.1	1.4	9.5
IE (1 VI 66)				
surface	1.9	1.7	1.7	14.1
mid-depth	2.0	2.1	1.5	10.6
IIIC (31 V 66)				
surface	2.5	3.1	2.0	20.4
mid-depth	1.8	2.5	2.7	38.1
1 m off bot.	2.7	2.9	1.7	17.0
VF (31 V 66)				
surface	1.7	1.3	1.3	8.7
mid-depth	2.1	2.5	1.5	10.2
SUS (9 VIII 66)				
surface	1.4	1.5	3.6	85.9
mid-depth	1.5	1.6	3.3	71.8
1 m off bot.	1.7	2.4	3.3	56.4

TABLE A-1 Continued

Station, Date, and Depth	Mean ( $\mu$ )	Standard Deviation ( $\mu$ )	Skewness	Kurtosis
IE (9 VIII 66)				
surface	1.7	1.5	2.3	28.4
mid-depth	1.8	1.6	2.0	21.1
1 m off bot.	1.9	2.1	2.7	41.3
IIIC (22 VIII 66)				
surface	1.3	0.9	1.9	21.2
mid-depth	1.5	1.6	3.2	58.9
1 m off bot.	1.7	1.9	3.9	87.9
VF (25 VII 66)				
surface	2.0	1.5	1.8	17.1
mid-depth	2.4	2.1	1.8	22.0
SUS (12 I 67)				
surface	1.1	0.6	2.5	43.7
mid-depth	1.2	0.7	2.8	52.4
1 m off bot.	1.1	0.7	2.9	62.8
IE (12 I 67)				
surface	1.5	1.2	2.4	32.7
mid-depth	1.4	1.3	2.3	30.9
1 m off bot.	1.5	1.5	3.0	52.6

TABLE A-1 Continued

Station, Date, and Depth	Mean ( $\mu$ )	Standard Deviation ( $\mu$ )	Skewness	Kurtosis
IIIC (12 I 67)				
surface	1.5	1.2	1.8	21.4
mid-depth	1.5	1.2	2.0	29.5
1 m off bot.	1.7	1.5	2.8	57.1
VF (12 I 67)				
surface	1.8	1.6	1.7	15.6
mid-depth	1.9	1.5	1.4	11.8
1 m off bot.	1.8	1.7	1.8	17.7

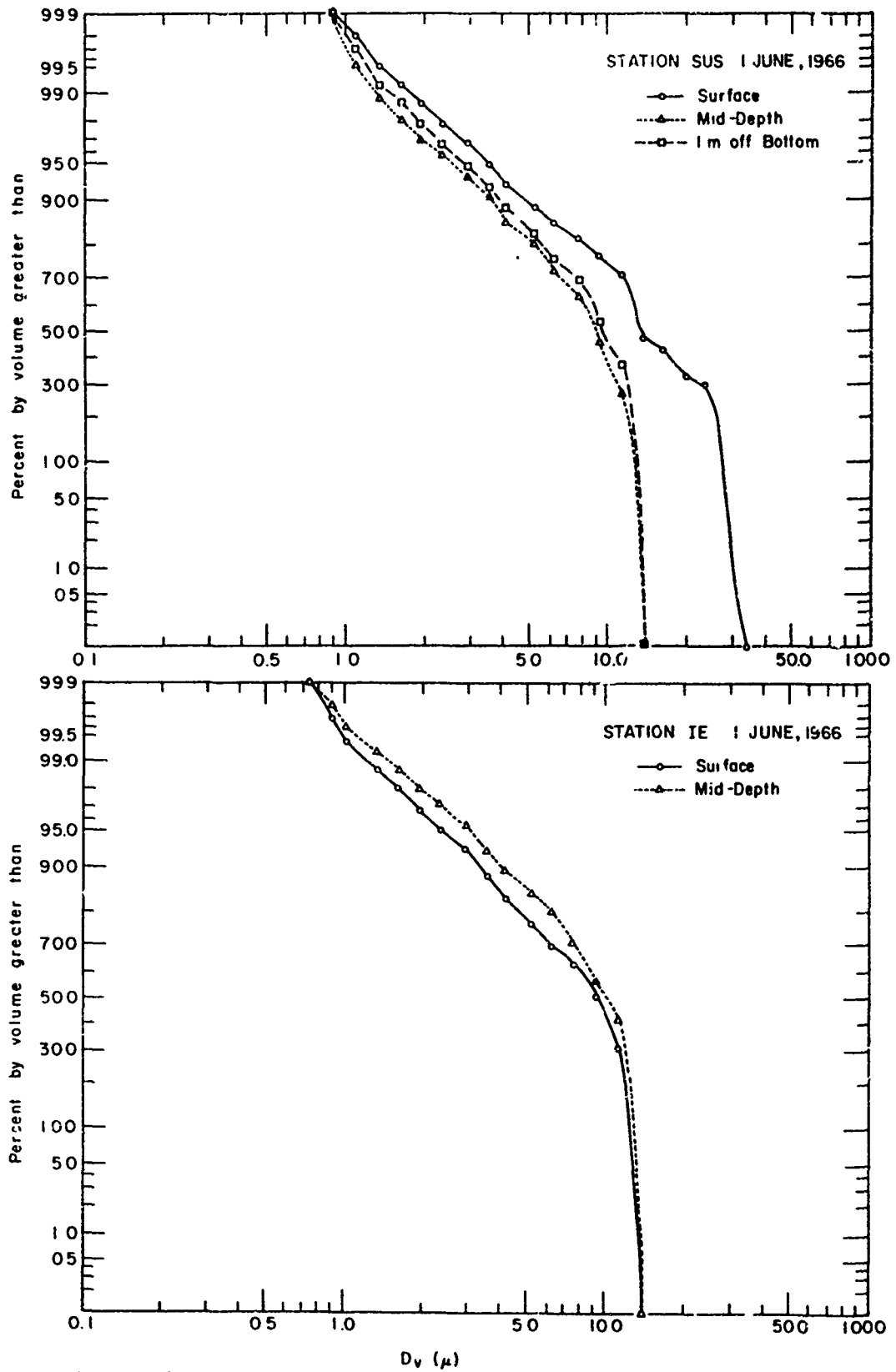


Fig. A 7 Volume-Size Distribution Curves obtained by Transformation of Number-Size Data.

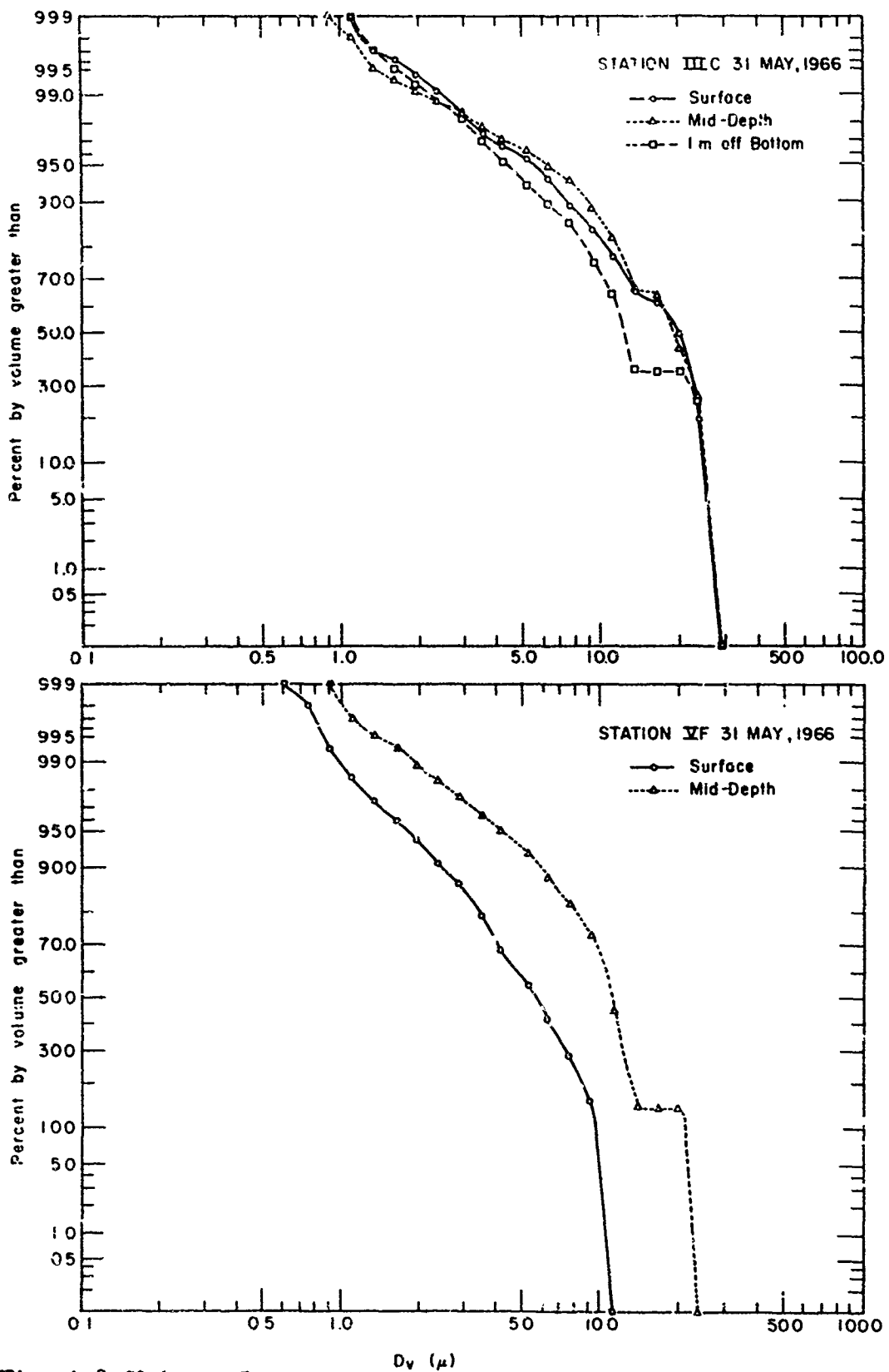


Fig. A 8 Volume-Size Distribution Curves obtained by Transformation of Number-Size Data.

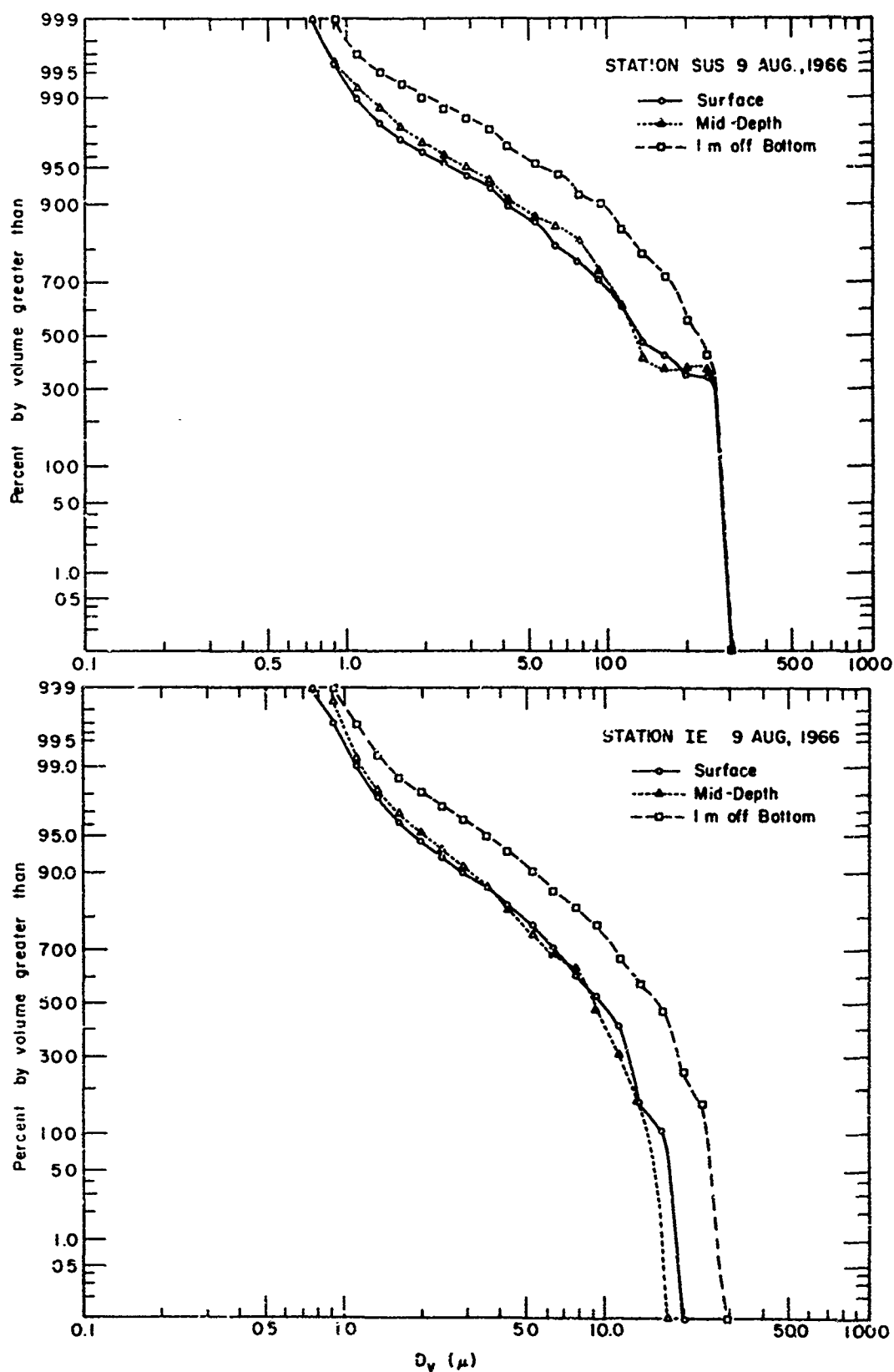


Fig. A 9 Volume-Size Distribution Curves obtained by Transformation of Number-Size Data.

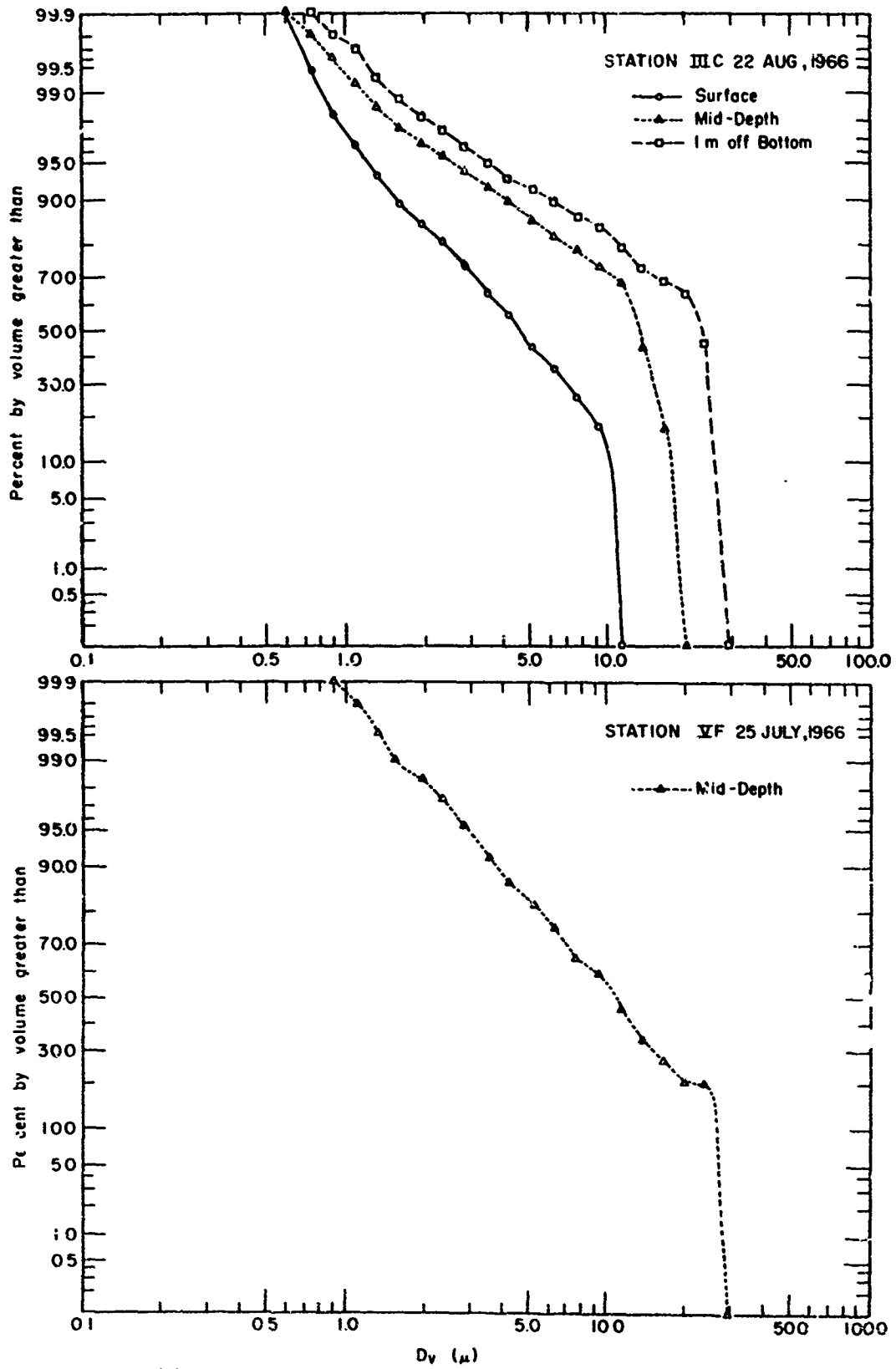


Fig. A 10 Volume-Size Distribution Curves obtained by Transformation of Number-Size Data.

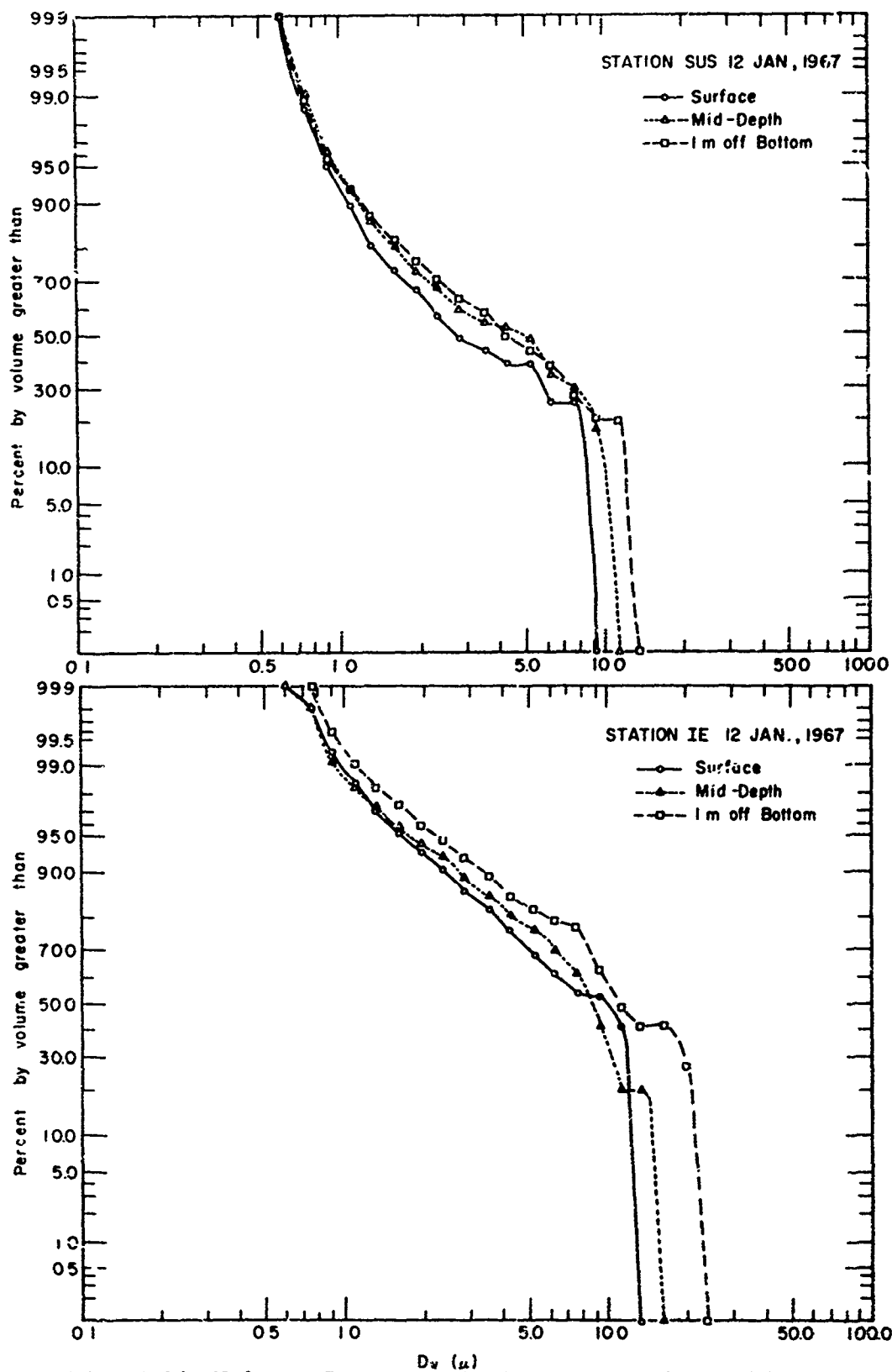


Fig. A 11 Volume-Size Distribution Curves obtained by Transformation of Number-Size Data.

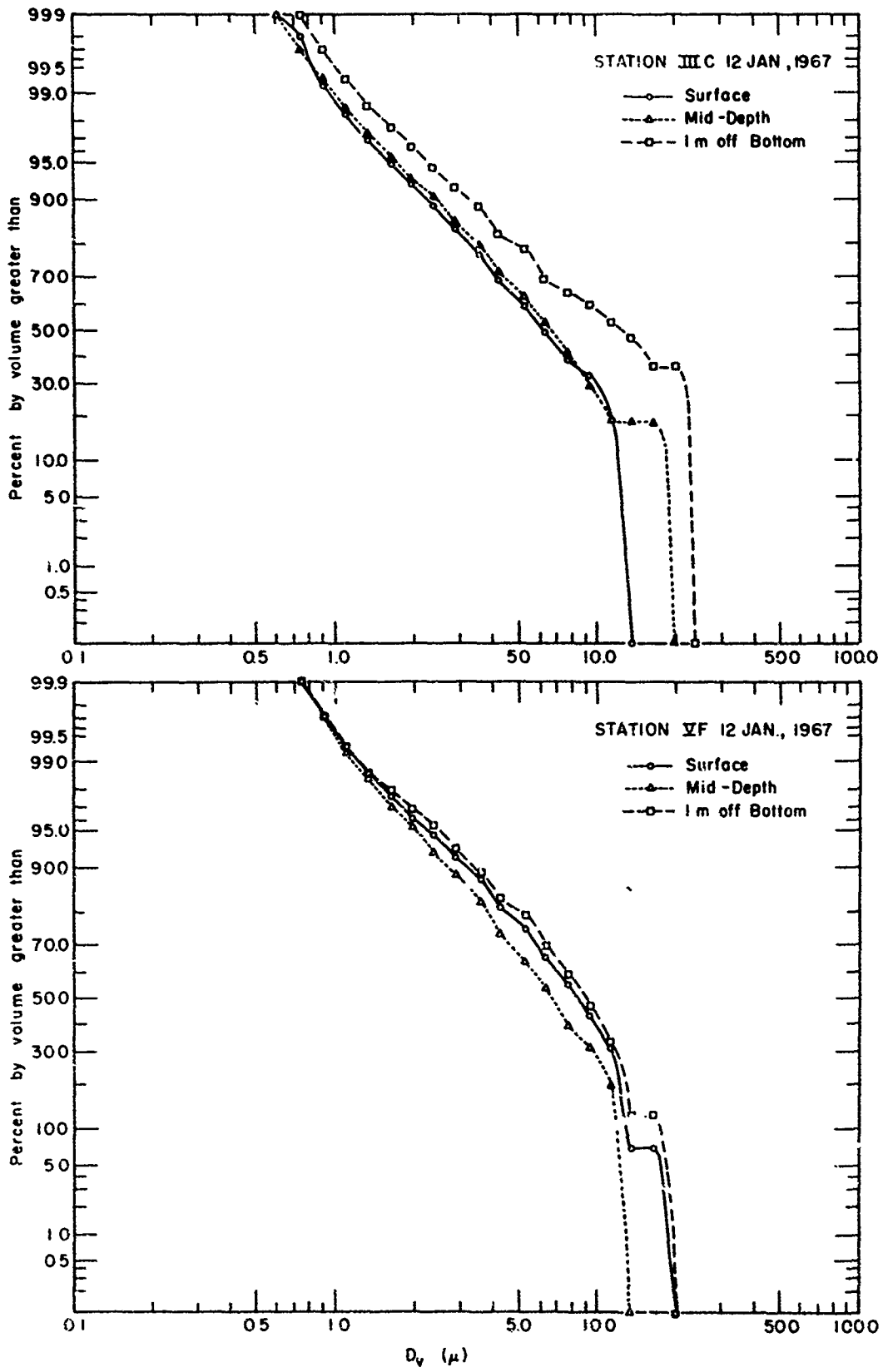


Fig. A 12 Volume-Size Distribution Curves obtained by transformation of Number-Size Data.

TABLE A-2

Statistical Properties of Particle Size Distributions Shown in Figures 55 and 56 and in Figures A7 through A12.

Station, Date, and Depth	Mean $\bar{D}_v$ ( $\mu$ )	Standard Deviation	Skewness	Kurtosis
SUS (14 XI 66)				
surface	10.2	6.7	0.1	- 1.6
mid-depth	15.3	9.2	0.0	- 1.6
1 m off bot.	10.8	5.8	- 0.1	- 1.5
IE (14 XI 66)				
surface	5.1	2.5	0.1	- 0.8
mid-depth	10.6	6.5	0.3	- 1.0
1 m off bot.	9.9	5.0	0.0	- 1.3
IIIC (14 XI 66)				
surface	8.8	5.5	0.2	- 1.2
mid-depth	7.1	3.5	0.2	- 1.2
1 m off bot.	6.5	3.5	0.2	- 0.9
VF (14 XI 66)				
surface	6.5	3.9	0.2	- 1.3
mid-depth	16.3	10.4	0.1	- 1.6
1 m off bot.	8.9	5.5	0.3	- 1.0
SUS (1 VI 66)				
surface	16.4	8.6	0.1	- 1.3
mid-depth	8.7	3.5	- 0.2	- 1.0
1 m off bot.	9.4	3.6	- 0.2	- 1.0
IE (1 VI 66)				
surface	8.8	3.8	- 0.2	- 1.2
mid-depth	9.6	3.5	- 0.3	- 0.7
IIIC (31 VI 66)				
surface	17.9	7.2	- 0.2	- 0.9
mid-depth	19.1	7.8	- 0.1	- 1.0
1 m off bot.	15.8	8.5	0.0	- 1.2

Table A-2 Continued

Station, Date, and Depth	Mean $\bar{D}_v$ ( $\mu$ )	Standard Deviation	Skewness	Kurtosis
VF (31 V 66)				
surface	5.9	2.6	- 0.1	- 1.0
mid-depth	11.6	4.8	0.3	0.3
SUS (9 VIII 66)				
surface	16.6	10.1	0.1	- 1.5
mid-depth	16.7	10.1	0.1	- 1.5
1 m off bot.	21.3	8.2	- 0.3	- 0.8
IE (9 VIII 66)				
surface	9.6	4.9	- 0.1	- 0.8
mid-depth	9.1	4.4	0.0	- 1.1
1 m off bot.	16.2	8.2	0.1	- 1.0
IIIC (22 VIII 66)				
surface	5.3	3.0	0.2	- 1.0
mid-depth	14.2	6.3	- 0.3	- 1.0
1 m off bot.	21.1	9.2	- 0.4	- 0.9
VF (25 VIII 66)				
mid-depth	12.5	7.8	0.3	- 0.8
SUS (12 I 67)				
surface	4.1	2.8	0.2	- 1.4
mid-depth	5.2	3.5	0.1	- 1.4
1 m off bot.	5.8	4.5	0.4	- 0.9
IE (12 I 67)				
surface	8.5	4.4	- 0.1	- 1.6
mid-depth	8.8	4.6	0.2	- 0.8
1 m off bot.	12.8	6.7	0.0	- 1.3
IIIC (12 I 67)				
surface	7.1	4.0	0.2	- 1.2
mid-depth	8.3	6.0	0.5	- 0.2
1 m off bot.	14.0	8.6	0.2	- 1.6
VF (12 I 67)				
surface	8.6	4.3	0.1	- 0.7
mid-depth	7.1	3.5	0.1	- 1.2
1 m off bot.	9.2	4.6	0.1	- 0.8

APPENDIX B--Determining Starting and Stopping Corrections For  
MSA Centrifuges.

It is necessary to apply starting and stopping corrections to the times calculated from (14) since these times are based upon the assumption that each centrifuge runs at a constant speed for the entire calculated time interval. This of course, is not true, and therefore either the starting and stopping times must be balanced, or a correction time factor must be used. The latter is the simpler solution and is the one used for the MSA centrifuges. From (12) we see that the settling velocity of a particle at any radius,  $r$  from the axis of rotation, is proportional to  $\omega^2$ . Therefore, if we plot  $\omega^2$  vs. time the area under the curve will be proportional to the distance a particle will settle in that time interval. A typical curve of  $\omega^2$  vs. time (Obce) is shown in Fig. B1. The distance which a particle would settle during the time period  $t$  is given by (12) as being proportional to the area Oacd. In fact, the distance of settling is proportional to the area cbce since the centrifuge does not run at a constant  $\omega$  for the entire timer setting. We want to select a new timer setting,  $t_2$ , during which a particle will settle the same distance as it would if it were centrifuged at constant  $\omega$  for the time period,  $t_1$ . The determination of the new timer setting,  $t_2$ , requires that the area Obc<sup>1</sup>e<sup>1</sup> equal the area Oacd, and consequently that the cc<sup>1</sup>d<sup>1</sup>d be equal to the difference between the areas Oab and dce.

The corrective time factor,  $\tau_{\omega}$ , for the 1200 r.p.m. centrifuge used by the author was determined in the following way. A stroboscope was used to determine the starting and stopping curves of the centrifuge, Fig. B2, and the area over the starting curve and the area under the stopping curve were then determined by planimetry. Their difference was taken and this area was divided by the area equivalent of unit time at  $\omega^2 = \text{constant}$ --the area of the rectangle whose length is given by the distance to the  $\omega^2 = \text{constant}$  line and whose width is equal to the distance equivalent of 1 second. This gives the required corrective time factor  $\tau_{40\pi}$  in seconds.

$$\tau_{40\pi} = \frac{(\text{Area over starting curve}) - (\text{Area under stopping curve})}{\text{Area equivalent of unit time at } \omega^2 = \text{constant}}$$

$$\tau_{40\pi} = \frac{(181.0 - 63.7) \text{ cm}^2}{(20.6 \times .5) \text{ cm}^2 \text{ sec}^{-1}}$$

$$\tau_{40\pi} = 11.4 \text{ sec.}$$

The manufacturer recommends that starting and stopping times be checked every six months.

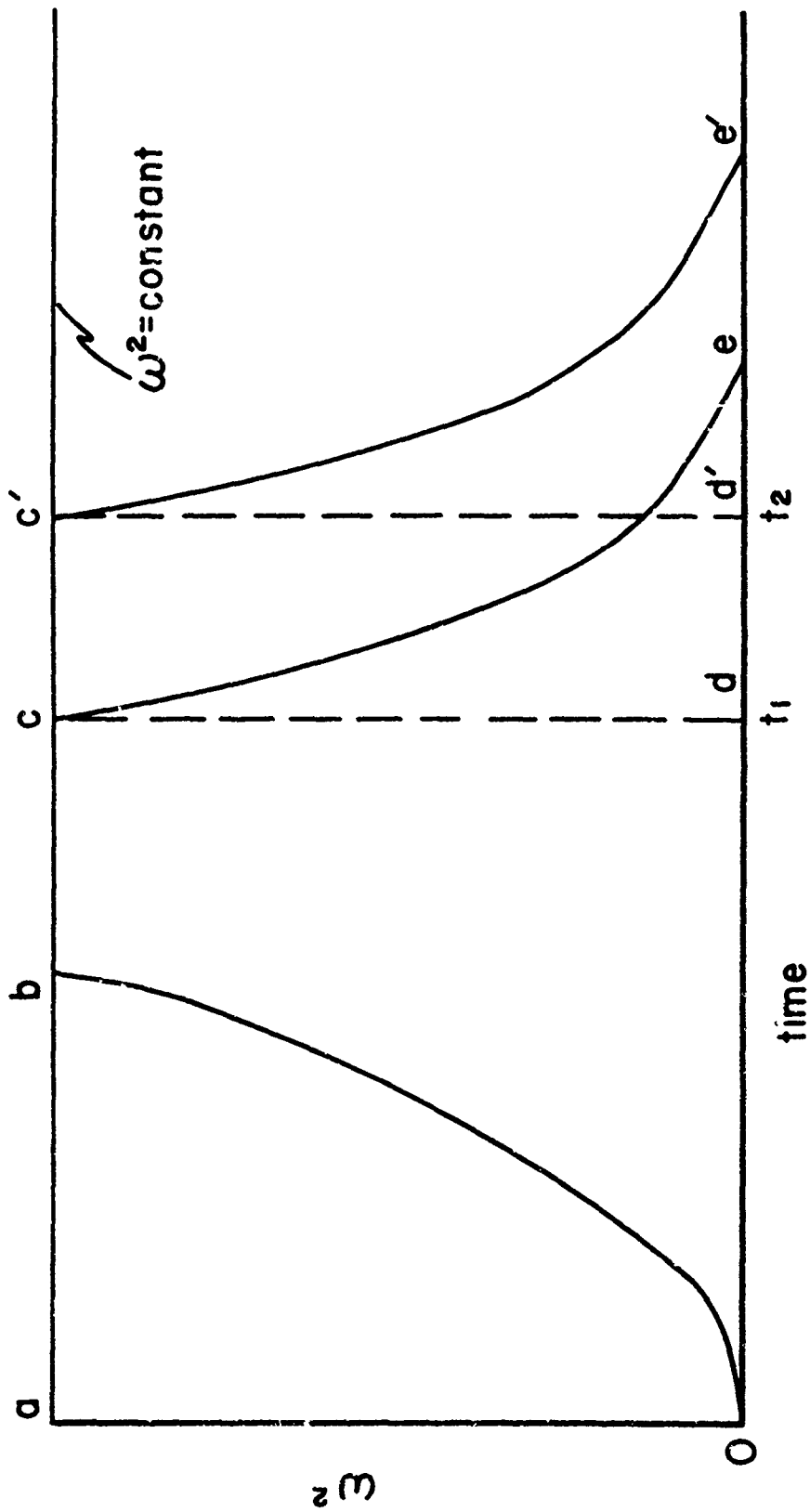


Fig. B1 Typical Acceleration Curves of MSA Centrifuge Used to Determine Starting-Stopping Correction Term.

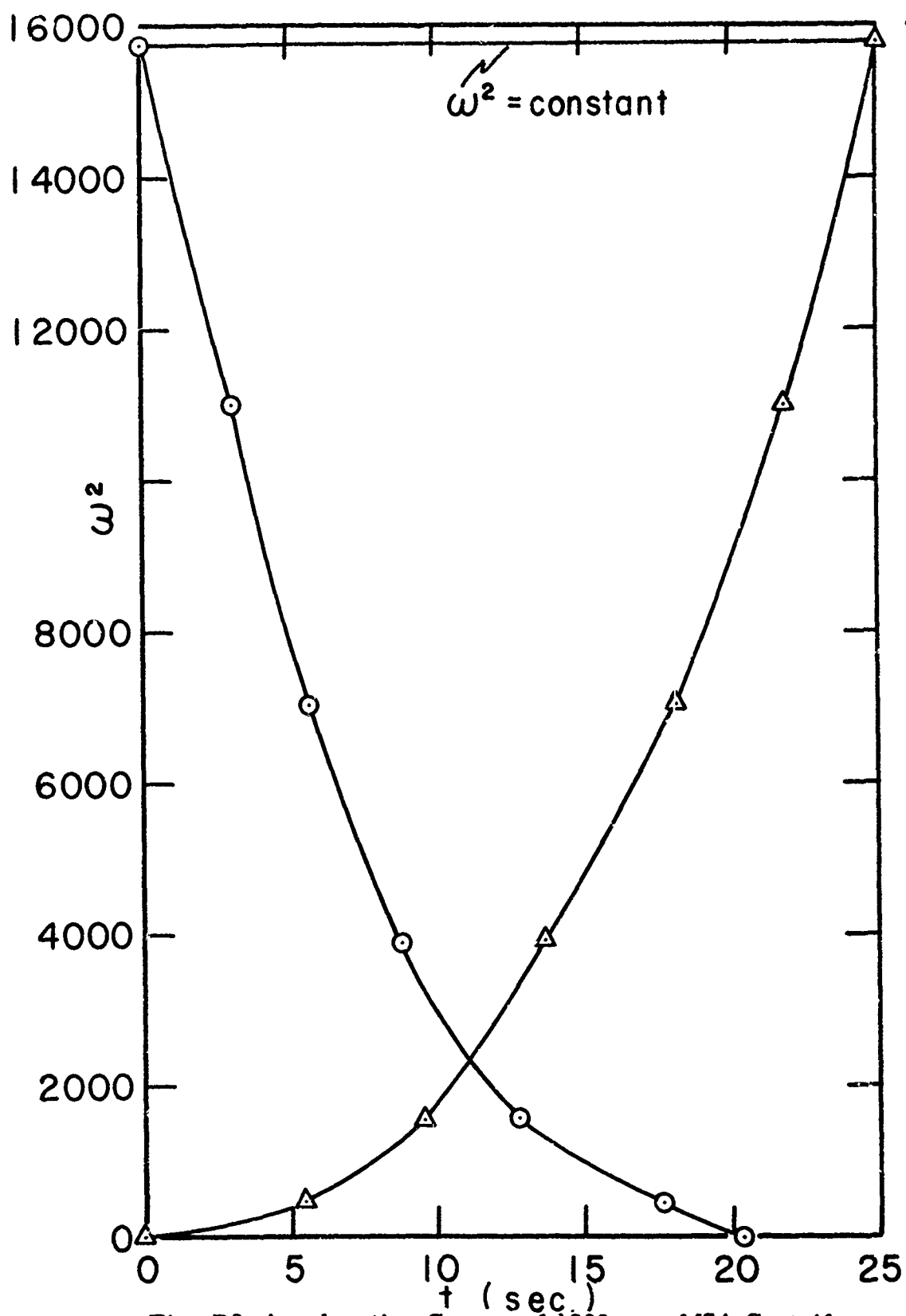


Fig. B2 Acceleration Curves of 1200 rpm MSA Centrifuge Used to Determine Starting-Stopping Correction Term. Plotted Points Determined with a Stroboscope.

APPENDIX C-- Preparation of a Reading Schedule for an MSA  
Size Analysis.

The sample of suspended sediment was dispersed in distilled water at 23°C. The following values were used in the preparation of reading schedule.

Temperature = 23°C

$$\mu_{\text{H}_2\text{O}} = 0.936 \times 10^{-2} \text{ poise}$$

$$\rho_0 \equiv \rho_{\text{H}_2\text{O}} = 0.998 \text{ gm cm}^{-3}$$

$$\rho \equiv \rho_{\text{sediment}} = 2.30 \text{ gm cm}^{-3}$$

$$g = 980 \text{ cm sec}^{-2}$$

$$\omega = 20\pi, 40\pi, 60\pi \text{ rad sec}^{-1}$$

$$r_0 = 3.3 \text{ cm}$$

$$r_2 = 13.3 \text{ cm}$$

$$h = 10 \text{ cm}$$

$$D_s = 10\mu \text{ (last particle size settled by gravity)}$$

$$\tau_{20\pi} = 8.4 \text{ sec}$$

$$\tau_{40\pi} = 11.4 \text{ sec}$$

$$\tau_{60\pi} = 30.1 \text{ sec}$$

Equation (21) is used to determine the reading times for the gravity portion of the reading schedule.

$$K_g = \frac{18 \times 10^8 \mu h}{(\rho - \rho_0)g} = \frac{18 \times 10^8 (0.936 \times 10^{-2}) 10}{(2.30 - 0.998) 980}$$

$$K_g = 13.199 \times 10^4 \text{ cm}^2 \text{ sec.}$$

$$t_g = \frac{K_g}{D^2} \quad (21)$$

For an 80 $\mu$  diameter sphere we have

$$t_g = \frac{13.199 \times 10^4}{(80)^2} = 21 \text{ sec}$$

For a 40  $\mu$  diameter sphere we have

$$t_g = \frac{13.199 \times 10^4}{(40)^2} = 82 \text{ sec}$$

and for 20  $\mu$  and 10  $\mu$  spheres we have

$$t_g = 5 \text{ minutes } 30 \text{ seconds, and } t_g = 22 \text{ minutes.}$$

Normally the gravity period would not be extended over this long a period, however the calculation of centrifuge timer settings is simplified by using a  $D_g$  of 10  $\mu$ .

Next, we must calculate the  $K_\omega$  for each centrifuge.

We have

$$K_{20\pi} = \frac{g}{h\omega^2} K_g = 3276 \text{ cm}^2 \text{ sec}$$

$$K_{40\pi} = \frac{g}{h\omega^2} K_g = 819 \text{ cm}^2 \text{ sec}$$

$$K_{60\pi} = \frac{g}{h\omega^2} K_g = 364 \text{ cm}^2 \text{ sec}$$

If 8  $\mu$  is the next size of interest, then using the 600 r.p.m. centrifuge we have

$$t_1 = t_1' - t_0' + \tau_{20\pi}$$

$$t_1 = \frac{K_{20\pi}}{D^2} \ln \frac{r_2}{r_0 + \frac{hD^2}{D_g}} - t_0' + \tau_{20\pi} = 16.2 - 0 + 8.4$$

$$t_1 = 25 \text{ sec}$$

For a 5  $\mu$  sphere at 600 r.p.m. we have

$$t_2 = t_2' - t_1' + \tau_{20\pi} \quad (t_1' \text{ is obtained from the previous calculation})$$

$$t_2 = \frac{K_{20\pi}}{D^2} \ln \frac{r_2}{r_0 + \frac{hD^2}{D_g}} - t_1' + \tau_{20\pi}$$

$$t_2 = 108.6 - 16.2 + 8.4 \text{ sec} = 101 \text{ sec} = 1 \text{ min } 41 \text{ sec.}$$

For a 3.5  $\mu$  sphere at 600 r.p.m.

$$t_3 = t_3' - t_2' + \tau_{20\pi}$$

$$t_3 = \frac{K_{20\pi}}{D^2} \ln \frac{r_2}{r_0 + \frac{hD^2}{D_g}} - t_2' + \tau_{20\pi}$$

$$t_3 = 188 \text{ sec} = 3 \text{ min } 08 \text{ sec.}$$

For a 2  $\mu$  sphere at 600 r.p.m.

$$t_4 = t_4' - t_3' + \tau_{20\pi} = 767 \text{ sec} = 12 \text{ min } 47 \text{ sec}$$

For a 1  $\mu$  sphere at 1200 r.p.m. we have

$$t_5 = t_5' - t_4' \left(\frac{20\pi}{40\pi}\right)^2 + \tau_{40\pi}$$

$$t_5 = \frac{K_{40\pi}}{D^2} \ln \frac{r_2}{r_0 + \frac{hD^2}{D_g}} - \frac{1}{4} t_4' + 11.4$$

$$t_5 = 867 \text{ sec} = 14 \text{ min } 27 \text{ sec}$$

For an  $0.5 \mu$  sphere at 1800 r.p.m. we have

$$t_6 = t_6' - t_5' \left( \frac{40\pi}{60\pi} \right)^2 + \tau_{60\pi}$$

$$t_6 = \frac{K_{60\pi}}{D^2} \ln \frac{r_2}{r_0 + \frac{hD^2}{D_g^2}} - \frac{4}{9} t_5' + \tau_{60\pi}$$

$$t_6 = 1552 \text{ sec} = 25 \text{ min } 52 \text{ sec}$$

For an  $0.25 \mu$  sphere at 1800 r.p.m. we have

$$t_7 = t_7' - t_6' + \tau_{60\pi}$$

$$t_7 = 6130 \text{ sec} = 102 \text{ min } 10 \text{ sec}$$

It is convenient to tabulate the times in a table similar to that shown in Fig. Cl.

## MSA DATA SHEET

SAMPLE NO. 1 ROOM TEMP. 23 CSAMPLE MATERIAL susp. sediment TUBE SIZE 0.75 mmSAMPLE DENSITY 2.3 gm cm<sup>-3</sup> SED. LIQUID waterFEEDING LIQUID none WETTING AGENT noneDISPERSING AGENT distilled H<sub>2</sub>O $R_0 = \underline{3.3 \text{ cm}}$  $R_2 = \underline{13.3 \text{ cm}}$  $K_g = \underline{13.199 \times 10^4}$ 

$D_\mu$	RPM	TIME	SED. Ht.(mm)	CORR.SED. Ht.(mm)	% > D	% < D	COMMENTS
80	Gravity	:21					
40	Gravity	1:22					
20	Gravity	5:30					
10	Gravity	22:00					
8	600	:25					
5	600	1:41					
3.5	600	3:08					
2	600	12:47					
1	1200	14:27					
0.5	1800	25:52					
0.25	1800	102:10					

REMARKS: \_\_\_\_\_

\_\_\_\_\_

\_\_\_\_\_

OPERATOR JRSDATE 5 JULY 1966

Fig. C1 MSA Data Sheet.

APPENDIX D--Volume-Size Distributions and their Statistical  
Properties of Suspended Sediment Samples from  
Selected Space-time Positions in the Upper  
Chesapeake Bay. Data obtained with a Mine  
Safety Appliance Particle Size Analyzer.

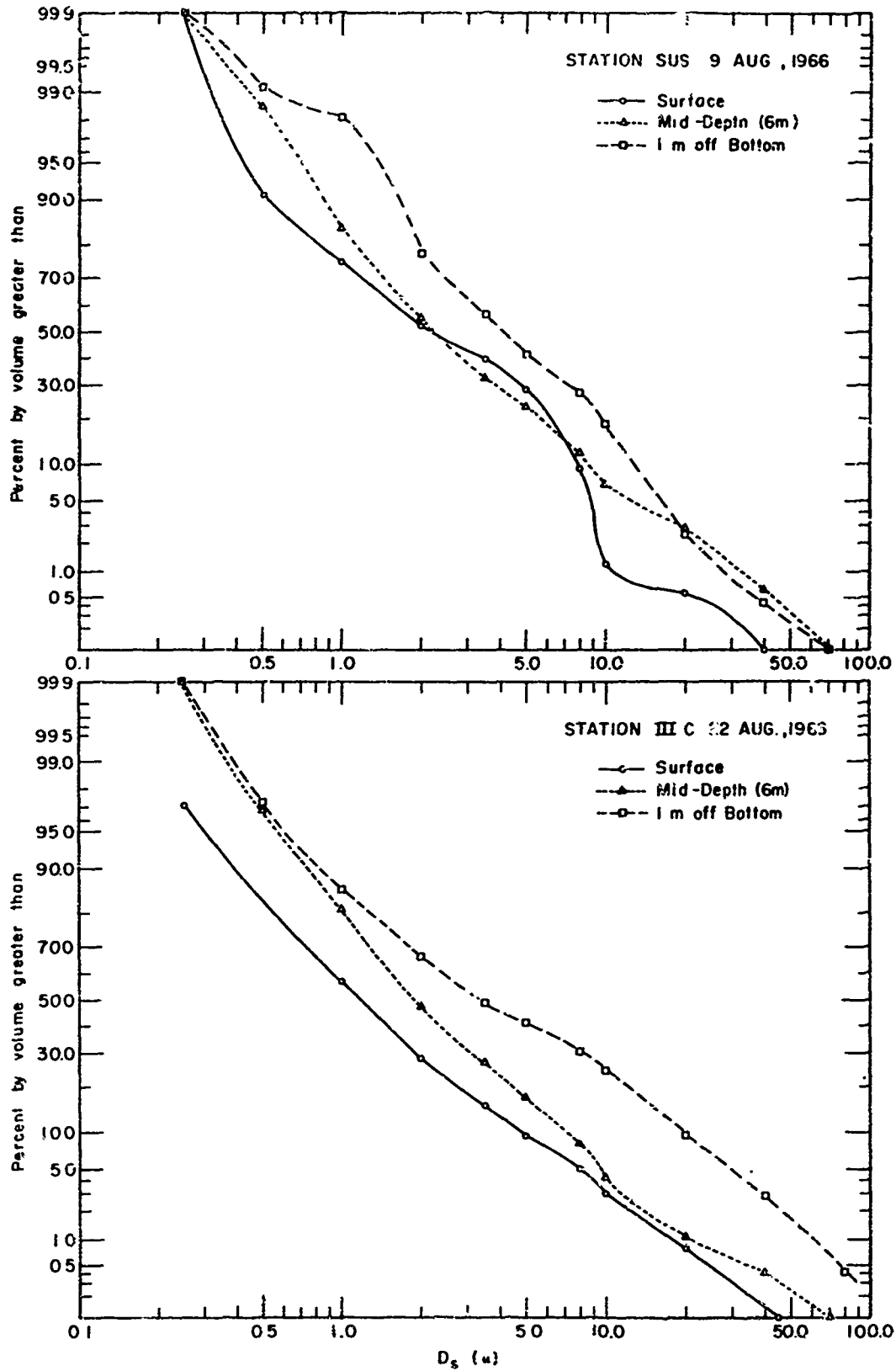


Fig. D1 MSA Centrifuge determined Volume-Size Distributions of Selected Samples of Suspended Sediment from the Upper Bay.

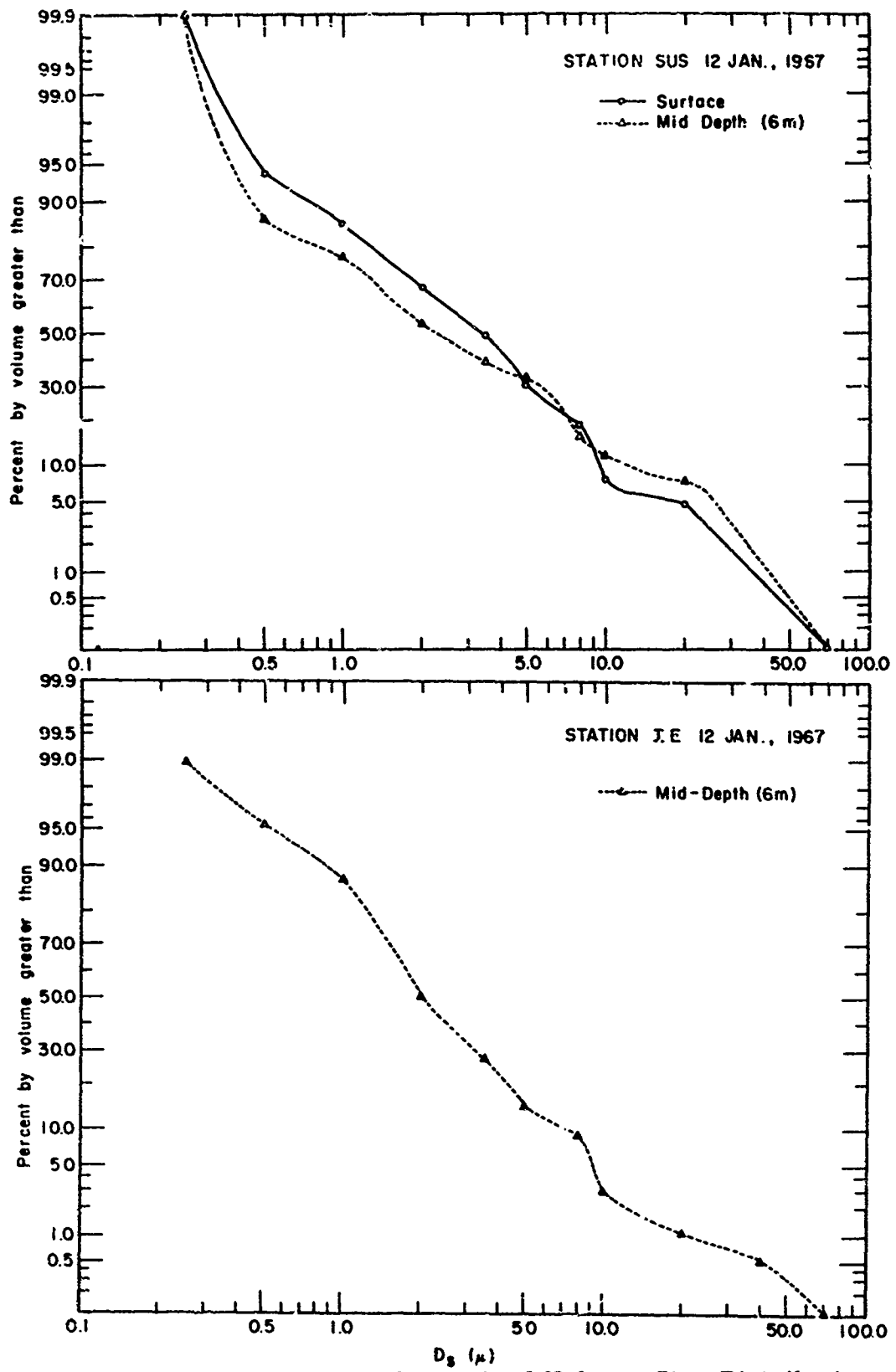


Fig. D2 MSA Centrifuge determined Volume-Size Distributions of Selected Samples of Suspended Sediment from the Upper Bay.

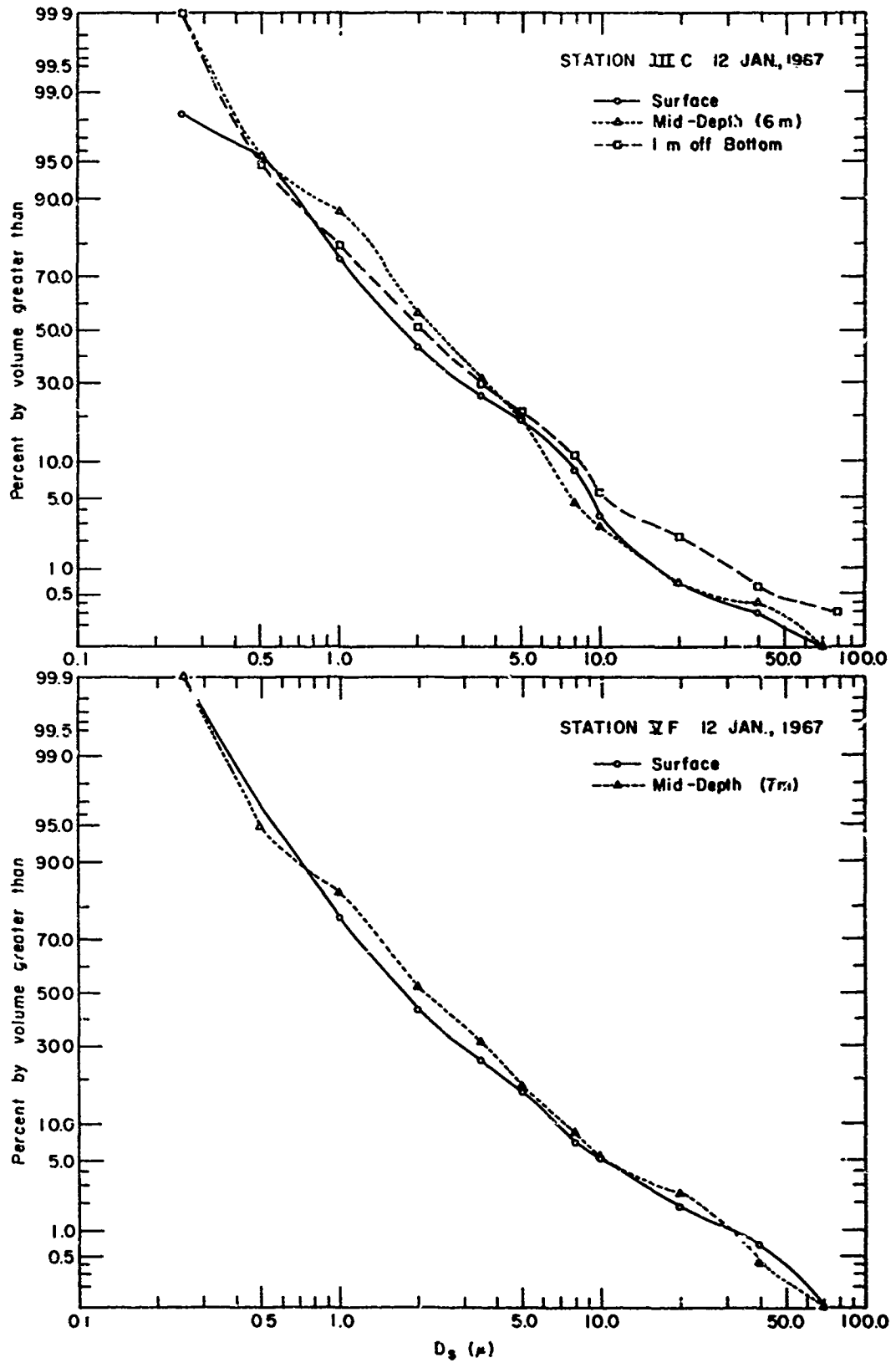


Fig. D3 MSA Centrifuge determined Volume-Size Distributions of Selected Samples of Suspended Sediment from the Upper Bay.

TABLE D-1

Statistical Properties of Particle Size Distributions Shown in Figures D1 through D3.

Station, Date, and Depth	Mean $D_s$ ( $\mu$ )	Standard Deviation ( $\mu$ )	Skewness	Kurtosis
SUS (9 VIII 66)				
surface	3.6	3.5	1.5	18.3
mid-depth	4.4	6.7	2.4	30.4
1 m off bot.	6.6	6.8	1.5	16.3
IIIC (22 VIII 66)				
surface	2.3	3.6	2.3	28.2
mid-depth	3.5	5.2	3.2	59.2
1 m off bot.	8.6	13.2	2.0	22.8
SUS (12 I 67)				
surface	6.0	9.9	2.1	19.3
mid-depth	6.6	12.2	1.7	11.3
IE (12 I 67)				
mid-depth	3.4	5.2	3.6	69.4
IIIC (12 I 67)				
surface	3.3	4.7	3.3	67.0
mid-depth	3.5	4.7	3.9	85.7
1 m off bot.	4.3	8.5	4.5	107.9

TABLE D-1 Continued

Station, Date, and Depth	Mean $D_s$ ( $\mu$ )	Standard Deviation ( $\mu$ )	Skewness	Kurtosis
VF (12 I 67)				
surface	3.6	6.1	3.3	53.7
mid-depth	3.9	6.0	2.6	36.5

## BIBLIOGRAPHY

- American Society for Testing Materials, 1951. Tentative recommended practice for analysis by microscopical methods for particle size distributions of particulate substances of subsieve sizes. American Society for Testing Materials Pub. E 20-51T, Phila., Pa. p. 1574-1584.
- Arnold, H., 1911. Limitations imposed by slip and inertia terms upon Stokes' law for the motion of spheres through liquids. *Phil. Mag.*, 6th Ser., 22:755-775.
- Bagnold, R.A., 1966. An approach to the sediment transport problem from general physics. U.S. Geological Survey Prof. Pap. 422-I, 37 p.
- Bennett, A.H., H. Jupnik, H. Osterberg, and O.H. Richards, 1951. *Phase Microscopy, principles and applications.* John Wiley and Sons, New York.
- Biggs, R.B., 1963. Deposition and early diagenesis of modern Chesapeake Bay muds. PhD. Thesis, Lehigh Univ., Bethlehem, Pa., 119 p.
- Bond, G.C., R.H. Meade, 1966. Size distributions of mineral grains suspended in Chesapeake Bay and nearby coastal waters. *Chesapeake Sci.*, 7:208-212.
- Burt, W.V., 1952. Scattering of light in turbid water. PhD. Thesis, Univ. of Calif., Los Angeles, 64 p.
- , 1953. Extinction of light by filter passing matter in

- Chesapeake Bay waters. *Science*, 118:386-387.
- , 1955a. Interpretation of spectrophotometer readings on Chesapeake Bay waters. *J. Mar. Res.*, 14:33-46.
- , 1955b. Distribution of suspended materials in Chesapeake Bay. *J. Mar. Res.*, 14:47-62.
- Cadle, R.C., 1965. *Particle Size, Theory and Industrial Applications*. Reinhold Pub. Co., New York, 390 p.
- Cartwright, L.M. and R.Q. Gregg, 1958. A liquid sedimentation method for particle size distributions, p. 127-142. In: *Symposium on Particle Size Measurement*. Amer. Soc. for Testing Materials, Spec. Tech. Pub. 234, Philadelphia, Pa.
- Daniel, F., and R.A. Alberty, 1961. *Physical Chemistry*, 2nd ed. John Wiley and Sons, Inc., New York, 744 p.
- Davies, C.N., 1947. The sedimentation of small suspended particles. *Instn. Chem. Engrs. and Soc. Chem. Ind.* Symposium Series No. I, *Symposium on Particle Size Analysis*. Suppl. to *Trans. Instn. of Chem. Eng.* 25:25-39.
- Fairs, G.L., 1943. The use of the microscope in particle size analysis. *Chem. and Ind.*, 62:374.
- Gans, R., 1928. Zur Theorie der Brownschen Molekularbewegung. *Ann. d. Physik*, 86:628-656.
- Glasstone, S., 1946. *The Elements of Physical Chemistry*. D. Van Nostrand Co., Inc., New York, 695 p.
- Goldberg, E.D., M. Baker, and D.L. Fox, 1952. Microfiltration in oceanographic research. I. Marine Sampling with the

- molecular filter. *J. Mar. Res.*, 11:194-204.
- Goldstein, S., 1929. The steady flow of viscous fluid past a fixed spherical obstacle at small Reynolds numbers. *Proc. Roy. Soc. London*, 123:225-235.
- , [ed.], 1938. *Modern Developments in Fluid Dynamics*, Vol. 2, p. 491. Oxford University Press.
- Grabau, A.W., 1904. On the classification of sedimentary rocks. *Am. Geol.*, 33:228-247.
- Hamilton, R.J., J.F. Holdsworth, and W.H. Walton, 1954. Factors in the design of a microscope eyepiece graticule for routine dust counts, p. 101-105. *Br. J. Appl. Phys.*, Suppl. No. 3.
- Harrison, W., M.P. Lynch, and A.G. Altschaeffl, 1964. Sediments of lower Chesapeake Bay, with emphasis on mass properties. *J. Sedim. Petrol.*, 34:727-755.
- Hawksley, P.G.W., 1951. The physics of particle size measurement: Part I, fluid dynamics and the Stokes diameter. *Mon. Bull. Br. Coal Util. Res. Ass.* 15:105-145.
- Herdan, G., 1960. *Small Particle Statistics*, 2nd ed. Butterworths, London, 418 p.
- Irani, R.R., and C.F. Callis, 1963. *Particle Size: Measurement, Interpretation, and Application*. John Wiley and Sons, Inc., New York, 165 p.

- Jackson, M.L., 1956. Soil Chemical Analysis, Advanced Course.  
Published by author, Dept. of Soil Science, U. of  
Wisconsin, Madison, Wis., 991 p.
- Jarrett, B.A. and H. Heywood, 1954. A comparison of methods for  
particle size analysis, p. 21-28. Brit. Jour. of Appl.  
Phys., Suppl. No. 3.
- Jobst, G., 1925. Zur Farbentheorie Kolloidaler Metall suspensionen.  
Ann. d. Physik, 76:863-888.
- Krumbein, W.C. and F.J. Pettijohn, 1938. Manual of sedimentary  
Petrography. Appleton-Century Co., New York, 549 p.
- Kunkel, W.D., 1948. Magnitude and character of errors pro-  
duced by shape factors in Stokes' law estimate of particle  
radius. J. Appl. Phys., 19:1056-1058.
- Ladenburg, R., 1907. Über den Einfluß von Wänden auf die  
Bewegung einer Kugel in einer reibenden Flüssigkeit.  
Ann. d. Physik, 23:447-458.
- Lamb, H.H., 1932. Hydrodynamics, 6th ed. Dover Pub., New York,  
738 p.
- Lisitsin, A.P., 1961. Distribution and composition of suspended  
materials in seas and oceans. In: Recent Sediments of the  
Seas and Oceans, U.S.S.R. Academy of Sciences, Commission  
on Sediments, Division of Geological and Geographical  
Sciences. Moscow, p. 175-231. In Russian.

- Loveland, R.P., 1959. Methods of particle-size analysis, p. 57-86. In: Symposium on Particle Size Measurement, Amer. Soc. for Testing Materials, Spec. Tech. Pub. 234, Phila. , Pa.
- Mie, G., 1908. Beitrage zur Optik truber Medien, Speziell kolloidaler Metallosungen. Ann. d. Physik, 25:377-445.
- Mine Safety Appliance Co., MSA Particle Size Analyzer Operating Procedures and Applications. Pittsburgh, Pa., 35 p.
- Oseen, C.W., 1910. Zur Hydrodynamik der Kugel. Ark. Mat. Astron. Fys. 6:1-75.
- Patterson, H.S. and W. Cawood, 1936. The determinations of size distribution in smokes. Trans. Faraday Soc., 32: 1084-1088.
- Pritchard, D.W., 1952. Estuarine hydrography, p. 243-280. In: H.E. Landsberg ed. , Advances in Geophysics, Vol. 1, Academic Press, New York.
- , 1955. Estuarine circulation patterns. Amer. Soc. Civil Eng. Proc. Hydraulics Div., 81:11. Separate No. 717.
- , 1956. The dynamic structure of a coastal plain estuary. J. Mar. Res., 15:33-42.
- Rayleigh, Lord, 1881. On the electromagnetic theory of light. Phil. Mag. Ser. 5, 12:81-101.
- Rose, H.E., 1945. An investigation into the laws of flow of fluids through beds of granular materials. Proc. Instn. Mech. Engrs. 153:141-147.

- Rubey, W.W., 1933. Settling velocities of gravel, sand, and silt particles. *Am. Jour. Sci.*, 25:325-338.
- Ryan, J.D., 1955. The Sediments of Chesapeake Bay. Md. Dept. of Geology, Mines and Water Resources Bull. 12, 120 p.
- Schubel, J.R., 1967. On suspended sediment sampling by filtration. *Southeastern Geol.*, 8:85-87.
- Shepard, F.P., 1963. *Submarine Geology*, 2nd ed. Harper and Row Pub. Inc., New York, 557 p.
- , 1964. Criteria in modern sediments useful in recognizing ancient environments, p. 1-25. In: L.M.J.U. Van Straaten [ed.], *Developments in Sedimentology*, Vol. 1, Deltaic and Shallow Marine Deposits, Elsevier Pub. 6, Amsterdam, 464 p.
- Singewald, J.T. and T.H. Slaughter, 1949. Shore Erosion in Tidewater Maryland. Md. Dept. Geol., Mines and Water Resources, Bull. 6, 140 p.
- Stephenson, L.W., C.W. Cook, W.C. Mansfield, 1933. Chesapeake Bay Region. Guidebook 5, 16th International Geological Congress, 49 p.
- Stokes, G.G., 1850. On the theories of the internal friction of fluids in motion, and of the equilibrium and motion of elastic solids. *Cambr. Phil. Soc. Trans.* 8:287-319.
- Wadell, H., 1932. Volume, shape, and roundness of rock particles. *Jour. Geol.* 40:443-451.
- , 1936. Some practical sedimentation formulas. *Geol. Foren. Forhandl.* 58:397-408.

Winneberger, J.H., J.H. Austin, and C.A. Klett, 1963. Membrane filter weight determinations. *J. Wat. Pollut. Control Fed.*, 35:807-813.

Young, D.K., 1962. Chemistry of Chesapeake Bay sediments. M.S. Thesis, School of Marine Science, College of William and Mary, Williamsburg, Va., 38 p.